CM Aprvd ✓ ISSUED 2008/10/13

911125
Revision 0

ENGINEERING SERVICES FOR THE NEXT GENERATION NUCLEAR PLANT (NGNP) WITH HYDROGEN PRODUCTION

NGNP Composites R&D Technical Issues Study

Prepared by General Atomics
For the Battelle Energy Alliance, LLC

Subcontract No. 00075309
Uniform Filing Code UFC: 8201.3.1.2

GA Project 30302

GENERAL ATOMICS

Rolls-Royce
URS Washington Division
TOSHIBA Leading Innovation >>>
FE
ОКБМ
Korea Atomic Energy Research Institute

GENERAL ATOMICS

GA 1485 (REV. 08/06E)

ISSUE/RELEASE SUMMARY

☐ R & D ☐ DV&S ☒ DESIGN ☐ T&E ☐ NA	APPVL LEVEL	DISC	QA LEVEL	SYS	DOC. TYPE	PROJECT 30302	DOCUMENT NO. 911125	REV 0

TITLE:

NGNP Composites R&D Technical Issues Study

			APPROVAL(S)			
CM APPROVAL/ DATE	REV	PREPARED BY	ENGINEERING	QA	PROJECT	REVISION DESCRIPTION/ W.O. NO.
7 RELEASED OCT 1 3 2008	0	for R. Vollman	A. Shenoy	K. Partain	J. Saurwein	Initial Issue W.O # A30302-0040

CONTINUE ON GA FORM 1485-1

NEXT INDENTURED DOCUMENT(S)

N/A

COMPUTER PROGRAM PIN(S)

N/A

☐ GA PROPRIETARY INFORMATION

THIS DOCUMENT IS THE PROPERTY OF GENERAL ATOMICS. ANY TRANSMITTAL OF THIS DOCUMENT OUTSIDE GA WILL BE IN CONFIDENCE. EXCEPT WITH THE WRITTEN CONSENT OF GA, (1) THIS DOCUMENT MAY NOT BE COPIED IN WHOLE OR IN PART AND WILL BE RETURNED UPON REQUEST OR WHEN NO LONGER NEEDED BY RECIPIENT AND (2) INFORMATION CONTAINED HEREIN MAY NOT BE COMMUNICATED TO OTHERS AND MAY BE USED BY RECIPIENT ONLY FOR THE PURPOSE FOR WHICH IT WAS TRANSMITTED.

☒ NO GA PROPRIETARY INFORMATION

PAGE ii OF *

LIST OF CONTRIBUTORS

Name	Organization
Russell Vollman	Vollman Engineering Services
Richard Phelps	General Atomics
Dave Carosella	General Atomics
John Saurwein	General Atomics
Jonathan Taylor	Roll Royce, PLC
John Shoesmith	Roll Royce, PLC
Anthony Donaldson	Roll Royce, PLC
Paul Andrews	Roll Royce, PLC
Jiso Jun	KAERI

EXECUTIVE SUMMARY

The nominal reactor outlet helium temperature in Modular Helium Reactor (MHR) designs has increased from 700°C - 750°C in steam-cycle plant designs to 850°C in the gas-turbine modular helium reactor (Refs. 1 and 2), and the Department of Energy (DOE) has recently selected a very-high temperature gas-cooled reactor (VHTR) having a nominal reactor outlet helium temperature of 950°C as the reactor type for the Next Generation Nuclear Plant (NGNP) Project. And in the MHR, with its passively safe features, some reactor system components are subject to gas temperatures substantially higher than 950°C during conduction cool down (CCD) events. Because of these high reactor helium temperatures, it is necessary to modify some of the reactor system components that were designed for earlier steam-cycle plants to accommodate higher-temperature service. This requires selection of alternate materials of construction that can withstand the higher operating temperatures, helium coolant impurities, and the neutron radiation environment. These alternate materials include high-temperature metal alloys, ceramics, and ceramic composites. Ceramic composites as discussed herein (and sometimes referred to simply as “composites”) include both carbon/carbon (C/C) composites (i.e., carbon fibers in a carbonaceous matrix) and SiC/SiC composites (i.e., SiC fibers in a SiC matrix).

The subject study began with an evaluation of the need to use ceramics and ceramic composites as the materials of construction for reactor system components in a 600-MWt prismatic-block NGNP operating with a reactor outlet helium temperature of 950°C and a reactor inlet helium temperature ranging from 490°C to 590°C. The operating conditions (e.g., temperatures and neutron fluence) and material requirements were established for these components, and the materials best suited to these operating conditions and requirements were selected based on a review of the properties of candidate materials, including high-temperature metallic alloys, ceramics, and ceramic composites. The R&D issues associated with the use of ceramic and ceramic composite materials in the NGNP were identified, and conclusions and recommendations were developed with respect to the technology development activities needed to advance the technology readiness of the components fabricated from these materials to the technology readiness level required to support completion of component final design and fabrication in a time frame consistent with the goal to start up the NGNP by 2021.

The Reactor System components that were the subject of this study include:

- Control rod assemblies, specifically the structural part that contain the B_4C compacts
- Control rod and reserve shutdown material guide tubes
- Upper core restraint elements
- Permanent side reflector seal sleeves

- Upper plenum shroud thermal barrier assembly
- Lower plenum sidewall thermal barrier assembly
- Hot duct thermal barrier assembly
- Metallic core support thermal barrier load bearing thermal insulators
- Shutdown cooling system inlet tube assembly
- Shutdown cooling system heat exchanger thermal barrier assembly

The primary conditions that drive the choice of materials for these reactor components are as follows:

- The neutron fluence acquired by the component over its life
- The long term operational temperature
- The cumulative effect of transient increases in temperature during CCD events
- The effect of impurities in the primary coolant on material properties over the life of the component

The technology issues identified in the study and the proposed resolutions are summarized in Table 7-1 of Section 7 of this report.

Key conclusions and recommendations from this study are as follows:

1. The control rods should be fabricated from FMI-222 C/C composites to withstand the nearly 1000°C maximum temperature during normal operation and the 1500°C maximum CCD temperature. These control rods will have an 8-year life. An alternate material choice is a SiC/SiC composite that could last the full lifetime of the reactor, but this is a longer-term alternative because additional technology development would be required to extend the temperature ceiling for SiC/SiC use above 1400°C to accommodate the CCD maximum temperature of 1500°C.

2. The remaining high temperature structures can be made from C/C composites since their 60-year life time fluence is low. These components are:

    - Control rod and reserve shutdown material guide tubes
    - Upper core restraint elements
    - Upper plenum shroud thermal barrier cover plates and structural hardware
    - Lower plenum sidewall thermal barrier cover plates and structural hardware
    - Hot duct thermal barrier cover plates and structural hardware
    - Shutdown cooling system inlet tube structural elements

3. The permanent side reflector (PSR) seals should be made from graphite as hollow dowels.

4. The metallic core support load-bearing insulator pads should be made from a readily available glassy ceramic.

5. The shutdown cooling system thermal barrier should be made from metallic cover plates and hardware with either solid ceramic insulation or fibrous insulation blankets.

6. It is recommended that the fibrous insulation blankets used in past MHR designs be replaced with solid ceramic insulation of the type used for insulating high-temperature furnaces.

7. High priority is required on tasks that are needed to complete the design and the development of ASME, ASTM, and ASM test standards for ceramic composite materials. This is essential to the selection and conduct of the tests needed to support the technology program and to provide the tools for completing the design on schedule. A group that has responsibility for providing these standards should be established and held responsible for meeting the schedule.

8. Corrosion and neutron radiation effects screening tests should be expedited to confirm final material selections.

9. The screening test program for radiation and corrosion tests should be expedited so that final material selections can be made as early as possible.

10. High priority should be given to completing test plans for round-robin testing of standard test specimens so that the data being generated by these tests will be obtained on generally acceptable specimens.

11. An activity should be initiated to prepare ASTM and ASM specifications to control fabrication of ceramic composite materials.

12. An activity should be initiated to define the ceramic composite material and failure models for design computer codes so that the proper tests will be conducted to validate the models for the design activity.

13. An organization should be assigned to incorporate the material models and design criteria into design analysis codes and to maintain the schedule for completion of this work.

14. The material control processes should be reviewed by comparing the planned composites technology program with what is being done in the aerospace business with the composite materials that have been in use for about 20 years.

15. The conclusions and recommendations of this study should be incorporated to the extent practical into the overall NGNP technology development program plan.

16. No data with respect to corrosion of C/C composites in an impure helium environment were found during this study. Consequently, there is an apparent need for such corrosion data to validate lifetime predictions of C/C composite materials in the NGNP reactor environment. The NGNP composites technology development program should include the testing needed to generate this data.

Additional conclusions and recommendations are provided in Section 8.

At this writing, strong consideration is being given to reducing the nominal reactor outlet helium temperature for the NGNP from 950°C into the range of 750°C to 800°C (with a corresponding reduction in the reactor inlet helium temperature), and it appears that this change will be officially adopted by DOE. However, this composites R&D issues study was started and largely completed while the reactor outlet helium temperature objective for NGNP was still 950°C. Thus, the focus of the study was to evaluate the need for composites and the composites R&D issues associated with a reactor operating at this temperature. However, a cursory evaluation was performed as a late add-on to the study to assess the potential impact of the expected reduction in helium coolant temperatures on the need to use ceramic and ceramic composite materials for reactor system components in the NGNP. It was determined that for reactor outlet helium temperatures up to 750°C, most of the C/C composites can be eliminated and replaced with high-temperature metallic alloys, except for the control rods, upper core restraint elements, and possibly the hot duct T/B cover plates (based on a conservative maximum hot streak temperature). For a reactor outlet helium temperature of 800°C, C/C composites also become the likely material choices for the lower plenum sidewall T/B cover plates and the SCS entrance tubes. Table E-1 summarizes the results of this evaluation. Needless to say, the NGNP composites technology development program would be impacted with respect to both scope and cost if the reactor outlet and inlet helium temperatures were to be reduced, and this impact would be greater at 750°C than at 800°C.

Table E-1. RS Component Material Selections for Various Reactor Outlet Gas Temperatures

Component	Material Choice			
	687°C Reactor Outlet	750°C Reactor Outlet	800°C Reactor Outlet	950°C Reactor Outlet
Control Rod	C/C Composite	C/C Composite	C/C Composite	C/C Composite
Control Rod & RSM Guide Tube	Hastelloy X	Hastelloy XR	Hastelloy XR	C/C Composite
Upper Core Restraint	C/C Composite	C/C Composite	C/C Composite	C/C Composite
Upper Plenum Shroud T/B Cover Plates	Hastelloy X	Hastelloy X	Hastelloy X	C/C Composite
Permanent Side Reflector Seal Sleeves	Graphite	Graphite	Graphite	Graphite
Metallic Core Supt Load Bearing Insulators	Macor Glass Ceramic	Macor Glass Ceramic	Macor Glass Ceramic	Macor Glass Ceramic
Hot Duct T/B Assy	Hastelloy X	C/C Composite (Possibly Haynes 230)	C/C Composite	C/C Composite
Cross Vessel T/B Assy	Not Needed	Not Needed	Not Needed (Cross Vessel just at 371°C Temp limit)	Alloy 800H
Lower Plenum Sidewall T/B Assy	Hastelloy X	Hastelloy XR	C/C Composite (Possibly Haynes 230)	C/C Composite
SCS Entrance Tubes	Hastelloy XR	Hastelloy XR	C/C Composite	C/C Composite
SCS Heat Exchanger T/B Assy	Alloy 800H	Alloy 800H	Alloy 800H	Alloy 800H

TABLE OF CONTENTS

LIST OF FIGURES

LIST OF TABLES

ACRONYMS AND ABBREVIATIONS

AMRC	Advanced Manufacturing Research Centre
ASME	American Society of Mechanical Engineers
ASTM	American Society for Testing and Materials
ATR	Advanced Test Reactor
CAMTEC	Composites and Advanced Materials Technology Centre
C/C composite	Continuous carbon fiber-reinforced carbon-matrix composite
CFC	Carbon fiber composite
CCD	Conduction cool-down
CR	Control rod
CTE	Coefficient of thermal expansion
CVD	Chemical vapor deposition
CVI	Chemical vapor infiltration
DDN	Design data need
DPA or dpa	Displacements per atom
GA	General Atomics
GT-MHR	Gas-Turbine Modular Helium Reactor
HFIR	High Flux Isotope Reactor
HTGR	High Temperature Gas-cooled Reactor
HTTR	High Temperature Test Reactor (JAERI)
HX	Heat Exchanger
INL	Idaho National Laboratory
JMTR	Japan Material Test Reactor (Japan)
KAERI	Korea Atomic Energy Research Institute (Republic of Korea)
MCS	Metallic core support
NGNP	Next Generation Nuclear Plant
NRC	United States Nuclear Regulatory Commission
ORNL	Oak Ridge National Laboratory
PBMR	Pebble Bed Modular Reactor
PBMR Pty Ltd.	Pebble Bed Modular Reactor (Pty) Limited (Republic of South Africa)
PCS	Polycarbosilane
PIRT	Phenomena Identification and Ranking Table

PSR	Permanent side reflector
QA	Quality assurance
R&D	Research and development
RS	Reactor System
RSM	Reserve shutdown material
SCS	Shutdown Cooling System
S/S	Steady state
SiC	Silicon carbide
SiC/SiC composite	Continuous silicon carbide fiber-reinforced silicon carbide-matrix composite
T/B	Thermal barrier
UCR	Upper core restraint
UPS	Upper plenum shroud
VHTR	Very High Temperature Reactor (900°C to 1000°C outlet temp)

1 INTRODUCTION

The nominal reactor outlet helium temperature in Modular Helium Reactor (MHR) designs has increased from 700°C - 750°C in steam-cycle plant designs to 850°C in the gas-turbine modular helium reactor (Refs. 1 and 2), and the Department of Energy (DOE) has recently selected a very-high temperature gas-cooled reactor (VHTR) having a nominal reactor outlet helium temperature of 950°C as the reactor type for the Next Generation Nuclear Plant (NGNP) Project. And in the MHR, with its passively safe features, some reactor system components are subject to gas temperatures substantially higher than 950°C during conduction cool down (CCD) events. Because of these high reactor helium temperatures, it is necessary to modify some of the reactor system components that were designed for earlier steam-cycle plants to accommodate higher-temperature service. This requires selection of alternate materials of construction that can withstand the higher operating temperatures, helium coolant impurities, and the neutron radiation environment. These alternate materials include high-temperature metal alloys, ceramics, and ceramic composites[1].

The subject study began with an evaluation of the need to use ceramics and ceramic composites as the materials of construction for reactor system components in a 600-MWt prismatic-block NGNP operating with a reactor outlet helium temperature of 950°C and a reactor inlet helium temperature ranging from 490°C to 590°C. The operating conditions (e.g., temperatures and neutron fluence) and material requirements were established for these components, and the materials best suited to these operating conditions and requirements were selected based on a review of the properties of candidate materials, including high-temperature metallic alloys, ceramics, and ceramic composites. The R&D issues associated with the use of ceramic and ceramic composite materials in the NGNP were identified, and conclusions and recommendations were developed with respect to the technology development activities needed to advance the technology readiness of the components fabricated from these materials to the technology readiness level required to support completion of component final design and fabrication in a time frame consistent with the goal to start up the NGNP by 2021.

At this writing, strong consideration is being given to reducing the nominal reactor outlet helium temperature for the NGNP from 950°C into the range of 750°C to 800°C, and it appears that this change will be officially adopted by DOE. However, this composites R&D issues study was started and largely completed while the reactor outlet helium temperature objective for NGNP was still 950°C. Thus, the focus of the study was to evaluate the need for composites and the composites R&D issues associated with a reactor operating at this temperature. However, a cursory evaluation of the impact of a lower reactor outlet helium temperature on the need to use

---

[1] Ceramic composites as discussed herein (and sometimes referred to simply as "composites") include both carbon/carbon (C/C) composites (i.e., carbon fibers in a carbonaceous matrix) and SiC/SiC composites (i.e., SiC fibers in a SiC matrix).

ceramic and ceramic composite materials for reactor system components in the NGNP was performed as a late add-on to the study. The results of this evaluation are presented in Section 9.

2 IDENTIFICATION OF COMPONENTS

2.1 Reactor System Components

The purpose of this section is to describe the Reactor System in general and to show the location and hierarchy of the Reactor System components that are candidates for fabrication from ceramic composite materials.

The Reactor System consists of the reactor core and the reactor internals. The reactor core components are those directly involved in the production of neutrons such as the fuel element assemblies, the various graphite reflectors, the boron shielding, and the neutron control materials including the control rods and reserve shutdown material. There are other components in the core, but they are not relevant to this study. The reactor internals components are those that support the reactor core assembly and insulate the various metallic structural elements from the high-temperature gas of the primary coolant system. The Reactor System diagram is shown in Figure 2-1. A cross section of the Reactor System illustrating the various physical components is shown in Figure 2-2.

2.2 Components to be evaluated in this study

The reactor system components that are considered to be candidates for fabrication from high-temperature materials are as follows:

- Control rods assemblies, specifically the structural part that contain the B_4C compacts
- Control rod guide tubes
- Upper core restraint elements
- Permanent side reflector seal sleeves
- Upper plenum shroud thermal barrier assembly
- Lower plenum sidewall thermal barrier assembly
- Hot duct thermal barrier assembly
- Metallic core support thermal barrier assembly
- Shutdown cooling system inlet tube assembly
- Shutdown cooling system heat exchanger thermal barrier assembly

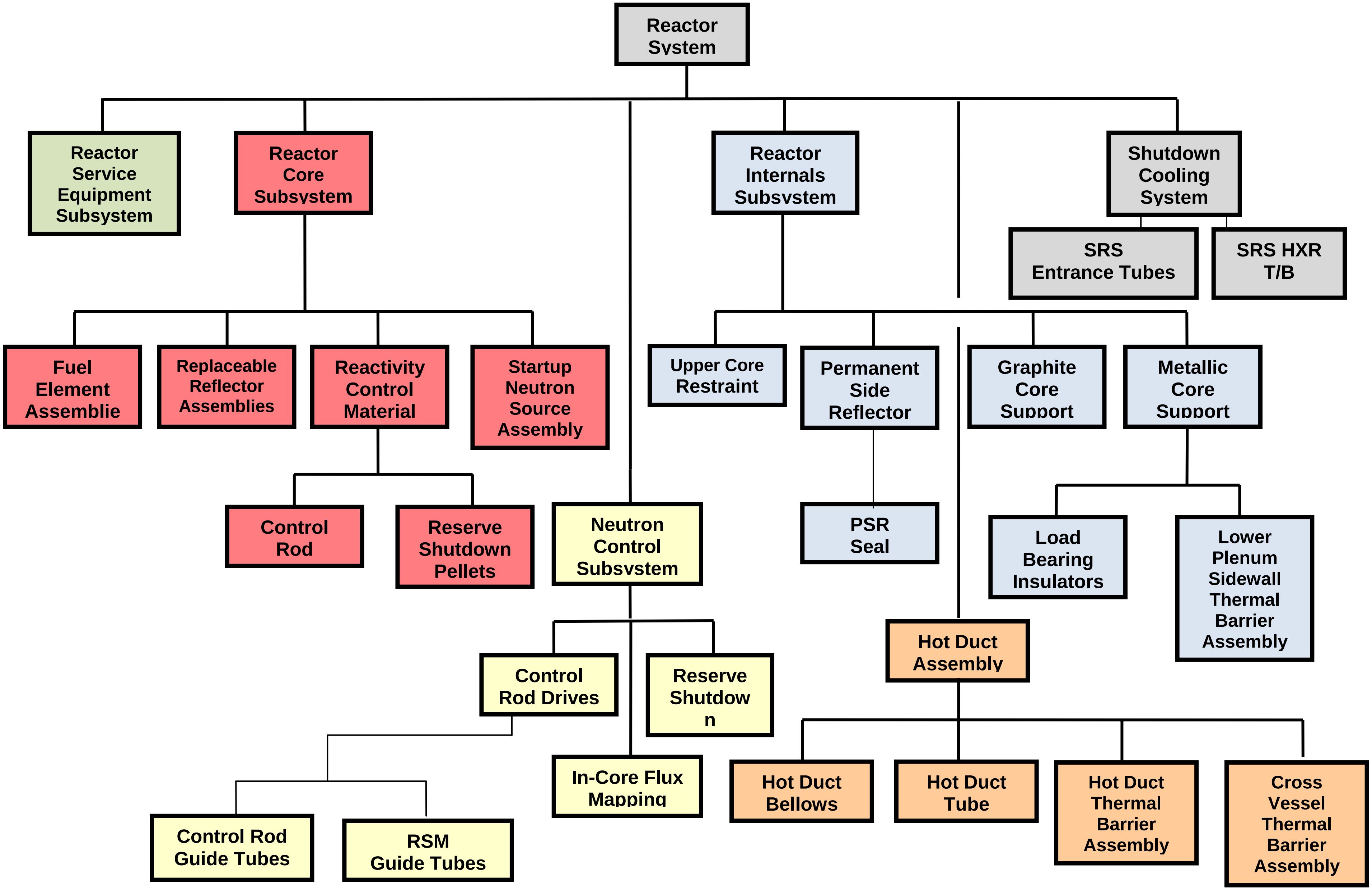

Figure 2-1. Reactor System Hierarchy

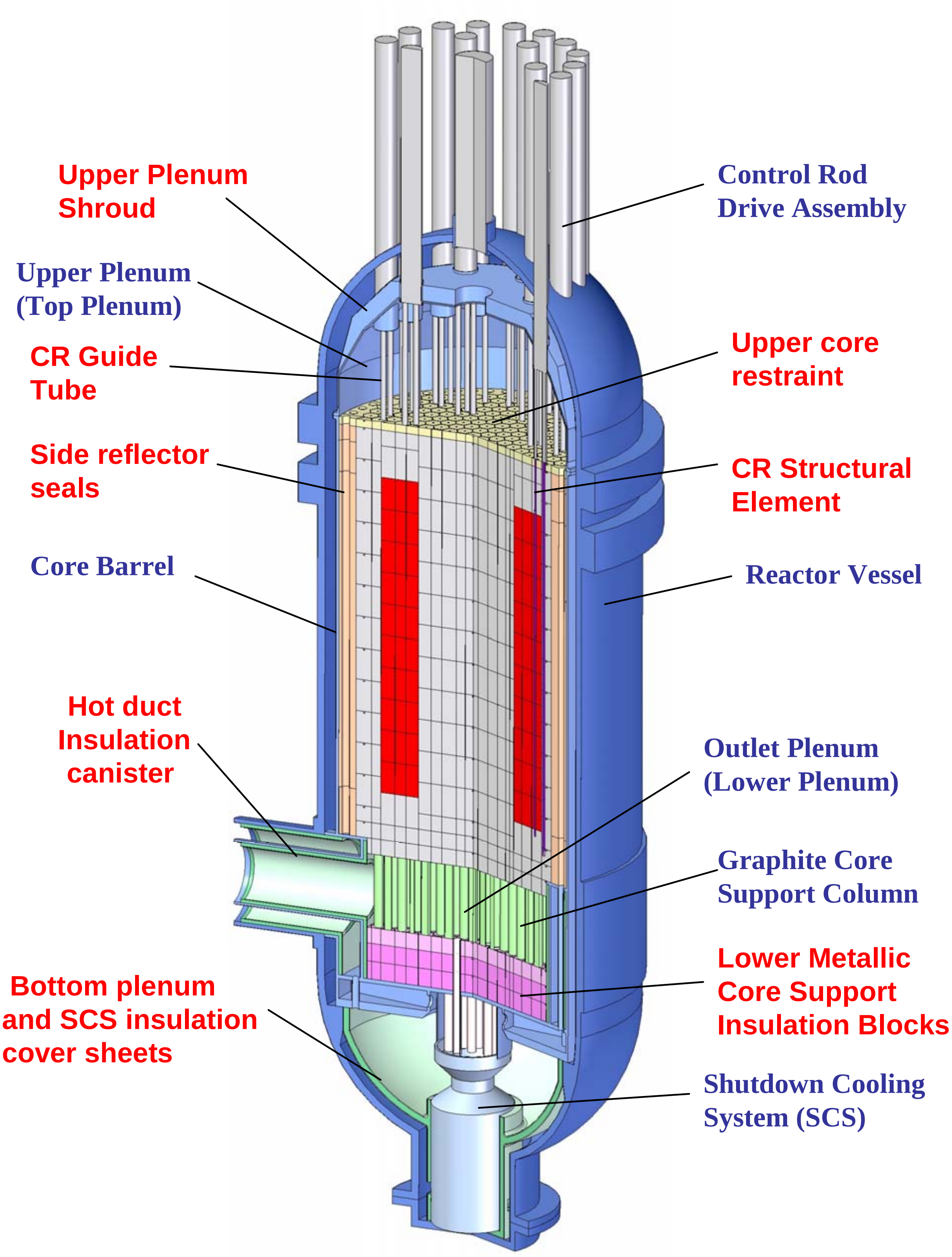

Figure 2-1. Physical location of Reactor System high temperature hardware

3 DESIGN CONDITIONS & REQUIREMENTS

3.1 Normal Operation and Off-Normal Conditions

The purpose of this section is to define the operating conditions and design requirements for the high-temperature components that are candidates to be fabricated from ceramic composites. It is not intended to be an exhaustive set of conditions and design requirements, as would be found in the design specification, but just those needed to select materials of construction. These requirements will be compared with the material capabilities in Section 4 as the basis for materials selection.

As discussed in Section 2, a groundrule for this study is that the materials selected for the reactor system components must provide the capability for the NGNP to operate with a nominal reactor outlet helium temperature up to 950°C. The reactor inlet helium temperature is assumed to be between 490°C and 590°C. For material evaluation, the worst case inlet temperature is used. For example, in determining the thickness of candidate insulation materials, the maximum temperature difference between the hot side and cold side is used. Conversely, for the maximum temperature effect, the maximum cold-side temperature is used. In all cases, the maximum hot-side temperature of 950°C is used.

The primary conditions that drive the choice of materials for the reactor core and internals components are as follows:

- neutron fluence received by the component
- long term operational temperature
- the cumulative effect of transient increases in temperature during conduction cool down transients
- the effect of impurities in the primary coolant on material properties over the life of the component

3.2 Summary of Thermal Fluid Analysis of the NGNP

Thermal conditions have been calculated by the Korea Atomic Energy Research Institute (KAERI) for the GA-proposed NGNP design in a series of analyses for NGNP normal operation and conduction cool down (CCD) conditions (Ref. 4). KAERI performed analyses for reactor inlet/outlet temperatures of 490°C/950°C and 590°C/950°C. The maximum temperatures calculated for selected key reactor core components during steady state 100% power operation and CCD events are summarized in Tables 3-1 and 3-2, respectively. These tables were taken directly from Ref. 4, which is included as Appendix I in this report. The temperatures calculated for the reactor system components that are being considered in this study for fabrication from ceramic or ceramic composite materials are presented in Section 5.

In Table 3-1, the maximum temperature of the fuel and fuel block are lower for the 590°C case than for the 490°C case because the core flow rate is substantially higher to maintain the same heat extraction from the reactor core with a smaller coolant temperature ΔT over the length of the core. The higher flow rate has the effect of lowering the differences in fuel temperature above and below the average, resulting in lower maximum fuel temperatures. This is a desirable result for fuel performance because it reduces fission product release from the hottest fuel in the core.

Table 3-1. RS Component Maximum Temperatures for Normal Operation

Components	490°C Core Inlet (C)	590°C Core Inlet (C)
Fuel Compact	1133	1110
Fuel Block	1081	1057
Replaceable Top Reflector	553	637
Replaceable Central Reflector	900	897
Replaceable Side Reflector	762	788
Replaceable Bottom Reflector	1018	1004
Core Barrel (Alloy 800H)	481	578
Reactor Pressure Vessel (SA 508)	333	390

.

Table 3-2. Reactor System Component Maximum Temperatures for CCD Events

Components	Pressurized CCD Event		De-pressurized CCD Event	
	490°C Core Inlet (C)	590°C Core Inlet (C)	490°C Core Inlet (C)	590°C Core Inlet (C)
Fuel Compact	1243	1280	1487	1511
Fuel Block	1243	1279	1487	1511
Replaceable Top Reflector	1195	1225	964	990
Replaceable Central Reflector	1232	1267	1473	1497
Replaceable Side Reflector	951	980	1153	1174
Replaceable Bottom Reflector	1019	1005	1018	1004
Core Barrel (Alloy 800H)	597	608	693	706
Reactor Press Vessel (SA 508)	456	468	540	553

3.3 Neutron Fluence at the Reactor System Components

Neutron fluxes and fluence were estimated from prior program information and gleaned from Design Data Needs (Ref. 2). In addition, a detailed nuclear analysis including components outside the permanent side reflector was used (Ref. 3). The results for this study are presented in Appendix B. The neutron fluence for each component is listed in Table 3-3.

Table 3-3. Reactor Internals Lifetime Neutron Fluence

Component	Design Life	Lifetime Fluence	
		n/m^2	dpa (estimate)
Control Rods	8 y	3.22×10^{26}	4.0
Control Rod & RSM Guide Tubes	60 y	1.03×10^{23}	0.00128
Upper Core Restraint	60 y	3.49×10^{24}	0.0434
Upper Plenum Shroud Thermal Barrier	60 y	1.20×10^{22}	0.00098
Permanent Side Reflector Seal Sleeves	60 y	3.22×10^{24}	0.0400
Metallic Core Support Load Bearing Insulators	60 y	8.50×10^{21}	0.00011
Hot Duct & Cross Vessel Thermal Barrier	60 y	8.50×10^{21}	0.00011
Lower Plenum Sidewall Thermal Barrier	60 y	8.50×10^{21}	0.00011
Shutdown Cooling System Entrance Tubes	60 y	8.50×10^{21}	0.00011
Shutdown Cooling System HX Thermal Barrier	60 y	8.50×10^{21}	0.00011

3.4 Primary Coolant Chemistry

The coolant chemistry levels required for design are shown in Table 3-4. This data was taken from DDN 11.07.01 (Ref. 2). This chemistry is not in equilibrium with the temperatures in the primary coolant loop, but represents probabilistic maximum values. The expected values of oxidants in the coolant are shown in Table 3-5. These values are for lower core inlet/outlet temperatures, but are shown here to provide an indication of what might be expected during normal operation. The primary coolant impurity levels for which the components must sustain operation are considerably higher than the expected values for equilibrium conditions due to uncertainty in predicting the levels of oxidants in the primary coolant.

Table 3-4. Design Levels of Primary Coolant Impurities for Reactor Internals Components

Parameter	Value	Units	Ref	Comment
Design Primary He Coolant Impurities at S/S 100% power			2	This is an equilibrium coolant chemistry at 100% power for Tin = 490°C and Tout = 850°C.
H_2O	2.0	ppmV		140 microatm
CO_2	2.0	ppmV		140 microatm
CO	5.0	ppmV		350 microatm
H_2	10.0	ppmV		700 microatm
CH_4	2.0	ppmV		140 microatm
N_2	10.0	ppmV		700 microatm
Particulates	10.0	lb/yr		

Table 3-5. Expected Levels of Primary Coolant Impurities for Reactor Internals Components

Parameter	Value	Units	Ref	Comment
Expected Primary He Coolant Impurities at S/S 100% power (For reference only)			2	This is an equilibrium coolant chemistry at 100% power for Tin = 490°C and Tout = 850°C.
H_2O	0.5	ppmV		35 microatm
CO_2	1.0	ppmV		69.7 microatm
CO	2.0	ppmV		140 microatm
H_2	3.0	ppmV		210 microatm
CH_4	0.1	ppmV		7 microatm
N_2	2.0	ppmV		140 microatm
Particulates	1.0	lb/yr		

3.5 Summary List of Reactor System Design Requirements for Material Selection

Table 3-6 is a partial compilation of the expected conditions for a prismatic NGNP with a mixed mean reactor outlet helium temperature of 950°C. The table contains 2 cases: Case 1 – reactor inlet/outlet of 490°C/950°C, and Case 2 – reactor inlet/outlet of 590°C/950°C. The design requirements are compiled in Table 3-6 to aid in selection of materials for the high-temperature structures of this study. The source of the data is shown as a reference number in the column just to the left of the comment column. The references are listed in Section 10. Because of the size of this compilation, only a portion of it is presented in Table 3-6. The entire compilation is provided in Appendix A.

In most cases, the values included in Table 3-6 (and Table A-1) are directly from the referenced source. In other cases, some margin has been added to account for uncertainty. One example of such margin is for the primary coolant impurity levels for which the components must sustain operation; these are considerably higher than the expected values for equilibrium conditions due to uncertainty in predicting the levels of oxidants in the primary coolant. Another example is the primary coolant hot streaks emanating from the reactor core, where the values are based on past analyses. The hot streak maximum increase in temperature above the mean outlet temperature of 950°C is conservatively assumed to be 250°C directly below the core and 225°C at the entrance to the hot duct. The actual hot streaks may be well below these maximums. The choice of materials should be based on these assumed hot streak temperatures until an updated analysis is performed to obtain more accurate values.

Table 3-6. NGNP RI Components Conditions for Normal Operation and CCCD Transients

(Complete Table in Appendix A)

Location	Component	Parameter	Value	Units	Ref	Comment
Overall Reactor System						
	Overall Sys Parameter	Reactor Thermal Power (100% Power)	600.0	MW(t)	1	GT-MHR was 490/850°C Tin/Tout of the Reactor Core
	Overall Sys Parameter	Core Avg Power Density	6.6	MW/m^3	1	Was 6 MW/m^3 for 550 MWt 102 Col Core. Increased power density 10% for the 600MWt 102 col core. His I the stretched version of the 102 col core.
	Electric Gen Loop	Power Split to Electric Power Gen Loop	525.0	MW(t)	?	Electric generation loop
	Process Heat Loop	Power Split to Process Heat Loop	65.0	MW(t)	?	Process Heat Loop
	Overall Sys Parameter	System Pressure (100% power)	7.1	MPa abs	1	(1025 psia)
	Overall Sys Parameter	Reactor Vessel Relief Valve set pressure	7.8	MPa abs	Calc	(1128 psia) set at 10% above Operating press.

Location	Component	Parameter	Value	Units	Ref	Comment
	Overall Sys Parameter	**Case 1: Core Tin/Tout 490/950°C**				To be used in cases where the 490°C inlet temp is most critical to the design (e.g., Thermal barrier thickness calculations).
		Core Inlet He Temp	490.0	C	4	
		Core outlet He Temp	950.0	C	4	A capability requirement to set to maximize PCS and Process heat performance.
		Primary He coolant total flow rate	248.5	kg/s	4	
	Overall Sys Parameter	**Case 2: Core Tin/Tout 590/950°C**				To be used in cases where the 590°C inlet temp is most critical to the design (e.g., Thermal barrier cover plate operating temp).
		Core Inlet He Temp	590.0	C	1	Was 490°C, but changed to 590°C to reduce hot streaks in core He flow and localized hot spots in fuel. Not the same as 600MW KAERI analysis of 250.4 kg/s for Tin=490°C & Tout=950°C due to higher Core delta T.
		Core outlet He Temp	950.0	C	1	Was 850°C, but rose to 950°C to set max capability. Raised core inlet temp 100°C to bring to 590°C to maintain the same core ΔT. A capability requirement to set to maximize PCS and process heat performance
		Primary He coolant total flow rate	320.0	kg/s	1	Same as 600MWt GT-MHR flow rate. This flow rate is for a Tin=490°C and Tout=850°C. Assumed that hot streaks above mean temp not affected since axial temp increase across core the same.
	Overall Sys Parameter	He Coolant Loop Sustained noise level	160.0	dB	2	Transient spectrum up to 160 dB. For noise induced vibration. (DDN C.11.02.02)
	Application to specific Components	PCC & DCC Temp Profiles	*		4	* See Ref 4 for temps in KAERI T/H analysis Report. Specific Temp Maximums will be called out for the components below.
	Overall Sys Parameter	Max rate of depressurization during a breach of Primary Pressure Boundary	152.0	kPa/sec	2	(22 psi/s) System Pressure vs. time at key locations better. (DDN C.11.02.02)
	Reactor Vessel	Max Avg Reactor Vessel Allowable Metal Temp during normal operation	371.0	C	5	(700F) All Reactor Internal Components, in conjunction with other equipment, must function to maintain vessel temp at or below 371 C during Normal Operation.
	Reactor Vessel	Reactor Vessel Fluence shall not Exceed:			1	All Reactor Internal Components, in conjunction with other equipment, must function to maintain vessel neutron fluence at or below at or below the fluence listed below during Normal Operation for the 60-year life of the reactor plant.
	Reactor Vessel	E > 0.9 MeV	9.9×10^{21}	n/m^2	1	
	Reactor Vessel	0.1 < E < 0.9 MeV	4.8×10^{22}	n/m^2	1	
	Reactor Vessel	3.05eV < E < 0.1 eV	9.9×10^{22}	n/m^2	1	

Location	Component	Parameter	Value	Units	Ref	Comment
	Reactor Vessel	e < .01 eV	3.3×10^{22}	n/m^2	1	
	Reactor Vessel	Total for all neutron Energy Levels	1.84×10^{23}	n/m^2	1	
	Applies to all comp in primary coolant loop. Use for design.	Design Required Primary He Coolant Impurities @ S/S 100%pwr:			2	All of these values are for a core T_{in} = 490C & core $T_{out\ let}$ = 850C. DDN.11.07.01 They apply to all equipment in the reactor primary coolant. The Values are maximums to be used for design and are not in equilibrium with each other.
		H2O	2.0	ppmV		140 microatm
		CO2	2.0	ppmV		140 microatm
		CO	5.0	ppmV		350 microatm
		H2	10.0	ppmV		700 microatm
		CH4	2.0	ppmV		140 microatm
		N2	10.0	ppmV		700 microatm
		Particulates	10 .0	lb/yr		
	Reference only - Do not use for design.	Expected Primary He Coolant Impurities @ S/S 100%pwr: (For reference only)			2	All of these values are for a core T_{in} = 490C & core $T_{out\ let}$ = 850C This is an equilibrium coolant chemistry at 100% power for an Tin = 490 C and Tout = 850 C.
		H2O	0.5	ppmV		35 microatm
		CO2	1.0	ppmV		69.7 microatm
		CO	2.0	ppmV		140 microatm
		H2	3.0	ppmV		210 microatm
		CH4	0.1	ppmV		7 microatm
		N2	2.0	ppmV		140 microatm
		Particulates	1.0	lb/yr		
Permanent Side Reflector Assy						
	PSR Seal Sleeves	Case 1: Max Normal op Helium Coolant Core Inlet Temp @ 100% power	490.0	C	4	Predicted sleeve temp so close to coolant temp. Use Coolant Temp as component Design Temp for Normal op. (Ref 4)
		Case 1: Total Flow Rate @ 100% power	248.5	kg/s	4	
		Case 2: Max Normal op Helium Coolant Core Inlet Temp @ 100% power	590.0	C	1	Predicted sleeve temp very close to coolant temp. Use Coolant Temp as component design Temp for Normal op. (Ref 4). Was 490C, but changed to 590C. Maintained same core delta T so hot streaks are about same as 600MWt NGNP.
		Case 2: Total Flow Rate @ 100% power	320.0	kg/s	1	
		Max Seal Sleeve Temp	590.0	C	4	

Location	Component	Parameter	Value	Units	Ref	Comment
		Max PCC Temp sustained for about 150 hours per event. Case 2	643.0	C	4	See Transient temp vs. time curve in Ref 4.
		Max DPCC Temp sustained for about 150 hours per event. Case 2	743.0	C	4	See Transient temp vs. time curve in Ref 4.
		Maximum Neutron Flux (Full spectrum)	2.0×10^{17}	$n/m^2/s$	3	EOC Flux. May be a little lower than average, but within error of calc at this point.
		Maximum Total Neutron Fluence (Full spectrum)	3.2×10^{26}	n/m^2	3	60-year plant life at 85% plant capacity factor
Upper Plenum						
	All of Upper Plenum	Case 1: Max Normal op Helium Coolant Core Inlet Temp @ 100% power	490.0	C	4	
		Case 1: Total Flow Rate @ 100% power	248.5	kg/s	4	
		Case 2: Max Normal op Helium Coolant Core Inlet Temp @ 100% power	590.0	C	1	
		Case 2: Total Flow Rate @ 100% power	320.0	kg/s	1	
	UPS Thermal Barrier Cover Plates & Fasteners	Case 2 max Normal Op Temp @ 100% power	541.0	C	4	Adjust Ref 4 temp for a 490°C Core inlet to a 590°C core inlet by adding 100°C to 490°C results to account for higher gas temp.
		Max PCC Temp sustained for about 150 hours per event.	926.0	C	4	(1697°F) Occurs at full system pressure
		Max DCC Temp sustained for about 350 hours per event.	540.0	C	4	(1004°F) Occurs at blow down pressure of approx 1 atm

4 MATERIAL PROPERTIES AND CAPABILITIES

The purpose of this section is to identify potential materials that will meet the design requirements identified in Section 3 and to list the relevant properties of these materials. In addition, the properties will be evaluated to determine their design limits so they can be evaluated against the design requirements to determine which materials can be used for the hardware of the Reactor System. Limits on useful temperature and neutron fluence, and corrosion properties are identified for the materials. The ability of the materials to meet life requirements is noted. Selection of materials for fabrication of parts is based on the material properties, material limits, manufacturing feasibility, and availability. Of course, the materials must have the capability to meet the design requirements to be acceptable for use in the hardware.

4.1 Material Properties

This subsection catalogues the material properties of the candidate materials with the objective of developing the service limits for the selected candidates. Three types of materials are being considered for use in the high temperature areas of the reactor core and Internals structures. They are high-temperature metallic alloys, monolithic ceramics, and ceramic composites. Properties of these types of materials have been obtained from a myriad of sources and organized into groups for possible use. These properties are displayed in tables in the following subsections.

4.1.1 Metallic material properties

Table 4-1 lists the material properties for high-temperature metallic alloys.

Table 4-1. High-Temperature Alloy Properties at Maximum Allowable Temperatures

Mat'l	ASME Code Info			Mechanical Properties at Code Temp Limit						Physical Properties at Code Temp Limit			Environmental Effects			Comment
	Applicable Codes & Stds	Code Temp Limit		Elastic Mod	Min UTS	Min YS	S_m	S_o	Temp	CTE (Mean)	Conductivity	Cobalt Content	Corrosion & Fluence Limits			
		F	C	10^3 KSI	KSI	KSI	KSI	KSI	F	in/in/°F	W/m.K	%	Codes & Stds	n/m^2	DPA	
718 AMS5596C	ASME Sect III, Div 1	1,200	649	23.6	146.3	122.1	41.2	6.7	1,200	8.3	22.3	1.2 Max	Owners Responsibility. Maintain at least 10% ductility.	3.0E+22	0.00246	Fluence of 1.2E23 is all thermal fluence. High energy neutrons don't affect ductility Gamma & Gamma-Prime formation causes increase in strength and reduction in ductility with increasing temp ** Note: Could not find 1800F data before completion of report.
800H SB-409	ASME Sect III, Div 1	1,400	760	21.9	30.6	14.0	11.0	3.6	1,400	10.2	23.8	2.0	Owners Responsibility. Maintain at least 10% ductility.	3.0E+22	0.00246	
617	ASME Sect VIII, Div 1 Code Case 1956-7	1,650	899	21.9	126.5 *	58.3*	39.1	?	1,650	8.7	26.7	10 to 15	Owners Responsibility. Maintain at least 10% ductility.	3.0E+22	0.00246	
617	ASME Sect VIII, Div 1 Code Case 1982-1	1,800	982	19.0	**	**	**	**	1,800	9.0	28.4	10 to 15	Owners Responsibility. Maintain at least 10% ductility.	3.0E+22	0.00246	
Hast X AMS5536G	ASME Sect VIII, Div 1	1,600	871	19.8	30.3	17.0	11.1	1.3	1,600	9.0	25.6	0.5-2.5	Owners Responsibility. Maintain at least 10% ductility.	3.0E+22	0.00246	
Mitsubishi Hast XR	Not in Code Yet. Code Case 2315 Sect Viii, Div. 1	1700?	927	**	**	**	**	**	1,700	**	**	0 to 1.0	Owners Responsibility. Maintain at least 10% ductility.	3.0E+22	0.00246	** Note: Could not find 1700F data before completion of report.
Haynes 230	ASME Sect VIII, Div 1 Code Case 2384	1,800	982	30.9 RT	35.0	21.0	11.6	< 0.8	1,800	7.0	8.9 RT	5.0 Max	Owners Responsibility. Maintain at least 10% ductility.	3.0E+22	0.00246	

4.1.2 Monolithic Ceramic Material Properties

Table 4-2 lists monolithic ceramic material properties followed by a description of the important classes of ceramics. Material suppliers are listed in Appendix G.

Table 4-2. Monolithic Ceramic Material Properties

Manufacturer	**Product Name**	**Density (Fired) g/cm^3**	**Porosity (apparent) (%)**	**Thermal Expansion Coefficient (10E-6/°C)**	**Thermal Conductivity (W/m.K)**	**Specific Heat (J/kg.K)**	**Thermal shock (Delta °C)**	**Poisson's Ratio**
Morgan Advanced Ceramics	Alumina (typical of fully dense grades)	3.75 - 3.95	0	6.9 - 8.9 (RT) 8.5 - 9.0 (800°C)	25.6 - 30.0 (RT) 12.5 (400°C)	880	160 - 210	
Kyocera	Alumina (A479SS) 99.5%	3.9		7.2 (400°C) 8.0 (800°C)	32 (20°C)	780	250	0.23
Morgan Advanced Ceramics	Zirconia Toughened Alumina (ZTA)	4.32	0	8.3 (RT)	20 (RT)			0.24
Morgan Advanced Ceramics	MgO Stabilized Zirconia (Z500)	5.6 - 5.7	0	10 (RT) 10 (800°C)	2.5 (RT)	460	300	
Kyocera	Zirconia (Z-220)	5.6		10 (400°C 10.5 (800°C)		460	450	0.31
Saint Gobain Ceramics	Hexaloy SA SiC	3.1		4.02 (700°C)	125 (RT) 103 (200°C)	670		0.14
Saint Gobain Ceramics	Hexaloy SP SiC	3.04		4.2 (700°C)	110 (RT)	590		0.14
Kyocera	Silicon carbide (SC-211)	3.2		3.7 (400°C) 4.4 (800°C)	60	670	400	0.16
Morgan Advanced Ceramics	Silicon Carbide	2.7 - 3.1	0.1 - 5.0	4.5 - 5.0 (1000°C)	35 - 124 (200°C)			
Morgan Advanced Ceramics	Cordierite	2.4	0	3.0 (RT)	2.0 (RT) 3.0 (400°C)	950	300	
Morgan Advanced Ceramics	Aluminum Silicates	2.3 - 3.0	0 - 11	2.9 (RT) 5.7 - 6.3 (1000°C)	1.4 - 6.0 (200°C)	800 - 900		55 - 150
Morgan Advanced Ceramics	Fused Silica	1.35 - 2.0	0	0.5 (RT)	0.9 (RT)			
Morgan Advanced Ceramics	RBSN	2.5	20	3.1 (1000°C)	12 (RT)	1100	> 600	
Morgan Advanced Ceramics	SSN	3.2	0	3.3 (RT)	15 (RT)	900	> 600	
Kyocera	Silicon Nitride (SN - 240)	3.3		2.8 (400°C) 3.3 (800°C)	27	650	> 800	0.28
Corning / Morgan	MACOR	2.52	0	11.4 (25-600ºC)	1.46	790		0.29
Morgan Advanced Ceramics	Cordierite	2.4	0	3.0 (RT)	2.0 (RT) 3.0 (400°C)	950	300	
	Aluminosilicate glass-ceramics							

Manufacturer	**Product Name**	**Density (Fired) g/cm^3**	**Porosity (apparent) (%)**	**Thermal Expansion Coefficient (10E-6/°C)**	**Thermal Conductivity (W/m.K)**	**Specific Heat (J/kg.K)**	**Thermal shock (Delta °C)**	**Poisson's Ratio**
Morgan Advanced Ceramics	Mullite Alumina (typical of fully dense grades)	1500 - 1725	14.3 - 18.5	310 - 500	2000 - 2500		4 - 5.9	
Kyocera	Alumina (A479SS) 99.5%	1600	16	360	2350		4	
Morgan Advanced Ceramics	Zirconia Toughened Alumina (ZTA)			430				
Morgan Advanced Ceramics	MgO Stabilized Zirconia (Z500)	1000	11	500-550	2000		8.4	
Kyocera	Zirconia (Z-220)		10.7	750			7.0 - 8.0	
Saint Gobain Ceramics	Hexaloy SA SiC	1900	2800 Knoop 0.1Kg	380 (4 Point)	3900		4.6	
Saint Gobain Ceramics	Hexaloy SP SiC	1900	2800 Knoop 0.1Kg	240 (4 Point)			4.3	
Kyocera	Silicon carbide (SC-211)	1200	22	540			4.0 - 5.0	
Morgan Advanced Ceramics	Silicon Carbide	1300 - 1650		80 - 400				
Morgan Advanced Ceramics	Cordierite	1000		88.1	500			
Morgan Advanced Ceramics	Aluminum Silicates	1150 - 1350		64	275			
Morgan Advanced Ceramics	Fused Silica	1000 - 1100		125	850 - 900			
Morgan Advanced Ceramics	RBSN	1300		200	650			
Morgan Advanced Ceramics	SSN	1000	16	650	> 3000			
Kyocera	Silicon Nitride (SN - 240)	1200	14	1020			7	
Corning / Morgan	MACOR	1000		345			1.53	
Morgan Advanced Ceramics	Cordierite	1000		88	500			
	Aluminosilicate glass-ceramics					950ºC, 15MPa: 1.7x10-8 s-1 (ref 5). Compressive, 1300ºC, 15MPa: 10-4 s-1 (ref 6)		

Manufacturer	**Product Name**	**Density (Fired) g/cm^3**	**Porosity (apparent) (%)**	**Thermal Expansion Coefficient (10E-6/°C)**	**Thermal Conductivity (W/m.K)**	**Specific Heat (J/kg.K)**	**Thermal shock (Delta °C)**	**Poisson's Ratio**
	Mullite					Tensile, 1300ºC, 15MPa: <10-8 s-1. At 45MPa: 3x10-8 s-1 (ref 1). Compressive, 1300ºC, 15MPa: 4.8x10-8 s-1 (ref 2)		

4.1.2.1 Silicon Nitride

Silicon Nitride (Si_3N_4) is a hard monolithic ceramic with excellent resistance to thermal shock, corrosion, chemical reaction and with excellent refractory properties. It is produced either from powder or directly via reaction bonding. If produced from powder, it can be hot pressed or sintered, giving Hot Pressed Silicon Nitride (HPSN) and Sintered Silicon Nitride (SSN). Si_3N_4 cannot be conventionally sintered owing to the decomposition of Si_3N_4 at 1850ºC (3350ºF); it must be liquid-phase sintered using small quantities of metal oxide additives to promote the formation of intergranular eutectic phases. Hot pressing reduces this problem, giving a purer product. Both HPSN and SSN are fully dense, and exhibit similar properties. Fully dense Si_3N_4 has similar strength to alumina but is tougher. It suffers many of the same drawbacks as alumina, such as vulnerability to creep, not least because of the existence of intergranular phases produced from sintering aids. However, it is markedly superior to alumina in thermal shock.

Reaction Bonded Silicon Nitride (RBSN) is manufactured by the infiltration of nitrogen gas into a silicon powder compact under high temperature. The process of nitriding causes ~20% volume expansion, however it is impossible to form fully dense, stoichiometric bodies via this process as the infiltrating gas must remain free to permeate. Thus, RBSN retains around 20% porosity, with a consequent reduction in strength and Young's modulus. RBSN also tends to contain small quantities of unnitrided silicon. However, since component volume change during nitriding is minimal owing to material expansion into the pore structure, and since silicon powder can easily be lightly compacted, RBSN can be formed as near-net or net-shape complex components.

Fully dense grades of Si_3N_4 have high thermal diffusivity. Thermal diffusivity is the ratio of a material's thermal conductivity to its specific heat capacity, and gives a measure of the rate of heat transfer through the material.

Silicon nitride is highly resistant to chemical attack across a wide range of temperatures and in a wide range of atmosphere. Nonetheless, Si_3N_4 will oxidize in atmospheres containing even small quantities of oxygen at temperatures above ~1300ºC (2350ºF), forming cristobalite and enstatite scales.

A literature search did not show any systematic study of the effect of neutron damage on Si_3N_4. Silica films at grain boundaries of SiC are prone to bubble formation; therefore, one may expect oxides at grain boundaries of Si_3N_4 to be similarly affected.

4.1.2.2 Alumina

Alumina is an extensively-studied and readily available material, manufacturable into finished parts via sintering and hot isostatic pressing. Many different grades of alumina are available, ranging from 80% pure to over 99.9% pure. Alumina powder is amongst the cheapest available ceramic powders, and produces exceptionally strong and chemically inert products. Alumina's weaknesses are, as previously mentioned, its vulnerability to creep and thermal shock. Alumina is also susceptible to reduction when in elevated temperature contact with reactive metals and in contact with carbon in a reducing atmosphere at temperature.

In terms of radiation damage, it is known that alumina swells by over 2% when neutron irradiated at 1000K; however, this work was undertaken at very high fluence of over 10^{26} n/m^2. For comparison, monolithic graphite fluence limits (turn-around from shrinking to swelling) are expected to be about $2x10^{26}$ n/m^2 at 1000K.

Fully dense grades of alumina have the highest thermal diffusivity of any commonly-available ceramic.

4.1.2.3 Zirconia

The use of pure zirconia (ZrO_2) is rare, given that it experiences two phase transitions on heating which on cooling produce such internal stresses in the material that it shatters. Zirconia is almost always used in a toughened form, in which small additions of other metal oxides (MgO, Y_2O_3) stabilize one of the crystal phases, minimizing this problem. Judicious use of these oxide additives can precipitate a dual-phase structure – generally tetragonal precipitates in a cubic matrix – in which the stress field of an approaching crack tip causes the transformation of the tetragonal precipitate to the cubic phase, with the associated volume increase causing a crack closing stress on the crack tip. This mechanism toughens the zirconia, meaning that it is the toughest of the monolithic ceramics.

The most common grades are, as discussed above, those stabilized with magnesia (MgO) or yttria (Y_2O_3). Yttria stabilization provides the highest toughness but these grades have limited temperature capability without losing the toughening mechanism – only around 200ºC can be tolerated. Magnesia stabilized zirconia can be used up to 1000ºC.

Zirconia is also famed for its resistance to wear, abrasion, and corrosion.

All forms of zirconia have comparatively low thermal diffusivity, given the material's low thermal conductivity and high density. Conductivity tends to decrease with increasing deviations from purity.

4.1.2.4 Silicon Carbide

Silicon Carbide (SiC) is in reality a broad term for a wide class of materials based around SiC. Like silicon nitride, it can be formed by a variety of methods: pressureless sintering of SiC powder; reaction bonding in which molten silicon is infiltrated into a graphite powder compact; Chemical Vapor Deposition (CVD) in which solid SiC is deposited onto a substrate directly from gaseous precursors.

CVD SiC is enormously expensive, very pure, and with such electrical and thermal properties that it is mostly used in the electronics industry. CVD SiC has thermal conductivity and diffusivity an order of magnitude higher even than alumina.

Industrial uses of SiC focus around sintered SiC and reaction bonded material (RBSC). These materials are exceptionally strong, creep resistant, and oxidation resistant, except as already described in the section on SiC/SiC composites.

4.1.2.5 Boron Nitride

Boron Nitride (BN) exists in two crystal forms: cubic (cBN) and hexagonal (hBN). cBN, also known as Borazon, is a well-known abrasive, one of the very tiny class of materials able to scratch diamond. cBN, however, is difficult and expensive to produce, and brittle. Thus, most engineering applications of BN are for the hexagonal form.

hBN, also known as 'white graphite', has the same layered atomic structure as graphite. As a result, it has a very high degree of anisotropy in thermal, electrical and mechanical properties, similar to graphite. For example, parallel to its atomic sheets (the 'a' direction), it exhibits a thermal conductivity two orders of magnitude higher than that perpendicular to the atomic sheets (the 'c' direction). In its strongest directions; however, it exhibits exceptionally high strength at elevated temperature.

Whilst polycrystalline hBN is available, the anisotropy of properties within single crystals reduces the integrity of this material drastically.

The greatest uses of hBN are in lubrication and molten metal working, owing to its excellent lubricity at high temperatures in oxidizing atmospheres and even in vacuum, and also owing to its high surface energy in contact with most molten metals. It is rarely used as a structural ceramic.

4.1.2.6 Fused Silica

Fused silica is a cheap, readily available refractory material exhibiting low strength and elastic modulus, but also low thermal conductivity and thermal expansion. It is manufactured by the sintering of silica powder.

The high-temperature creep rate of fused silica is very difficult to determine because the effect of creep is obscured at temperatures >1300ºC by the phase transition to cristobalite. Much of the as-produced structure of fused silica is quartz, which, along with cristobalite and tridymite, is a crystalline allotrope of SiO_2. However, quartz is denser than cristobalite, and it has been calculated that conversion of 6.5% of remnant quartz in fused silica to cristobalite causes volumetric expansion of 1%. This phenomenon means that prediction of the high-temperature viscoplastic deformation of fused silica is very problematic. At low stress levels and high temperatures fused silica can even be seen to expand parallel to a compressive stress axis.

One point that should be the subject of further investigation is that ballistic damage by incident neutrons is not the only mechanism of radiation damage in silica; there is a radiolytic damage mechanism (Ref. 8). Incident ionizing electromagnetic radiation can cause valence electron excitations in silica which, through affecting the covalent bonding, lead to Frenkel defects just as ballistic neutron damage does. Therefore, if silica is to be used, the complete radiation spectrum experienced by the relevant component must be considered.

4.1.2.7 Mullite

There are various chemical forms of mullite, which is a form of aluminosilicate material which is considered distinct enough to merit its own category. The most common engineering mullite composition is called ‘3:2 mullite’ because it consists of alumina and silica in the ratio 3:2, as $3Al_2O_3.2SiO_2$. This material, however, is not a mixture, nor a composite; it is a true compound.

Mullite, as discussed above in Section 4.1.3, exhibits very low creep, reasonable strength, and very good resistance to corrosion, to thermal degradation and to thermal shock. Mullite, being a simple combination of alumina and silica, is also a cost-effective material.

Data given for creep of mullite vary widely when compared to, for example, alumina. This is likely to be caused by the wide variety of different variables between different creep experiments: temperature, stress level, and stress sense in particular. By the most pessimistic measure, mullite is superior to alumina in creep by a factor of around 2. By other measures, as discussed previously, it can be superior to alumina in tensile creep by two orders of magnitude.

4.1.2.8 Glass Ceramics and Aluminosilicates

Glass-ceramics are a class of materials which could be described as heat-treatable glasses. The design intent behind glass-ceramics is that they be castable as amorphous glasses but then heat-treatable to produce crystalline phases. Commercially-available glass-ceramics focus around the reactive metal oxide/alumina/silica ternary phase system, with the two main candidates being magnesium aluminosilicate (MAS) and lithium aluminosilicate (LAS).

A major advantage of glass-ceramics is that by careful control of the composition, the thermal expansivity can be tailored over a wide range, from zero up to matching or exceeding nickel alloys.

LAS in particular is also highly refractory, exhibiting maximum use temperatures in excess of those for alumina ceramics, and is highly resistant to thermal shock and creep.

4.1.2.9 Insulation Materials

Products for insulation applications are likely to be based on fibrous blankets, or materials that contain a high volume fraction pore structure. Methods of producing a pore structure include the incorporation of hollow spheres in a matrix or the production of foamed ceramics with a tailorable volume fraction of porosity.

Commercially available insulation products are offered based on microporous insulation systems. These materials are used in the aerospace, power generation, steel and non-ferrous and glass industries at temperatures up to 1150°C and offer the lowest thermal conductivity at minimum dimensions. Suppliers of such product are Microtherm and Armil CFS.

A wide variety of fibrous blankets are offered for high temp insulation. These blankets are available commercially under a variety of trade names and can be made from alumina/silica fibers, needled ceramic fiber blankets (2300 – 2600°F), polycrystalline mullite fibers (3000°F), silica fibers (1800°F), or silica/magnesia fibers (2300°F) offering the temperature limits indicated. These ceramic fibers can also be formed into boards or blocks for insulation and hot face lining applications with similar temperature capabilities. Suppliers of such product are Armil CFS or Kitsons Thermal Supplies, but there is likely to be a large number of other suppliers in the network.

Whilst offering very low thermal conductivity, drawbacks of fibrous insulation are the poor mechanical integrity, the likelihood that dust will be produced and the degradation of thermal properties if fretting leads to breakdown in the structure of the blanket. It is conceivable that the microporous products that are offered as an alternative to fibrous insulation avoid these problems whilst still offering ~~a~~ thermal insulation and a compliant layer between structures to accommodate thermal expansion mismatches.

Provision of a detailed review of insulation materials is beyond the scope of this report, but it is recommended that further detailed investigations are performed.

4.1.2.10 Refractory Materials

A mature supplier base exists for the supply of refractory materials to a broad range industries that include metal production, power generation, petro-chemical, waste incineration and thermal processing. A cursory examination of the products available indicates that a broad range of refractory materials are offered for these applications, with material compositions being tailored to cope with resistance to molten metals, slags, glasses and a range of gaseous environments. The refractory materials therefore appear to offer good resistance to a range of aggressive environments. Details of mechanical and physical properties for the refractory materials are not readily available, but apart from chemical inertness these materials are characterized by a high degree of open porosity (10% to 20%) and are assumed to offer good thermal insulation.

Despite the lack of information on refractory materials provided in this report it is considered that these materials may offer a possible alternative to the engineering and fine ceramics described above in some of the nuclear reactor component applications. In addition to the ability of these materials to operate in aggressive high temperature environments other perceived benefits are likely to be the relatively low cost of these materials and the ability to make the large monolithic blocks required for some of the components. To this end it is recommended that further discussions are held with refractory suppliers to determine the strengths and weaknesses of these materials.

Provision of a detailed review of refractory materials is beyond the scope of this report, but it is recommended that further detailed investigations are performed.

4.1.3 Ceramic Composite Material Properties

Table 4-3 lists ceramic composite material properties. General material characteristic of composite materials, such as anisotropy, are listed in Appendix F. Material suppliers are listed in Appendix G.

4.1.3.1 Carbon / Carbon Composites

Carbon fiber-reinforced carbon (C/C) composites were developed in the 1960s and 1970s for the NASA Space Shuttle. They are a class of materials exhibiting similar characteristics and design intents to SiC/SiC composites, however with increased high-temperature strength retention but much reduced oxidation resistance compared to SiC/SiC. C/C composites have high thermal conductivity and good thermal shock resistance, yet low thermal expansivity.

There are two major routes for part fabrication in C/C composites: pyrolysis and graphitization, and CVI. In the first, parts are laid up using any of the techniques available to polymer matrix composites: filament winding, resin transfer molding, prepregging and so on. Subsequent pyrolysis causes thermal decomposition of the polymer resin which, when adequately controlled, leaves pure carbon. Further high-temperature heat treatment can result in the graphitization of the carbon deposit.

CVI of C/C composites involves the production of an empty fiber network within which carbon fibers are in the orientation in which they are intended to be in the final component. Acetylene (C_2H_2) or methane (CH_4) is then infiltrated into the fiber network under heat, causing the acetylene to decompose to give soot. Further heat treatment graphitizes the soot.

Table 4-3. Ceramic Composite Material Properties

Mat'l	Density	Conductivity			CTE	Tensile Strength	Fract Toughness	Use Temp	Fluence Limit		Codes & Stds	Comment
	g/cc	W/m.^{o}K	Temp C	Direction	$10^{-6}/^{o}C$	MPa	MPa-m$^{1/2}$	C	n/m^2	DPA		
C/C* FMI-222 3-D	1.48	160	21	In Pl		~175		2000	3.2E+26	4.00	ASTM, ASM. Industry Practice. Designer Responsibility.	Control Rod Life 8 years. Guide Tube Life 60 years. Cov Pl Life 60 Years
		100	800	In Pl		~175						
		93	1200	In Pl		~175						
		90	1600	In Pl		~175						
SiC/SiC Hi-Nicalon 2-D**	2.60	30	21	In Pl	4.5	150-300	20-30	1400	2.4E+27	> 30	ASTM, ASM. Industry Practice. Designer Responsibility.	Control Rod Life 60 Years.
		15	1000	In Pl		150-300	20-30					
		15	21	Trans Thickness	**4.5**	20-30						
		8	1000	Trans Thickness		20-30						
A/N720 (Ox/Ox)	2.61	4.21	21	In Pl	3.5	218	na	1150		na	industry Practice Owners Responsibility	COIC
		2.39	1200	“	6.0	“	“					
SiC/SiC (Ideal Matl)	2.6	9-35	21	In Pl	4.7	na	na	1200		na	“	“
		8-20	1000	“	na							

One of the complexities in the manufacture of C/C composites is the variation in properties, and especially neutron radiation resistance, of different types of carbon fiber. Carbon fibers are produced by two main methods:

- PAN Fiber: PAN stands for polyacrylonitrile, which is, in the case of a carbon fiber precursor, a slight misnomer – the resin used tends to be a copolymer the main component of which is acrylonitrile. To manufacture carbon fiber, PAN is drawn into filaments and paralyzed to give carbon. PAN fibers are made up of sheets of carbon atoms, similar to graphite, however these sheets are folded over each other randomly.

- Pitch fiber: pitch fiber is produced via a similar process, substituting pitch for PAN. This affects the crystallization kinetics during carbonization, and results in pitch fiber being composed of stacked flat graphene sheets, like graphite crystals. This tends to give pitch fiber a higher modulus but lower tensile strength than PAN fiber.

Crucially, the greater purity and crystallinity of graphitized pitch fiber leads to it having a much greater resistance to neutron damage than PAN fiber.

C/C composites, like graphite, oxidize rapidly at temperatures above ~600ºC in air or any oxidizing atmosphere. As with SiC/SiC, the presence of water severely exacerbates oxidation of C/C. Electrical contact between a C/C composite and steel will render even stainless steel more susceptible to corrosion than normal. Carbon/carbon itself is very resistant to chemical corrosion. Providing a non-oxidizing atmosphere can be maintained and electrical contacts between parts properly designed, C/C composites exhibit enormous high-temperature capability.

4.1.3.2 Silicon Carbide / Silicon Carbide (SiC/SiC) Composites

SiC/SiC composites are a class of material incorporating SiC fiber reinforcement within a SiC matrix. Monolithic SiC is an exceptionally hard, durable material that is very resistant to corrosion and to the degradation of its properties at high temperatures. However, it suffers severely from the drawback of many ceramics in that it has very low toughness and so is, in its monolithic form, not suitable for structural applications. The reinforcement of a SiC matrix with SiC fiber is intended to improve the fracture toughness and impact properties by crack diversion.

SiC/SiC composites have excellent resistance to thermal shock, very high thermal conductivity, and a moderate thermal expansion coefficient when compared to alumina.

SiC/SiC composites can be manufactured by a variety of methods. Each method relies upon the prefabrication of the preform of SiC fiber reinforcement. Once this is done, the SiC matrix must be produced within the reinforcement. There are several methods for this:

- Chemical Vapor Infiltration (CVI): Invented by Roger Naslain at the University of Bordeaux, CVI produces the purest, most stoichiometric and most crystalline SiC matrix. It relies on the infiltration of a mixture of methyltrichlorosilane ($Si(CH_3)Cl_3$) gas into the SiC fiber preform, then slow decomposition of the $Si(CH_3)Cl_3$ to SiC under heating. The SiC thus formed is deposited from the gas phase onto the SiC fiber preform. CVI is the most expensive and slowest manufacturing method for SiC/SiC composites

- Melt Infiltration (MI): MI uses a different chemical route to achieve the formation of a SiC matrix. SiC fibers are laid up within a polymer resin, often in prepreg sheets. Following this, the SiC/polymer composite is paralyzed in a high-temperature furnace to convert the matrix to carbon. Molten silicon, or occasionally a silicon alloy, is then infiltrated into the porous carbon matrix, reacting with the matrix to produce a SiC matrix. However, full reaction is not achieved and free silicon and carbon remain in the composite.

- Polymer Infiltration and Pyrolysis (PIP): The PIP process involves soaking a fiber preform or powder compact with a liquid polymer precursor that converts to ceramic material upon pyrolysis. Pre-ceramic polymers are available that form silicon carbide, silicon nitride, silicon oxycarbide, and silicon oxynitride. Stoichiometric SiC produced by this method is claimed to have good thermal stability to 1900°C in air.

SiC fibers can be crystalline or amorphous, and can vary fairly widely from the ideal 1:1 Si:C atomic ratio. The current major manufacturers and brands are UBE Tyranno, Nippon-Carbon’s Nicalon™ and Hi-Nicalon™ ranges, and Dow-Corning’s Sylramic™ fiber. These fibers can be formed by a CVD process or derived from polymers using complex curing and pyrolysis steps to produce the desired properties. The polymer derived fibers generally contain nanocrystalline β-SiC grains and it is possible for carbon, oxygen and an amorphous phase to be present in varying amounts depending on the fiber. Sintering aids such as titanium, boron and aluminum are also added to some fibers giving rise to the formation of secondary phases such as TiB_2 in the Sylramic fiber or Al_2O_3 in the LOX formed Tyranno fiber.

For nuclear applications, it is known that the degradation of SiC in a neutron flux is badly affected by deviation from a stoichiometric composition, especially in favor of excess carbon. Evidently then stoichiometric fiber is preferred. In the Tyranno and Nicalon™/Hi-Nicalon™ ranges there are both near-stoichiometric fibers and fibers with excess carbon – near-stoichiometric grades include Tyranno-SA and Hi-Nicalon™-S. Sylramic™ fiber is near-stoichiometric. It has been found in the literature however that in some of these fibers the stoichiometry is only skin-deep, and that in the centre of the fibers excess carbon still exists. Carborundum formerly manufactured an alpha-SiC fiber that avoided this problem, but have discontinued this.

Extensive research has been conducted at ORNL into the effects of neutron irradiation on Hi-Nicalon™, Hi-Nicalon™ Type-S and Sylramic™ fibers. The essential conclusion is that Sylramic™ is the poorest fiber in terms of radiation swelling and in terms of the degradation of mechanical properties following neutron irradiation. It is postulated that a contributory factor to this is that Sylramic™ fiber contains boron, which, under neutron irradiation, transmutes to helium (Refs. 9 & 10).

Adherence to stoichiometry and increased crystallinity also improve the thermal stability of the fibers, with grades such as Sylramic™ exhibiting maximum use temperatures of 1400°C.

The natural thermal oxide of SiC is SiO_2, which tends to form a scale on the SiC surface under highly oxidizing conditions. The oxidization of SiC is strongly promoted by the presence of water vapor in the atmosphere. In atmospheres containing high water vapor content, the protective SiO_2 layer reacts with the H_2O to form $Si(OH)_4$ which is volatile. In these circumstances the SiC is not protected and continued oxidation leads to recession of the substrate.

4.1.3.3 Oxide / Oxide Composites

Oxide/Oxide Composites are a wide class of materials where metal oxides are used both for the reinforcing fibers and the matrices. The variety comes from the breadth of different oxides available for both purposes, each with different properties. For example, fibers can be manufactured from yttrium aluminum garnet (YAG), single- or poly-crystalline alumina, yttria, zirconia-toughened alumina (ZTA), mullite, and any of the various forms of alumina/mullite combination. Matrices are even more diverse including all of the above plus spinels, beryllia, calcia, thoria and so on. Each of these fibers and matrices has its own properties, and the various possible combinations produce such a variety of properties that a full discussion would be a fitting subject for a sizeable textbook.

This report, therefore, will select oxides as if they were monolithic based on desirable properties and will then deal with various fiber/matrix combinations of these. It should be noted that the only oxide/oxide CMC systems which is currently fully commercially available are Nextel™/Alumina systems.

Alumina offers desirable strength properties, and is very readily available. It is, however, chronically susceptible to creep and thermal shock in its pure form. Further comparative statements are made relative to the performance of high-purity alumina below.

Mullite ($3Al_2O_3.2SiO_2$) and YAG are of interest because they exhibit the lowest available creep rates; however, the trade off is decreased strength and modulus relative to alumina.

Alumina/Mullite combinations are of interest, especially as fibers, owing to their useful combination of strength and creep resistance.

ZTA is of interest for its combination of strength and creep resistance.

The principal supplier of Alumina and Alumina/mullite fibers is 3M, supplying through their Nextel™ range. 3M have expended a great deal of effort trying to overcome alumina's poor creep performance, culminating in Nextel™ 610 and 720 fibers. 610 is an yttria-doped alumina fiber and 720 is an alumina/mullite fiber. 720 fiber is ~2 orders of magnitude superior to 610 fiber in creep, but has a lower tensile strength. Nextel™ 650 is a new ZTA fiber, demonstrating creep rates 2 orders of magnitude lower than Nextel™ 610 whilst maintaining strength.

Standing far out ahead of all forms of alumina or mullite in creep performance is YAG fiber, for which there is currently no commercial manufacturing route. YAG fiber of suitable diameters for weaving has been fabricated in laboratories, but manufacturing defects currently reduce its strength to unacceptable levels (~1 GPa / 145 ksi).

The property advantages of the fiber materials discussed above hold equally when the same materials are discussed as matrices. However, cost and processability also become issues to be considered. YAG, for example, remains an attractive material based on properties alone, but at ~$1M/ton, it is not cost-effective.

The best oxide/oxide composite for high temperature strength, creep resistance, thermal shock resistance and cost effectiveness would therefore currently be a Nextel™ 720/mullite composite; however, Nextel™ 650 may increase in availability and may be considered superior for its strength characteristics. In the future, YAG/mullite composites may well be available which will be superior.

All oxide ceramics, but of those considered especially mullite, are affected by alkalis at high temperature. For example, mullite exposed to sodium nitrate at temperatures around 1000ºC will form a porous scale at a rate of 10 microns/hr. Beyond reactions with strong acids and alkalis, most metal oxides are very inert. Some more complex oxides, such as aluminum titanate, can decompose to simpler oxides at high temperature. In the case of aluminum titanate the decomposition products are alumina and titania above 1250ºC.

Being oxides already, oxides do not oxidize. However, recession of oxides can take place at much reduced rates compared to SiC in high temperature environments containing water vapor (Ref. 11). The principal environmental interactions are with themselves, in that ceramic compositions that are not purely stoichiometric tend to change structure at very elevated temperatures. For example, aluminum-rich mullite phases can precipitate alumina and a silicon-rich mullite. Good ceramic system design such as is present in most modern engineering ceramic systems avoids this.

4.1.3.4 Mixed Fiber / Matrix Combinations

As well as the composite materials described above, it is also feasible to manufacture composites that are mixed fiber and matrix combinations. For example, a mixed system that is commercially available is based on carbon fibers in a silicon carbide matrix. Other mixed systems that have been investigated in the past are silicon carbide fibers in an alumina matrix. Issues that are described above for fibers and matrices are likely to be equally applicable to these mixed systems.

4.2 Material Limits

The purpose of this subsection is to list the selected candidate materials and their limits for comparison with design requirements.

4.2.1 Metallic Material Limits

Typical metallic materials for high temperature nuclear applications are Alloy 800H, Hastelloy X, Hastelloy XR, Inconel 617, and Haynes Alloy 230.

Table 4-4 shows the limits for temperature and fluence for the various metallic materials. Cobalt content is also a discriminator due to activation and subsequent transport of radioactive cobalt throughout the coolant loop.

4.2.2 Monolithic Ceramic Material Capabilities and Limits

Table 4-5 shows the limits for temperature and fluence for the various monolithic ceramic materials considered in this study.

Table 4-4. Metallic Material Capabilities and Limits

Material	Temperature Capability				Cobalt Content		Neutron Fluence Limit			Comment
	C	F	S_o KSI	Codes & Standards	%	Use In n-Irradiation Environment?	n/m^2 (HTGR Spectrum)	dpa	Codes & Standards	
Alloy 800H	760	1400	3.6	ASME Sect III, Div 1	2.0	Yes	$3.0x10^{22}$	0.00246	Owners Responsibility. At least 10% Ductility.	Fluence of $3x10^{22}$ is all thermal energy. High energy neutrons don't have significant effect.
"	816	1500	2.0	Push Beyond Code & validate performance by test.	"	"	"	"	"	Might be useful at 1500°F (816°C) for thermal barrier cover plates and fasteners.
Inconel 617	982	1800	12.8	ASME Sect VIII, Div 1	10 to 15	No. Cobalt too high	$3.0x10^{22}$	0.00246	Owners Responsibility. At least 10% Ductility.	Eliminated because cobalt is too high.
Hastelloy X	899	1600	1.3	ASME Sect VIII, Div 1	0 to 1.0	Yes	"	"	"	Can use up to 1600°F (871°C)
"	927	1700	?	Push Beyond Code & validate performance by test.	"	"	$3.0x10^{22}$	0.00246	Owners Responsibility. At least 10% Ductility.	Eliminated for use at 1700°F (927 °C) because strength too low.

Material	Temperature Capability				Cobalt Content		Neutron Fluence Limit			Comment
	C	F	S_o KSI	Codes & Standards	%	Use In n-Irradiation Environment?	n/m^2 (HTGR Spectrum)	dpa	Codes & Standards	
Mitsubishi Hastelloy XR	899	1700	?	Not In Code. Complete code work.	“	“	$3.0x10^{22}$	0.00246	Owners Responsibility. At least 10% Ductility.	Eliminated for use at 1700°F (927 °C) because strength too low.
Haynes 230	982	1800	~ 0.8	ASME Sect VIII, Div 1	5.0	No. Cobalt too high	$3.0x10^{22}$	0.00246	Owners Responsibility. At least 10% Ductility.	Eliminated because Cobalt too high.

Table 4-5. Monolithic Ceramic Material Capabilities and Limits

Material	Density	Conductivity		CTE	Bend Strength	Use Temperature		Codes & Stds	Neutron Fluence Limit			Ref No.	Comment
	g/cc	k W/m.^{o}K	Temp C	$10^{-6}/^oC$	MPa	C	F		n/m^2 (HTGR Spectrum)	dpa	Codes & Stds		
Kaowool In helium (For Ref Only)	na	0.11	21	na	na	1000	1832	Industry practice. Owner's responsibility.	Unavail	Unavail	Owners Responsibility	7	Data from CEA experiments in 1970s.
	na	0.65	982	na	na	1000	1832	“	“	“	“	7	“
Fused Silica GA	2.01	0.72	400	0.8	14.0	1000	1832	ASTM, ACMAASTM, ACMA Industry Ceramic Design Practice for Brittle Mat'ls Owners Responsibility.	“	“	“	8	Data from Large HTGR program tests
	2.01	1.13	850	0.8	16.0	“	“	“	“	“	“	8	
Fused Silica GA	1.68	0.09	21	0.5	125	1000	1832	“	“	“	“	“	
Alumina-fully dense	3.75-3.95	25.6-30	21	7.9	310	1500	2732	“	“	“	“	20	Morgan Adv Ceramics
	“	12.5	400	8.75								“	“
Alumina (A479SS) 99.5%	3.9	32	21	7.2	360	1600	2912	“	“	“	“	21	Kyocera
Zirconia Toughened Alumina (ZTA)	4.32	20	21	8.3	430	NAa	NA	“	“	“	“	20	Morgan Adv Ceramics
MgO Stabilized Zirconia (Z2500)	5.6	2.5	21	10	500	1000	1832	“	“	“	“	20	Morgan Adv Ceramics

Material	Density	Conductivity		CTE	Bend Strength	Use Temperature		Codes & Stds	Neutron Fluence Limit			Ref No.	Comment
	g/cc	k W/m.°K	Temp C	10^{-6}/°C	MPa	C	F		n/m^2 (HTGR Spectrum)	dpa	Codes & Stds		
Zirconia (Z-220)	5.6	na	na	10	750	na	na	Owners Responsibility	na	na	Owners Responsibility	21	Kyocera
Hexaloy SA SiC	3.1	103	200	4.02	380	1900	3452	“	“	“	“		St.Gobain Ceramics
Hexaloy SP SiC	3.04	110	21	4.2	240	1900	3452	“	“	“	“		St.Gobain Ceramics
Silicon Carbide (SC 211)	3.2	60	21	4.4	540	1200	2192	“	“	“	“	21	Kyocera
Silicon Carbide	2.9	35-124	200	4.8	80-400	1300	2372	“	“	“	“	20	Morgan Adv Ceramics
Cordierite	2.4	2	21	3.0	88	1000	1832	“	“	“	“	20	Morgan Adv Ceramics
		3	400										
Aluminum Silicates	2.7	4.5	200	3.0	64	1150	2102	“	“	“	“	20	Morgan Adv Ceramics
Fused Silica	1.7	0.9	21	0.5	125	1000	1832	“	“	“	“	20	Morgan Adv Ceramics
RBSN	2.5	12	21	3.1	200	1300	2732	“	“	“	“	20	Morgan Adv Ceramics
SSN	3.2	15	21	3.3	650	1000	1832	“	“	“	“	20	Morgan Adv Ceramics
Silicon Nitride (SN-240)	3.3	27	21	3.3	1020	1200	2129	“	“	“	“	20	Morgan Adv Ceramics
Macor	2.52	1.46	21	11.4	345	1000	1832	“	“	“	“	20	Coming & Morgan Adv Ceramics

4.2.3 Ceramic Composite Material Limits

Table 4-6 shows the limits for temperature and fluence for the acceptable ceramic composite materials. Materials without irradiation data were omitted from consideration.

Table 4-6. Ceramic Composite Material Capabilities and Limits

Mat'l	Density	Conductivity			CTE	Tensile Strength	Fract Tough	Use Temp	Fluence Limit		Codes & Stds	Comment
	g/cc	W/m. ^{o}K	Temp C	Direction	$10^{-6}/^{o}C$	MPa	MPa-m$^{1/2}$	C	n/m^2	dpa		
C/C* FMI-222 3-D	1.48	160	21	In Pl		~175		2000	3.2E+26	4.00	ASTM, ASM. Industry Practice. Designer Responsibility.	Control Rod Life 8 years. Guide Tube Life 60 years. Cov Pl Life 60 Years
		100	800	In Pl		~175						
		93	1200	In Pl		~175						
		90	1600	In Pl		~175						
SiC/SiC Hi-Nicalon 2-D**	2.60	30	21	In Pl	4.5	150-300	20-30	1400	2.4E+27	> 30	ASTM, ASM. Industry Practice. Designer Responsibility.	Control Rod Life 60 Years.
		15	1000	In Pl		150-300	20-30					
		15	21	Trans Thickness	**4.5**	20-30						
		8	1000	Trans Thickness		20-30						

5 MATERIALS SELECTION EVALUATION

The basis for the selection of materials for the various reactor core and internals components is explained in this section. A component-by-component evaluation is presented based on materials that meet the design requirements in Section 3 above. The following is a list of the materials selected for each component.

Component	Structural Material	Insulator Material
Control Rod Structural Elements	C/C Composite SiC/SiC long term	na
Control Rod & RSM Guide Tubes	C/C Composite	na
Upper Core Restraint	C/C Composite	na
Upper Plenum Shroud Thermal Barrier	C/C Composite	Ceramic blocks
PSR Seal Sleeves	Graphite	na
Metallic Core Support Load Bearing Insulators	Monolithic Ceramic	na
Hot Duct Thermal Barrier	C/C Composite	Ceramic blocks
Cross Vessel Thermal barrier	Metal - Alloy 800H	Fibrous Blankets
Lower Plenum Sidewall Thermal Barrier	C/C Composite	Ceramic blocks
SCS Gas Entrance Tubes	C/C Composite	Ceramic blocks
SCS Heat Exchanger Thermal Barrier	Metal - Alloy 800H	Fibrous Blankets

The material evaluation and selection are summarized in Table 5-1. The individual sections that follow this summary explain in detail the basis for the choices of materials on a component-by-component basis. The issues that need to be addressed and the technology development activities needed to bring the component to the technology readiness level needed to complete the design and initiate fabrication are defined for each component.

Table 5-1. Reactor Internal Materials Selection Summary

Component	Design Life	Normal Op Design Temp		Off-Normal Design Temp		Temp Limit	Design Fluence		Fluence Limit		Mat'l Selection	Remark
		C	F	C	F		n/m^2	dpa	n/m^2	dpa		
Control Rod	8y Replaceable	905	1631	1500	2732	> 2000C	3.22E+26	4.00000	3.22E+26	4	C/C Composite	Norm Op & CCD Temp to high for metal structure. Fluence to high. SiC/SiC Alternate for longer life. CR Replaced every 8 years or sooner if needed.
Control Rod & RSM Guide Tube	60y Replaceable. Can be less than 60y	583	1081	989	1812	> 2000C	1.03E+23	0.00128	3.22E+26	4	C/C Composite	Norm Op Temp O.K. for Alloy 800H. Fluence to hi for 60-y life if metal. O.K. for compos. Off-Norm Temp to high for metals. Must use compos. Replaceable component. Life can be less than 60y.
Upper Core Restraint	60y Replaceable. Can be less than 60y	553	1027	1094	2001	> 2000C	3.49E+24	0.04340	3.22E+26	4	C/C Composite	Norm Op Temp O.K. for Alloy 800H. Fluence to hi for 60-y life if metal. O.K. for compos. Off-Norm Temp to high for metals. Must use compos. Replaceable component. Life can be less than 60y.
Upper Plenum Shroud T/B Cov Plates and Hw	60y	541	1006	926	1699	> 2000C	1.20E+22	0.00098	3.00E+22	0.002 46	C/C Composite	C/C a safe choice. Hast x close. Investigate Hast X further. Off-Normal Temp to high for Hast X.
Permanent Side Reflector Seal Sleeves	60y	602	1116	743	1369	2400C	3.22E+24	0.04340	4.00E+26	5	Graphite	Temps low for Compos. Dowel & Socket connection function preserved. Graphite preferred in this application. Compatible with reflector environment. Make blocks longer & control tolerances to minimize flow leakage.

Component	Design Life	Normal Op Design Temp		Off-Normal Design Temp		Temp Limit	Design Fluence		Fluence Limit		Mat'l Selection	Remark
		C	F	C	F		n/m^2	dpa	n/m^2	dpa		
Metallic Core Supt Load Bearing Insulators	60y	860	1580	860 Temp Drops Exponentially.	1580	1250C	8.50E+21	0.00011	?	?	Top- Alumino Silicate Ceramic	Composites not needed. Solid Ceramic. Alumina top. Fused Silica bottom.
	60y	653	1207	653 Temp Drops Exponentially.	1207	1000C	8.50E+21	0.00011	?	?	Bottom- Macor Glass Ceramic	
Hot Duct T/B Assy	60y	949 MM 1174 HS	1740 MM 2145HS	949 720-50Hr 700-450hr	1740 1328-50hr 1292-450hr	> 2000C	8.50E+21	0.00011	3.22E+26	4	C/C Composite	Norm Op & Transient Temps to hi for metals Hot streak temps preclude metals. Off-Norm Temp declines. Fluence so low no problem.
Cross Vessel T/B Assy	60y	589	1092	589 Drops Exponentially.	1092s Exponentially	1400F	8.50E+21	0.00011	3.22E+26	4	800H	Temps low enough to allow use of 800H.
Lower Plenum Sidewall T/B Assy	60y	877 MM 1127 HS	1611 MM 2061 HS	877 720-50Hr 700-450hr	1611 1328-50hr 1292-450hr	> 2000C	8.50E+21	0.00011	3.22E+26	4	C/C Composite	Norm Op & Transient Temps to hi for metals Hot streak temps preclude metals. Off-Norm Temp declines. Fluence so low no problem.
SCS Entrance Tubes	60y	949 MM 1199 HS	1710 MM 2160 HS	949 Temp Drops Exponentially	1710 Temp Drops Exponentially	> 2000C	8.50E+21	0.00011	3.22E+26	4	C/C Composite	Normal Op Hot Streak Temp to Hi for metals.
SCS HX T/B Assy	60y	580	1076	580 Drops Exponentially	1076 Drops Exponentially	1400F	8.50E+21	0.00011	3.00E+22	0.00246	Alloy 800H	Norm Op & Off Norm Temp O.K. for Metals. Fluence O.K.

5.1 Control Rods

The control rods are located in two general areas of the reactor core. There is a circle near the inner boundary of the fuel and central replaceable reflector elements (12 rods). There is another circle near the outer boundary between the fuel and outer replaceable reflector reflectors (18 rods) as shown in Figure 5-1. The outer control rods are used to control the power in the core and are inserted during normal operation. The inner rods are withdrawn during normal operation and are only used to shut down the nuclear reaction. There are six inner and six outer reserve shutdown columns with a channel for insertion of boronated graphite pellets in the unlikely event that the control rods cannot be inserted.

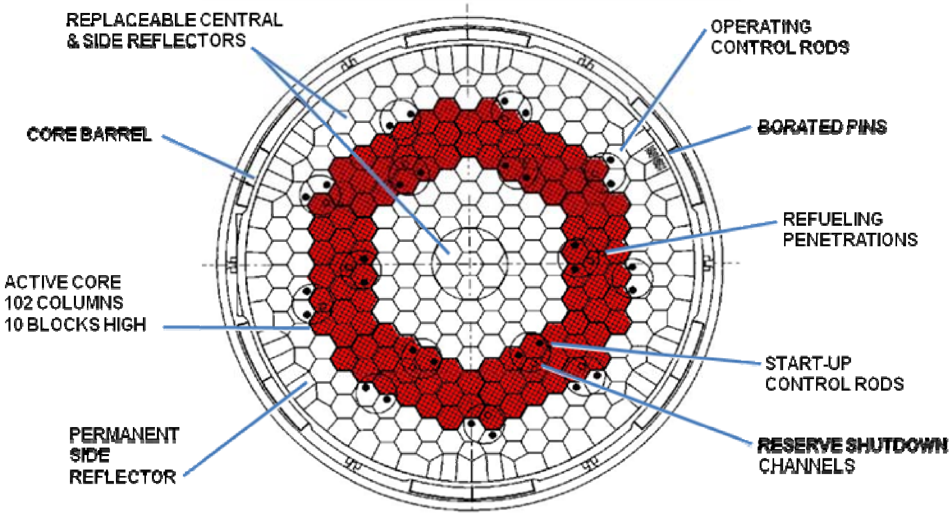

Figure 5-1. Cross-section of reactor core

The control rod is shown in Figure 5-2. It is a linear assemblage of rigid links filled with boronated graphite compacts within a cylindrical sleeve. Flexibility of the rod assembly is accommodated by the joints between rigid links. The sleeves and joints are the structural elements that contain the nonstructural absorber compacts and transfer the operational loads to the control rod drive. All control rods are identical to accommodate interchangeability. Figure 5-2 shows the structural elements that contain the boronated graphite neutron absorber compacts. The dimensions are in mm. Some control rod designs do not have a central spine and rely on the sleeve and connections for load carrying capability. The final configuration of the control rods will be determined in the final design phase.

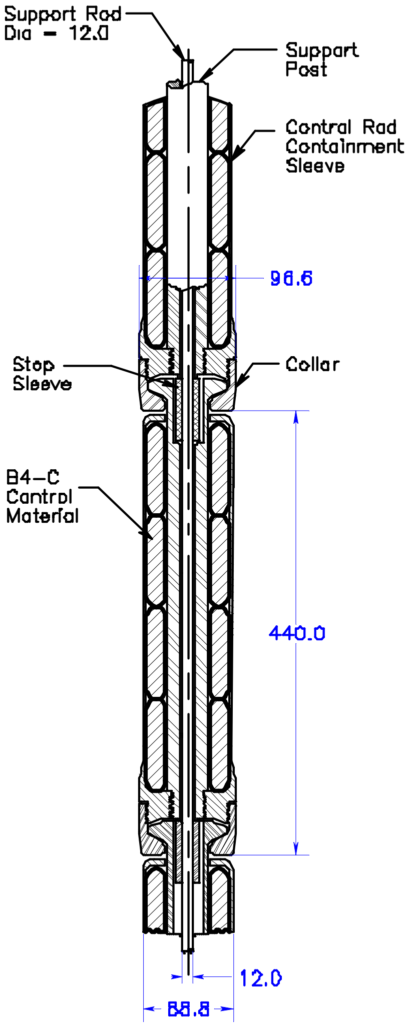

Figure 5-2. NGNP control rod

Maximum control rod temperatures during normal operation and during CCD events are given in Tables 5-2 and 5-3, respectively. During a scram, all the control rods are inserted into the core. If, in addition to the scram, a loss of forced circulation of the primary coolant occurs, then the already inserted control rods will increase in temperature during the CCD transient as shown in Figures 5-3 and 5-4.

Table 5-2. Control Rod Maximum Steady State Temperatures

Location	Max Temp (Inlet 490°C) (C)	Max Temp (Inlet 590°C) (C)	Z (m)*
Top of Core	514	606	9.491
Core Mid Height	706	759	5.746
Bottom of Core	895	906	1.786
*Z(m) is the distance in meters from a reference point below the bottom of the core as defined in Ref. 4			

Table 5-3. Control Rod Maximum Temperatures during CCD Events

Location	Pressurized CCD Event		De-pressurized CCD Event	
	490°C Core Inlet (C)	590°C Core Inlet (C)	490°C Core Inlet (C)	590°C Core Inlet (C)
Bottom of Core	1273	1500	1474	1236

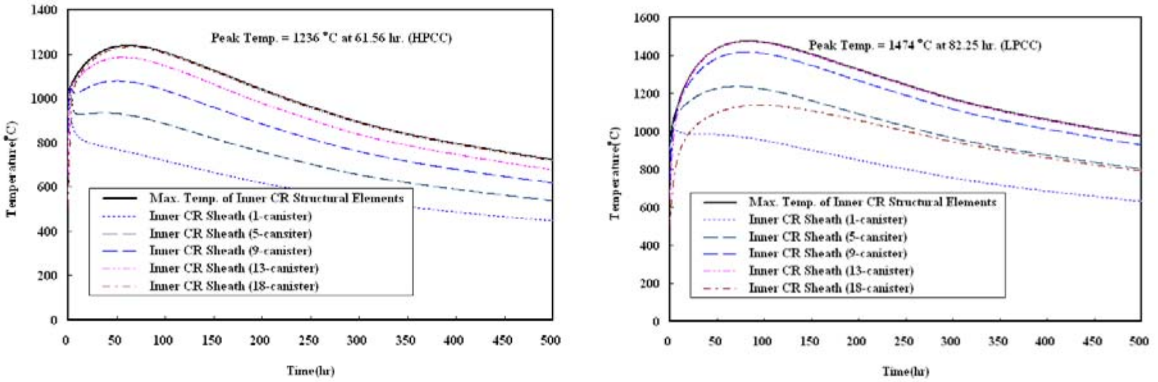

Pressurized Conduction Cool Down
Peak Temp = 1236°C

De-pressurized Conduction Cool Down
Peak Temp = 1474°C

Figure 5-3. Control rod temperatures for CCD transients with T_{in} of 490°C

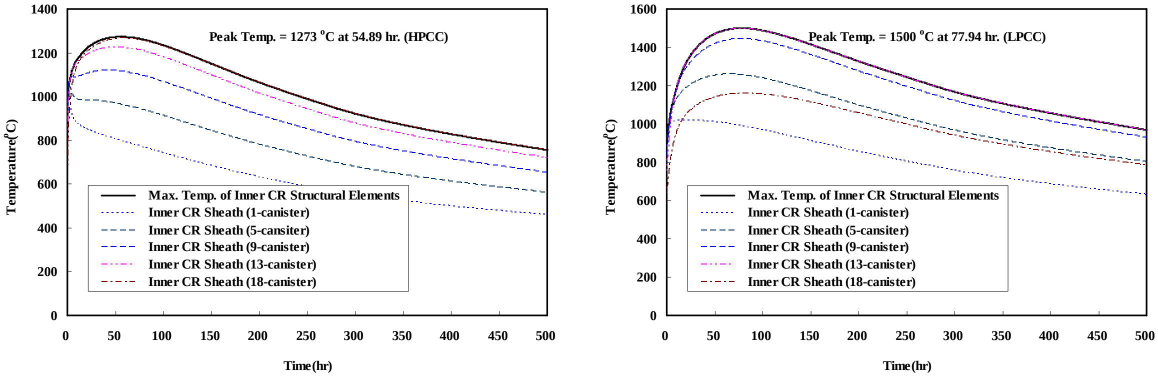

Pressurized Conduction Cool Down
Peak Temp = 1273°C

De-pressurized Conduction Cool Down
Peak Temp = 1500°C

Figure 5-4. Control rod temperatures for CCD transients with T_{in} of 590°C

The neutron fluence that the control rods experience varies depending on the location in the reactor core. The outer control rods experience the largest fluence because they are inserted throughout power operation to control the reactor. The inner rods are only inserted during shutdown. However, the inner control rods experience the highest temperatures during a CCD event. All control rods are interchangeable, so they are designed to meet a combination of the worst conditions. The highest total neutron fluence is 3.2×10^{26} n/m^2, or 4.0 dpa (taken from Tables 3-3 and 3-6). It takes 8 years of operation to accumulate this fluence. It is planned to replace the control rods at that time to refresh the boronated graphite absorbers.

Metallic control rods may not withstand this fluence, and they cannot withstand the conduction cool down temperatures in the inner circle positions. SiC/SiC composites have the capability to withstand this fluence quite easily with a fluence limit (see Table 4-6) greater than the lifetime fluence for 60 years of reactor operation. However, the SiC/SiC composites have a temperature limit of 1400°C. Thus, they will not meet the maximum conduction cool down temperature of 1500°C. C/C composites will just meet the 8-year life of the control rods, but they will easily meet the maximum design temperature because C/C has a temperature limit greater than 2000°C. Therefore, the control rods should be fabricated from C/C composites to meet the combined conditions.

No data was found in this study on corrosion of C/C composites in a helium environment with the reactor coolant design impurities shown in Table 3-4. Therefore, this is an issue that must be addressed in the technology development program. There is a need for corrosion data to validate the life of C/C composite materials in the NGNP reactor environment.

The control rod sleeve components receive the highest radiation dose of any components in the scope of this study, $5.5x10^{25}$ nm^{2}. Also, this component receives the highest temperature considered in this study, 1500°C during a pressurized CCD event.

It should be noted that there is no manufacturable material that is not subject to creep at these temperatures, and therefore the design must consider the unavoidable viscoplastic effects on the control rod. However, it is anticipated that the duration of any transient temperature increases will be short enough for creep not to be a problem.

The control rod sleeves vary in cross section; therefore, the best option appears to be that control rod sleeves and support posts be manufactured from filament- or tape-wound fiber-reinforced carbon-based composites, either C/C or SiC/SiC. The neutron fluence is near the limit of that acceptable for C/C, but given the superior high-temperature strength retention of C/C composites and the 8-year component life, coupled with the 1-2 order of magnitude cost increase to move to SiC/SiC, C/C composite appears to be the best option. The choice of fiber reinforcement and the degree of graphitization of the matrix are likely key to the resistance of the component to the neutron radiation.

It is recommended that the SiC/SiC composite option be pursued as a backup to C/C composites because it may be possible to use the SiC/SiC at 1500°C. The control rod life and reliability would be greatly enhanced with this option.

5.2 Control Rod & Reserve Shutdown Material Guide Tubes

The control rod (CR) guide tubes functions to assure that the control rods enter the reactor core when lowered by the control rod drives. The reserve shutdown material (RSM) guide tubes function to assure that the boronated graphite pellets can be dropped into the RSM core channels in the event that the control rods do not insert on command. These simple tubes span the gap in the upper plenum between the CR and RSM drives and the top of the core. They have a telescoping feature to accommodate differential movement between the top of the reactor core and the control rod drives. They have holes in the sidewall of the tubes that meter helium coolant past the control rods to maintain acceptable temperatures of the CR structural elements. The guide tubes insert into the top of the fuel columns at an engineered interface with the upper core restraint (UCR) blocks. They must accommodate the motion of the design basis earthquake and still ensure insertion of the control rods or the RSM pellets. A 60-year design life is desirable, but not required, since they are easily removed and replaced during refueling if necessary.

A typical guide tube and its interface with the UCR block are shown in Figure 5-5.

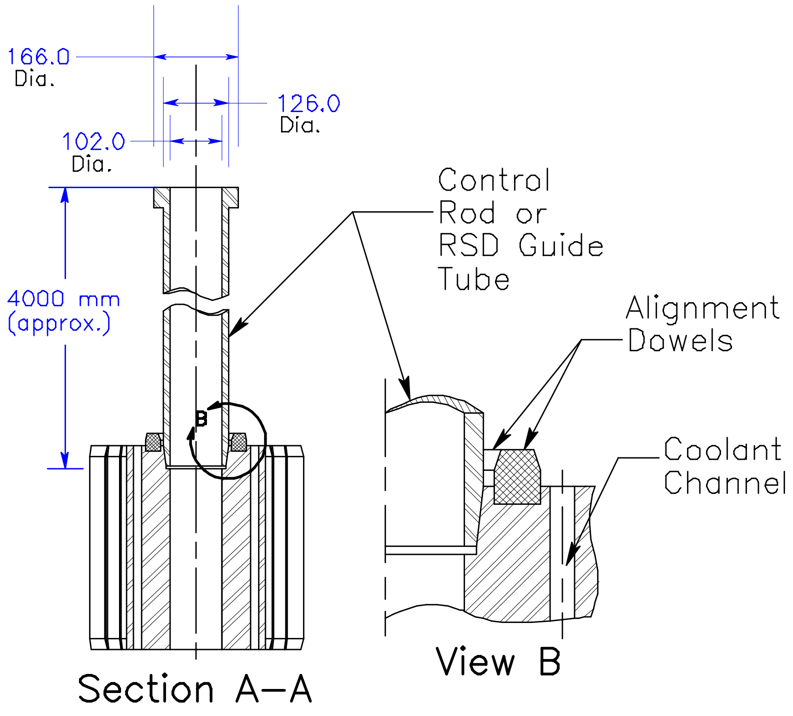

Figure 5-5. Control rod and RSM guide tube interface with upper core restraint blocks

Control Rod and RSM guide tube steady state temperatures are shown in Table 5-4 (Ref. 4). The transient temperatures for pressurized and de-pressurized CCD events are shown in Table 5-5 and Figures 5-6 and 5-7.

Table 5-4. CR & RSM Guide Tube Maximum Steady State Temperatures

Location	**Temp (490°C Inlet) (C)**	**Temp 590°C Inlet (C)**	**Z (m)**
Top of Guide Tube	331	365	16.01
Mid Height of Guide Tube	335	371	13.64
Bottom of Guide tube (Top of Reactor Core)	486	584	11.74

Table 5-5. CR & RSM Guide Tube Maximum Temperatures during CCD Events

Location	Pressurized CCD Event		De-pressurized CCD Event	
	490°C Core Inlet (C)	590°C Core Inlet (C)	490°C Core Inlet (C)	590°C Core Inlet (C)
Bottom of Guide tube (Top of Reactor Core)	974	989	533	584

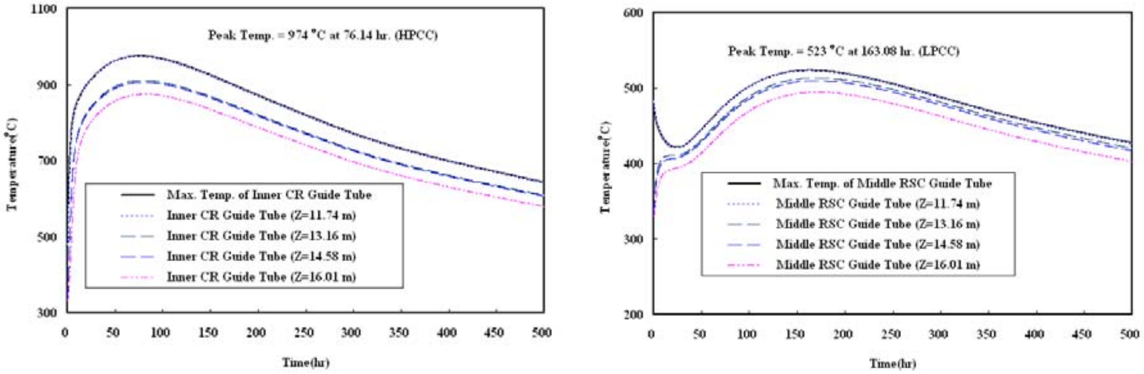

Pressurized Conduction Cool Down
Peak Temp = 974°C

Depressurized Conduction Cool Down
Peak Temp = 523°C

Figure 5-6. CR & RSM guide tube temperatures for CCD transients with T_{in} of 490°C

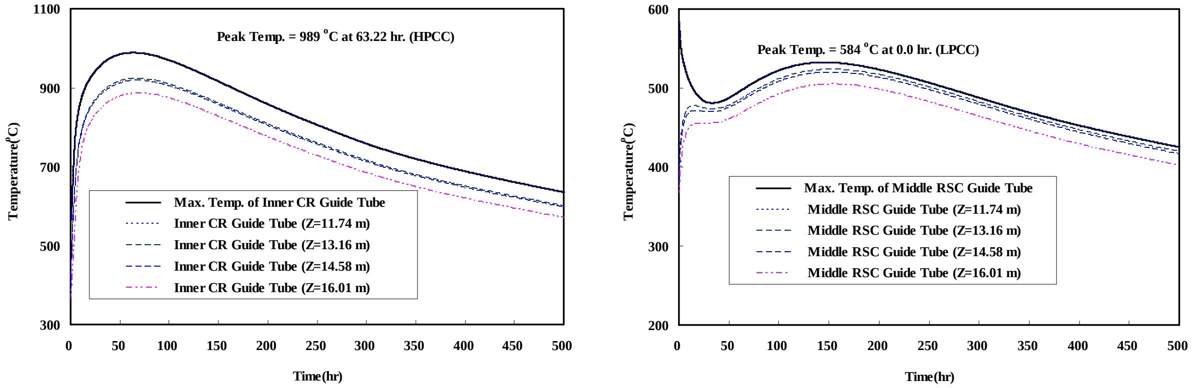

Pressurized Conduction Cool Down
Peak Temp = 989°C

Depressurized Conduction Cool Down
Peak Temp = 584°C

Figure 5-7. CR & RSM guide tube temperatures for CCD transients with T_{in} of 590°C

The neutron fluence that the CR and RSM guide tubes experience vary depending on the location above the reactor core. The fluence is quite low in the upper plenum due to neutron shielding surrounding the reactor core. The CR and RSM tubes experience a maximum fluence of $1.03x10^{23}$ n/m^2, or 0.00128 dpa. The guide tubes are subjected to a maximum temperature of about 583°C during normal operation. This fluence and temperature would allow the tubes to be fabricated from alloy 800H. However, the temperature of the tube reaches a maximum of about 989°C during a pressurized CCD event, which is substantially above the allowable temperature of any candidate metallic alloy in Table 4-4. C/C composite material has the capability (Table 4-6) to easily withstand the fluence and the maximum expected temperature. Because the fluence is so low, the more expensive SiC/SiC composite material is not needed in this application. Thus, C/C composite material is selected as the material for the guide tubes.

These parts are ~about 4000-mm long tubes having an inner diameter of about 100-mm and an outer diameter of about 120-mm. They are not expected to experience a significant amount of internal wear, but can experience high temperatures in a CCD event. This composite could be manufactured by filament- or tape-winding of the tube using a polymer/pitch fiber prepreg, followed by pyrolysis of the matrix and graphitization of the resulting carbon matrix. Careful choice of the fiber orientation could be used to tailor the thermal expansion coefficient.

Alternatively, the same manufacturing technique could be applied to an oxide-oxide low-creep ceramic system. However, there is a lack of irradiation data for this composite. Thus, it is not recommended for use until further study is completed, including irradiation effects.

5.3 Upper Core Restraint

The upper core restraint (UCR) assembly sits on top the reactor core and permanent side reflector assemblies. It functions to maintain the fuel and replaceable columns centered with respect to the bottom of the core. This prevents the fuel columns from leaning against one another, and it maintains somewhat even spaces around each column such that helium coolant flows relatively evenly around the columns preventing bi-stable lateral movements of the fuel columns.

The UCR must accommodate radial thermal expansion of the graphite blocks within the surrounding metallic core support structure. In addition, it must accommodate vertical relative movement of the individual fuel and reflector columns caused by differential thermal expansion and irradiation induced dimensional change of the graphite elements. The UCR is in the way of refueling operations, so it must be designed to be removed and replaced during refueling. Therefore, the UPS elements are designed to have nearly the same cross section and handling features as the fuel elements to facilitate remote handling by the fuel handling machine. The UCR interfaces with the control rods, the RSM pellets, the CR and RSM guide tubes, the fuel handling machine, and the coolant channels in the permanent side reflector. Figure 5-8 illustrates the various UCR elements that, when assembled together atop the reactor core, act like a solid plate connecting the loose assemblage of fuel and reflector columns at their center lines to the core barrel. The keys and keyways of these elements interlock to form a stable structure in the horizontal plane above the core. Vertical relative movement is allowed by the sliding key/keyway joints. Figure 5-9 shows the "T-key" arrangement and dowel locators for the fuel handling machine in a typical UCR element.

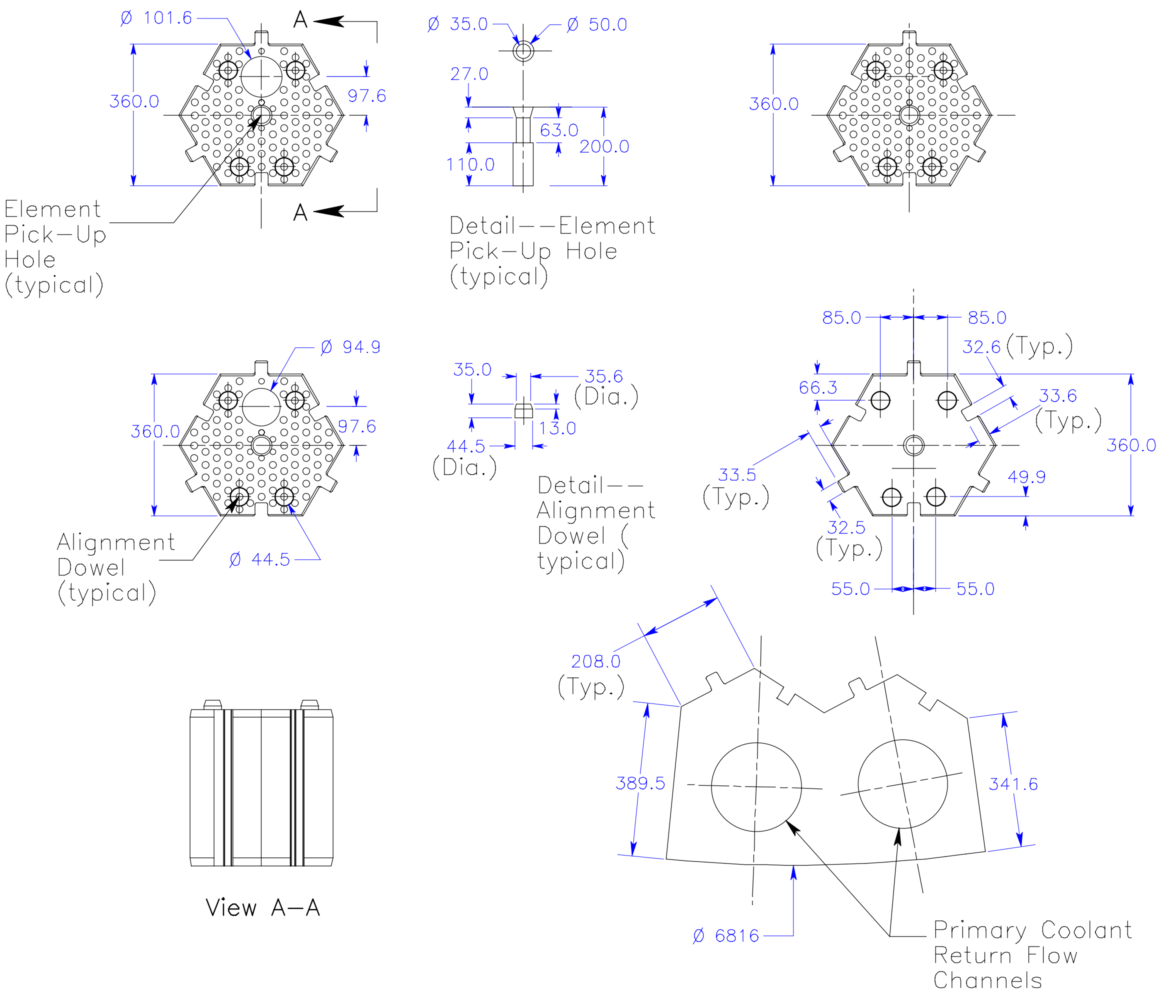

(Dimensions in mm)

Figure 5-8. Geometries of the various upper core restraint elements

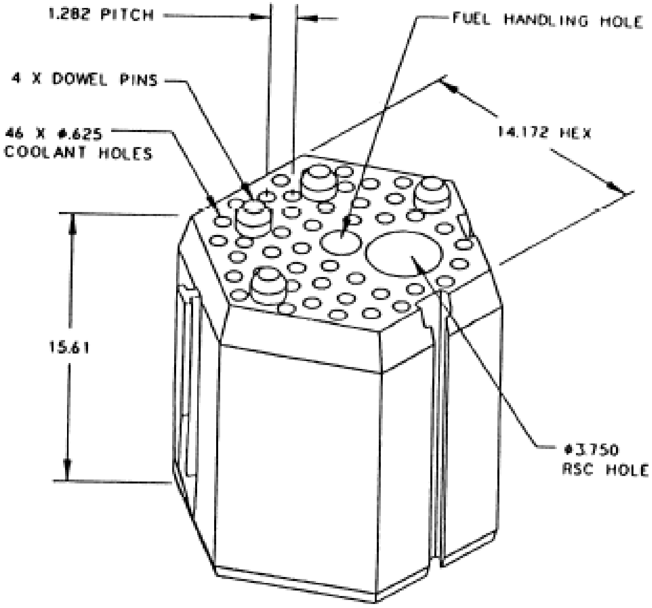

(Dimensions in inches)

Figure 5-9. UCR element showing "T-key" arrangement and dowel locators for fuel handling

The operating temperature of the UCR is about the same as the reactor inlet helium temperature. Temperatures during a CCD event are quite high due to welling up of hot gas from lower in the core into the upper plenum. The UCR must withstand all design basis earthquakes without failure to assure subsequent insertion of control rods and/or the RSM if needed, and to ensure that core cooling can be maintained. The neutron fluence level is low on top of the reactor core because of neutron shielding around the core. The maximum total neutron fluence at the UCR is 3.5×10^{24} n/m^2, or 0.0434 dpa.

UCR steady state temperatures are shown in Table 5-6 (Ref. 4). The temperatures during pressurized and de-pressurized CCD events are shown in Table 5-7 and Figures 5-10 and 5-11.

Table 5-6. UCR Maximum Steady State Temperatures

Location	Height	Temp (490°C Core Inlet) (C)	Temp (590°C Core Inlet) (C)	Z (m)
Central Reflector Column	Top	457	538	11.50
	Bottom	485	584	11.30
Fuel Assy Column	Top	460	543	11.50
	Bottom	486	584	11.30
Replaceable Side Reflector Column	Top	461	544	11.50
	Bottom	485	584	11.30
PSR Column	Top	466	555	11.50
	Bottom	486	584	11.30

Table 5-7. UCR Maximum Temperatures during CCD Events

Location	Pressurized CCD Event		De-pressurized CCD Event	
	490°C Core Inlet (C)	590°C Core Inlet (C)	490°C Core Inlet (C)	590°C Core Inlet (C)
Bottom of UCR Block (Top of Reactor Core)	1075	1094	642	655

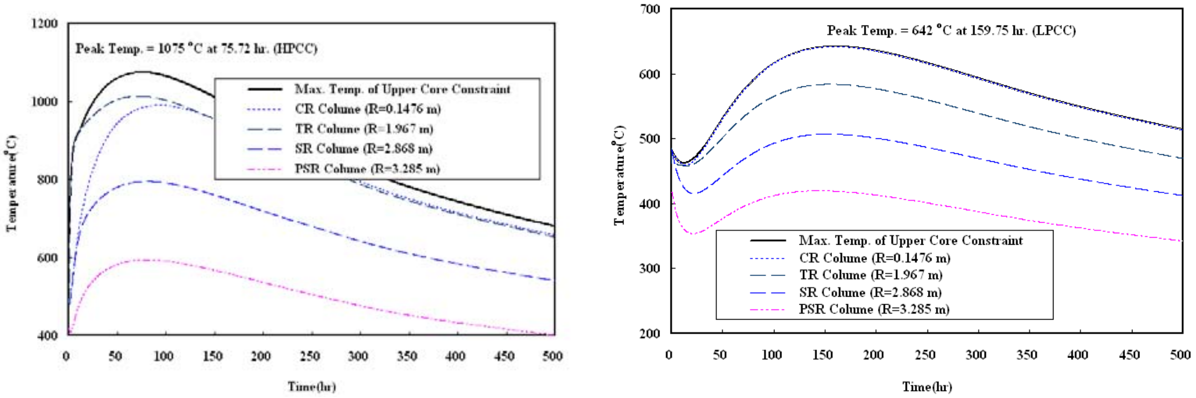

Pressurized Conduction Cool Down
Peak Temp = 1075°C

Depressurized Conduction Cool Down
Peak Temp = 642°C

Figure 5-10. UCR temperatures for CCD transients with T_{in} of 490°C

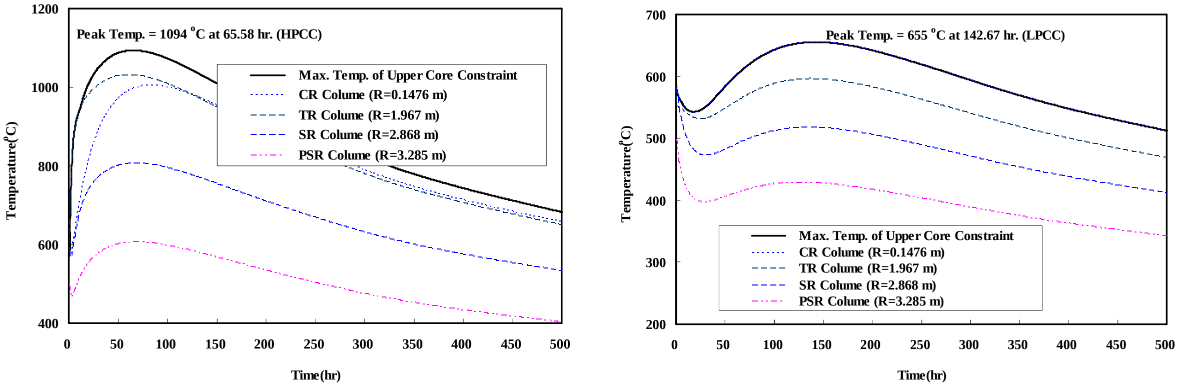

Pressurized Conduction Cool Down
Peak Temp = 1094°C

Depressurized Conduction Cool Down
Peak Temp = 655°C

Figure 5-11. UCR temperatures for CCD transients with T_{in} of 590°C

In previous HTGR designs, the UCR material was alloy 800H. Normal operation temperatures are low enough to retain this material. However, the maximum temperature during a pressurized CCD event (1094°C) is too high for alloy 800H. Thus, a C/C composite is the material of choice because the neutron fluence is low. SiC/SiC composites could also be used, but with the low fluence the more expensive material is not needed. The complexity of this component requires that the manufacturer be involved in the design at the onset.

5.4 Upper Plenum Shroud Thermal Barrier

The upper plenum shroud (UPS) forms a gas plenum above the reactor core to uniformly distribute the primary helium coolant to the fuel columns as shown in Figure 5-12. Coolant flows out of the PSR coolant channels into the upper plenum where it mixes and then flows from the upper plenum through the reactor core to the lower plenum at the bottom of the core. The UPS has a thermal barrier to prevent heat up of the UPS structure and the reactor vessel. The upper plenum operates at the reactor inlet helium temperature. It also heats up during the conduction cool down events from natural convection currents welling up from the core. The maximum temperatures during normal operation and during CCD events are high enough to require that the upper plenum shroud have thermal barrier features that prevent overheating of the reactor vessel during both normal and off-normal operation. In addition, the control rod and RSM channels in the reactor core allow some neutron streaming to the UPS. To reduce the neutron fluence to an acceptable level, there is boronated graphite placed between the thermal barrier and the UPS primary structure, which is alloy 800H.

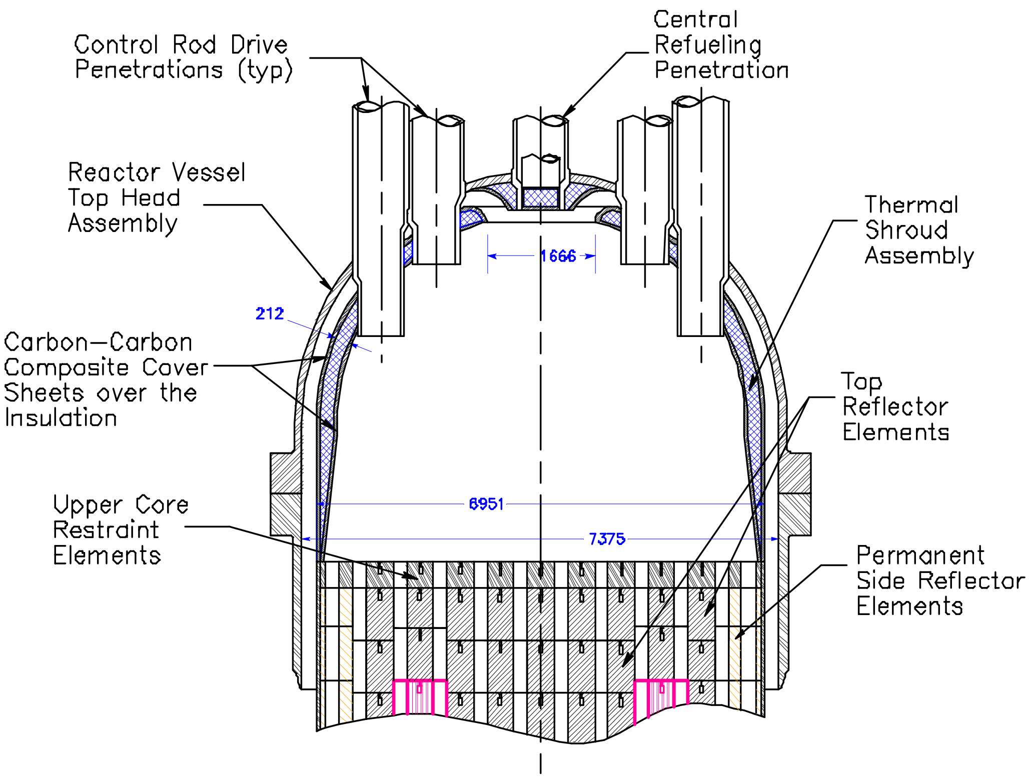

Figure 5-12. Upper Plenum Shroud

The neutron fluence on the thermal barrier cover plates is $1.2x10^{22}$ n/m^2.

Upper plenum shroud steady state temperatures are given in Table 5-8. The transient temperatures for pressurized and depressurized CCD events are given in Table 5-9 and Figures 5-13 and 5-14.

Table 5-8. UPS Thermal Barrier Maximum Steady State Temperatures

Location	Temperature (C)				Z (m)
	C/C Hot Side	Kaowool	Boronated Graphite	C/C Cold Side	
490°C Core Inlet					
Top of UPS	342	334	327	327	15.42
Mid Height of UPS	374	343	314	314	13.78
Bottom of UPS	458	387	317	316	12.23
590°C Core Inlet					
Top of UPS	383	371	359	358	15.42
Mid Height of UPS	433	389	345	345	13.78
Bottom of UPS	541	444	349	348	12.23
C/C thickness = .0125 m Kaowool thickness = 0.06 m					

Table 5-9. UPS Thermal Barrier Maximum Temperatures during CCD Events

Location	Pressurized CCD Event		De-pressurized CCD Event	
	490°C Core Inlet (C)	590°C Core Inlet (C)	490°C Core Inlet (C)	590°C Core Inlet (C)
T/B Cov Pl Hot Side	914	926	513	540

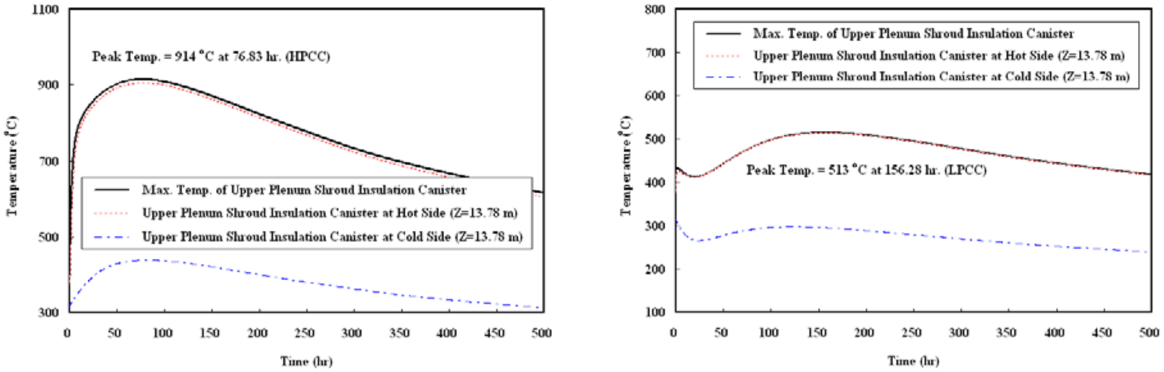

Pressurized Conduction Cool Down
Peak Temp = 914°C

Depressurized Conduction Cool Down
Peak Temp = 513°C

Figure 5-13. UPS temperatures for CCD transients with T_{in} of 490°C

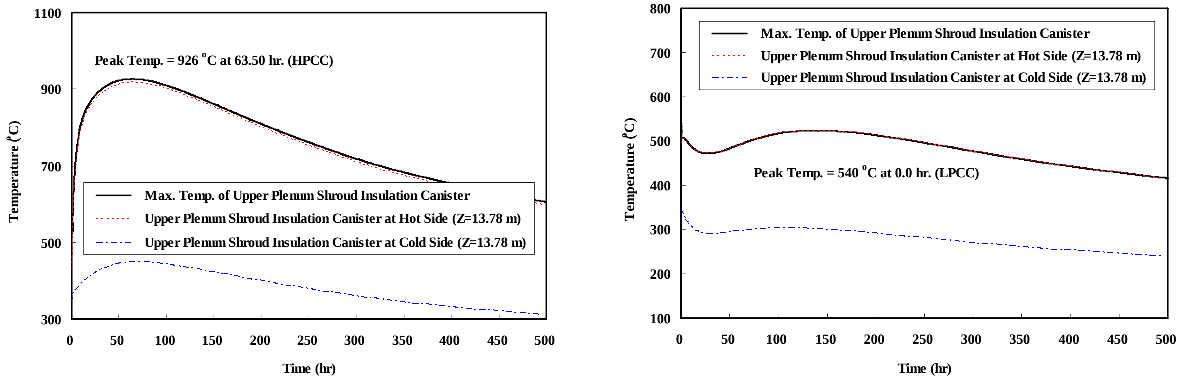

Pressurized Conduction Cool Down
Peak Temp = 926°C

Depressurized Conduction Cool Down
Peak Temp = 540°C

Figure 5-14. UPS temperatures for CCD transients with T_{in} of 590°C

The thermal barrier cover plates could be fabricated from a metallic material such as alloy 800H or Hastelloy X if designed only for the maximum expected temperature during normal operation. The neutron fluence does not appear to be a problem for Hastelloy X, but the effect of neutrons streaming through the control rod channels has not been calculated for this study, so local areas could exceed the allowable thermal neutron fluence of $3.0x10^{22}$ n/m^2. However, the maximum calculated temperature during a pressurized CCD event (926°C) is higher than the maximum allowable temperature in the ASME code for either alloy 800H or Hastelloy X (see Table 4-4). Both Haynes 230 and alloy 617 have sufficiently-high temperature limits for this application, but their high cobalt content is a concern[2]. Therefore, the choice for this application is a C/C composite, which can easily handle both the fluence and temperature. SiC/SiC composites are not considered for this application because the fluence is to low.

The thermal insulation material for this application in prior MHR designs has been ceramic fiber blankets with trade names Quartz-et-Silice and Kaowool. Concerns with respect to the use of these insulation materials are that: (1) relaxation of the fibers during operation may allow natural convection cells to form, (2) depressurization/pressurization cycles could lead to fatigue failure of the fibers, and (3) mechanical fatigue of the fibers might occur due to noise in the cooling circuit. To overcome these concerns, it is recommended that use of solid ceramics blocks instead of the fibrous insulation be investigated.

---

[2] Except for their high cobalt content, either alloy 617 or Haynes 230 would be a good choice as the material for the UPS cover plates. Given that the neutron flux at the locations of these cover plates is quite low, it is uncertain if there would be sufficient neutron activation of the cobalt to be a problem. An analysis should be performed to verify the somewhat arbitrary rejection of these materials in this study based on their high cobalt content.

Solid ceramic insulation materials are available that contain a high-volume-fraction pore structure. Methods of producing a pore structure include incorporation of hollow spheres in a matrix or the production of foamed ceramics with a tailorable volume fraction of porosity. Commercially available insulation products based on microporous insulation systems are available. These materials are used in the aerospace, power generation, steel and non-ferrous and glass industries at temperatures up to 1150°C and offer the lowest thermal conductivity at minimum dimensions. Suppliers of such product are Microtherm and Armil CFS.

If it is determined that fibrous blankets are needed, the legacy materials such as Quartz-et-Silace and Kaowool will need to be replaced with higher-temperature blanket materials. A wide variety of fibrous blankets are offered for high-temperature insulation. These blankets are available commercially under a variety of trade names and can be made from alumina/silica fibers. Needled ceramic fiber blankets (2300 – 2600°F), polycrystalline mullite fibers (3000°F), silica fibers (1800°F), or silica/magnesia fibers (2300°F) are all suitable for the indicated temperature service. These ceramic fibers can also be formed into boards or blocks for insulation and hot face lining applications with similar temperature capabilities. Suppliers of such product are Armil CFS or Kitsons Thermal Supplies, but there are likely to be a large number of other potential suppliers.

While offering very low thermal conductivity, fibrous insulation has some drawbacks, which include poor mechanical integrity, the likelihood of dust production, and degradation of thermal properties if fretting leads to breakdown in the structure of the blanket. It is conceivable that the microporous products that are offered as an alternative to fibrous insulation avoid these problems while still offering adequate thermal insulation and a compliant layer between structures to accommodate thermal expansion mismatches.

A detailed review of insulation materials was beyond the scope of this study, so it is recommended that a further investigation be performed to confirm the selection of insulation material.

No data was found in this study on the corrosion of solid ceramics or ceramic fiber blankets in a helium environment with the reactor coolant design impurities shown in Table 3-4. Therefore, this is an issue that must be addressed in the technology development program. There is a need for corrosion data to validate the life of ceramic materials in an NGNP reactor environment.

5.5 Permanent Side Reflector Seal Sleeves

The permanent side reflector (PSR) blocks are made of highly purified graphite. The primary function of the PSR is to reflect neutrons back into the reactor core to minimize neutron leakage. The neutrons that do make it through both the replaceable side reflectors and the PSR are mostly reduced to thermal energy levels. The thermal neutron fluence to the reactor vessel is reduced to an acceptable level by placing boron carbide pins in the outer portion of the PSR. It is the combination of a thickness of graphite and the boron pins that perform both the neutron reflection and vessel shielding functions.

Past reactor designs had alloy 800H coolant channels attached to the core barrel through which the helium returning to the reactor from the power conversion system flowed to the UCP. In the current NGNP design, the return helium flows to the UCP through channels in the PSR. Since the PSR is made of graphite blocks, these channels will leak helium to the core to some extent. Seal sleeves made of C/C composites as shown in Figure 5-15 are envisioned as being needed to minimize this leakage.

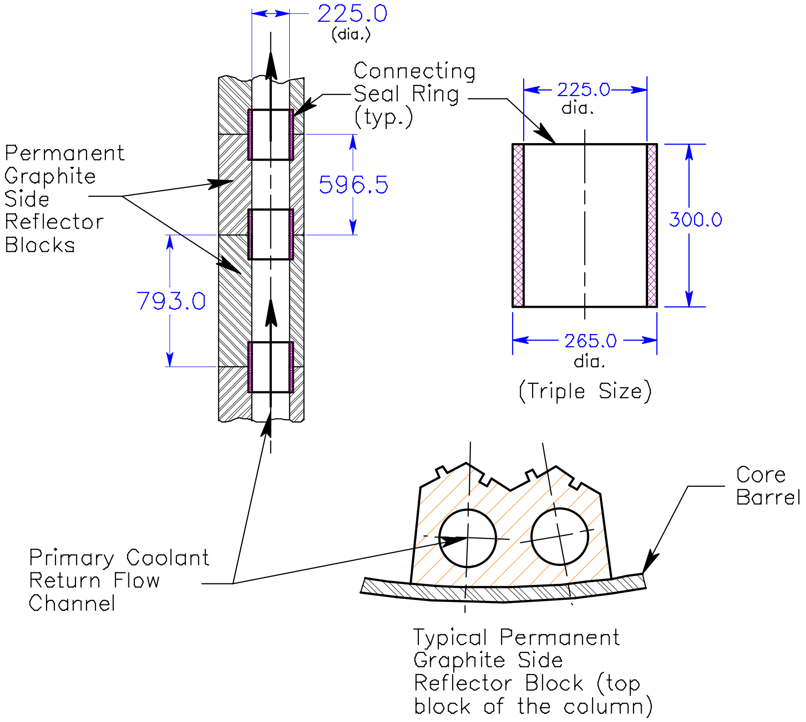

Figure 5-15. PSR seal sleeve concept for primary coolant passages in PSR blocks

The PSR graphite blocks rest one-upon-the-other in a stack. There are joints between blocks that require a shear connection to maintain alignment of the blocks in a stack. Graphite dowels were used in previous designs to maintain coolant-hole alignment and keep as much pure graphite in the PSR as possible. These dowels maintain the blocks in alignment during normal and off normal operation and during earthquakes. These dowels can be replaced with rings of graphite surrounding the coolant channels to form a hollow dowel that permits coolant flow to pass through it while maintaining the purified graphite material needed for reflection of neutrons.

By placing the coolant channels in the PSR, a new function has been introduced, which is to minimize coolant flow leakage to the core through the gaps in the coolant passages between PSR blocks. This function can be achieved with the proper gaps between the graphite hollow dowels and by reducing the number of blocks (i.e., number of horizontal gaps between blocks) in a column. A helium leakage analysis was performed for this study to determine the feasibility of controlling leakage in this manner. The results show that it is possible to control the bypass flow to acceptable levels in this manner. The analysis is provided in Appendix E.

The neutron fluence for the seal location is 3.2×10^{24} n/m^2 (0.0434 dpa) after 60 years of operation. This is not a problem for nuclear graphite.

The PSR seal sleeve steady state temperatures are shown in Table 5-10. The transients for pressurized and depressurized CCD events are shown in Table 5-11 and Figures 5-16 and 5-17.

Table 5-10. PSR Seal Sleeve Maximum Steady State Temperatures

Location	Max Temp (Inlet 490°C) (C)	Max Temp (Inlet 590°C) (C)	Z (m)
Top of PSR	484	582	10.71
Bottom of PSR	487	585	0.3965

Table 5-11. PSR Seal Sleeve Maximum Temperatures during CCD Events

Location	Pressurized CCD Event		De-pressurized CCD Event	
	490°C Core Inlet (C)	590°C Core Inlet (C)	490°C Core Inlet (C)	590°C Core Inlet (C)
Top of PSR	631	643	729	743

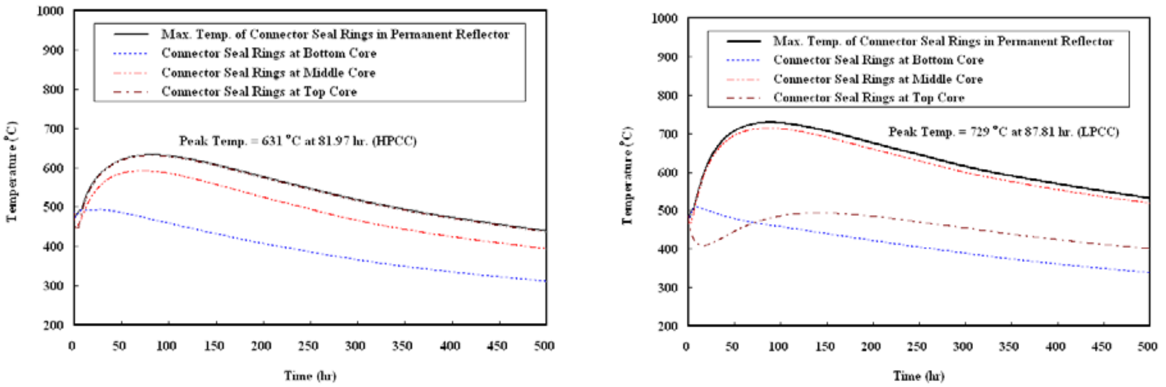

Pressurized Conduction Cool Down
Peak Temp = 631°C

Depressurized Conduction Cool Down
Peak Temp = 729°C

Figure 5-16. PSR seal sleeve temperatures for CCD transients with T_{in} of 490°C

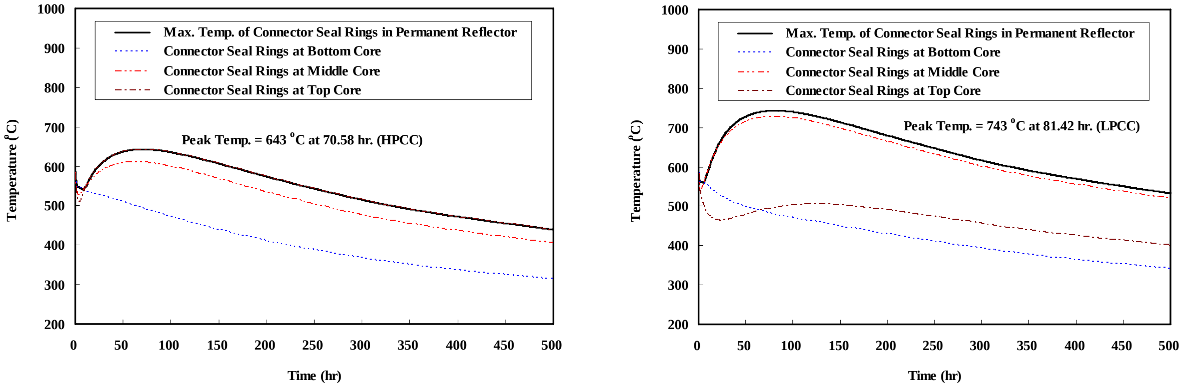

Pressurized Conduction Cool Down
Peak Temp = 643°C

Depressurized Conduction Cool Down
Peak Temp = 743°C

Figure 5-17. PSR sleeve temperatures for CCD transients with T_{in} of 590°C

The maximum temperatures of the PSR sleeves during normal operation and CCD events, and the neutron fluence are well below the limits for either C/C composites or graphite. Thus, it is not necessary to use a relatively expensive C/C composite material for this application. Hollow graphite dowels will perform well for this function while maintaining compatibility of material within the PSR assembly. Choosing graphite for the seal sleeves does not require any new technology development for the NGNP (i.e., because an extensive graphite development program is already being conducted to qualify new nuclear grade graphites for the NGNP).

5.6 Metallic Core Support Load Bearing Insulators

The metallic core support (MCS) load-bearing insulators function to reduce heat flow from the lower plenum gas to the metallic core support to prevent over heating. The MCS is made of alloy 800H, which cannot tolerate the 950°C core outlet temperature[3]. The load bearing insulators are located below the graphite core support posts as shown in Figure 5-18. In past reactors designs such as Ft. St. Vrain, these insulators were made from monolithic ceramic materials arranged in layers to accommodate thermal gradients. Low-conductivity material was selected to minimize insulator thickness. Alumina, fused silica, and Masrock ceramics were used. Ceramic composites could be used for this application but they would do not offer any advantage over monolithic ceramic pads since the loads pass directly through them in compression.

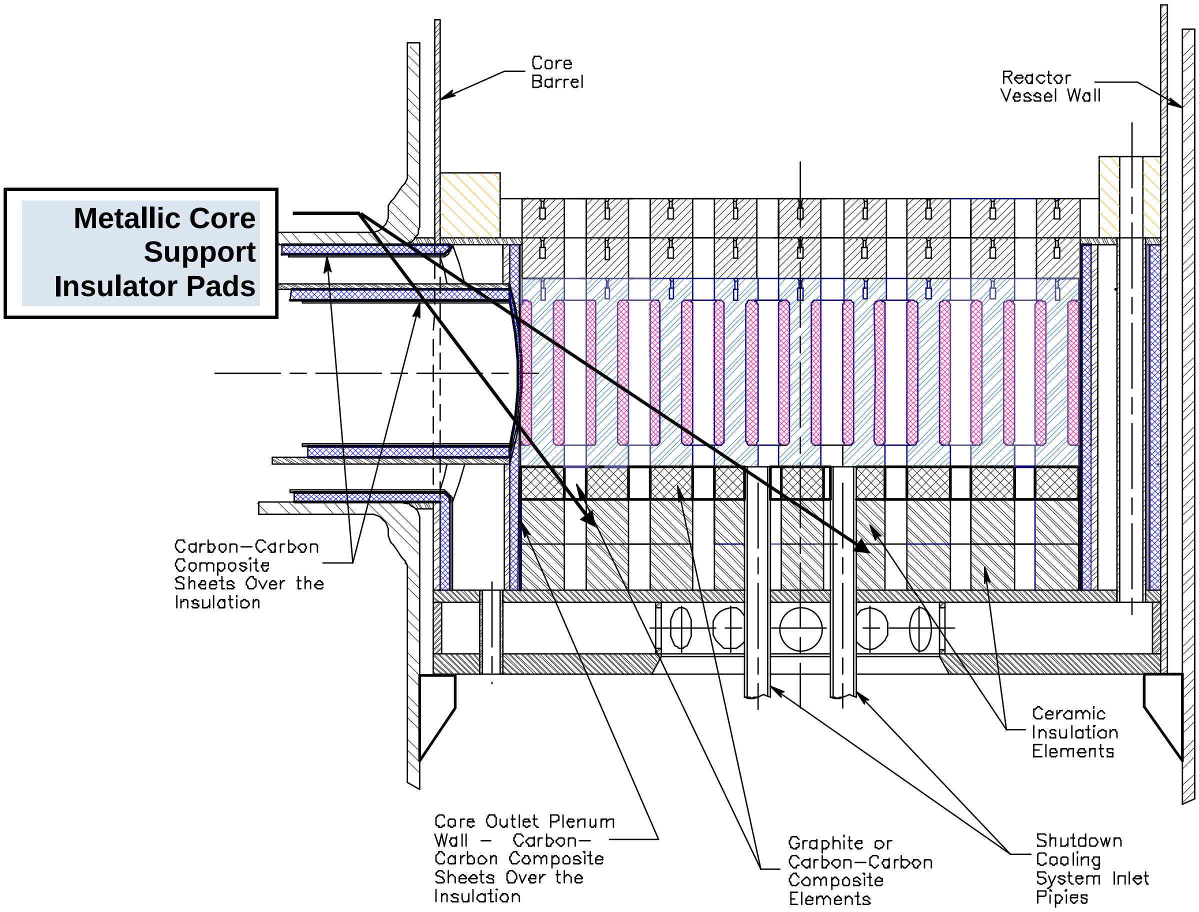

Figure 5-18. Location of insulation assemblies in the lower plenum of NGNP configuration

The neutron fluence at this location is 8.5x10^{21} n/m^{2} (0.00011dpa), which is very low. However, no neutron irradiation data was found for these ceramics. While most ceramics are relatively

---

[3] The limiting temperature for 800H is 760°C for a primary load carrying structure like the metallic core support designed and fabricated to the rules of the ASME Code.

unaffected by neutron radiation compared to metals and graphitic materials, data needs to be developed to confirm the suitability of ceramics for this application.

The load bearing insulator steady state temperatures are shown in Table 5-12. The temperatures for pressurized and depressurized CCD events are shown in Table 5-13 and Figures 5-19 and 5-20.

Table 5-12. MCS Thermal Insulator Maximum Steady State Temperatures

Location	Height	Temp (490°C Core Inlet) (C)	Temp (590°C Core Inlet) (C)	Z (m)
SCS Inlet Pipe Zone	Top	838	860	-2.006
	Bottom	631	697	-2.417
Core Zone	Top	825	851	-2.006
	Bottom	620	689	-2.417

Table 5-13. MCS Thermal Insulator Maximum Temperatures during CCD Events

Location	Pressurized CCD Event		De-pressurized CCD Event	
	490°C Core Inlet (C)	590°C Core Inlet (C)	490°C Core Inlet (C)	590°C Core Inlet (C)
SCS Inlet Pipe Zone	837	860	837	860

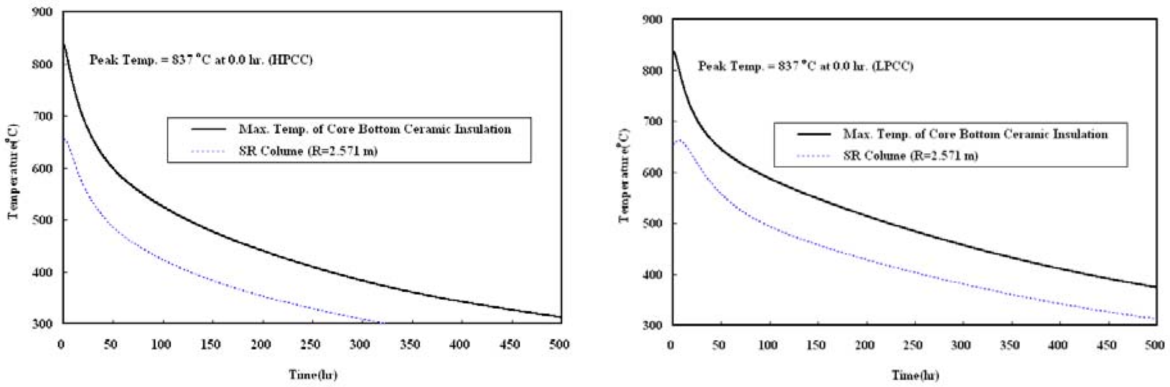

Pressurized Conduction Cool Down
Peak Temp = 837°C

Depressurized Conduction Cool Down
Peak Temp = 837°C

Figure 5-19. MCS thermal insulator temperatures for CCD transients with T_{in} of 490°C

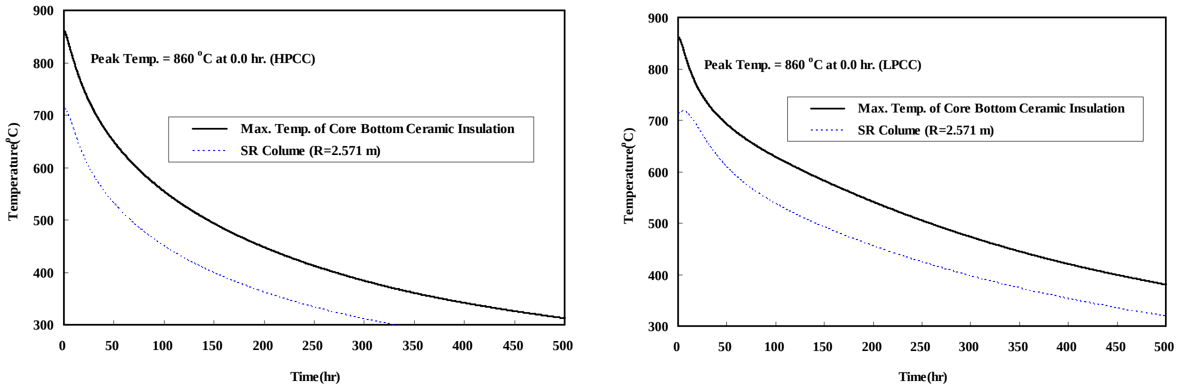

Pressurized Conduction Cool Down
Peak Temp = 837°C

Depressurized Conduction Cool Down
Peak Temp = 860°C

Figure 5-20. MCS thermal insulator temperatures for CCD transients with T_{in} of 590°C

There are a large number of ceramics available that may meet the requirements for this application. This component, or set of components, must insulate the 800H core support floor from the core heat. In normal operation, it must withstand a 300ºC temperature drop over a 200-mm thickness. However, abnormal operating conditions may cause considerable thermal transients. Further work must be done to understand these transients.

As part of the assessment of these monolithic ceramic insulators, thermal analyses were performed to scope out the possible temperatures and thermal gradients during steady state operation and normal transients. The calculations are presented in Appendix C. Based on these calculations, the thermal gradients were judged to be too high for Alumina type ceramics, which have very low thermal shock resistance. Mullite and glassy ceramics were judged to be capable of handling these thermal gradients. Thus, the glassy ceramic MACOR (see Table 4-5) was chosen to be an optimum material for this application.

Although it is intended to be removable should the need arise, the MCR thermal insulator is a 60-year life component. Originally it was proposed to either cover the lower plenum wall diameter with hexagonal insulating plates, one plate to each fuel column, or with 12 pieces. If these components are to be removable, then the former is recommended to promote lower component weight, though this does complicate manufacture and installation.

The status of these parts as 60-year life components requires very high creep resistance, even under the low compressive stresses of ~1ksi (6.9 MPa). Resistance to thermal transients requires a certain degree of thermal shock resistance. Full determination of this engineering requirement requires a full analysis of thermal transients which should be completed in further work. The pads have been chosen to be 3 inches thick (76.2mm). There are two of them stacked one on top of the other. The worst-case thermal gradient calculated for Macor insulator pads is 21°C/cm. Macor is judged to be able to withstand this gradient and still maintain structural integrity.

The choice of Macor needs to be confirmed in the technology development program. Additional thermal-stress analysis is also needed to confirm this choice.

5.7 Concentric Hot Duct and Cross Vessel Thermal Barrier Assemblies

Figure 5-21 shows the concentric hot duct and cold return duct assembly.

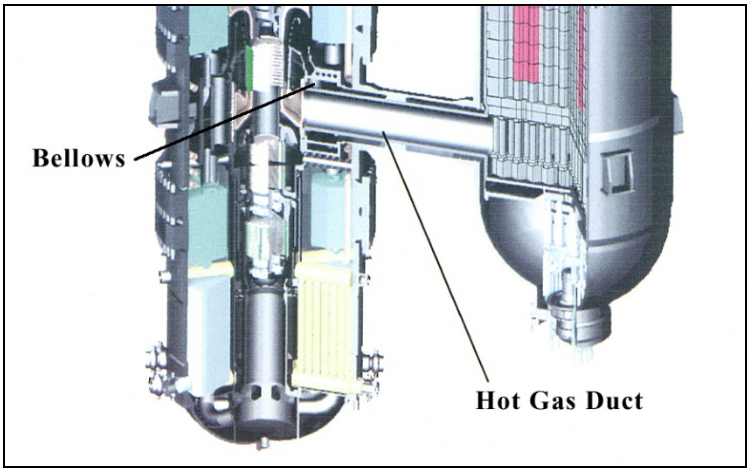

Figure 5-21. Concentric hot duct and cross vessel

Figure 5-22 shows the hot duct and cross vessel relationship. The hot duct has primary helium coolant gas flowing from the reactor core through the center of the hot duct while return gas at the core inlet temperature returns to the core in the annular region between the cross vessel and hot duct. The hot tube is bathed in return gas at up to 590°C. The tube is subjected to the core pressure drop of about 15 psid radially inward to put the tube in hoop compression. A leak through this pressure boundary would result in a short circuit of primary coolant at the core inlet temperature directly into the hot gas exiting the reactor core. Thus, the hot duct must be a highly reliable internal pressure boundary to prevent leakage flow from occurring. It is fabricated from alloy 800H, which has an ASME code temperature limit of 760°C, so it must be protected from the 950°C core outlet gas, with hot streaks up to 225°C above the mean mixed temperature. The hot streaks can be as high as 1175°C. A high-temperature thermal barrier system has been designed for past reactors to protect the alloy 800H tube. The hot duct is designed to have a life of 60 years.

It is planned to fabricate the cross vessel from SA508/SA533 steel, which is the material used to fabricate the vessels for light water reactors (LWRs). Section III of the ASME code limits the maximum steady state temperature for this material to 371°C. This is far lower than the return gas temperature of up to 590°C. Therefore, the cross vessel must be insulated on the inside and cooled on the outside by blowing air through a shroud around the outside of the cross vessel. This results in a two-layer insulation system, one on the inside of the hot duct and one on the inside of the cross vessel, as shown in Figure 5-23. A cross-vessel thermal hydraulic analysis was performed as part of this study and confirmed the feasibility of this cooling scheme. The analysis is presented in Appendix D.

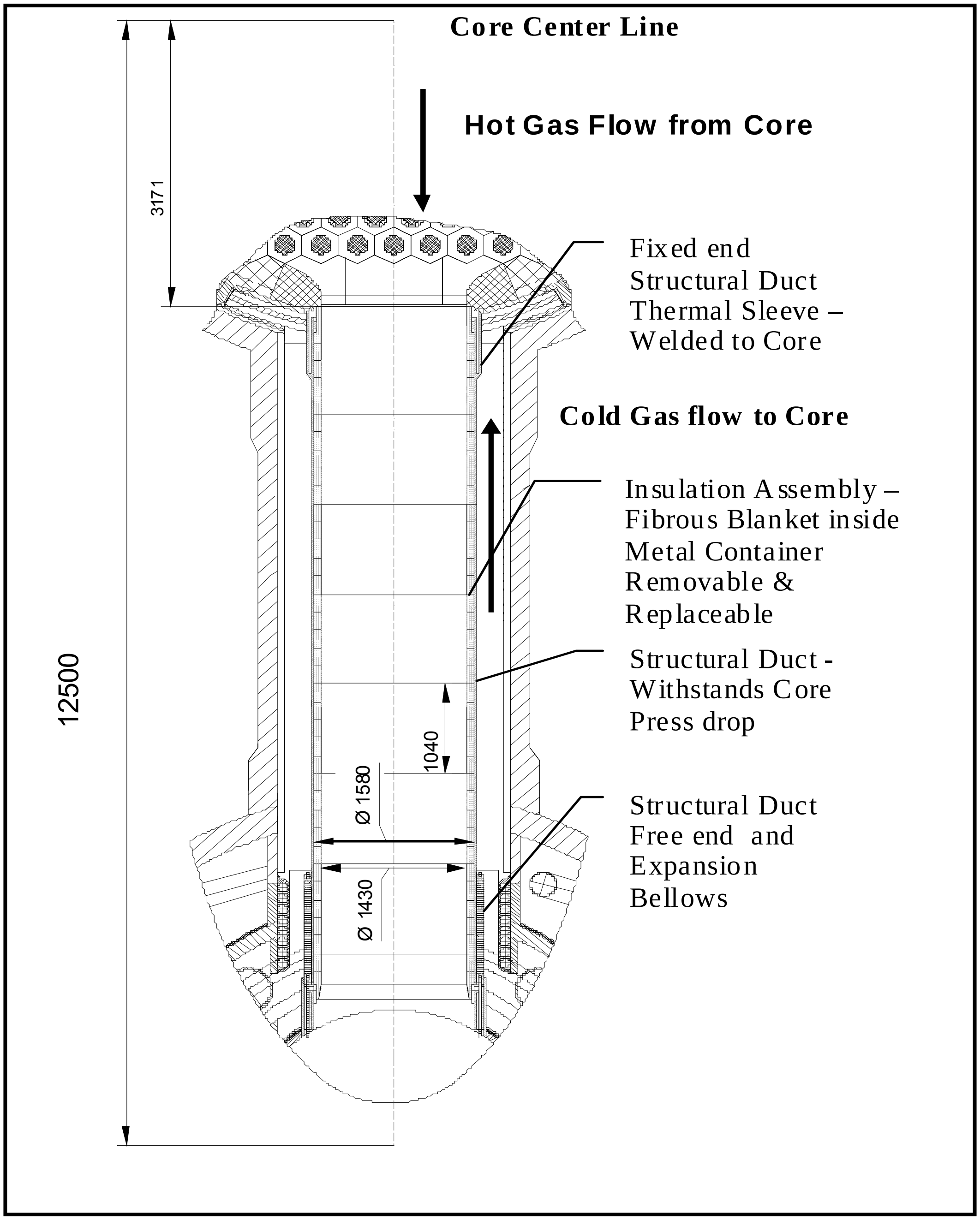

Figure 5-22. Hot duct and cross vessel relationship

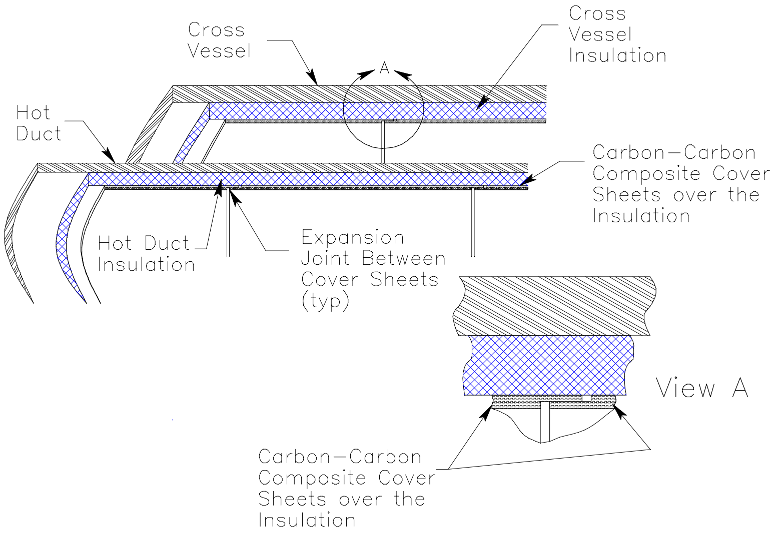

Figure 5-23. Hot duct and cross vessel insulation details

The lower plenum sidewall, hot duct, and cross vessel experience a neutron fluence of 8.5x10^{21} n/m^2 (0.00011dpa) over the 60-year life of the NGNP. This is a very low fluence for the materials being considered for these applications.

The hot duct and the lower plenum side wall thermal barrier experience the complex temperature environment of the core exit plenum (or lower plenum). The lower plenum is the volume into which primary helium gas exits after passing through the reactor core. The helium coolant exits each fuel column at a different temperature because the gas flowing through the fuel columns is not controlled to achieve a uniform exit temperature and the flow resistance in each fuel column varies due to geometry differences[4] and gas buoyancy effects. The gas temperature also varies within a fuel element column due to power tilts across the column. The gas exiting the fuel columns mixes in the lower plenum as it is flows towards the hot duct. The variation in the helium temperatures exiting the various fuel columns has been estimated to be as high as ±250°C, and it is conservatively estimated that mixing in the lower plenum reduces these hot streaks by only about 25°C at the entrance to the hot duct. These hot streaks have been found to be 25 to 50 cm in diameter and to result in locally high gas temperatures impinging on the cover plates of the lower plenum sidewall and hot duct thermal barrier.

Thus, the lower plenum sidewall and the hot duct thermal barrier must be designed for this

---

[4] The geometries of the fuel columns are essentially the same except for the control rod and reserve shutdown columns, which have large holes for insertion of control rods and reserve shutdown material.

complex mixture of temperatures. To accommodate this complexity without conducting detailed thermal analyses for specific thermal barrier configurations, materials will be chosen on a worst case basis.

The hot side of the thermal barrier will be designed based on two temperatures. The thickness of the insulation system will be based on the mixed mean temperature, and the thermal barrier cover plate material will be selected based on the conservatively estimated maximum hot streak temperature. Thus, the service temperature for the lower plenum sidewall hot-side cover plate material is specified to be the mixed mean gas temperature plus the maximum hot streak temperature of 250°C. Similarly, the hot duct cover plate material will be chosen to withstand the mixed mean gas temperature plus a hot streak temperature of 225°C. The hot duct assembly steady state temperatures, including hot streaks, are shown in Table 5-14.

The transient temperature declines exponentially from the steady state temperature in all CCD events. Thus, the peak temperatures during the CCD events are the same as the steady state maximums. Hot duct maximum CCD temperatures are shown in Table 5-15. The hot duct transient temperatures for CCD events are shown in Figures 5-24 and 5-25.

Table 5-14. Hot Duct and Cross Vessel Through-thickness Temperatures

Component	Location	Component Temperatures (490°C Inlet Temp) (C)		Component Temperatures (590°C Inlet Temp) (C)	
		Mixed Mean Gas Temp	Hot Streak Gas Temp	Mean Temp Gas	Hot Streak Gas
Hot Duct Thermal Barrier & Metallic Tube	Hot Side C/C Composite Cover Pl	949	1174	949	1174
	Kaowool Insulation Blanket	712	?	764	?
	Hot Side Hot Duct Metallic Tube	495	?	594	?
	Center thickness Metallic Tube	493	?	593	?
	Cold Side Hot Duct Metallic Tube	491	?	591	?
Cross Vessel thermal Barrier & Metallic Vessel	Hot Side T/B Cover Pl	490	na	589	na
	Kaowool Insulation Blanket	379	na	414	na
	Hot Side Cross Vessel Metal wall	273.2*	na	247.8	na
	Center thickness Metal wall	272.9*	na	247.2	na
	Cold Side Cross Vessel Metal Wall	272.8*	na	246.6	na
Note: * The cross vessel temperature varies from 273 to 253°C along its length. Cross vessel cooling was modeled on the outside of the cross vessel wall. Note: ? No local heat transfer analysis performed for this study. Note: Temp profile thru-the-thickness is nearly constant along length of ducts. Hot streaks are local and mixing is not accounted for in these estimates.					

Table 5-15. Hot Duct Thermal Barrier Maximum Temperatures during CCD Events

Location	Pressurized CCD Event		De-pressurized CCD Event	
	490°C Core Inlet (C)	590°C Core Inlet (C)	490°C Core Inlet (C)	590°C Core Inlet (C)
T/B Cov Pl Hot Side	954	954	849	949

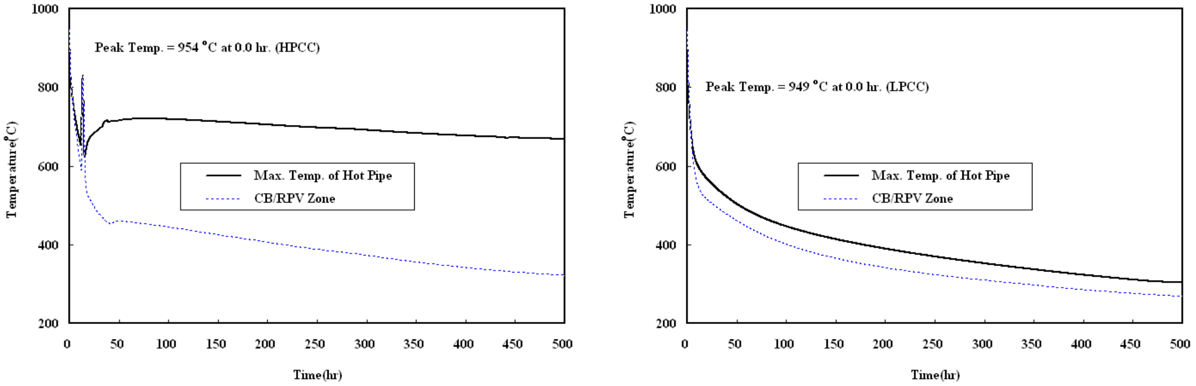

Pressurized Conduction Cool Down
Peak Temp = 949°C

Depressurized Conduction Cool Down
Peak Temp = 954°C

Figure 5-24. Hot duct T/B cover plate temperatures for CCD transients with T_{in} of 490°C

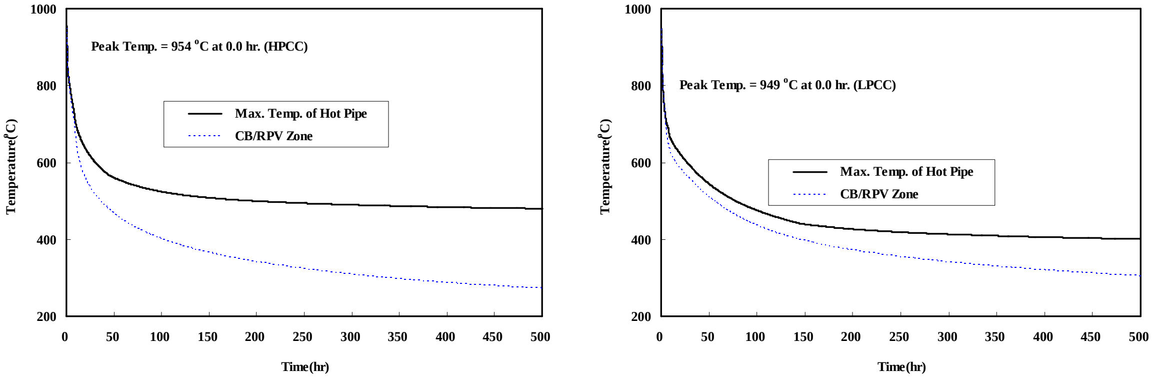

Pressurized Conduction Cool Down
Peak Temp = 949°C

Depressurized Conduction Cool Down
Peak Temp = 954°C

Figure 5-25. Hot duct T/B cover plate temperatures for CCD transients with T_{in} of 590°C

The hot duct thermal barrier cover plates are much too hot at 949°C, with hot streaks of up to 1174°C, to use metallic materials. Thus, the hot duct thermal barrier cover plates should be made from a ceramic composite to obtain the strength needed at these high temperatures. Since this is a low neutron fluence area, C/C composites are preferred. The shapes and sizes can be made to accommodate the hot duct and sidewall geometries. In order to withstand the hot streak temperature and to redistribute the heat across the insulation, a filament- or tape-wound C/C composite appears to be the best option for the cover plate.

The thermal insulation material used in the past was fibrous insulation blankets such as Kaowool and Quartz-et-Silice. Relaxation of these fibers at high temperature reduces the effectiveness of the insulation. There are solid ceramic materials specifically produced for use as high-temperature insulation. Two candidates identified by Rolls-Royce are (1) high-pore-volume ceramics specifically designed for use as thermal insulators, and (2) refractory ceramics with very low conductivities. These materials should be thoroughly investigated before making a final choice. Interlocking blocks of insulation can be used that will be much more tolerant to noise in the primary coolant loop, withstand the sudden pressure changes of the cooling loop, and not relax during operation. This will remove the uncertainty of the life of fibrous insulation blankets over the 60-year life of the NGNP.

These are the same insulation materials selected for the UPS thermal barrier. Commercially available insulation products are available based on microporous insulation systems. These materials are used in the aerospace, power generation, steel, and non-ferrous and glass industries at temperatures up to 1150°C, and offer the lowest thermal conductivity at minimum dimensions. Suppliers of such products include Microtherm and Armil CFS (see Appendix G).

The maximum temperature for the hot duct metallic tube is 495°C per Table 5-14. The maximum temperature would be somewhat higher based on the hot streak temperature instead of the mixed-mean gas temperature, but the temperature should still be low enough to permit use of alloy 800H, and alloy 800H is recommended for this application.

5.8 Lower Plenum Sidewall Thermal Barrier Assembly

The lower plenum side wall experiences the same gas conditions as the hot duct except the hot streaks are slightly higher at 250°C above the mean gas temperature. This thermal barrier assembly surrounds the lower plenum as a cylinder with its axis vertical as shown in Figure 5-26. The lower plenum sidewall thermal barrier is a high-temperature insulation system much like the hot duct, but it is much larger in diameter with the axis in the verticle direction. It protects the alloy 800H metal core support from 950°C gas.

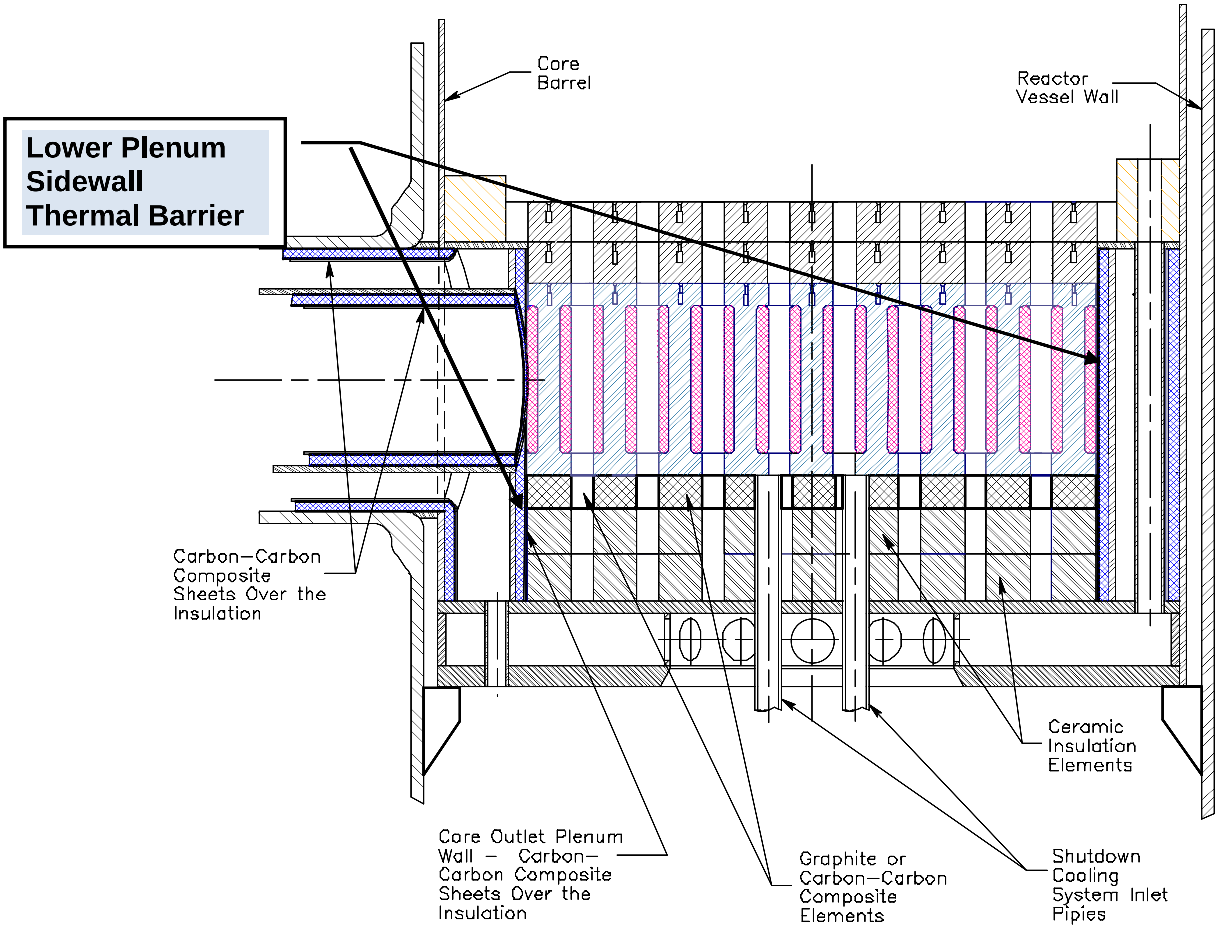

Figure 5-26. Lower plenum sidewall thermal barrier surrounding the core exit plenum

The neutron fluence incident on the thermal barrier is the same as incident on the hot duct, 8.5×10^{21} n/m^2 (0.00011 dpa).

The lower plenum sidewall thermal barrier steady state temperatures are shown in Table 5-16. The transient temperature declines exponentially from the steady state temperature in all CCD events. Thus, the peak temperatures during the CCD are the same as the steady state maximums. The response to the CCD transients is essentially the same as for the hot duct. The steady state temperatures are sustained and are far too high for metallic materials. Thus, the recommended material for the T/B cover plates is a C/C composite given that the neutron fluence is very low.

Table 5-16. Lower Plenum Sidewall Thermal Barrier Maximum Steady State Temperatures

Location	Temperature (C)				
	Cover Plate Hot Side		Kaowool	800H Cold Side	Z (m)
	Mean Temp Gas	Hot Streak Gas**			
490°C Core Inlet					
Top of Lower Plenum	676	926	584	494	-0.300
Three quarter height	857	1107	677	499	-0.900
Mid Height of Lower Plenum	686	936	589	494	-1.500
Quarter height	597	847	547	498	-2.006
Bottom of lower plenum	529	779	511	495	-2.417
590°C Core Inlet					
Top of Lower Plenum	727	977	659	593	-0.300
Three quarter height	874	1124	734	596	-0.900
Mid Height of Lower Plenum	733	983	662	593	-1.500
Quarter height	665	915	630	595	-2.006
Bottom of lower plenum	616	866	604	591	-2.417
C/C thickness = .005 m Kaowool thickness = 0.005 m ** Hot streak temps were estimated by adding 250°C to mean gas temp.					

The insulator should be a solid refractory ceramic specifically developed for use as high-temperature insulation. This is the same recommendation as was made for the hot duct. The technology development program should include candidate refractory ceramics because of their durability in the NGNP environment and their low conductivity. Irradiation effects are not expected to be large for the low fluence areas, but this needs to be verified by evaluation. In addition, the effects of corrosion on ceramic insulation materials needs to be determined.

5.9 Shutdown Cooling System (SCS) Gas Entrance Tubes

The SCS gas entrance tubes provide a flow path for the primary coolant from the reactor core outlet plenum to the entrance of the SCS heat exchanger as shown in Figure 5-27. These tubes pass through the bottom layers of the graphite core support and the metallic core support load bearing insulator pads. Continuing, they pass through the metallic core support bottom plate and exit above the SCS heat exchanger.

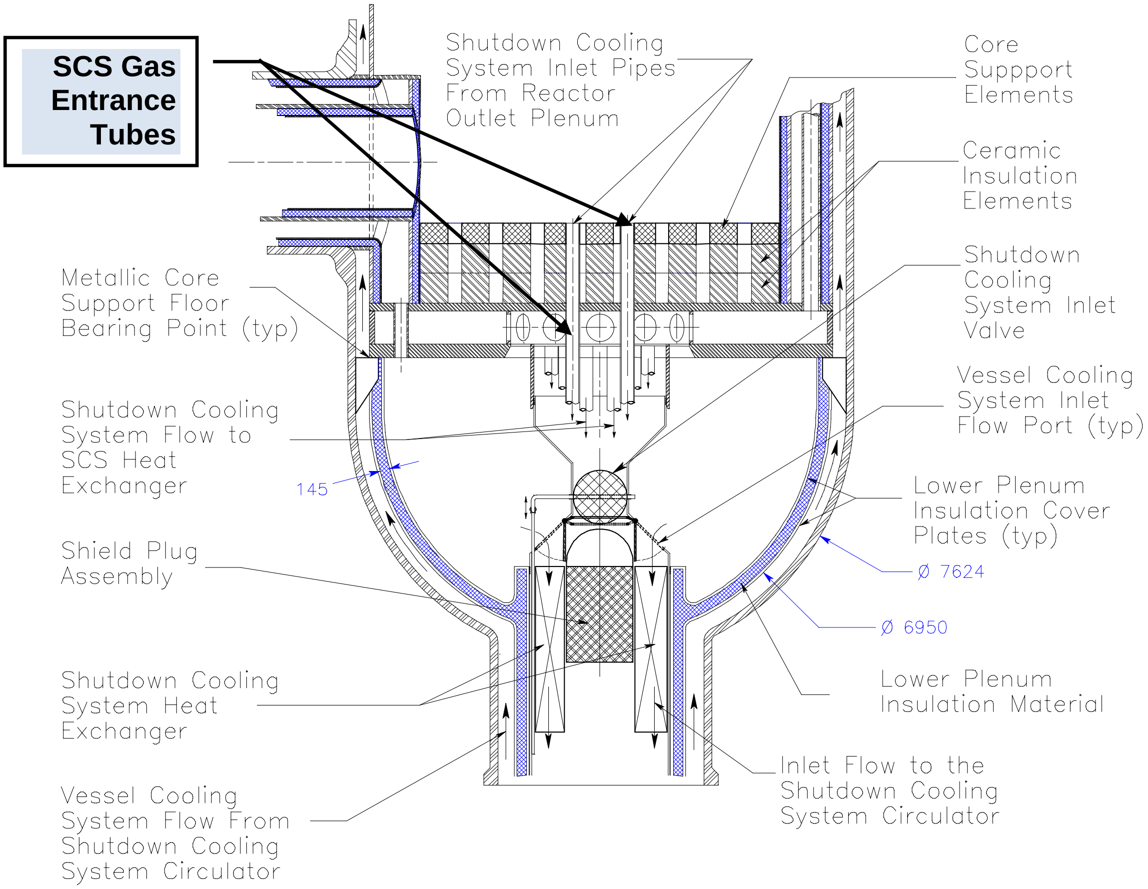

Figure 5-27. SCS entrance tubes connect reactor exit plenum with entrance to SCS HX

During reactor power operation, the SCS entrance tubes are valved closed and no primary coolant flows through them. However, the upper ends of the tubes interface with the graphite core support. Thus, during normal operation and CCD transients, the upper ends of the tubes come in contact with the complex flow and associated hot streaks of the primary coolant. To shut down the reactor, the control rods are inserted and the latent heat of the reactor graphite pile is removed by the main heat transport system. After this, the SCS is activated to remove core decay heat.

When the SCS is operational, the entire length of the SCS entrance tubes experience the hot gas exiting from the core. During a CCD event, there is the option to turn on the SCS for additional cooling, if needed. The SCS entrance tubes may experience very hot gas at the beginning of this type of operation until the core is cooled sufficiently to bring the gas temperature down to about 950°C.

The neutron radiation fluence in this area is low as it is for the whole lower plenum region. The SCS entrance tubes will experience a fluence of 8.5×10^{21} n/m^2 (0.00011 dpa) over the 60-year life of the reactor. These tubes are to be designed for the complete reactor lifetime of 60 years.

The SCS entrance tubes steady state temperatures at full reactor power are listed in Table 5-17. The temperatures decline exponentially from the steady state temperatures during a CCD transient in the same fashion as for all components in the lower plenum area. The upper ends of the entrance tubes are exposed to lower plenum hot streaks that are potentially 250°C higher than the mixed mean gas temperature.

Table 5-17. SCS Entrance Tube Steady State Temperatures

Component	**Location**	**Temperature (490°C Inlet Temp) (C)**		**Temperature (590°C Inlet Temp) (C)**	
		Mean Temp Gas	**Hot Streak Gas**	**Mean Temp Gas**	**Hot Streak Gas**
SCS Entrance Tubes	Lower Plenum End Entrance	949	1199**	949	1199**
	SCS End Exit	~ 949*	NC	~ 949*	NC

* The tube temperature at the SCS end is probably lower than this conservative estimate.

** Hot streak temps were estimated by adding 250°C to the mixed mean gas temperature. They should be concentrated at the lower plenum end of the tube (upper end of tube).

NC = Not calculated

The low fluence and very high temperature at the top end of the SCS entrance tubes makes a compelling case for selecting a C/C composite for this application. Metallic tubes could not withstand the high temperatures. The SCS entrance tubes are about 2600-mm long, with a diameter of 200mm. Given the similarity in fit, form, and function of these tubes to the control rod and RSM guide tubes, it is likely that these tubes would also be fabricated from filament- or tape-wound fiber-reinforced C/C composites.

The thermal barrier assembly for the tubes means that this component will be made from two concentric tubes made from C/C composites with insulation material between them. The selection of this insulation material will favor hard ceramic materials. The selection of the specific ceramic will need to be the subject of a more detailed design study in the future.

5.10 Shutdown Cooling System Heat Exchanger (HX) Thermal Barrier Assembly

The SCS thermal barrier forms a heat flow barrier between the core inlet gas, which is at a temperature of up to 590°C, and the vessel coolant gas, which is at about 250°C, as shown in Figure 5-28[5]. It also limits heat flow from the SCS heat exchanger entrance gas at up to 950°C and the vessel coolant gas. Localized high temperature in the immediate areas of the gas exiting the SCS entrance tubes may be as high as 950°C. Most of the barrier will be experiencing gas at 590°C.

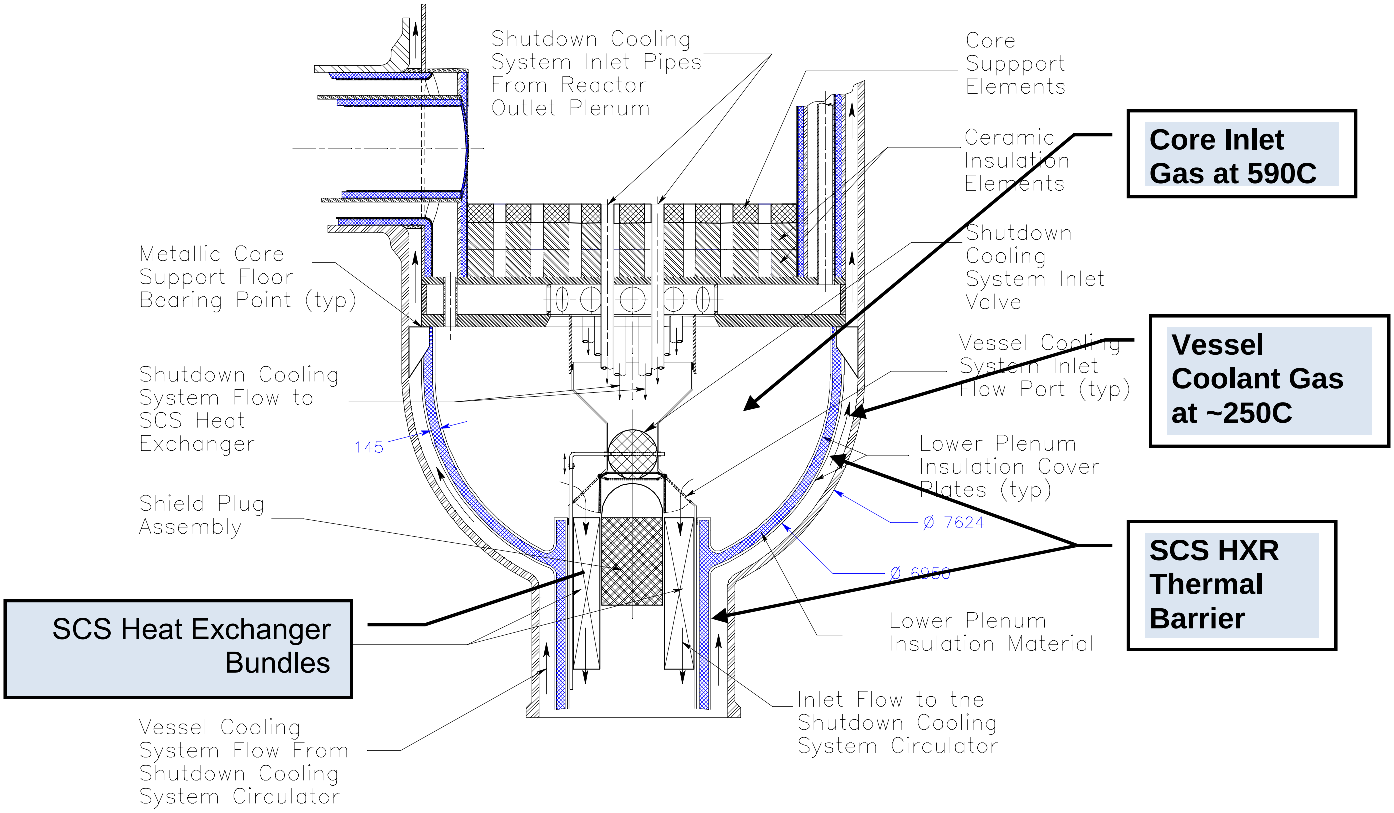

Figure 5-28. SCS HX thermal barrier assembly

---

[5] Figure 5-28 illustrates a pre-conceptual concept for a reactor vessel cooling system in which the SCS is the source of the cold helium used to directly cool the vessel. This reactor vessel cooling concept is just one of a number of options that are under consideration, and it should not be assumed that it is the preferred option at this time. The design of the reactor vessel cooling system for the NGNP, if direct vessel cooling is determined to be required, will be developed during NGNP conceptual design.

The thermal barrier in this area is required to last the complete reactor lifetime of 60 years.

The neutron radiation fluence in this area is low as it is in the whole lower plenum region. These structures will experience a fluence of 8.5×10^{21} n/m^2 (0.00011 dpa) over the entire 60-year life of the reactor.

The SCS heat exchanger thermal barrier is expected to experience the steady state temperatures listed in Table 5-18. The thermal analysis that generated these temperatures (Ref. 4), assumed that the insulation material was Kaowool and that there was boronated graphite shielding in the assembly. The actual thermal barrier will not have boronated graphite shielding. The insulation may not be Kaowool, but a solid ceramic insulator. This does not affect the predicted temperatures much because the area is dominated by 590°C gas on one side and ~250°C gas on the other side of the thermal barrier. The temperatures decline exponentially from the steady state temperatures during a CCD event as shown in Figures 5-29 and 5-30.

Table 5-18. SCS HX T/B Assembly Steady State Temperatures

Component	**Location**	**Temperature (C)**	
		490°C Inlet Temp	**590°C Inlet Temp**
SCS Heat Exchanger T/B Assy	Hot Side T/B Cover Pl	483	580
	Kaowool Insulation Blanket	368	423
	Boronated graphite Shielding	255	270
	Cold Side Metallic Structure	254	269

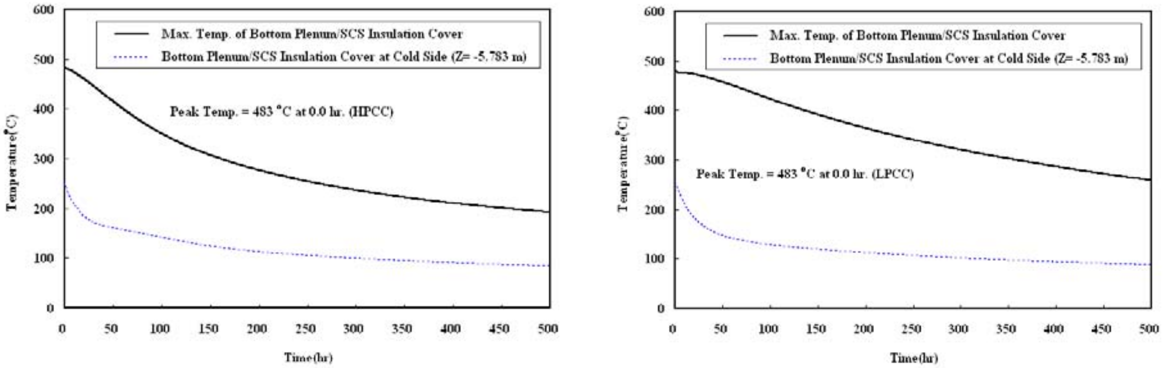

Pressurized Conduction Cool Down
Peak Temp = 483°C

Depressurized Conduction Cool Down
Peak Temp = 483°C

Figure 5-29. SCS HX T/B cover plate temperatures for CCD transients with T_{in} of 490°C

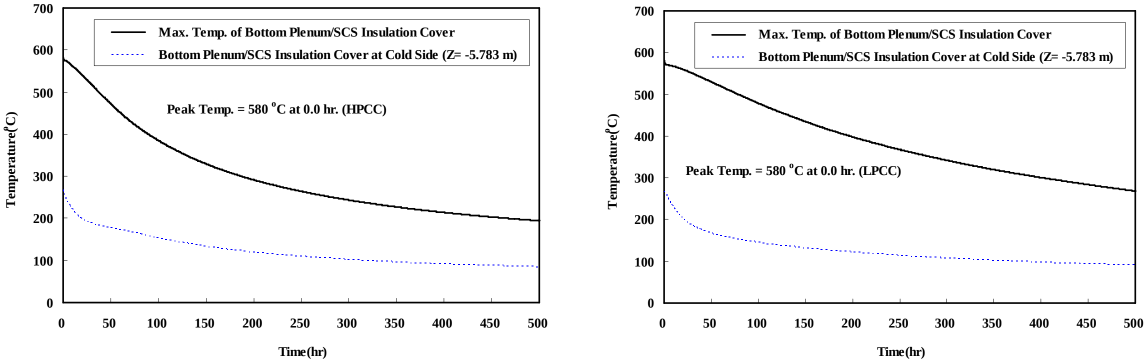

Pressurized Conduction Cool Down
Peak Temp = 580°C

Depressurized Conduction Cool Down
Peak Temp = 580°C

Figure 5-30. SCS HX T/B cover plate temperatures for CCD transients with T_{in} of 590°C

According to the thermal analysis, the maximum temperature this component experiences is 580°C. This temperature is not high enough to require the use of ceramic or C/C composite materials. Therefore, a metallic solution (e.g. Alloy 800H, or Hasteloy X) should be more cost-effective in this application.

The choice of materials for this region can be metallic cover plates with either ceramic fiber blankets or solid ceramic insulators. The final choice will be made in the detail design phase. Suffice to say that ceramic composites are not needed for this application.

6 ANTICIPATED CODIFICATION REQUIREMENTS

This section assesses the readiness level of the industry standards needed for design, fabrication and quality control of the metallic, ceramic, and ceramic composite materials to be potentially used for high-temperature components of the NGNP Reactor System.

Metallic materials are well codified. The only challenge with respect to the metallic material codes is to determine how to extend the codes to higher temperatures (which is no small task). The calendar time required to obtain high temperature data, convert it to design information, and obtain ASME code committee approval is typically too long for a nuclear plant that is scheduled to be deployed in the year 2021 because the design would have to be completed by the end of 2014 to be able to complete fabrication and installation of components by 2019. That leaves only five years from 2009 to test the materials, evaluate the data, modify the code, and obtain approval by the committee members to extend the existing metallic alloys to higher temperature applications. This is considered by the author to likely be too little time to make such changes.

Work on the ASME code has been on-going at various organizations for ceramic composites based on the ASME Code approach for graphite. Work is also on-going on ASTM test standards and material specifications, ASM standards, and industry standards for material testing and design where no standards exist. Some ASTM and ASM standards are complete, but many are in draft form or have not been started.

6.1 Applicable ASME Codes

6.1.1 Metallic Materials

The ASME Code, Section III, Div. 1, and high temperature code cases for metallic materials (Ref. 5) are applicable to the design and fabrication of high temperature metallic components. Extension of these metals to higher temperature limits is possible, but of marginal value for the NGNP with a 950°C reactor outlet helium temperature and a 490°C to 590°C reactor inlet helium temperature. Non-metallic materials are required to provide the capability for these high-temperature components.

6.1.2 Ceramic Materials

There is an ASME code section being developed for the design and fabrication of ceramic composites for nuclear applications. The code section is to be developed along the lines of the nuclear graphite code section. Currently, the ASME Code, Section III, Div. 2, Subsection CE for Graphite (Ref. 6) is well under way (it has been in progress for at least 20 years). The current chairman of the Working Group for this code is Dr. Timothy Burchell of ORNL. The ceramic composite code section is also being developed by this working group at the present time.

The committee is just getting started and a large increase in effort will be needed to get the standard for ceramic composites up to par and accepted by the main committee. This effort should be given high priority in the NGNP technology development program. From a cursory review of the INL and ORNL proposed technology programs, this priority is well recognized by the material technologists working the graphite and ceramics areas.

The introduction of ceramic composite materials helps reduce the effect of brittleness associated with monolithic ceramics because the composites posses cross-linked fibers that act as crack stoppers. The apparent toughness is higher in these materials allowing them to be used in components with high tensile stresses. These ceramic materials are excellent replacements for metals where the temperatures are too high.

Design standards are available for monolithic ceramics and low-temperature C/C composites, but high-temperature ceramic composites are relatively new and the existing standards need to be extended to higher temperatures. As a minimum, new ASME code cases are required for the materials concerned. The process for this is well understood for metallic materials with every issue of the ASME boiler and pressure vessel code, Section II, for material properties, prefaced by guidelines for approval of new materials.

How these guidelines translate for approval of ceramic and ceramic composite materials is not currently clear. The ASME Subgroup on Graphite Core Components has the job of investigating this question, and producing a strategy for the approval of new materials. As of September 2008, it has produced few guidelines for the codification of ceramic or ceramic composite materials. However, it is anticipated that similar processes for the acquisition of technology will be followed as are current in the aerospace industry where experience using ceramics and ceramic composites is extensive.

It is anticipated that design and material standards developed for use in reactors, whether sponsored by the ASME Code committees or some other industry standards, will require data for selected materials of at least three identical heats/casts/cures, for different weave architectures, from different sample component sizes and temperatures, and in different directions to account for the orthotropic nature of ceramic composites. Properties to be obtained include:

- Mechanical Properties
  - Strength (tensile, compressive, flexural)
  - Modulus
  - Poisson’s ratio
  - Toughness
  - Creep rate

  - Fatigue properties
  - Fracture Toughness & Crack Propagation Rates
  - Phase stability
- Physical Properties
  - Bulk density
  - Thermal expansion
  - Thermal conductivity
  - Specific heat
- Environmental Effects
  - Nuclear Radiation Effects
  - Corrosion Effects in an impure reactor helium coolant
- Joining Processes

It should be noted that, while the legacy procedures for metallic materials have generally been for ASME to incorporate an ASTM or ASM standard directly into the Boiler and Pressure Vessel Code, the guidelines permit the incorporation of standards from other bodies, such as ISO. Extension of the design standards, material behavior models, methods of fabrication and quality control from the aerospace industry is a good place to start the development of these standards.

Incorporation of ceramic or ceramic composite materials into the code will require a national or international standardization authority, such as ASTM, ASM, ISO, or SAE AMS to develop a standard which can then be presented to the ASME Code Committee for consideration.

6.1.3 ASTM Standards

ASTM standards for testing ceramic materials operate under Committee C28 on Advanced Ceramics. The current chairman of this committee is Dr. Stephen Gonczy of Gateway Materials Technologies. The Committee is made up of several subcommittees. The committee for monolithic ceramics is C28.01. The committee for Ceramic Matrix composites is C28.07, which is chaired by Dr. Yutai Katoh of ORNL. Currently the test methods for composites are being developed at INL and ORNL and codified in the C28.07 subcommittee. The program plan is well thought out. Test specimens have been developed and are to be tested in a planned round-robin set of tests involving ORNL, INL, and CEA (with help from Prof. Jacques Lamon, of the University of Bordeaux, Apessac, France) (Ref. 8). This program is behind schedule due to reduced activity in 2006 and 2007. Test specimen standardization needs to be given high priority to support deployment of the NGNP in year 2021.

ASTM specifications for controlling the performance and quality of ceramic materials are much further behind the testing standards because the emphasis has been on characterizing the materials in a nuclear environment.

6.2 ASM Standards

ASM has two series of standards for applicable materials, the Cer- and Cp- series. For example, ASM Cp-19 deals with ceramic fiber reinforced alumina composites. The status of these standards needs to be investigated further because there was not enough time to investigate them thoroughly during this study.

6.3 Other Standards

The purpose of this section is to identify industry standards that could be used in lieu of American standards that have not yet been developed to the extent that they are readily available. It is also anticipated that non-commercial design and material standards exist that can be used for design purposes.

There are commercial standards used in the design of components using ceramic materials. Statistical failure models are the norm since ceramics generally exhibit high strength, but brittle behavior with relatively low fracture toughness. The introduction of ceramic composite materials helps reduce the effect of brittleness with cross-linked fibers that act as crack stoppers. The apparent toughness is higher in these materials allowing them to be used in components with high tensile stresses.

There was insufficient time available during this current study to fully investigate these commercial standards and their applicability to the NGNP project. This should be part of a further investigation to establish which standards will be adopted for design, quality control and fabrication. Further study of how the aerospace industry developed and uses design standards, material models, and fabrication controls should be conducted as a starting point for the development of such standards for nuclear reactor design and fabrication (see Appendix H).

The following is an example of how Rolls-Royce works with commercial standards for ceramics and ceramic composite structures. Rolls-Royce operates and controls its own internal system for specifications, processes and procedures to control all aspects associated with the development and operation of components and systems in safety critical applications across all the business sectors in which the company operates. These business sectors are civil aerospace, defense aerospace, marine (which includes nuclear power generation plants) and energy (also including civil nuclear power).

Rolls-Royce has an internal structure to produce and control specifications and standards for materials (MSRR), manufacturing processes (RPS), quality (RQS), design (JDS), engineering (JES) and all other processes operated within the Company.

For the introduction of new materials, Rolls-Royce uses a process that is based on the NASA technology readiness level (TRL) system together with internal controls. The material capability acquisition process (GQP X.T.1.4) operated within the company is a gated review process that at local and senior management level involves three and two review stages respectively before these management panels. The issues covered within the process are customer needs and requirements, material supply and processing, material development program, health and safety, cost considerations, a program risk review, component operating environment, methodologies to support life assessment and design, material property databases, required documentation, arising IPR, and validation of material technology. A similar process is operated for the introduction of new manufacturing processes (MCRL). A Materials Advisory Board consisting of a panel of independent academic experts is also available to assess new materials and processes.

The generation of material property data required to support the introduction of a new material is also closely controlled within Rolls-Royce. The test equipment and methods operated by Rolls-Royce or sub-contractors is controlled by either Rolls-Royce or international standards for operation and calibration, and subject to audit by Rolls-Royce personnel. The raw data generated from mechanical test programs is closely controlled within Rolls-Royce, and procedures exist that specify the level of testing required to generate design quality data for the different levels of component classification (critical, sensitive etc). Design curves are generated from the raw test data using established analysis routines and stored electronically within the company for access by the design and life assessment routines that are used in the component definition process.

Personnel from Rolls-Royce actively participate in the committees of several international bodies that exist to review and introduce new standards and specifications for materials and associated test requirements to maintain currency.

7 TECHNOLOGY DEVELOPMENT REQUIREMENTS

Development issues have been identified in Section 5 for the materials needed for the NGNP reactor system high-temperature components and in Section 6 for design and material standards. This section summarizes the technology issues associated with the use of ceramics and ceramic composites in the NGNP and outlines the technology development needed to resolve the issues. The priority for both design and fabrication needs is driven by the NGNP program notional schedule to deploy the NGNP by the year 2021. Section 7.1 discusses a notional schedule for the interaction between NGNP design and the technology program, Subsection 7.2 covers technology needs in the form of DDNs, and Subsection 7.3 discusses the technology issues that fall out of the examination of the technology notional schedule and the issues arising from the engineering assessments in Section 5.

7.1 Technology Development Schedule

The NGNP is to be deployed by 2021. Thus, to determine the timing of the technology development program, one must lay out a practical schedule as a framework for executing a technology program that gives priority to what can be reasonably accomplished in the available time. A reasonable notional schedule is shown in Figure 7-1.

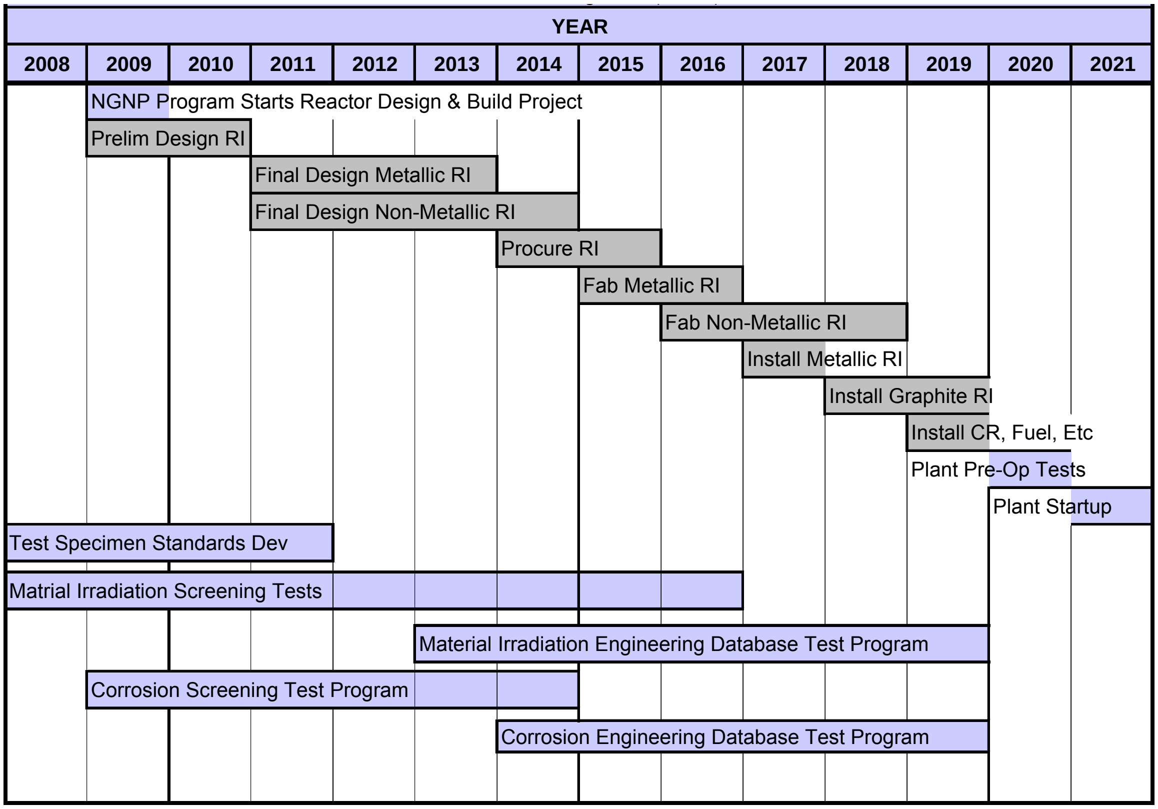

Figure 7-1. Summary-level composites technology development schedule

This is a very ambitious notional schedule that has the following features:

- The design-fabricate-install-startup program starts in earnest at the beginning of 2009
- The preliminary design is completed by the end of 2011
- The final design is competed by the end of 2014
- Procurement of hardware starts in 2014 and is complete at the end of 2015 (this is ordering the hardware)
- Fabrication starts in 2015 for the large metallic components
- The non-metallic fabrication starts in 2016
- Installation of components is phased and must be complete by the end of 2019
- The year 2020 is reserved for preoperational tests
- In year 2021, the plant is in the start up mode

Ideally, the technology program should be completed prior to completion of the final design phase so that the basis for the design is well established. This is six years into the program. Thus, all screening tests and engineering database tests need to be completed in six years. Completing the technology program in six years would only be possible if there were very few technology issues to solve. Since new materials are being introduced into this reactor to handle high-temperature service conditions, there is a considerable amount of testing needed to screen materials and obtain an engineering database. Thus, the technology program will likely run into the fabrication phase, and possibly into the installation phase. This means the design will have a certain amount of risk associated with less-than-complete data sets for the design basis.

The technology program has to have certain elements to be complete. These elements are as follows:

- Standards for test specimens and material specifications (ASTM/ASM)
- Design and fabrication criteria completion, such as ASME Code changes
- Conduct screening tests to select materials
    - Nuclear effects screening
    - Corrosion effects screening
    - Initiation of material models
    - Initiation of design criteria
    - Aspects in the tests that support material model development
- Engineering data base phase with a statistically significant quantities of data
    - Nuclear effects tests on selected materials
    - Corrosion effects tests on selected materials
    - Completion and validation of material models against test data
    - Completion and validation of design criteria against test data

These elements are shown in the notional technology development schedule in Figure 7-2. By laying out the test program that supports the design and build effort, one can see what has to be emphasized in the test program to provide the information needed for the various stages of the overall effort.

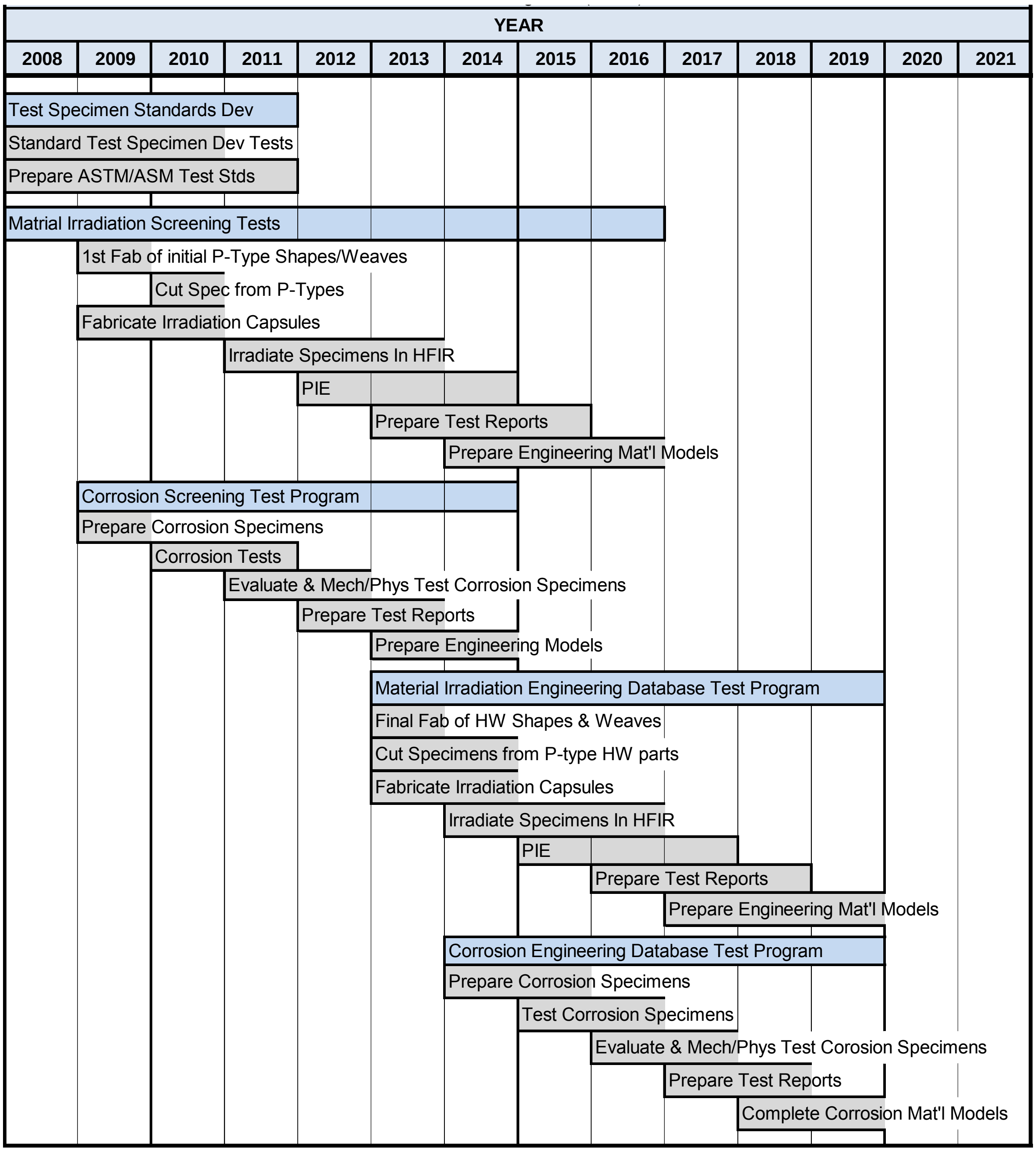

Figure 7-2. NGNP reactor materials technology development notional schedule

It is obvious that the standards for testing must be established before much testing is completed to have confidence in the data being generated. Second, but not so obvious, is that the tests to be performed must necessarily be influenced by the material behavior models, the failure models, and the design criteria being used for design validation. Past experience compels us to make sure that the models are well understood so that the proper tests will be performed to provide the particular test data necessary to derive the coefficients in the material behavior and failure models.

The program laid out in Figure 7-2 goes all the way to the final installation of the hardware. This means that there will be some risk that the hardware being fabricated and installed will not meet requirements if the needed test data is not available. Rework of hardware in the fabrication phase usually results in delays in the schedule and in added cost.

The issues derived from the notional schedule are as follows:

1. Standards (ASTM/ASM) for tests and material specifications are not being pursued fast enough to be ready for the accelerated test program. This jeopardizes the validity of the test data that will be obtained from the tests that are performed. Round-robin tests to confirm test specimen configuration need to be completed.

2. Irradiation tests are not being performed fast enough to support deployment of NGNP by 2021. This is especially true if more candidate materials are introduced into the test program. At present, there are only two ceramic composites being tested for irradiation affects; FMI-222 C/C composite, and Hi-Nicalon^{TM} SiC/SiC composite. PAN fiber C/C composites may work in a low-radiation environment.

3. Corrosion tests are needed, but are not being performed at this time. Screening tests should be performed at the earliest possible date to determine if C/C composites have a problem in the NGNP environment. Engineering database tests also need to be performed once final material selection has been completed.

4. Composite material models and design criteria are not available for NGNP test development, and to support the design effort. Tests must to be designed with known material models so that the correct tests will be performed. The design effort must show how the design meets the design and safety requirements. It is necessary that the design criteria that will be used in the design process are well formulated so the designers can assess how well their designs meet requirements. They don't have to have all the data until the end of design when the final design analyses are completed, but any missing data adds risk to the design as it goes into production. However, this happens all the time for design of new systems and should not be a deterrent to moving forward.

5. Design Standards are inadequate. The upgrading of design standards, such as the ASME code, takes a long time and should get started in earnest to meet the notional schedule.

6. A disciplined materials development, engineering, and manufacturing process is lacking in the Technology Program. The methodology for this very important process can be borrowed from the Aerospace industry. Appendix H describes the elements of a ceramic material technology program being conducted by Rolls-Royce for the controlled development of ceramic composite materials for use in aerospace and nuclear power structures.

7.2 Technology Needs

The technology readiness levels (TRLs) of the high-temperature hardware of the reactor system are mostly at 2 and 3. The type of data needed for monolithic ceramics and ceramic composites is fundamental materials data reflecting the need to understand the basic behavior of the material and the effects of both neutron irradiation and corrosion on the life of the components to be fabricated from these materials. There are 36 new DDNs identified for the reactor internals recommended to be made from ceramic composites. These are associated with six different components and are shown in Table 7-1. Each component has the same set of DDNs with slightly different conditions. The types of DDNs are: 1) irradiation effects, 2) basic material properties, 3) corrosion effects in an impure helium environment, and 4) manufacturing process development. Maintaining DDNs on a component basis allows tracking of where the request for data arose and the specific conditions needed for the data. It also gives insight into how the data will be used in the engineering process so tests can be tailored accordingly. The new DDNs for each component should be prepared to identify the required data and testing, and the identified tests should be included in the technology development program.

DDNs already exist for the monolithic ceramics, so no new DDNs are needed for components to be fabricated from these materials. The test program for monolithic ceramics should be expanded to include solid ceramic insulation as a potential replacement for fibrous insulation. However, fibrous insulation will most likely still be used in areas where the temperatures are sufficiently low.

7.3 Summary of Technology Issues

Technology issues have been identified as part of the process of selecting materials for the Reactor System high temperature components. In addition, the technology program as a whole has been evaluated. The issues have been integrated into common areas and are listed in Table 7-2 along with proposed resolution activities.

Table 7-1. New Design Data Needs for Reactor System Internals

DDN NO.	DDN TITLE	SOURCE
C.11.00	REACTOR System (RS)	
C.11.01	Neutron Control System	GT-MHR
N.11.01.12	CR & RSM Guide Tubes - Effect of Low Level Irradiation on Composite Materials	New
N.11.01.13	CR & RSM Guide Tubes - Composite Material Properties	New
N.11.01.14	CR & RSM Guide Tubes - Effects on Composites of Primary He and Temperature	New
N.11.01.15	CR & RSM Guide Tubes - Composite Component Manufacturing Process Development	New
C.11.02	Reactor Internals and Hot Duct	GT-MHR
N.11.02.17	Hot Duct & LP Sidewall T/B - Effect of Low Level Irradiation on Composite Materials	New
N.11.02.18	Hot Duct & LP Sidewall T/B - Composite Material Properties	New
N.11.02.19	Hot Duct & LP Sidewall T/B - Effects on Composites of Primary He and Temperature	New
N.11.02.20	Hot Duct & LP Sidewall T/B -Composite Component Manufacturing Process Development	New
N.11.02.21	UPS-Effect of Low Level Irradiation on Composite Materials	New
N.11.02.22	UPS-Composite Material Properties	New
N.11.02.23	UPS- Effects on Composites of Primary He and Temperature	New
N.11.02.24	UPS-Composite Component Manufacturing Process Development	New
N.11.02.25	UCR-Effect of Low Level Irradiation on Composite Materials	New
N.11.02.26	UCR-Composite Material Properties	New
N.11.02.27	UCR- Effects on Composites of Primary He and Temperature	New
N.11.02.28	UCR-Composite Component Manufacturing Process Development	New
C.11.03	Reactor Core	GT-MHR
N.11.03.53	Control Rod - Effect of High Level Irradiation on Composite Materials	New
N.11.03.54	Control Rod - Composite Material Properties	New
N.11.03.55	Control Rod - Effects on Composites of Primary He and Temperature	New
N.11.03.56	Control Rod - Composite Component Manufacturing Process Development	New
C.14.04	Shutdown Heat Exchanger (SHE)	GT-MHR
N.14.04.13	SCS Entrance Tube T/B - Effect of Low Level Irradiation on Composite Materials	New
N.14.04.14	SCS Entrance Tube T/B - Composite Material Properties	New
N.14.04.15	SCS Entrance Tube T/B - Effects on Composites of Primary He and Temperature	New
N.14.04.16	SCS Entrance Tube T/B - Composite Component Manufacturing Process Development	New

Table 7-2. Technology Issues for Reactor System High Temperature Components

Issue	Proposed Resolution Activity
There are not enough high temperature composites in the technology program. Only two serious candidates: • FMI-222 C/C Composite, and • Hi-Nicalon^{TM} SiC/SiC Composite	Broaden program to include: • PAN Fiber C/C for low fluence application • Other SiC/SiC composites • Reduce dominance of hi-fluence needs of Fusion program • 2-tiered program needed separated by fluence level: o Hi-Fluence up to 30dpa o Low fluence < 0.04 dpa and lower
Acceptable level of Cobalt in hi-temp metallic alloys not defined rigorously enough causing rejection of good hi-temperature alloys like Haynes 230.	• Develop a sound technical basis for allowable Cobalt concentration in metal alloys • Determine adverse effect of Cobalt in alloys on Reactor Sys.
Fibrous blanket insulation missing from technology program	• Select candidate fibrous blanket insulation materials for thermal barrier • Include them in test program
Solid ceramic thermal insulation materials not included in the technology program to replace fibrous blankets.	• Select solid ceramic insulation to replace ceramic fiber blankets in thermal barrier. • Test these materials for NGNP environments • Establish an engineering database • Develop Engineering material models for design and system assessments • Establish supply chain.
Monolithic ceramics for use in load bearing insulators not included in test program	Add monolithic ceramics to test program • Test these materials for NGNP environments • Establish an engineering database • Develop Engineering material models for design and system assessments • Establish supply chain
Composite manufacturing input to design process is lacking	Include fabricators input to avoid testing wrong materials: • Early in program to assure components can be produced • Assure choice of composite and it's architecture are correct for product • Assure the correct composites are tested

Issue	Proposed Resolution Activity
ASTM/ASM Standards for material tests and specifications are not being pursued fast enough to be ready for accelerated test program	Expedite Stds development • Complete std spec design ASTM, ASM, other • Complete planned round-robin tests on standard specimens • Complete standards prep by end 2011
Irradiation test not being performed fast enough to meet year-2021 deployment	Expedite Irradiation tests • Develop test program that will complete irradiation tests by end 2013 • Expedite screening tests on candidate composites • Select Final Composites for test
Corrosion tests not being performed	Expedite Corrosion tests • Develop test program that will complete corrosion tests by end 2011 • Select labs to do corrosion tests • Expedite screening tests on candidate composites • Select Final Composites for test
Composite material models and design criteria not available for NGNP test and design effort	Expedite task to develop composite behavior models and design criteria: • Mat'l behavior models • Failure Models • Design Criteria • Define tests that support Material Models & Criteria
Design Standards are inadequate	• Escalate design standards through the ASME code development. • Use the aerospace industry experience for material testing, design and fabrication standards as a model to modify for use in nuclear reactors
Test Program not emphasize acquisition of engineering database of statistical significance	Develop 2-tiered test program • Screening tests to confirm material selections (Currently on-going at low level) • Engineering Database test program o Large database on composites needed o Need to include variation in properties from lot-to-lot and part to part of composite components o Support and Validate mat'l models & design criteria
A disciplined Materials Development, Engineering, Manufacturing, process is lacking in the Technology Program.	• Develop a materials control program like those used in the aerospace industry (See Appendix H)

8 CONCLUSIONS AND RECOMMENDATIONS

This section lists the essential conclusions of this study regarding the choice of materials for the high-temperature components of the Reactor System and the technology issues associated with use of these materials for the NGNP. It also presents recommendations that, if adopted, should enhance the potential for successful deployment of high-temperature ceramics and ceramic composite materials in the NGNP Reactor System.

8.1 Conclusions

1. The control rod structural elements, which experience a very high radiation fluence, should be fabricated from a 3-dimensional C/C composite because the maximum temperature during a CCD event is 1500°C. Currently, FMI-222 is the only candidate that has enough radiation data to be selected for the control rods. The maximum life appears to be eight years. This life is adequate because the control rods can be replaced easily. The corrosion resistance of this material in the expected NGNP reactor helium environment must be evaluated on an expedited basis to ensure there are no life-limiting corrosion effects.

   A longer term choice for this material is a SiC/SiC composite, possibly Hi-Nicolan^{TM}, due to its apparent much greater radiation and corrosion tolerance. However, at this time it is limited to a temperature of 1400°C. If this limit can be increased, a SiC/SiC composite would be a better choice because the control rod lifetime could be 60 years if this material is used. However, more tests need to be conducted on this material, including corrosion tests, to verify that this choice is correct. Also, the final choice of architecture and SiC/SiC material needs to be completed.

2. The high-temperature components in low fluence locations (<0.04 dpa) should be made from FMI-222 C/C composite or a suitable alternative. These components are:

   - Control rod and RSM guide tubes
   - Upper core restraint elements
   - Upper plenum shroud thermal barrier cover plates and structural hardware
   - Lower plenum sidewall thermal barrier cover plates and structural hardware
   - Hot duct thermal barrier cover plates and structural hardware
   - Shutdown cooling system inlet tube structural elements

   Corrosion tests in the NGNP reactor helium environment should be conducted to determine what life limiting aspects may exist and whether any protective coatings are needed. Alternate materials such as PAN fiber composites might be a less expensive alternate to FMI-222. Verification of radiation and corrosion tolerance for PAN fiber composites needs to be completed before a decision to switch to this lower-cost material can be made.

3. The load bearing thermal insulator pads above the metallic core support should be made of monolithic ceramics. The favored choice for this application is Macor, a glassy ceramic containing a mixture of the oxides of aluminum, lithium, and silicon. It becomes a true compound after heat treatment, instead of a mixture. This material is very stable and can have its thermal expansion varied to match the alloy 800H structure upon which it rests. The number of ceramics available is very large. Thus, the final choice needs to be reviewed to assure the optimum material is chosen for this application. Radiation and corrosion tests need to be conducted to verify the choice before proceeding to full fabrication.

4. The use of fibrous ceramic insulation material for thermal barrier assemblies should be questioned. Legacy fibrous blanket materials Kaowool and Quartz-et-Silice will not withstand the NGNP operating temperatures. There are a number of fibrous blanket insulations on the market that will meet the temperature requirements. However, their capability to withstand the noise vibration and thermal cycling for 60 years of operation without failure is questionable.

5. Thermal barrier solid block insulation material for sandwich type insulation assemblies should be considered. There are a number of microporous sintered ceramics available that are used in solid block form. These are expected to have superior fatigue-life properties over fibrous blanket insulation materials and are more likely to meet the 60-year life requirement in the reactor environment. These products have the lowest conductivity of candidate insulators. Further information about these materials should be obtained from suppliers like Microtherm and Armil CFS (see Appendix G).

6. The Shutdown Cooling System thermal barrier should be the legacy metallic cover plate and fastener design with the fibrous blankets replaced by solid ceramic insulation.

7. In this study, some potentially useable high-temperature metallic alloys such as Haynes 230 and alloy 617 were rejected as potential materials for some reactor components because of their cobalt content. The allowable level of cobalt in reactor system components in very-low fluence locations should be defined and justified to verify whether or not the rejection of these materials was warranted.

8. The permanent side reflector seal sleeves should be made from graphite. There is no need to use C/C composites for this application. The seal sleeves can be an adaptation of the graphite dowels that were used in previous designs by merely replacing the previous solid dowels with hollow dowels that serve the same load-alignment function. The PSR

blocks should be made as large as possible to minimize flow leakage paths around the blocks.

9. The number of composites in the technology program should be increased. There are only two main candidates; FMI 222 3-D C/C composite, and Hi-Nicalon^{TM} SiC/SiC 2-D composite. These have been chosen either for high-temperature capability (the C/C composite) or for high tolerance to radiation (the SiC/SiC composite). For low neutron fluence, PAN Fiber C/C composite, or equivalent, should be added to the program.

10. Completion of the ASME standards for design and fabrication of ceramic composites should be given high priority and expedited to support the design and fabrication of hardware that must be procured in the 2014-2015 time period and fabricated in the 2015 through 2018 time period.

11. Near-term completion of the ASTM and ASM standards for material property testing should be given high priority and expedited to support the screening tests and tests to obtain the engineering data bases that are needed for the material models and design criteria. The confidence in the data will be greatly enhanced if accepted standard test specimens are used.

12. Completion of the ASTM and ASM standards for material specifications used to control fabrication of ceramic composite materials should be given high priority and completed in time to support hardware that is to be procured in the 2014-2015 time period and fabricated in the 2015 through 2018 period.

13. The materials test program should be completed no later than the end of 2016 to support deployment of the NGNP in the year 2021.

14. Start of corrosion tests of materials in the primary coolant helium environment should be expedited to assure that the candidate ceramic materials, both composite and monolithic, will meet the life requirements of the NGNP. Corrosion tests should be completed by 2014.

15. The activity to choose the material behavior and failure models for ceramic composites should start in the year 2009 to assure that the test program obtains the correct data to support these models.

16. The activity for incorporating the material and failure models into design analysis computer codes should start in 2013 to support the design effort. An organization should be assigned to initiate and lead this task.

17. The screening test program should be expedited within the technology program to finalize material selections as early as possible.

18. There is a need to establish quality control procedures that assure the engineering database is governed by standards that will produce repeatable data and correct application to the design and fabrication of the NGNP reactor materials and equipment (see Appendix F).

8.2 Recommendations

1. Include other ceramic composites materials in the technology program such as PAN fiber C/C composites for low radiation applications.

2. Include a 3-D SiC/SiC composite material that can be used above 1500°C for long lived control rod structural elements.

3. Include selected monolithic ceramic materials in the technology program for load bearing thermal insulators and insulators to replace fibrous insulation blankets.

4. Initiate an activity to evaluate very-high-temperature ceramic fiber insulation materials identified in this report for use in sandwich-type insulation assemblies.

5. Initiate an activity to establish the level of cobalt that is permissible in reactor system components. This is needed to determine if high-temperature metallic alloys such as Haynes 230 and alloy 617, which have relatively high cobalt content, can be used for components that are subject to low neutron fluence.

6. Increase the activity level for preparation and completion of ASTM standards for ceramic composite materials irradiation test specimens.

7. Assign high-priority to completion of the round-robin test plans for the standard test specimens so that the data generated by the testing will be obtained on generally acceptable specimens.

8. Initiate an activity to prepare ASTM and ASM specifications to control fabrication of ceramic composite materials.

9. Initiate an activity to define the ceramic composite material and failure models for insertion in design computer codes so the proper tests will be conducted and the models will be ready for the design activity.

10. Initiate corrosion tests to aid in screening candidate ceramic materials. It is insufficient to select the materials based on radiation behavior only.

11. Evaluate the envisioned material control processes by comparing what the technology program is planning with what is now being done in the aerospace business for the composite materials they have been used for about 20 years.

12. The conclusions and recommendations of this study as presented herein should be incorporated to the extent practical into the overall NGNP technology development program plan.

9 IMPACT OF LOWER REACTOR OUTLET HELIUM TEMPERATURE ON NEED FOR COMPOSITES

At this writing, strong consideration is being given to reducing the nominal reactor outlet helium temperature for the NGNP from 950°C into the range of 750°C to 800°C (with a corresponding reduction in the reactor inlet helium temperature), and it appears that this change will be officially adopted by DOE. However, this composites R&D issues study was started and largely completed while the reactor outlet helium temperature objective for NGNP was still 950°C. Thus, the focus of the study was to evaluate the need for composites and the composites R&D issues associated with a reactor operating at this temperature. However, a cursory evaluation was performed as a late add-on to the study to assess the potential impact of the expected reduction in helium coolant temperatures on the need to use ceramic and ceramic composite materials for reactor system components in the NGNP.

The approach taken in this evaluation was to estimate the impact of reducing the reactor outlet helium temperature for the NGNP on the need for ceramic and ceramic composite materials by comparing the operating conditions for the reactor system components in a 600-MWt NGNP operating with a nominal reactor outlet temperature of 950°C (as developed in Sections 3 through 5 of this report) with those in the 350-MW steam-cycle Modular High Temperature Gas-Cooled Reactor (MHTGR) operating with a nominal reactor outlet gas temperature of 687°C. In the analysis, it was assumed that scaling up the steam-cycle plant power level from 350 MWt to 600 MWt does not change the key operating conditions that drive the choice of materials. It was also assumed that the neutron fluence levels and primary coolant impurities would not be sufficiently changed to impact the selection of materials. Table 9-1 compares the operating conditions for the two plants.

Reduced nominal reactor outlet helium temperatures of 750°C and 800°C were considered in this evaluation. The corresponding reactor inlet helium temperatures were obtained by assuming the core helium temperature rise to be 428°C, which is the same as in the 350-MWt steam-cycle plant. An adjustment was made to the maximum design temperatures for the various high-temperature components in the NGNP operating at 950°C reactor outlet helium temperature (as given in Table 5-1) to account for the reactor outlet helium temperatures differences. Materials were then selected based on the capability of the materials to withstand the adjusted temperatures. Tables 9-2 through 9-4 summarize the adjusted temperatures material evaluation and selection for reactor inlet/outlet helium temperatures of 259°C/687°C, 322°C/750°C, and 372°C/800°C, respectively.

Table 9-1. Operating Conditions for the NGNP and 350-MWt Steam Cycle MHTGR

Parameter	350-MWt SC		600-MWt NGNP	
	Value	Units	Value	Units
Reactor thermal power (100% power)	350.0	MWt	600.0	MWt
Core average power density	5.9	MW/m^3	6.6	MW/m^3
System pressure (100% power)	6.39	MPa abs	7.07	MPa abs
Reactor vessel relief valve set pressure (estimated)	7.0	Psia	7.8	Psia
Case 1: Core Tin/Tout 490/950°C				
Core inlet He temp	259.0	C	490.0	C
Core outlet He temp	687.0	C	950.0	C
Primary He total flow rate	157.1	kg/s	248.5	kg/s
Core pressure drop	34.5	KPa	62.4	
Case 2: Core Tin/Tout 590/950°C				
Core inlet He temp	259.0	C	590.0	C
Core outlet He temp	687.0	C	950.0	C
Primary He total flow rate	157.1	kg/s	320.0	kg/s
Core pressure drop	34.5	KPa	103.5	

Table 9-2. Reactor Internal Materials Selection Summary for Tin/Tout = 259°C/687°C

Component	Design Life	Normal Op Design Temp	Off-Normal Design Temp	Temp Limit	Design Fluence		Fluence Limit		Mat'l Selection
		C	C	C	n/m^2	dpa	n/m^2	dpa	
Control Rod	8y Replaceable	642	1368	> 2000	3.22E+26	4.00000	3.22E+26	4	C/C Composite
Control Rod & RSM Guide Tube	60y Replaceable Can be < 60y	252	858	871	1.03E+23	0.00128	3.00E+22	0.002	Hast X
Upper Core Restraint	60y Replaceable. Can be < 60y	222	963	> 2000	3.49E+24	0.04340	3.22E+26	4	C/C Composite
Upper Plenum Shroud T/B Cov Plates	60y	210	796	871	1.20E+22	0.00098	3.00E+22	0.002	Hast X
PSR Seal Sleeves	60y	271	611	2400	3.22E+24	0.04340	3.22E+26	4	Graphite
Metallic Core Supt Load Bearing Insulators	60y	597	597 Drops Exponentially	1000	8.50E+21	0.00011	?	?	Top- Macor Glass Ceramic
	60y	422	422 Drops Exponentially	1000	8.50E+21	0.00011	?	?	Bottom- Macor Glass Ceramic
Hot Duct T/B Assy	60y	686 MM 911 HS	686 Drops Exponentially	927	8.50E+21	0.00011	3.00E+22	0.002	Hast XR
Cross Vessel T/B Assy	60y	258	258 Drops Exponentially.	760	8.50E+21	0.00011	3.00E+22	0.002	Temp. low enough to eliminate T/B
Lower Plenum Sidewall T/B Assy	60y	614 MM 864 HS	614 Drops Exponentially	871	8.50E+21	0.00011	3.00E+22	0.002	Hast X
SCS Entrance Tubes	60y	686 MM 936 HS	686 Drops Exponentially	927	8.50E+21	0.00011	3.00E+22	0.002	Hast XR
SCS HXR T/B Assy	60y	249	249 Drops Exponentially	760	8.50E+21	0.00011	3.00E+22	0.002	Alloy 800H

Table 9-3. Reactor Internal Materials Selection Summary for Tin/Tout = 322°C/750°C

Component	Design Life	Normal Op Design Temp	Off-Normal Design Temp	Temp Limit	Design Fluence		Fluence Limit		Mat'l Selection
		C	C	C	n/m^2	dpa	n/m^2	dpa	
Control Rod	8y Replaceable	705	1400	> 2000	3.22E+26	4.00000	3.22E+26	4	C/C Composite
Control Rod & RSM Guide Tube	60y Replaceable Can be < 60y	315	885	927	1.03E+23	0.00128	3.00E+22	0.002	Hast XR
Upper Core Restraint	60y Replaceable. Can be < 60y	285	994	> 2000	3.49E+24	0.04340	3.22E+26	4	C/C Composite
Upper Plenum Shroud T/B Cov Plates	60y	278	826	871	1.20E+22	0.00098	3.00E+22	0.002	Hast X
PSR Seal Sleeves	60y	334	643	2400	3.22E+24	0.04340	3.22E+26	4	Graphite
Metallic Core Supt Load Bearing Insulators	60y	660	660 Drops Exponentially	1000	8.50E+21	0.00011	?	?	Top- Macor Glass Ceramic
	60y	385	385 Drops Exponentially	1000	8.50E+21	0.00011	?	?	Bottom- Macor Glass Ceramic
Hot Duct T/B Assy	60y	749 MM 974 HS	749 Drops Exponentially	> 2000	8.50E+21	0.00011	3.00E+22	0.002	C/C Composite (Possibly Haynes 230 with temp. limit of 982°C
Cross Vessel T/B Assy	60y	322	322 Drops Exponentially	760	8.50E+21	0.00011	3.00E+22	0.002	Temp. low enough to eliminate T/B
Lower Plenum Sidewall T/B Assy	60y	677 MM 927 HS	677 Drops Exponentially	871	8.50E+21	0.00011	3.00E+22	0.002	Hast X
SCS Entrance Tubes	60y	749 MM 999 HS	749 Drops Exponentially	927	8.50E+21	0.00011	3.00E+22	0.002	Hast XR
SCS HXR T/B Assy	60y	380	380 Drops Exponentially	760	8.50E+21	0.00011	3.00E+22	0.002	Alloy 800H

Table 9-4. Reactor Internal Materials Selection Summary for Tin/Tout = 372°C/800°C

Component	Design Life	Normal Op Design Temp	Off-Normal Design Temp	Temp Limit	Design Fluence		Fluence Limit		Mat'l Selection
		C	C	C	n/m^2	dpa	n/m^2	dpa	
Control Rod	8y Replaceable	755	1425	> 2000	3.22E+26	4.00000	3.22E+26	4	C/C Composite
Control Rod & RSM Guide Tube	60y Replaceable Can be < 60y	365	880	927	1.03E+23	0.00128	3.00E+22	0.002	Hast XR
Upper Core Restraint	60y Replaceable. Can be < 60y	365	985	> 2000	3.49E+24	0.04340	3.22E+26	4	C/C Composite
Upper Plenum Shroud T/B Cov Plates	60y	323	817	871	1.20E+22	0.00098	3.00E+22	0.002	Hast X
PSR Seal Sleeves	60y	384	634	2400	3.22E+24	0.04340	3.22E+26	4	Graphite
Metallic Core Supt Load Bearing Insulators	60y	642	642 Drops Exponentially	1000	8.50E+21	0.00011	?	?	Top- Macor Glass Ceramic
	60y	435	435 Drops Exponentially	1000	8.50E+21	0.00011	?	?	Bottom- Macor Glass Ceramic
Hot Duct T/B Assy	60y	799 MM 1024 HS	799 Drops Exponentially	> 2000	8.50E+21	0.00011	3.00E+22	0.002	C/C Composite
Cross Vessel T/B Assy	60y	371	371 Drops Exponentially	760	8.50E+21	0.00011	3.00E+22	0.002	Temp. low enough to eliminate T/B
Lower Plenum Sidewall T/B Assy	60y	727 MM 977 HS	727 Drops Exponentially	> 2000	8.50E+21	0.00011	3.00E+22	0.002	C/C Composite (Possibly Haynes 230 with temp. limit of 982°C)
SCS Entrance Tubes	60y	799 MM 1049 HS	799 Drops Exponentially	> 2000	8.50E+21	0.00011	3.00E+22	0.002	C/C Composite
SCS HXR T/B Assy	60y	362	362 Drops Exponentially	760	8.50E+21	0.00011	3.00E+22	0.002	Alloy 800H

The results of the evaluation show that the PSR seal rings and the load bearing ceramic pads do not change because the choice of materials is driven by requirements other than temperature. However, for most of the other components there is an effect. It was determined that for reactor outlet helium temperatures up to 750°C, most of the C/C composites can be eliminated and replaced with high-temperature metallic alloys, except for the control rods, upper core restraint elements, and possibly the hot duct T/B cover plates (based on a conservative maximum hot streak temperature). For a reactor outlet helium temperature of 800°C, C/C composites also become the likely material choices for the lower plenum sidewall T/B cover plates and the SCS entrance tubes. Table 9-5 summarizes the results of this evaluation. Needless to say, the NGNP composites technology development program would be impacted with respect to both scope and cost if the reactor outlet and inlet helium temperatures were to be reduced, and this impact would be greater at 750°C than at 800°C.

Another important conclusion of the evaluation is that an NGNP reactor operating at reactor outlet helium temperatures up to 800°C would not require direct cooling of the reactor vessel to use SA508/533 as the vessel material. Beyond 800°C, it appears that vessel cooling would be needed. However, the conditions for which vessel cooling is required need to be confirmed by a rigorous thermal hydraulic analysis of the Reactor System. In fact, all the conclusions from this cursory evaluation of the impact of reactor outlet and inlet helium temperatures on the materials of construction for reactor system components should be confirmed by a more rigorous evaluation.

Table 9-5. RS Component Material Selections for Various Reactor Outlet Temperatures

Component	Material Choice			
	687°C Reactor Outlet	750°C Reactor Outlet	800°C Reactor Outlet	950°C Reactor Outlet
Control Rod	C/C Composite	C/C Composite	C/C Composite	C/C Composite
Control Rod & RSM Guide Tube	Hastelloy X	Hastelloy XR	Hastelloy XR	C/C Composite
Upper Core Restraint	C/C Composite	C/C Composite	C/C Composite	C/C Composite
Upper Plenum Shroud T/B Cover Plates	Hastelloy X	Hastelloy X	Hastelloy X	C/C Composite
Permanent Side Reflector Seal Sleeves	Graphite	Graphite	Graphite	Graphite
Metallic Core Supt Load Bearing Insulators	Macor Glass Ceramic	Macor Glass Ceramic	Macor Glass Ceramic	Macor Glass Ceramic
Hot Duct T/B Assy	Hastelloy XR	C/C Composite (Possibly Haynes 230)	C/C Composite	C/C Composite
Cross Vessel T/B Assy	Not Needed	Not Needed	Not Needed (Cross Vessel just at 371°C Temp limit)	Alloy 800H
Lower Plenum Sidewall T/B Assy	Hastelloy X	Hastelloy XR	C/C Composite (Possibly Haynes 230)	C/C Composite
SCS Entrance Tubes	Hastelloy XR	Hastelloy XR	C/C Composite	C/C Composite
SCS Heat Exchanger T/B Assy	Alloy 800H	Alloy 800H	Alloy 800H	Alloy 800H

10 REFERENCES

1. 600MW(t) Gas Turbine-Modular Helium Reactor System Design Description, GA DRAFT Report No. DOE-MHR-100011 (RDI#2320-0007) Rev. 0, September 22, 1994.

2. 600MW(t) Gas Turbine-Modular Helium Reactor Design Data Needs, GA Report No. DOE-MHR-100217, Rev 0, August 29, 1996.

3. T.E. Blue, Miller, D.E., Nuclear Power Monitoring Using Silicon Carbide Semiconductor Radiation Detectors, NERI Quarterly Report for the Period April-June 2003, Project No. DE-FG03-02SF22620, Ohio State Univ.

4. Min-Hwan Kim, Jisu-Jun, Won Jae Lee, A thermal-Fluid Analysis for the Selection of Operating Conditions of Reactor Internals, KAERI Report No. NHDD-RD-08-005, Rev. 1, September 12, 2008.

5. ASME Code for Metals, Section III, Div. 1.

6. ASME Code for Graphite, Section III, Div. 2, Subsection CE.

7. ASTM Stds Committee C28 on Advanced Ceramics, “C” series ASTM standards on Ceramics and Ceramic Composites, Status Report Dated January, 2007.

8. R.E. Bullock, Cheney, H.H., High-Temperature Mechanical Properties of Alumina & Silica Materials in a Helium Environment, Project 7700, GA Technologies Report No. 907889. April 11, 1985.

9. Ferber, Weresczak and Henrik, Compressive creep and thermo physical performance of refractory materials, Oak Ridge National Laboratory Report ORNL/TM-2005/134, 2006

10. de Arellano-Lopez et al, Compressive creep of mullite containing Y2O3, Acta Materialia 50, pp. 4325-4338, 2002

11. Pitchford, J.E., Effects of Structure on Mechanisms and High Temperature Plastic Deformation in Oxide Ceramics. PhD thesis. University of Cambridge, UK, 1999

12. Ruggles-Wrenn, M.B. et al, Creep Behavior of Nextel™ 720/alumina ceramic composite with +/- 45º fibre orientation at 1200ºC, Composites Science and Technology 68, pp 1588-1595, 2008

13. Raj and Chyung, Solution-precipitation creep in glass-ceramics, Acta Metallurgica 29, pp. 159-166, 1980

14. Mercer and Chokshi, The elevated temperature compression creep behavior of a calcium aluminosilicate (anorthite) glass-ceramic, Scripta Metallurgica et Materialia 28, pp. 1177-1182, 1993

15. Hu, Li and Mao, Growth behavior, morphology and properties of lithium aluminosilicate glass ceramics with different amount of CaO, MgO and TiO2 additive, Ceramics International 34, pp. 1393-1397, 2008

16. Hobbs, Clinard, Zinkle and Ewing, Radiation effects in ceramics, Journal of Nuclear Materials 216, pp. 291-321, 1994

17. Osborne, Hubbard, Snead and Steiner, Neutron irradiation effect on the density, tensile properties and microstructural changes in Hi-Nicalon™ and Sylramic™ SiC fibers

18. Newsome et al, Evaluation of neutron irradiated silicon carbide and silicon carbide composites, Journal of Nuclear Materials 371, pp. 76-89, 2007

19. Savoini et al, Radiation damage in neutron-irradiated yttria-stabilized zirconia single crystals, Journal of Nuclear Materials 277, pp. 199-203, 2000

20. Morgan Technical Ceramics, Materials Data (Advanced Ceramics), data handbook, Sept 2005 issue

21. Kyocera Corp. Corporate Fine Ceramics Group, Mechanical & Industrial Ceramics, data handbook, 2006 issue

APPENDIX A – Compilation of Conditions for RS Components

The compilation of conditions for Reactor Internal components, which was partially provided in Table 3-6 is provided in its entirety in Table A-1.

Table A-1. NGNP Reactor Internals Components Normal Operating Conditions at 100% Power and for Conduction Cool-down Transients

Location	Component	Parameter	Value	Units	Ref	Comment
Overall Reactor System						
	Overall Sys Parameter	Reactor Thermal Power (100% Power)	600.0	MW(t)	1	GT-MHR was 490/850 C tin/Tout of the Reactor Core
	Overall Sys Parameter	Core Avg Power Density	6.6	MW/m^3	1	Was 6 MW/m^3 for 550 MWt 102 Col Core. Increased power density 10% for the 600MWt 102 col core. His I the stretched version of the 102 col core.
	Elec Gen Loop	Power Split to Electric Power Gen Loop	525.0	MW(t)	?	Electric generation loop
	Process Heat Loop	Power Split to Process Heat Loop	65.0	MW(t)	?	Process Heat Loop
	Overall Sys Parameter	System Pressure (100% power)	7.1	MPa abs	1	(1025 psia)
	Overall Sys Parameter	Reactor Vessel Relief Valve set pressure	7.8	MPa abs	Calc	(1128 psia) set at 10% above Operating press.
	Overall Sys Parameter	**Case 1: Core Tin/Tout 490/950C**				To be used in cases where the 490C inlet temp is most critical to the design (e.g., Thermal barrier thickness calculations).
		Core Inlet He Temp	490.0	C	4	
		Core outlet He Temp	950.0	C	4	A capability requirement to set to maximize PCS and Process heat performance.
		Primary He coolant total flow rate	248.5	kg/s	4	
	Overall Sys Parameter	**Case 2: Core Tin/Tout 590/950C**				To be used in cases where the 590C inlet temp is most critical to the design (e.g., Thermal barrier cover plate operating temp).

Location	Component	Parameter	Value	Units	Ref	Comment
		Core Inlet He Temp	590.0	C	1	Was 490C, but changed to 590C to reduce hot streaks in core He flow and localized hot spots in fuel. Not the same as 600MW KAERI analysis of 250.4 kg/s for Tin=490C & Tout=950C due to higher Core delta T.
		Core outlet He Temp	950.0	C	1	Was 850C. But rose to 950C to set max capability. Raised core inlet temp 100degC to bring to 590C to maintain the same Core Delta T. A capability requirement to set to maximize PCS and Process heat performance.
		Primary He coolant total flow rate	320.0	kg/s	1	Same as 600MW(t) GT-MHR flow rate. This flow rate is for a Tin=490C and Tout=850C. Assumed that hot streaks above mean temp not affected since axial temp increase across core the same.
	Overall Sys Parameter	He Coolant Loop Sustained noise level	160.0	dB	2	Transient spectrum up to 160 dB. For noise induced vibration. (DDN C.11.02.02)
	Application to specific Components	PCC & DCC Temp Profiles	*		4	* See Ref 4 for temps in KAERI T/H analysis Report. Specific Temp Maximums will be called out for the components below.
	Overall Sys Parameter	Max rate of depressurization during a breach of Primary Press Boundary	152.0	kPa/sec	2	(22 psi/s) System Pressure vs. time at key locations better. (DDN C.11.02.02)
	Reactor Vessel	Max Avg Reactor Vessel Allowable Metal Temp during normal operation	371.0	C	5	(700F) All Reactor Internal Components, in conjunction with other equipment, must function to maintain vessel temp at or below 371 C during Normal Operation.

Location	Component	Parameter	Value	Units	Ref	Comment
	Reactor Vessel	Reactor Vessel Fluence shall not Exceed:			1	All Reactor Internal Components, in conjunction with other equipment, must function to maintain vessel neutron fluence at or below at or below the fluence listed below during Normal Operation for the 60-year life of the reactor plant.
	Reactor Vessel	E > 0.9 MeV	9.9x10^21	n/m^2	1	
	Reactor Vessel	0.1 < E < 0.9 MeV	4.8x10^22	n/m^2	1	
	Reactor Vessel	3.05eV < E < 0.1 eV	9.9x10^22	n/m^2	1	
	Reactor Vessel	e < .01 eV	3.3x10^22	n/m^2	1	
	Reactor Vessel	Total for all neutron Energy Levels	1.84x10^23	n/m^2	1	
	Applies to all comp in primary coolant loop. Use for design.	Design Required Primary He Coolant Impurities @ S/S 100%pwr:			2	All of these values are for a core T_{inlet} = 490C & core $T_{out\ let}$ = 850C. DDN.11.07.01 They apply to all equipment in the reactor primary coolant. The Values are maximums to be used for design and are not in equilibrium with each other.
		H2O	2.0	ppmV		140 microatm
		CO2	2.0	ppmV		140 microatm
		CO	5.0	ppmV		350 microatm
		H2	10.0	ppmV		700 microatm
		CH4	2.0	ppmV		140 microatm
		N2	10.0	ppmV		700 microatm
		Particulates	10 .0	lb/yr		
	Reference only - Do not use for design.	Expected Primary He Coolant Impurities @ S/S 100%pwr: (For reference only)			2	All of these values are for a core T_{inlet} = 490C & core $T_{out\ let}$ = 850C This is an equilibrium coolant chemistry at 100% power for an Tin = 490 C and Tout = 850 C.
		H2O	0.5	ppmV		35 microatm
		CO2	1.0	ppmV		69.7 microatm

Location	Component	Parameter	Value	Units	Ref	Comment
		CO	2.0	ppmV		140 microatm
		H2	3.0	ppmV		210 microatm
		CH4	0.1	ppmV		7 microatm
		N2	2.0	ppmV		140 microatm
		Particulates	1.0	lb/yr		
Permanent Side Reflector Assy						
	PSR Seal Sleeves	Case 1: Max Normal op Helium Coolant Core Inlet Temp @ 100% pwr	490.0	C	4	Predicted sleeve temp so close to coolant temp. Use Coolant Temp as component Design Temp for Normal op. (Ref 4)
		Case 1: Total Flow Rate @ 100% pwr	248.5	kg/s	4	
		Case 2: Max Normal op Helium Coolant Core Inlet Temp @ 100% pwr	590.0	C	1	Predicted sleeve temp very close to coolant temp. Use Coolant Temp as component design Temp for Normal op. (Ref 4). Was 490C, but changed to 590C. Maintained same core delta T so hot streaks are about same as 600MWt NGNP.
		Case 2: Total Flow Rate @ 100% pwr	320.0	kg/s	1	
		Max Seal Sleeve Temp	590.0	C	4	
		Max PCC Temp sustained for about 150 hours per event. Case 2	643.0	C	4	See Transient temp vs. time curve in Ref 4.
		Max DPCC Temp sustained for about 150 hours per event. Case 2	743.0	C	4	See Transient temp vs. time curve in Ref 4.
		Maximum Neutron Flux (Full spectrum)	2.0x10^17	n/m^2/s	3	EOC Flux. May be a little lower than average, but within error of calc at this point.
		Maximum Total Neutron Fluence (Full spectrum)	3.2x10^26	N/m^2	3	60-year plant life at 85% plant capacity factor.
Upper Plenum						

Location	Component	Parameter	Value	Units	Ref	Comment
	All of Upper Plenum	Case 1: Max Normal op Helium Coolant Core Inlet Temp @ 100% pwr	490.0	C	4	
		Case 1: Total Flow Rate @ 100% pwr	248.5	kg/s	4	
		Case 2: Max Normal op Helium Coolant Core Inlet Temp @ 100% pwr	590.0	C	1	
		Case 2: Total Flow Rate @ 100% pwr	320.0	kg/s	1	
	UPS Thermal Barrier Cover Plates & Fasteners	Case 2 max Normal Op Temp @ 100% pwr	541.0	C	4	Adjust Ref 4 temp for a 490C Core inlet to a 590c core inlet by adding 100deg C to 490C results to account for higher gas temp.
		Max PCC Temp sustained for about 150 hours per event.	926.0	C	4	(1697F) Occurs at full system pressure.
		Max DCC Temp sustained for about 350 hours per event.	540.0	C	4	(1004F) Occurs at blow down pressure of approx 1 atm
		Neutron Flux & Fluence			2	
		Thermal neutron flux	7.46x10^12	n/m^2/s	2	
		E > 0.1 Mev neutron flux	5.22x10^13	n/m^2/s	2	
		Thermal neutron fluence	1.2x10^22	n/m^2	2	Max Fluence = 1.2x10^22 n/m^2 60year life at 85% capacity Factor. E<3.05 eV (DDN C.11.02.11)
		E > 0.1 Mev neutron fluence	8.4x10^22	n/m^2	2	Max Fluence = 8.4x10^22 n/m^2 60year life at 85% capacity Factor. E>0.1 MeV (DDN C.11.02.11)
	UPS Thermal Barrier Fibrous Insulation, or Solid Ceramic	Case 2 max Normal Op Temp @ 100% pwr	541.0	C	4	Adjust Ref 4 temp for a 490C Core inlet to a 590c core inlet by adding 100deg C to 490C results to account for higher gas temp.
		Max PCC Temp sustained for about 150 hours per event.	926.0	C	4	
		Max DCC Temp sustained for about 350 hours per event.	540.0	C	4	

Location	Component	Parameter	Value	Units	Ref	Comment
	UPS Thermal Barrier B4C Shielding Mat'l	Case 2 max Normal Op Temp @ 100% pwr	400.0	C	4	Adjust Ref 4 temp for a 490C Core inlet to a 590c core inlet by adding 100deg C to 490C results to account for higher gas temp.
		Max PCC Temp sustained for about 150 hours.	885.0	C	4	
		Max DCC Temp sustained for about 350 hours.	399.0	C	4	
	UPS Thermal Barrier Hardware-Cold Side	Case 2 max Normal Op Temp @ 100% pwr	390	C	4	Adjust Ref 4 temp for a 490C Core inlet to a 590c core inlet by adding 100deg C to 490C results to account for higher gas temp.
		Max PCCD Temp sustained for about 150 hours per event.	784.0	C	4	
		Max DCCD Temp sustained for about 350 hours per event.	398.0	C	4	
		Neutron Flux & Fluence			2	Opposite side of B4C from reactor.
		Thermal neutron Flux	1.5x10^9	n/m^2/s	2	
		Epithermal neutron Flux	5.9x10^13	n/m^2/s	2	
		Fast Neutron Flux	1.0x10^12	n/m^2/s	2	
		Total neutron Flux	6.0x10^13	n/m^2/s	2	
		Thermal neutron Fluence	2.5x10^18	n/m^2	2	Max Fluence based on 60-year life at 85% plant capacity Factor.
		Epithermal neutron Fluence	9.5x10^22	n/m^2	2	Max Fluence based on 60-year life at 85% plant capacity Factor.
		Fast Neutron Fluence	1.7x10^21	n/m^2	2	Max Fluence based on 60-year life at 85% plant capacity Factor.
		Total neutron Fluence	9.7x10^22	n/m^2	2	Max Fluence based on 60-year life at 85% plant capacity Factor.
	CR & RSM Guide Tubes	Case 2 max Normal Op Temp @ 100% pwr	583.0	C	4	Adjust Ref 4 temp for a 490C Core inlet to a 590c core inlet by adding 100deg C to 490C results to account for higher gas temp.

Location	Component	Parameter	Value	Units	Ref	Comment
		Max PCCD Temp above 1100C sustained for about 150 hours per event.	989.0	C	4	
		Max DCCD Temp above 1100C sustained for about 450 hours per event.	584.0	C	4	
		Thermal neutron flux	4.16x10^13	n/m^2/s	3	(DDN C.11.02.11)
		E > 0.1 Mev neutron flux	2.24x10^13	n/m^2/s	3	(DDN C.11.02.11)
		Total Neutron Flux	6.4x10^13	n/m^2/s	3	
		Thermal neutron fluence	6.7x10^22	n/m^2	3	Max Fluence based on 60-year life at 85% capacity Factor. (DDN C.11.02.11)
		E > 0.1 Mev neutron fluence	3.6x10^22	n/m^2	3	Max Fluence based on 60-year life at 85% capacity Factor. (DDN C.11.02.11)
		Total Neutron Fluence	1.03x10^23	n/m^2	3	Max Fluence based on 60-year life at 85% capacity Factor. (DDN C.11.02.11)
	Upper Core Restraint	Case 2 max Normal Op Temp @ 100% pwr - Top surface of UCR	553.0	C	4	Adjust Ref 4 temp for a 490C Core inlet to a 590c core inlet by adding 100deg C to 490C results to account for higher gas temp.
		Case 2 max Normal Op Temp @ 100% pwr - Bottom surface of UCR	584.0	C	4	Adjust Ref 4 temp for a 490C Core inlet to a 590c core inlet by adding 100deg C to 490C results to account for higher gas temp.
		Max PCCD Temp above 1000C sustained for about 175 hours per event.	1,094.0	C	4	Fairly uniform Temp anticipated at hottest block of USR.
		Max DCCD Temp above 600C sustained for about 175 hours per event.	655.0	C	4	Fairly uniform Temp anticipated at hottest block of USR.
		Mechanical Loads (DW+Core flow Press drop over length)+side loads on Key-Keyway combinations. Also must consider side loads from Earthquakes.	*	Kg		* Must calculate.
		Neutron flux & Fluence at top of Upper Core Restraint			2	

Location	Component	Parameter	Value	Units	Ref	Comment
		Thermal neutron flux	4.16x10^13	n/m^2/s	2	(DDN C.11.02.11)
		E > 0.1 Mev neutron flux	2.24x10^13	n/m^2/s	2	(DDN C.11.02.11)
		Total Neutron Flux	6.4x10^13	n/m^2/s		
		Thermal neutron fluence	6.2x10^22	n/m^2	2	Based on 60-year life at 85% capacity Factor. This is a replaceable component with fuel handling machine. E<3.05 eV (DDN C.11.02.11)
		E > 0.1 Mev neutron fluence	3.6x10^22	n/m^2	2	Based on 60-year life at 85% capacity Factor. E>0.1 MeV (DDN C.11.02.11)
		Total neutron fluence	9.8x10^22	n/m^2		
		Neutron flux and Fluence at bottom of Upper Core Restraint			2	
		Thermal neutron flux	2.12x10^15	n/m^2/s	2	(DDN C.11.02.11)
		E > 0.1 Mev neutron flux	5.41x10^13	n/m^2/s	2	(DDN C.11.02.11)
		Total neutron flux	2.17x10^15	n/m^2/s		
		Thermal neutron fluence	3.4x10^24	n/m^2	2	Based on 60-year life at 85% capacity Factor. E<3.05 eV (DDN C.11.02.11)
		E > 0.1 Mev neutron fluence	8.7x10^22	n/m^2	2	Based on 60-year life at 85% capacity Factor. E>0.1 MeV (DDN C.11.02.11)
		Total neutron fluence	3.49x10^24	n/m^2		
Reactor Core						
	Control Rods	Case 2 max Normal Op Temp @ 100% pwr	905.0	C	4	Adjust Ref 4 temp for a 490C Core inlet to a 590c core inlet by adding 100deg C to 490C results to account for higher gas temp.
		Max PCC Temp sustained above 1100C for about 150 hours per event.	1,273.0	C	4	
		Max DCC Temp sustained above 1100C for about 350 hours per event.	1,500.0	C	4	

Location	Component	Parameter	Value	Units	Ref	Comment
		Mechanical Loads (DW+Core Press drop distributed along length in vertical direction)	*	Kg		* Must calculate mechanical Loads (DW+Core Press drop distributed along length in vertical direction)
		Lateral Earthquake loads	*	Kg		* Must determine from seismic analysis.
		Total neutron flux	1.5x10^18	n/m^2/s	3	
		Total neutron fluence	3.2x10^26	n/m^2	3	Based on an 8-year life and replacement every eight years.
	Core Barrel	Case 1 max Normal Op Temp @ 100% pwr	481.0	C	1	(898F)
		Case 2 max Normal Op Temp @ 100% pwr	578.0	C	4	(1073F)
		Max PCC Temp sustained for about 150 hours per event.	608.0	C	4	(1097F)
		Max DCC Temp sustained for about 250 hours per event.	706.0	C	4	(1303F)
		Neutron flux at Top of Core Barrel				
		Thermal neutron flux	1.22x10^12	n/m^2/s		Max Fluence = 3.2x10^21 n/m^2-60year life at 85% capacity Factor. E<3.05 eV (DDN C.11.02.11)
		> 0.1 Mev neutron flux	6.84x10^12	n/m^2/s		Max Fluence = 1.1x10^22 n/m^2-60year life at 85% capacity Factor. E>0.1 MeV (DDN C.11.02.11)
		Neutron Flux & Fluence 2 inside surface of Core Barrel			2	Opposite side of B4C from reactor.
		Thermal neutron Flux	1.5x10^9	n/m^2/s	2	
		Epithermal neutron Flux	5.9x10^13	n/m^2/s	2	
		Fast Neutron Flux	1.0x10^12	n/m^2/s	2	
		Total neutron Flux	6.0x10^13	n/m^2/s	2	
		Thermal neutron Fluence	2.5x10^18	n/m^2	2	Max Fluence based on 60-year life at 85% plant capacity Factor.
		Epithermal neutron Fluence	9.5x10^22	n/m^2	2	Max Fluence based on 60-year life at 85% plant capacity Factor.

Location	Component	Parameter	Value	Units	Ref	Comment
		Fast Neutron Fluence	1.7x10^21	n/m^2	2	Max Fluence based on 60-year life at 85% plant capacity Factor.
		Total neutron Fluence	9.7x10^22	n/m^2	2	Max Fluence based on 60-year life at 85% plant capacity Factor.
Lower Plenum						
	Gen Lower Plenum	Avg He Temp out Bottom Reflector	950.0	C	1	
		Max Hot streak He outlet Temp above Bottom Reflector Avg Outlet Temp	250.0	°C	2	(DDN: 11.02.??) Need to confirm reference.
	Lower Plenum Sidewall T/B assy	Case 1-He Inlet Temp at Cold side of Sidewall T/B Assy	490.0	C	1	Use for max thickness calc of T/B. Want maximum temp difference across T/B.
		Case 2-He Inlet Temp at Cold side of Sidewall T/B Assy	590.0	C	1	Use for hardware design temps on cold side.
		Max Temp on Sidewall T/B Cov Pl	877.0	C	4	(1581F) This temp does not consider hot streaks.
		Max gas Hot streak Temp at sidewall T/B Cov Pl	1,127.0	C	2	(2061F) (DDN: 11.02.??) Need to confirm reference.
		Max Temp at Fibrous insulation in sidewall T/B	707.0	C	4	(1241F)
		Max Temp at steel side wall under sidewall T/B	519.0	C	4	(966F)
		Max PCC Temp per event.	877.0	C	4	Temp drops in about 50 hrs from the maximum to establish a temp of about 700C at 450hrs
		Max DCC Temp per event.	877.0	C	4	Temp drops in about 10 hrs from the maximum to 600C then decline exponentially over the next 400 hrs.
		Max Neutron flux & fluence at Sidewall T/B Cov Pl				
		Thermal neutron flux	5.23x10^12	n/m^2/s	2	(DDN C.11.02.02)
		E > 0.1 Mev neutron flux	6.22x10^10	n/m^2/s	2	(DDN C.11.02.02)
		Thermal neutron fluence	1.0x10^23	n/m^2	2	Max Fluence based on 60-year life at 85% plant capacity factor. (DDN C.11.02.02)

Location	Component	Parameter	Value	Units	Ref	Comment
		E > 0.1 Mev neutron fluence	3.9x10^21	n/m^2	2	Max Fluence based on 60-year life at 85% plant capacity factor. (DDN C.11.02.02)
		Sidewall T/B Sustained noise level	160.0	dB	2	Transient spectrum up to 160 dB. For noise induced vibration. (DDN C.11.02.02)
	Metallic Core Support Top Pl T/B Assy (Ceramic Pads)	Case 1-He Inlet Temp at cold side of Metallic Core Support pl coolant.	490.0	C	1	Use for max thickness calc of T/B. Want maximum temp difference across T/B.
		Case 2-He Inlet Temp at cold side of Metallic Core Support pl coolant.	590.0	C	1	Use for hardware design temps on cold side.
		Case 1-T/B Assy Temp at cold side against Metallic Core Support pl	631.0	C	4	
		Case 2-T/B Assy Temp at cold side against Metallic Core Support pl	653.0	C	4	
		Case 1-T/B Assy Temp at hot side towards lower plenum	838.0	C	4	
		Case 2-T/B Assy Temp at hot side towards lower plenum	860.0	C	4	
		Max heat transfer rate from lower plenum He to He just below Metallic Core Support top plate.	*			* Rate is assumed to be the same rate derived for the Hot duct on a per unit area basis.
		PCC max Temp at top of T/B Ceramic Pad	860.0	C	4	Temp Drops from 837C exponentially to 600C in about 50hrs and continues to drop.
		DCC max Temp at top of T/B Ceramic Pad	860.0	C	4	Temp Drops from 837C exponentially to 600C in about 100hrs and continues to drop.
		Max Neutron flux & fluence at Met Core Spt T/B				
		Thermal neutron flux	5.23x10^12	n/m^2/s	2	(DDN C.11.02.02)
		E > 0.1 Mev neutron flux	6.22x10^10	n/m^2/s	2	(DDN C.11.02.02)
		Thermal neutron fluence	1.0x10^23	n/m^2	2	Max Fluence based on 60-year life at 85% plant capacity factor. (DDN C.11.02.02)

Location	Component	Parameter	Value	Units	Ref	Comment
		E > 0.1 Mev neutron fluence	3.9x10^21	n/m^2	2	Max Fluence based on 60-year life at 85% plant capacity factor. (DDN C.11.02.02)
		Core Support Post Vertical Design Loads				
		DW + DP	3,273.0	kg	2	(7,200 lb) DW= Dead Weight, DP = Core Pressure Drop @ 100% pwr. Maximum offset of top of post relative to bottom is .01 m (4 in) (DDN C.11.02.01)
		DW + DP + OBE	6,318.0	kg	2	(13,900 lb) OBE= Operational basis Earthquake. Maximum offset of top of post relative to bottom is .01 m (4 in) (DDN C.11.02.01)
		DW + DP + SSE	8,500.0	kg	2	(18,700 lb) SSE= Safe Shutdown Earthquake. Maximum offset of top of post relative to bottom is .01 m (4 in) (DDN C.11.02.01)
Hot Duct Area	Hot Duct Assy					
		Case 1-He Flow Rate in Hot Ducts	284.5	kg/s	4	Can be derived from system flow rate and hot duct dimensions. There are at least 2 hot ducts; a large one for the steam cycle, and a small one for the H2 process loop.
		Large Hot duct - 89.17% of System Flow rate	253.7	kg/s	Calc	Assumes one large hot duct. Power split 525MWt
		Small Hot duct - 10.83% of System Flow rate	30.8	kg/s	Calc	Assumes one small hot duct. Power split 65MWt
		Case 2-He Flow Rate in Hot Ducts	320.0	kg/s	1	Can be derived from system flow rate and hot duct dimensions. There are at least 2 hot ducts; a large one for the steam cycle, and a small one for the H2 process loop.
		Large Hot duct - 89.17% of System Flow rate	285.3	kg/s	Calc	Assumes one large hot duct. Power split 525MWt
		Small Hot duct - 10.83% of System Flow rate	34.7	kg/s	Calc	Assumes one small hot duct. Power split 65MWt

Location	Component	Parameter	Value	Units	Ref	Comment
		He Velocity in Hot Duct	61.0	m/s	2	(200 ft/s) This velocity needs to be reconciled with sys coolant flow rate and hot duct Geometry. (DDN C.11.02.14)
		Avg He Temp at entrance to Hot Duct (Hot Side)	950.0	C	4	(1742F) See also (DDN C.11.02.14)
		Max Hot Streak He Temp at insulation hot surface	1,175.0	C	2	(2147F) Max delta T = 225 ^{o}C. There is mixing in the lower plenum due to L/D of streaks and core support posts. (DDN C.11.14.02)
		Case 1-Avg He Temp of Cold Side flow	490.0	C		
		Case 2-Avg He Temp of Cold Side flow	590.0	C		
		Case 1-Hot Duct T/B Assy Temps				
		Max Avg Temp of HD T/B Cover Pl	949.0	C	4	
		Max Avg Temp of T/B Fibrous Insulation	712.0	C	4	
		Max Temp of 800H Inner Tube Inside Wall	495.0	C	4	
		Max Temp 800H Inner Tube Outside Wall	491.0	C	4	
		Max Temp of Outer Tube T/B Cover Pl	490.0	C	4	
		Max Temp of Outer Tube Fibrous Insulation	379.0	C	4	
		Max Temp of Outer Tube Inside wall	273.0	C	4	
		Max Temp of Outer Tube Outside wall	273.0	C	4	
		Case 2-Hot Duct T/B Assy Temps (Add 100DegC to Case 1 Temps)				
		Max Avg Temp of HD T/B Cover Pl	949.0	C	4	
		Max Avg Temp of T/B Fibrous Insulation	766.0	C	4	
		Max Temp of 800H Inner Tube Inside Wall	595.0	C	4	
		Max Temp 800H Inner Tube Outside Wall	591.0	C	4	
		Max Temp of Outer Tube T/B Cover Pl	589.0	C	4	
		Max Temp of Outer Tube Fibrous Insulation	426.0	C	4	
		Max Temp of Outer Tube Inside wall	273.0	C	4	

Location	Component	Parameter	Value	Units	Ref	Comment
		Max Temp of Outer Tube Outside wall	273.0	C	4	
		Case 1 & 2 PCC Max Temp at Hot Duct T/B Cov Pl	954.0	C	4	Decays in 50 hrs to about 720C then drops slowly to 700C in about 450hrs.
		Case 1 & 2 DCC Max Temp at Hot Duct T/B Cov Pl	949.0	C	4	Decays in 15 hrs to about 600C then drops exponentially to 300C in about 500hrs.
		Max Neutron flux and fluence at Hot Duct				
		Thermal neutron flux	5.23x10^12	n/m^2/s	2	(DDN C.11.02.02)
		E > 0.1 Mev neutron flux	6.22x10^10	n/m^2/s	2	(DDN C.11.02.02)
		Thermal neutron fluence	1.0x10^23	n/m^2	2	Max Fluence based on 60-year life at 85% Plant Capacity Factor. (DDN C.11.02.02)
		E > 0.1 Mev neutron fluence	3.9x10^21	n/m^2	2	Max Fluence based on 60-year life at 85% Plant Capacity Factor. (DDN C.11.02.02)
		Hot Duct Sustained noise level	160.0	dB	2	Transient spectrum up to 160 dB. For noise induced vibration. (DDN C.11.02.02)
		Max rate of depressurization in Hot Duct during a breach of Primary Press Boundary	152.0	kPa/sec	2	(22 psi/s) System Pressure vs. time at key locations better. (DDN C.11.02.02)
		Max allowable He temp Rise between Hot Duct and Cross vessel	0.5	°C	Calc	The requirement for heat flow from the Hot Duct He to the Cross Vessel He is derived from this allowable temp rise.
Bottom Head of Reactor Vessel						
	Gen Bottom Head Area	Case 1- He Flow rate out of Cross Vessel into bottom head area	248.5	kg/s		Same as system total flow rate.
		Case 2- He Flow rate out of Cross Vessel into bottom head area	320.0	kg/s		Same as system total flow rate.
		Case 1-He Temp out of Cross Vessel into bottom head area	490.0	C		Does Not include losses.
		Case 2-He Temp out of Cross Vessel into bottom head area	590.0	C		Does Not include losses.

Location	Component	Parameter	Value	Units	Ref	Comment
		Vessel Cooling Sys He Temp in and out	474/260	C	4	An assumed Vessel cooling system using the SCS as the main cooler of vessel cooling gas.
		Vessel Cooling Sys He flow rate	4.1	kg/s	4	An assumed Vessel cooling system using the SCS as the main cooler of vessel cooling gas.
	SCS Entrance Tube & T/B	Max Temp of SCS Entrance Tube surface in contact with He gas	949.0	C	4	
		PCC Temp Profile in Bottom Head area	949.0	C	4	
		DCC Temp Profile in Bottom Head area	949.0		4	
		Neutron Flux & Fluence	**		4	** Use Same Flux/Fluence as Hot Duct above
	SCS HX T/B Assy	Case 1-Max Temp of SCS T/B surface in contact with He gas	483.3	C	4	
		Case 1-Max Temp of SCS T/B Fibrous Insulation	367.9	C	4	
		Case 1-Max Temp of SCS T/B support flow shroud	254.1	C	4	
		Case 1-PCC Max Temp at SCS T/B Cov Pl	483.0	C	4	Temp Declines exponentially to 240C in 500hrs.
		Case 1-DCC Max Temp at SCS T/B Cov Pl	483.0	C	4	Temp Declines exponentially to 280C in 500hrs.
		Case 2 Temps - Add 100degC to Case 1 Temps above	580.0	C	4	
		Case 1-Max Temp of SCS T/B Fibrous Insulation	414.0	C	4	
		Case 1-Max Temp of SCS T/B support flow shroud	255.0	C	4	
		Case 1-PCC Max Temp at SCS T/B Cov Pl	580.0	C	4	Temp Declines exponentially to 240C in 500hrs.
		Case 1-DCC Max Temp at SCS T/B Cov Pl	580.0	C	4	Temp Declines exponentially to 280C in 500hrs.
		Neutron Flux & Fluence	**		4	** Use Same Flux/Fluence as Hot Duct above

Appendix B – Neutron Fluence Estimate Analysis

Table B-1. GT-MHR Design Neutron Flux and Fluence for Reactor Internals (Part 1)

Location	**Component**	**EOC Flux From 600 MWt GT-MHR ($n/cm^2/s$)** (Core Avg Power Dens 6.6 W/cm^3)					
		MCNP Radial Locat'n (cm)	**Thermal**	**Epi-Thermal**	**Fast**	**Total**	
Reactor Core	Control Rods	148.0				1.5E+14	**TABLE** **Continued** **on** **Next** **Page**
RSR	Inside Surface RSR	241.5				1.5E+14	
RSR	Outside Surface RSR	308.8				3.0E+13	
PSR	Inside Surface PSR	308.8				5.0E+13	
PSR	Center of PSR	322.0				2.0E+13	
PSR	Outside Surface PSR	335.5				1.0E+13	
PSR	PSR Boron Pins-Inside Surface	335.5				1.0E+13	
PSR	PSR Boron Pins-Outside Surface	341.0	1.5E+05	5.9E+09	1.0E+08	6.0E+09	
Core Barrel	Core Barrel-Inside Surface	341.0	1.5E+05	5.9E+09	1.0E+08	6.0E+09	
RV	Reactor Vessel-Inside Surface	360.0	5.2E+04	2.0E+09	3.4E+07	2.0E+09	
RV	Reactor Vessel-Outside Surface	379.0	1.1E+04	4.0E+08	7.0E+06	4.1E+08	
**Ref. T.E.Blue, D.W.Miller, Nuclear Reactor Power Monitoring Using Silicon Carbide Semiconductor Radiation Detectors, NERI Report, Proj Number DE-FG03-02SF22620, Ohio State Univ.							

Table B-2. NGNP Design Neutron Fluence for Reactor Internals (Part 2)

Location	Component	Flux for 600MWt NPNG ($n/m^2/s$) (Core Avg Power Dens 6.6 MW/m^3)				Fluence for 600MWt NPNG (n/m^2)				Time Basis for Fluence		Comment
		Thermal	Epi-Thermal	Fast	Total	Thermal	Epi-Thermal	Fast	Total	Years	Plant Capacity Factor	
Reactor Core	Control Rods				1.5E+18				3.2E+26	8	0.85	Can be replaced on a shorter or longer interval if needed.
RSR	Inside Surface RSR				1.5E+18				2.0E+26	5	0.85	Can be replaced on a shorter or longer interval if needed.
RSR	Outside Surface RSR				3.0E+17				4.0E+25	5	0.85	Can be replaced on a shorter or longer interval if needed.
PSR	Inside Surface PSR				5.0E+17				8.0E+26	60	0.85	
PSR	Center of PSR				2.0E+17				3.2E+26	60	0.85	
PSR	Outside Surface PSR				1.0E+17				1.6E+26	60	0.85	
PSR	PSR Boron Pins-Inside Surface				1.0E+17				1.6E+26	60	0.85	
PSR	PSR Boron Pins-Outside Surface	1.5E+09	5.9E+13	1.0E+12	6.0E+13	2.5E+18	9.5E+22	1.7E+21	9.7E+22	60	0.85	
Core Barrel	Core Barrel-Inside Surface	1.5E+09	5.9E+13	1.0E+12	6.0E+13	2.5E+18	9.5E+22	1.7E+21	9.7E+22	60	0.85	
RV	Reactor Vessel-Inside Surface	5.2E+08	2.0E+13	3.4E+11	2.0E+13	8.3E+17	3.2E+22	5.5E+20	3.2E+22	60	0.85	
RV	Reactor Vessel-Outside Surface	1.1E+08	4.0E+12	7.0E+10	4.1E+12	1.7E+17	6.4E+21	1.1E+20	6.5E+21	60	0.85	

APPENDIX C – Thermal Analysis Supporting the Load Bearing Ceramic Design

SUMMARY: Both a steady state and a transient analysis were performed on the core support system as illustrated in Figure C-1. This analysis provided data to assure the following:

1. During steady state operation the heat transfer from the outlet helium (950°C) to the inlet helium (490°C) would not be excessive.
2. That during transient operation, the selected ceramic insulators that the support system sits upon would not be damaged by the thermal gradients that develop as the result of the transient operation.

This analysis had the following results:

1. During steady state operation at full power the maximum temperature rise in the inlet coolant was calculated to be less than 0.2°C for all cases considered. The maximum acceptable temperature increase is 0.5°C. Thus, it is clear that this design criterion is met.
2. The transient analysis of three configurations that used three different insulators has shown that large gradients (~ 250°C) will exist in the bottom insulator. Based on this preliminary evaluation it is clear that the ceramic insulator must be selected based on the ability to take large thermal gradients. It appears that the ceramic MACOR is the most likely choice. Plotted results of the transient analysis for the MACOR configuration are presented below.

SUPPORT SYSTEM DESCRIPTION: The support system (refer to Figure C-1) consists of the following:

1. A graphite cylindrical core support post that is caped at either end with a hexagonal end piece.
2. A hexagonal core support block.
3. Two insulating pads.
4. A metallic structure that makes up the upper surface of the inlet plenum.

The hot outlet helium is blown across the cylindrical portion of the support post. This helium enters the outlet plenum via cut outs in the upper hexagonal section of the support post. The heat transfer coefficient in this region is so large the post will operate at the helium temperature during steady state operation. There are contact gaps between the support post and the hexagonal support block, between the support block and the top layer of insulation, between the two layers of insulation and between the bottom layer of the insulation and the metallic structure. The inlet helium cools the metallic structure.

MODEL DESCRIPTION: Two different models were used for this analysis. The steady state analysis was performed two ways. One made use of a detailed MATHCAD model (Ref. 1) and the other made use of a TAC2D model (Ref. 2). Both the MATHCAD model and the TAC2D model predicted the same results within a couple degrees. TAC2D was used for the transient model. The two models will be described below.

MATHCAD Model – The MATHCAD model evaluates the temperature of the various components by using a series of heat balance equations at each location were the geometry and/or material changes. A set of 15 equations and 15 unknowns are solved simultaneously to determine the temperatures at each location. These temperatures are used to calculate the heat transfer from the outlet helium to the inlet helium. Three different insulator combinations were considered in this analysis. They were as follows:

1. Alumina on the top layer and silica on the bottom layer

2. MACOR on both layers
3. Carbon on both layers.

A copy of the model that uses MACOR is provided below. The other two models are identical except for the properties of the insulators.

TAC2D Model. The TAC2D model was a cylindrical model of a single core support assembly. The model was divided into a mesh of 7 radial divisions and 29 axial divisions for a total of 203 nodes. For the steady state analysis the computer code performs a heat balance on each of the nodes. For the transient analysis the computer code performances a transient central difference analysis on each of the nodes for a series of time steps. The following transient conditions were considered in this analysis.

1. Helium temperature change of 1000°C/minute.
2. Helium temperature change of 500°C/minute.
3. Helium temperature change of 250°C/minute.
4. Helium temperature change of 100°C/minute.
5. Helium temperature change of 50°C/minute.

For each of these transients it was assumed that the hot helium temperature, which starts at 950°C, would stabilize at 300°C while the cold helium temperature, which starts at 490°C, would stabilize at 100°C.

REFERENCES:

1. MATHCAD 11. Technical Calculation Tool
2. TAC2D A GENERAL PURPOSE TWO-DIMENSIONAL HEAT TRANSFER COMPUTER CODE

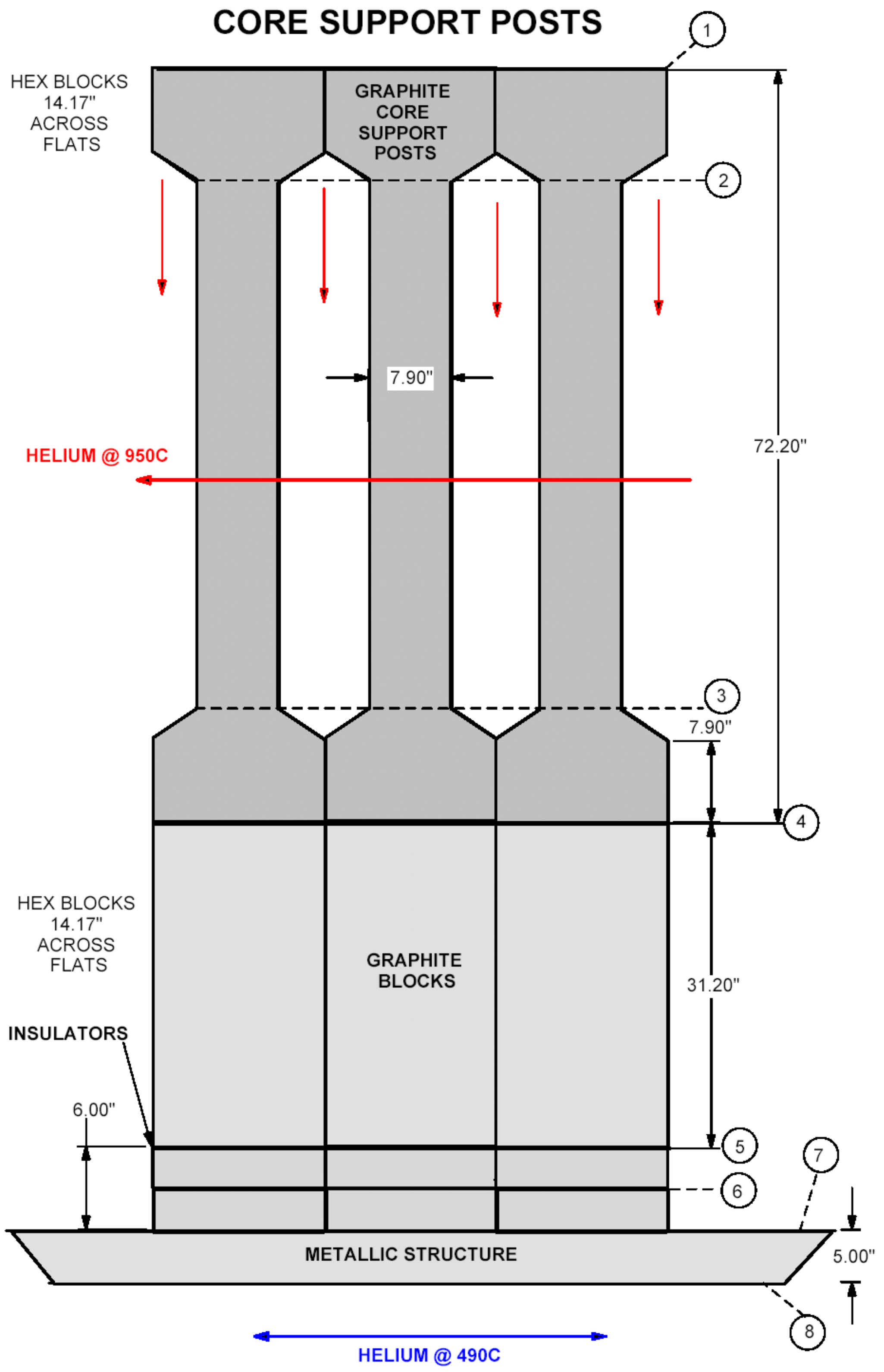
CORE SUPPORT POSTS
HEX BLOCKS 14.17" ACROSS FLATS
GRAPHITE CORE SUPPORT POSTS
1
2
3
4
5
6
7
8
7.90"
HELIUM @ 950C
72.20"
7.90"
HEX BLOCKS 14.17" ACROSS FLATS
GRAPHITE BLOCKS
31.20"
INSULATORS
6.00"
METALLIC STRUCTURE
5.00"
HELIUM @ 490C

Figure C-1

TRANSIENT RESULTS

Fifteen transient cases were run using TAC2D. These cases evaluated 3 different insulation material combinations for 5 different transients. The materials included the following configurations.

1. Alumina on the top and Silica on the bottom
2. Two layers of carbon
3. Two layers of MACOR

Of the three material combinations only MACOR was considered to be acceptable based on its ability to take the large gradients. The plotted transients for MACOR are presented below.

MACOR INSULATION - TOP PAD 3" THICK - 1000C/Min

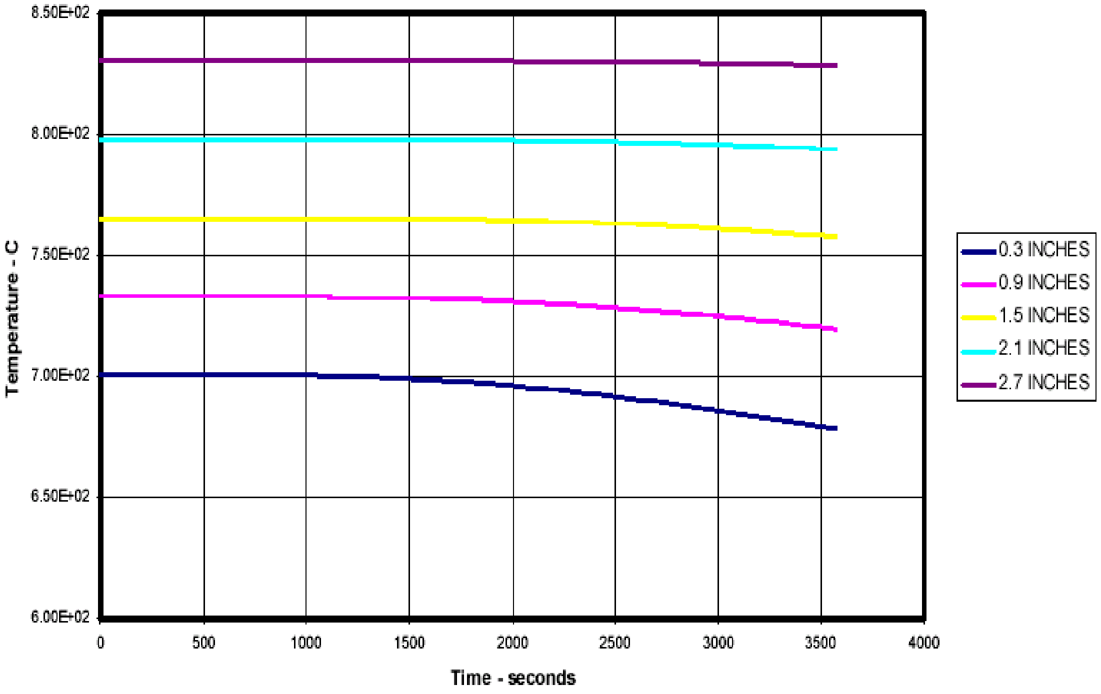

MACOR INSULATION - BOTTOM PAD 3" THICK - 1000C/Min

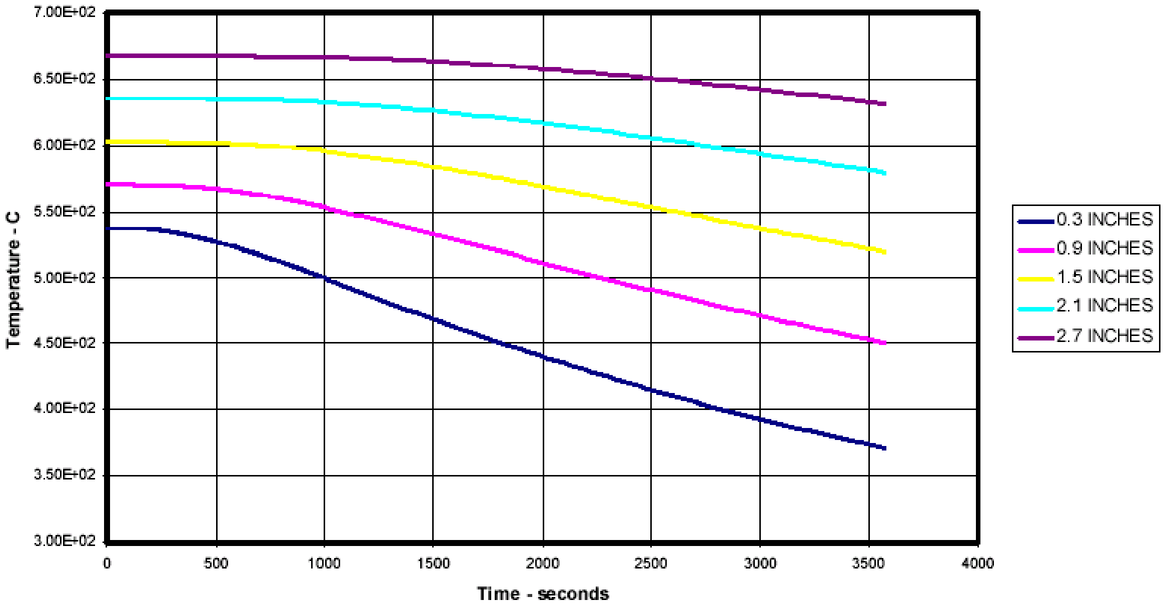

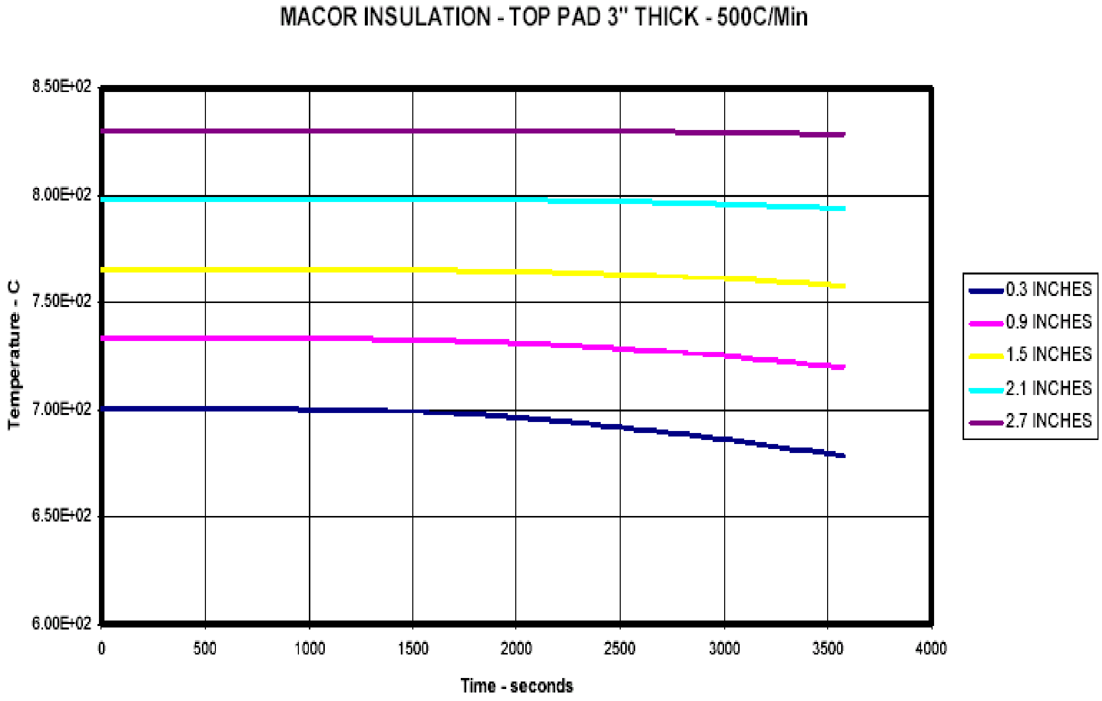
MACOR INSULATION - TOP PAD 3" THICK - 500C/Min
Temperature - C
8.50E+02
8.00E+02
7.50E+02
7.00E+02
6.50E+02
6.00E+02
0
500
1000
1500
2000
2500
3000
3500
4000
Time - seconds
0.3 INCHES
0.9 INCHES
1.5 INCHES
2.1 INCHES
2.7 INCHES

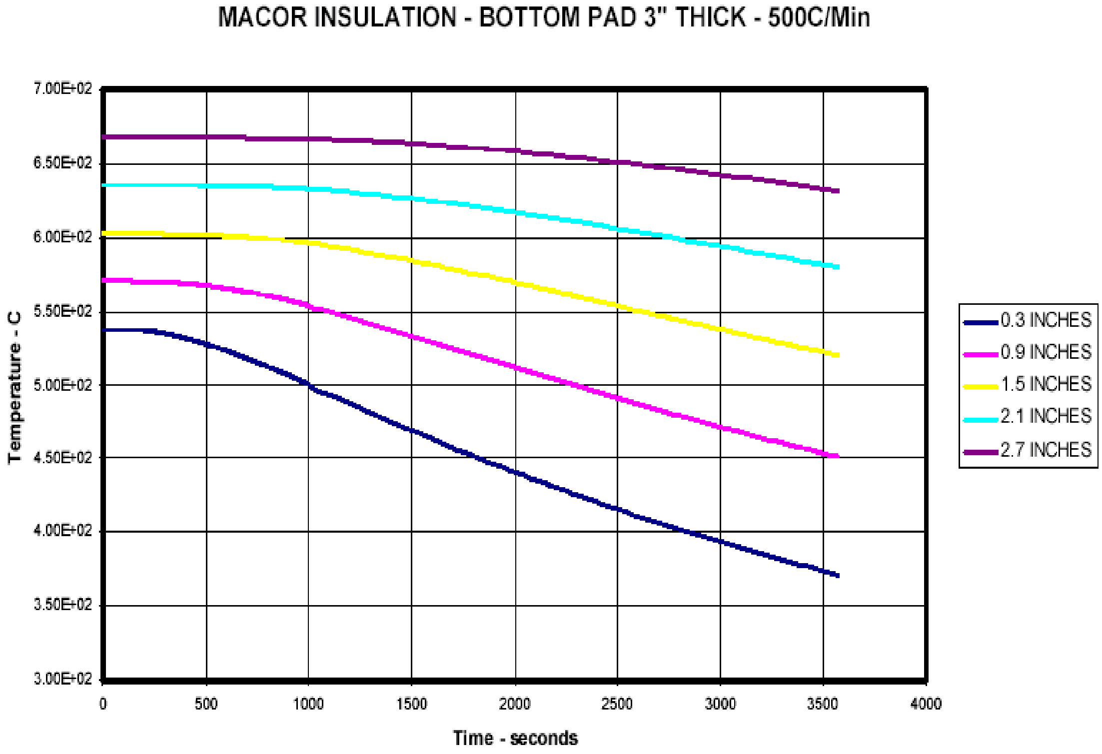
MACOR INSULATION - BOTTOM PAD 3" THICK - 500C/Min
Temperature - C
7.00E+02
6.50E+02
6.00E+02
5.50E+02
5.00E+02
4.50E+02
4.00E+02
3.50E+02
3.00E+02
0
500
1000
1500
2000
2500
3000
3500
4000
Time - seconds
0.3 INCHES
0.9 INCHES
1.5 INCHES
2.1 INCHES
2.7 INCHES

MACOR INSULATION - TOP PAD 3" THICK - 250C/Min

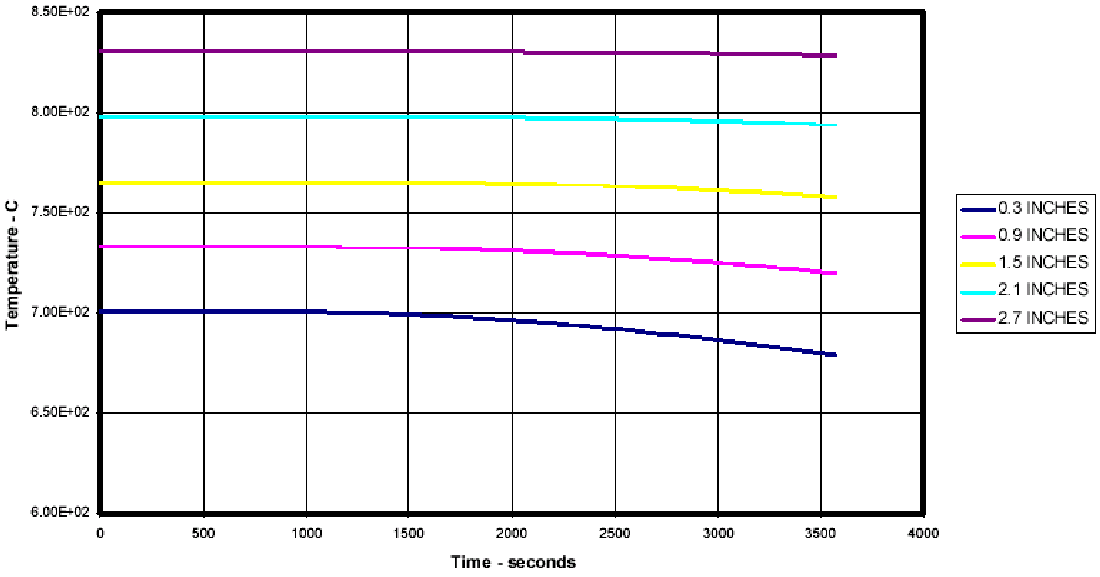

MACOR INSULATION - BOTTOM PAD 3" THICK - 250C/Min

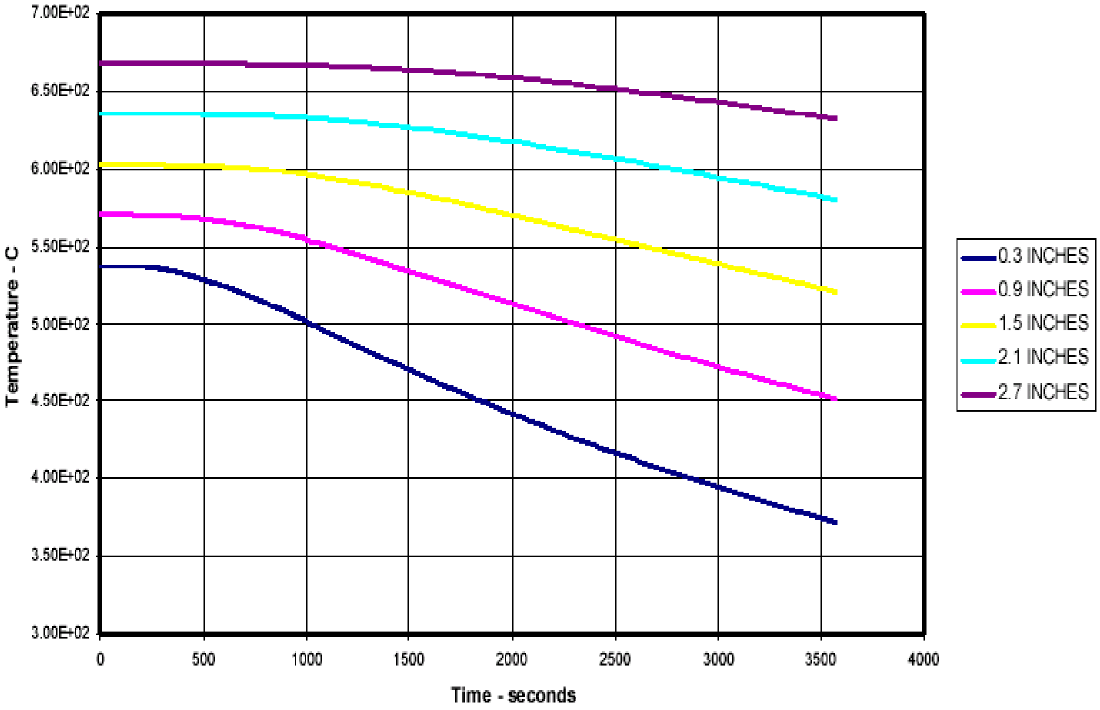

MACOR INSULATION - TOP PAD 3 " THICK - 100C/Min

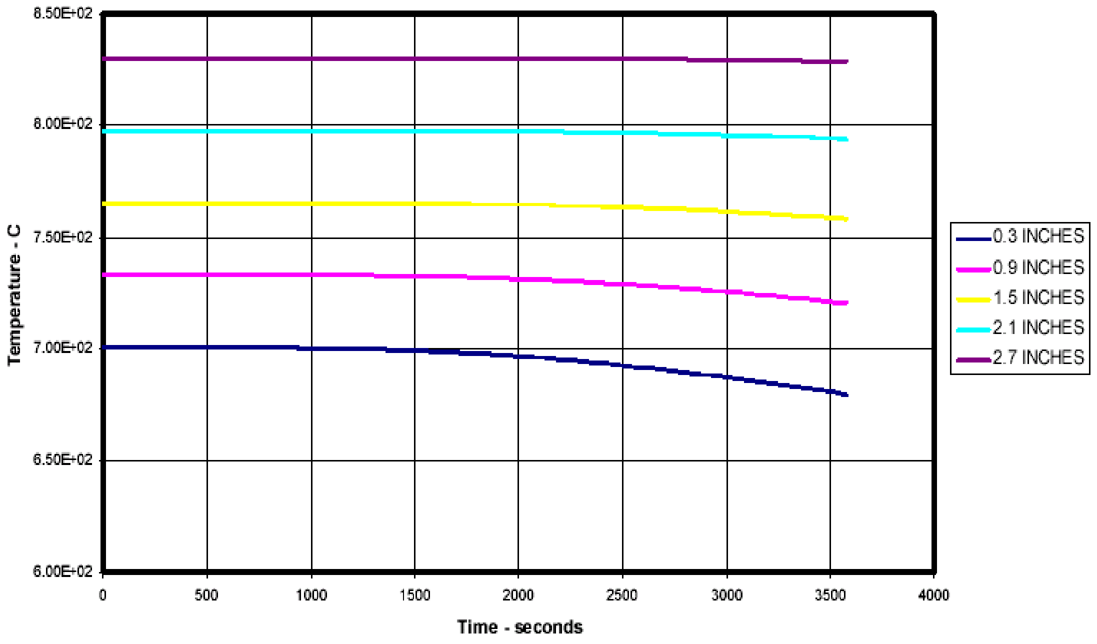

MACOR INSULATION BOTTOM PAD 3" THICK - 100C/Min

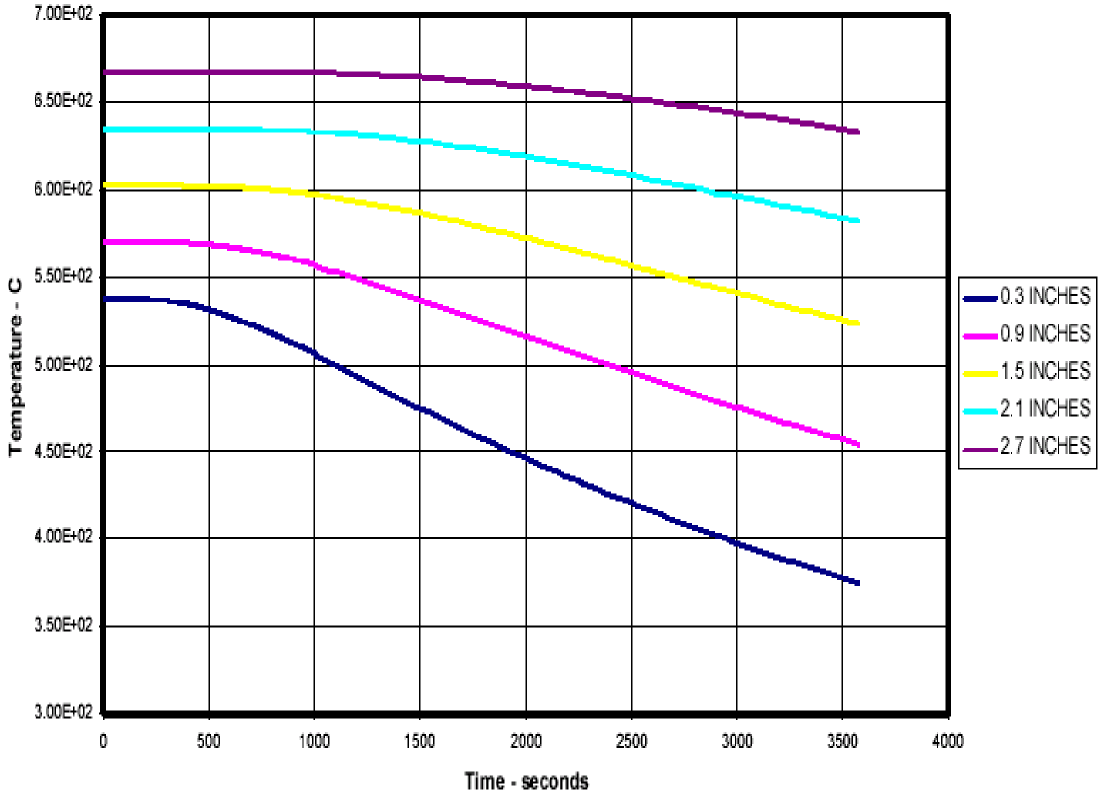

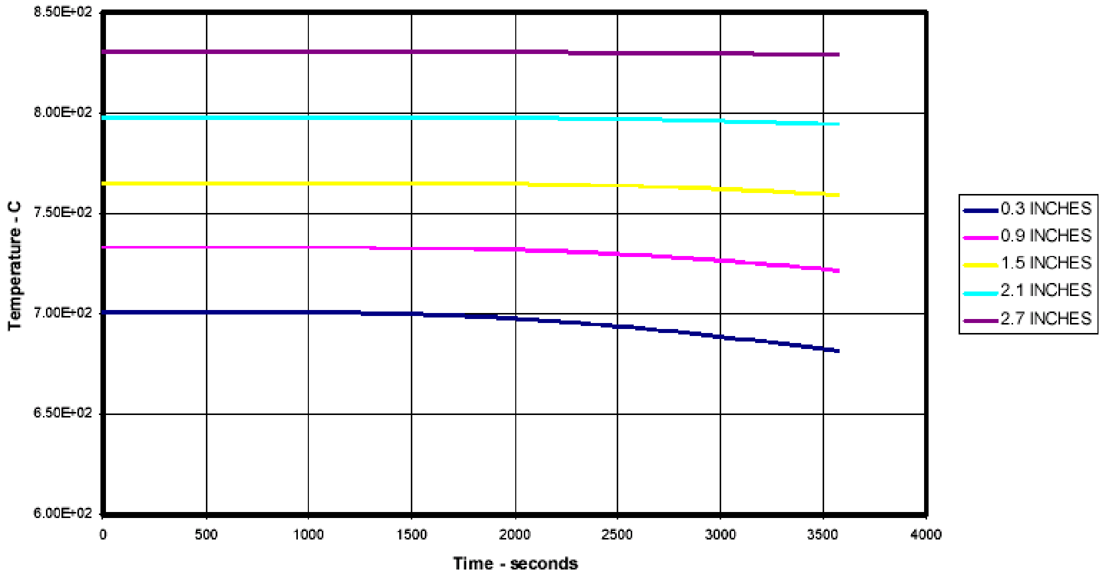
MACOR INSULATION - TOP PAD 3" THICK - 50C/Min

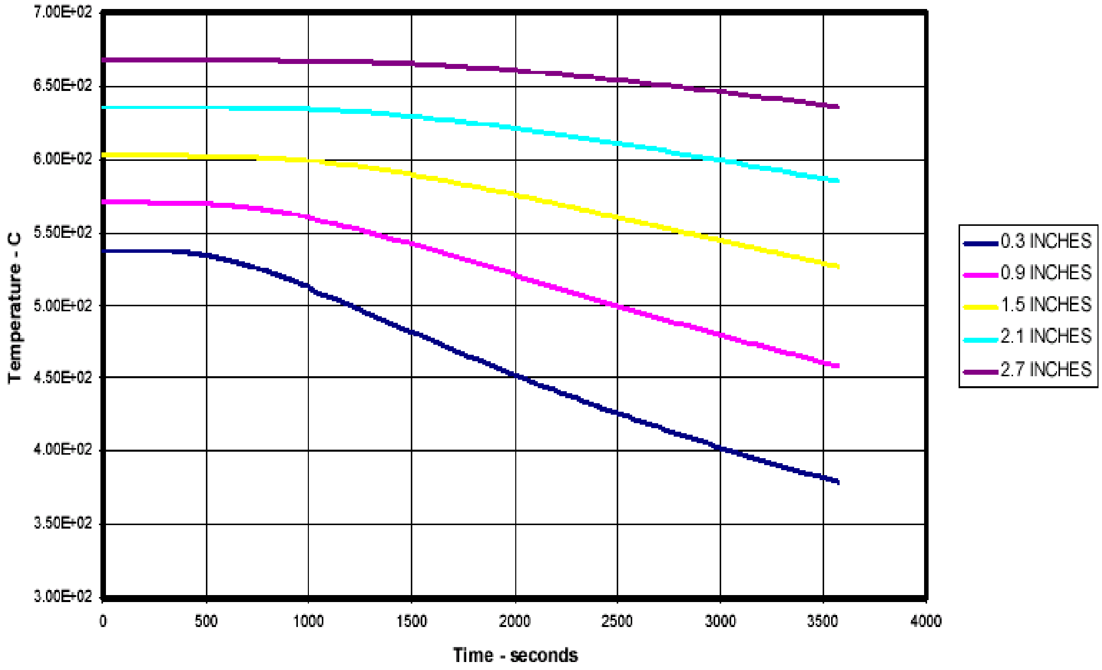
MACOR INSULATION - BOTTOM PAD 3" THICK - 50C/Min

MATHCAD MODEL

Three MATHCAD models were used for the steady state evaluation, one each for each of the three material combinations. All three models were the same expect for the material properties. The model for MACOR is described below.

NGNP
COMPOSITES
Calculation By: D. P. Carosella

General Atomics
Calculation Sheet
System CORE SUPPORT
Title: Establish Steady State Thermals and Input for TAC2D

Page No.: 1 of 23
Calculation No.:

I. INTRODUCTION

The reactor core is supported by a core support system as illustrated in Figure 1. This model will investigate means to control the heat loss from the hot helium (950ºC) to the cold helium (490ºC to 590ºC). During steady operation the temperature drop of the hot helium must be limited to 0.5ºC. This is achieved by the insulators that the core support system sits upon. This model will investigate insulation thickness and types to establish the required insulation to prevent excess heat loss. This model will also be used to define the geometry for the transient analysis which will be performed by the TAC2D code.

The constants function and properties required for this analysis follow:

Constants, Properties and Functions

$ORIGIN \equiv 1$

TC(T) converts the absolute temperature (T) to ºC. TF(T) converts the absolute temperature to ºF

$$TC(T) := \left(\frac{T}{K} - tc\right)\cdot °C \qquad TF(T) := \left(\frac{T}{R} - tr\right)\cdot °F$$

$kPa := Pa\cdot 1000$ $\quad tc \equiv 273.16$ $\quad tr \equiv 459.69$

$°C \equiv K$ $\quad °F \equiv R$

$MPa \equiv Pa\cdot 10^{6}$ $\quad bar \equiv .1\cdot MPa$ $\quad CFM \equiv ft^{3}\cdot min^{-1}$

$MW := watt\cdot 10^{6}$ $\quad kW := watt\cdot 10^{3}$ $\quad R_{gas} := 1545\,\frac{lbf\cdot ft}{lb\cdot R}$

Properties of Helium

$$Cp_{He} := 1.242\,\frac{BTU}{lb\cdot R} \qquad k_{He}(T) := 1.29\cdot 10^{-3}\,\frac{BTU}{hr\cdot ft\cdot R}\cdot\left(\frac{T}{R}\right)^{.674}$$

$$\mu_{He}(T) := 6.9\cdot 10^{-4}\,\frac{lb}{ft\cdot hr}\cdot\left(\frac{T}{R}\right)^{.674} \qquad Pr_{He}(T) := \frac{Cp_{He}\cdot\mu_{He}(T)}{k_{He}(T)} \qquad Mol_{He} \equiv 4$$

$$R_{He} := \frac{R_{gas}}{Mol_{He}} \qquad \gamma_{He} \equiv 1.667 \qquad \rho_{He}(T,P) := \frac{P}{R_{He}\cdot T}$$

NGNP
COMPOSITES
Calculation By: D. P. Carosella

General Atomics
Calculation Sheet
System CORE SUPPORT
Title: Establish Steady State Thermals and Input for TAC2D

Page No.: 2 of 23
Calculation No.:

Material Properties

Graphite:

$$k_{gr} := 18 \frac{BTU}{hr \cdot ft \cdot R} \qquad SPEC(T) := \left[13.9 + 41.3 \cdot \left[1 - e^{-1.04 \cdot 10^{-3} \cdot \left(\frac{T}{R} - tr \right)} \right] \right] \cdot \frac{BTU}{R \cdot ft^3}$$

Alumina:

$$CONLOG(T) := 4.4822 \cdot 10^{-7} \cdot \left(\frac{T}{R} - tr \right)^2 - 1.88686 \cdot 10^{-3} \cdot \left(\frac{T}{R} - tr \right) + 3.13055$$

$$k_{Al2O3}(T) := \exp(CONLOG(T)) \cdot \frac{BTU}{hr \cdot ft \cdot R}$$

$$\rho_{Al2O3} := 249 \frac{lb}{ft^3}$$

Specific Heat Data

$$T := \left[\begin{pmatrix} 32 \\ 122 \\ 212 \end{pmatrix} + tr \right] \cdot R \qquad Cp := \begin{pmatrix} .174 \\ .198 \\ .210 \end{pmatrix} \frac{BTU}{lb \cdot R}$$

$$vs := regress\left(\frac{T}{R}, \frac{Cp}{\frac{BTU}{lb \cdot R}}, 1 \right) \qquad vs = \begin{pmatrix} 3 \\ 3 \\ 1 \\ 0.077662 \\ 2 \times 10^{-4} \end{pmatrix}$$

$$\rho_{Al2O3} := 249 \frac{lb}{ft^3}$$

$$cf := \left(vs_4 + vs_5 \cdot \frac{T}{R} \right)$$

$$cf = \begin{pmatrix} 0.176 \\ 0.194 \\ 0.212 \end{pmatrix}$$

$$Cp_{Al2O3}(T) := \left(vs_4 + vs_5 \cdot \frac{T}{R} \right) \cdot \frac{BTU}{lb \cdot R}$$

Curve Fit of Al_2O_3 Heat Capacity Data

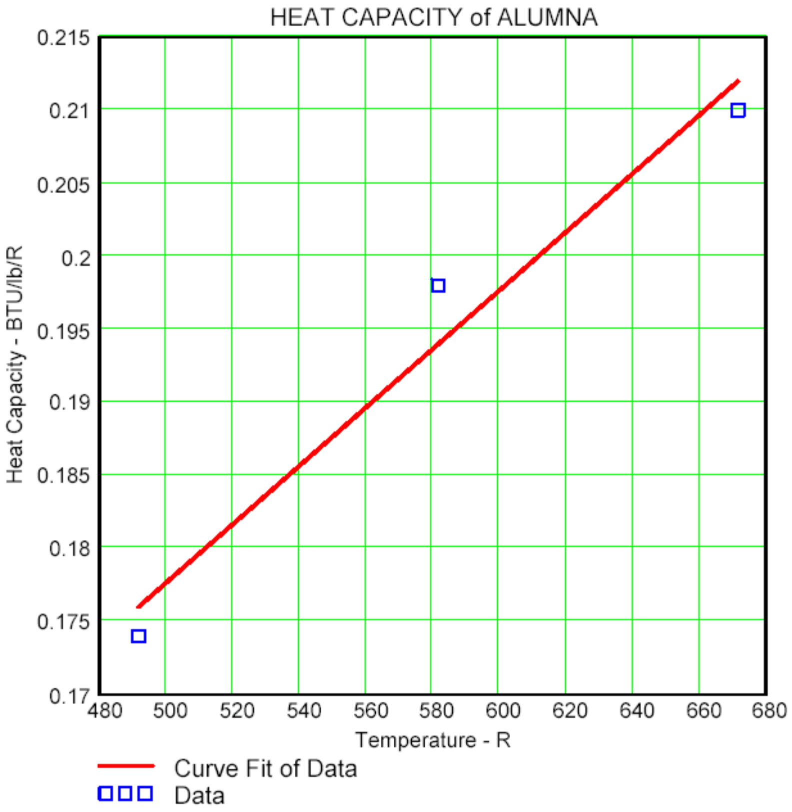

Silica (SiO_2)

Silica Conductivity (0% porosity)

$$Tx := \begin{pmatrix} 400 \\ 700 \\ 1300 \\ 1400 \end{pmatrix} \cdot K \qquad k_{SiO2} := \begin{pmatrix} 1.51 \\ 1.92 \\ 4.82 \\ 6.2 \end{pmatrix} \cdot \frac{watt}{m \cdot K} \qquad vs := regress\left(\frac{Tx}{K}, \frac{k_{SiO2}}{\frac{watt}{m \cdot K}}, 2\right)$$

$$vs = \begin{pmatrix} 3 \\ 3 \\ 2 \\ 2.6883 \\ -0.0049 \\ 5.1746 \times 10^{-6} \end{pmatrix}$$

$$T_1 := 400K$$

$$i := 2 .. 15$$

$$T_i := T_{i-1} + 100K$$

$$k_{fit}(T) := \left[vs_4 + vs_5 \cdot \frac{T}{K} + vs_6 \cdot \left(\frac{T}{K}\right)^2 \right] \cdot \frac{watt}{m \cdot K} \qquad k_{fit}[(700 + tc) \cdot K] = 1.6393 \frac{BTU}{hr \cdot ft \cdot R}$$

$k_{fit}(T) =$

	1
1	0.9032
2	0.8902
3	0.9369
4	1.0435
5	1.2099
6	1.436
7	1.722
8	2.0677
9	2.4733
10	2.9386
11	3.4638
12	4.0487
13	4.6934
14	5.398
15	6.1623

$\frac{BTU}{hr \cdot ft \cdot R}$

$$\rho_{SiO2} := 2.28 \cdot 62.4 \cdot \frac{lb}{ft^3}$$

$$\rho_{SiO2} = 142.272\, lb\, ft^{-3}$$

Curve Fit of SiO_2 Thermal Conductivity

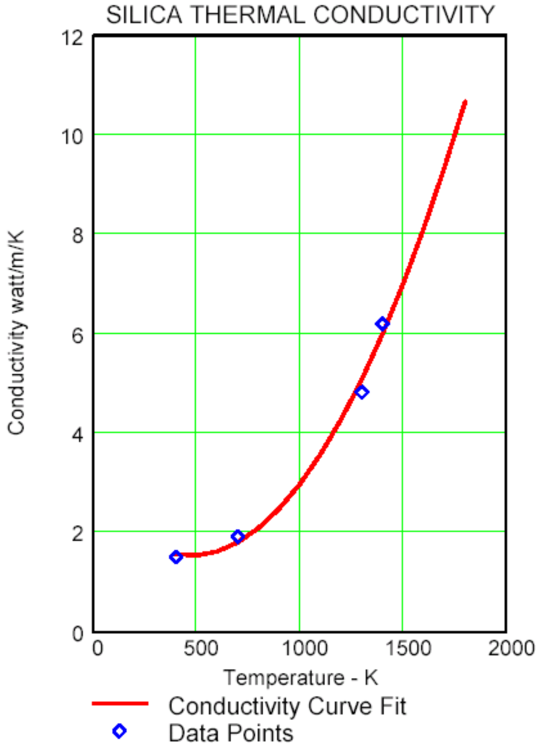

Silica Specific Heat (Reference 3)

$$T_{SiO2} := \left[\begin{pmatrix} 0 \\ 200 \\ 400 \\ 600 \\ 800 \\ 1200 \end{pmatrix} + tc\right] \cdot K \qquad Cp_{SiO2} := \begin{pmatrix} .2 \\ .237 \\ .270 \\ .282 \\ .285 \\ .291 \end{pmatrix} \frac{cal}{gm \cdot K}$$

$$vs := \text{regress}\left(\frac{T_{SiO2}}{R}, \frac{Cp_{SiO2}}{\frac{BTU}{lb \cdot R}}, 3\right) \qquad vs = \begin{pmatrix} 3 \\ 3 \\ 3 \\ 0.1077 \\ 2.3037 \times 10^{-4} \\ -9.9154 \times 10^{-8} \\ 1.4444 \times 10^{-11} \end{pmatrix}$$

$$Cp_{fit} := vs_4 + vs_5 \cdot \frac{T_{SiO2}}{R} + vs_6 \cdot \left(\frac{T_{SiO2}}{R}\right)^2 + vs_7 \cdot \left(\frac{T_{SiO2}}{R}\right)^3$$

Silica Specific Heat (Reference 3)

$$T_{SiO2} := \left[\begin{pmatrix} 0 \\ 200 \\ 400 \\ 600 \\ 800 \\ 1200 \end{pmatrix} + tc\right] \cdot K \qquad Cp_{SiO2} := \begin{pmatrix} .2 \\ .237 \\ .270 \\ .282 \\ .285 \\ .291 \end{pmatrix} \frac{cal}{gm \cdot K}$$

$$vs := \text{regress}\left(\frac{T_{SiO2}}{R}, \frac{Cp_{SiO2}}{\frac{BTU}{lb \cdot R}}, 3\right) \qquad vs = \begin{pmatrix} 3 \\ 3 \\ 3 \\ 0.1077 \\ 2.3037 \times 10^{-4} \\ -9.9154 \times 10^{-8} \\ 1.4444 \times 10^{-11} \end{pmatrix}$$

$$Cp_{fit} := vs_4 + vs_5 \cdot \frac{T_{SiO2}}{R} + vs_6 \cdot \left(\frac{T_{SiO2}}{R}\right)^2 + vs_7 \cdot \left(\frac{T_{SiO2}}{R}\right)^3$$

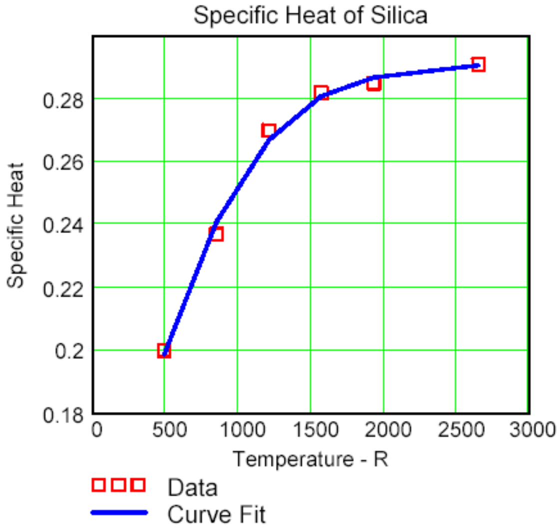

Alloy 800H

$k_{800H}(T) := \left[6.25 + .0055 \cdot \left(\frac{T}{R} - tr\right)\right] \cdot \frac{BTU}{hr \cdot ft \cdot R}$ $\quad Cp_{800H} := 0.12 \frac{BTU}{lb \cdot R}$

$\rho_{800H} := 501.12 \frac{lb}{ft^3}$

MACOR

$k_{mac} := 1.46 \frac{watt}{m \cdot K}$ $\quad k_{mac} = 0.8436 \frac{BTU}{hr \cdot ft \cdot R}$

$\rho_{mac} := 2.52 \frac{gm}{cm^3}$ $\quad \rho_{mac} = 157.3185\, lb\, ft^{-3}$

$Cp_{mac} := 790 \frac{joule}{kg \cdot K}$ $Cp_{mac} = 0.1887 \frac{BTU}{lb \cdot R}$

$SPEC_{mac} := Cp_{mac} \cdot \rho_{mac}$ $SPEC_{mac} = 29.6841 \frac{BTU}{R \cdot ft^3}$

HEAT TRANSFER CORRELATION

For the turbulent region the following heat transfer correlation was based on data on page 7-92 of the Heat Transfer Handbook, 1st Edition, 1973 (Ref. 1). For the laminar flow correlation has a correction factor to account for the channel width to length ratio (α) The laminar flow correlation is taken from London, A.L. & Shah, R. K., Laminar flow Forced Convection in Ducts (Ref. 2), The transition zone heat transfer is a linear approximation that fits between the limits of laminar and turbulent flow. The limits set in model are laminar flow: $Rel := 2300$ and turbulent flow: $Ret := 10000$. It should be noted that the transition zone heat transfer coefficient is only an approximation. It should also be noted that in the transition zone it is possible to oscillate between turbulent and laminar heat transfer.

$$Nu_{slot}(Re, Pr, Rel, Ret, \alpha) := \left| \begin{array}{l} Nu_t \leftarrow 0.0275 \cdot Re^{0.78} \cdot Pr^{0.3} \\ Nu_l \leftarrow 8.2449 - 17.005 \cdot \alpha + 25.512 \cdot \alpha^2 - 19.062 \cdot \alpha^3 + 5.8566 \cdot \alpha^4 \\ Nu1 \leftarrow 8.2449 - 17.005 \cdot \alpha + 25.512 \cdot \alpha^2 - 19.062 \cdot \alpha^3 + 5.8566 \cdot \alpha^4 \\ Nu2 \leftarrow .0275 \cdot Ret^{0.78} \cdot Pr^{0.3} \\ slope \leftarrow \dfrac{Nu2 - Nu1}{Ret - Rel} \\ B \leftarrow Nu1 - Rel \cdot slope \\ Nu_{tran} \leftarrow slope \cdot Re + B \\ Nu_t \text{ if } Re \geq Ret \\ Nu_l \text{ if } Re \leq Rel \\ Nu_{tran} \text{ otherwise} \end{array} \right.$$

NGNP
COMPOSITES
Calculation By: D. P. Carosella

General Atomics
Calculation Sheet
System CORE SUPPORT
Title: Establish Steady State Thermals and Input for TAC2D

Page No.: 10 of 23
Calculation No.:

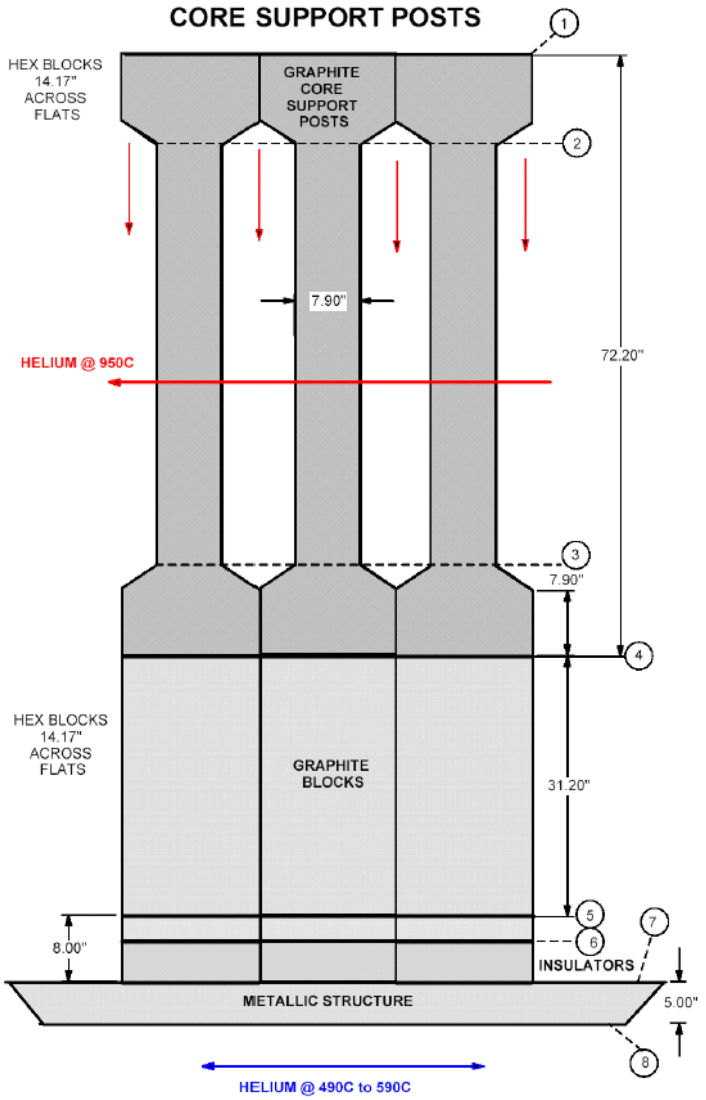

Figure 1: Core Support System

II. INPUT:

Geometric Parameters

Core Support Post Caps Hex Across Flats	$HexFlat := 14.17in$
Core Support Post Caps Hex Height	$HexH := 7.9in$
Core Support Post Total Length	$PostLen := 72.2in$
Post Diameter	$Postdia := 7.9in$
Graphite blocks height	
Case 1	$GraH_1 := 31.2in$
Case 2	$GraH_2 := .5 \cdot GraH_1$
Height of Ceramic Insulators	Variable
Metal Structure Thickness	$\Delta_{ms} := 5in$
Contact gap size (estimate)	$gap := .005in$
Diameter of holes in bottom reflector	$dia_{br} := 15.9mm$
Number of holes in bottom reflector	$No_{br} := 102$
Diameter of six helium groves in the core support post caps	$dia_{gr1} := 2 \cdot 27.4mm$
Diameter of 12 helium groves in the core support post caps	$dia_{gr2} := 2 \cdot 17.8mm$
Number of groves per post	$No_1 := 6$
	$No_2 := 12$
Number of Posts across the hot duct inlet	$No_{post} := 4$
Inlet Plenum height	$Pl_h := 500mm$
Plenum OD	$Pl_{od} := 6982mm$
Plenum ID	$Pl_{id} := 2900mm$
Number of Core Columns	$No_{col} := 259$

Thermodynamic Properties

Total Core Heat Generation	$Q_{tot} := 600MW$
Reactor Inlet Temperature	$T_{in} := (490 + tc) \cdot K$
Reactor Outlet Temperature	$T_{out} := (950 + tc) \cdot K$
Estimated Graphite Temp at Bottom of Core	$T_{gr} := (1000 + tc) \cdot K$
Helium Pressure	$P_{He} := 1025psi$

III. CALCULATIONS: This calculation is for two layers of MACOR

Referring to Figure 1, the following heat transfer paths can be defined in this problem.

1. Conduction down from the core to the core support posts at surface 1 (Figure 1). The core sits on 2 bottom reflectors and two flow distribution/support blocks (not shown) that are each half the height of a standard reflector block. This configuration results in five contact gaps between the core and the top of the core posts. The contact gaps are the primary heat transfer resistance between the core support posts and the active core.
2. Conduction in the top core support cap between surface 1 & 2. The core support cap contains groves for helium flow. Heat is transferred into the caps and is conducted down to the circular posts. The caps act as heat transfer fins.
3. The core support posts (surface 2 to 3) are subject to helium flow both in the vertical downward direction and in the horizontal direction. These flows generate large heat transfer coefficients. The posts act as thermal fins.
4. The bottom caps (surface 3 to 4) conduct heat from the posts to the graphite blocks.
5. The graphite blocks (surface 4 to 5) conduct heat downward into the insulating blocks.
6. The insulating blocks (surfaces 5 to 6 and 6 to 7) conduct heat downward into the metallic structure.
7. The metallic structure (surface 7 to 8) is cooled by the core inlet helium.
8. Gaps are located at surfaces 1, 4, and 5-7. These gaps also provide a major heat transfer resistance.

Geometric Calculations

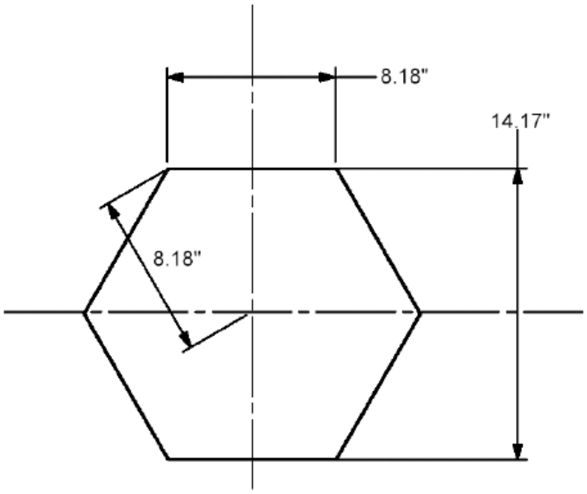

Figure 2: HEXAGONAL GRAPHITE BLOCK

Cross Sectional Area for the Hex

$$A_{hex} := 6\cdot\frac{HexFlat}{2}\cdot\frac{HexFlat}{3^{.5}}\cdot.5$$

$$A_{hex} = 1.2076\,ft^2$$

Cross Sectional Area of the Post

$$A_{post} := \frac{\pi}{4}\cdot Postdia^2$$

$$A_{post} = 0.3404\,ft^2$$

Flow area in the bottom reflector $A_{brflow} := No_{br} \cdot \left(\frac{\pi}{4} \cdot dia_{br}^{2} \right)$ $A_{brflow} = 0.218\,ft^{2}$

He Heat Transfer Area in a single bottom reflector: $A_{brht} := No_{br} \cdot \pi \cdot dia_{br} \cdot GraH_2$

$A_{brht} = 21.7308\,ft^{2}$

Flow area in flow control blocks and caps $A_{fc} := \pi \cdot \left(No_1 \cdot \frac{dia_{gr1}^{2}}{4} + No_2 \cdot \frac{dia_{gr2}^{2}}{4} \right) \cdot .5$

$A_{fc} = 0.1404\,ft^{2}$

He Heat Transfer Area in flow control blocks $A_{fcht} := \pi \cdot \left(No_1 \cdot \frac{dia_{gr1}}{2} + No_2 \cdot \frac{dia_{gr2}}{2} \right) \cdot GraH_2$

$A_{fcht} = 5.0649\,ft^{2}$

He Heat Transfer Area in post caps $A_{pcht} := \pi \cdot \left(No_1 \cdot \frac{dia_{gr1}}{2} + No_2 \cdot \frac{dia_{gr2}}{2} \right) \cdot HexH$

$A_{pcht} = 2.5649\,ft^{2}$

Gap Heat Transfer Resistance based on helium @ 950C

$$Res_{gap} := \frac{gap}{k_{He}(T_{out})} \qquad Res_{gap} = 0.0018\,hr \cdot ft^{2} \cdot \frac{R}{BTU}$$

Calculate the total He flow rate

$$W_{tot} := \frac{Q_{tot}}{Cp_{He} \cdot (T_{out} - T_{in})} \qquad W_{tot} = 552.9984\,lb\,sec^{-1}$$

Helium flow per column

$$W_{col} := \frac{W_{tot}}{102} \qquad W_{col} = 5.4216\,lb\,sec^{-1}$$

NGNP
COMPOSITES
Calculation By: D. P. Carosella

General Atomics
Calculation Sheet
System CORE SUPPORT
Title: Establish Steady State Thermals and Input for TAC2D

Page No.: 14 of 23
Calculation No.:

Bottom reflector heat transfer parameters

$$WP_{br} := No_{br} \cdot dia_{br} \cdot \pi$$

$$Re_{br} := \frac{4 \cdot W_{col}}{WP_{br} \cdot \mu_{He}(T_{out})} \qquad Re_{br} = 3.78 \times 10^{4}$$

$$Nu_{br} := .023 \cdot Re_{br}^{.8} \cdot Pr_{He}(T_{out})^{.4}$$

$$Nu_{br} = 89.6748$$

$$h_{br} := Nu_{br} \cdot \frac{k_{He}(T_{out})}{dia_{br}} \qquad h_{br} = 397.0957 \frac{BTU}{hr \cdot ft^{2} \cdot R}$$

UA products

$$UA_{cc} := h_{br} \cdot A_{brht} \qquad UA_{cc} = 8629.2038 \frac{BTU}{hr \cdot R}$$

Contact Gap

$$UA_{gap} := \frac{A_{hex} - A_{brflow}}{Res_{gap}} \qquad UA_{gap} = 548.6051 \frac{BTU}{hr \cdot R}$$

In the bottom reflector blocks the coolant holes will dominate the heat transfer

Estimate first block temperature

$$T_{rb1} := \frac{T_{out} \cdot UA_{cc} + T_{gr} \cdot UA_{gap}}{UA_{cc} + UA_{gap}} \qquad T_{rb1} = 1226.1488\,K$$

$$TC_{rb1} := TC(T_{rb1}) \qquad TC_{rb1} = 952.9888\,^{\circ}C$$

Based on the above calculation it is clear that the boundary at station 1 will be at 950ºC.

Heat Transfer Coefficients Around The Posts

Void Space per post: $Gap := HexFlat - Postdia$ $Gap = 0.5225\,ft$

Flow area at the hot duct inter face $A_{hdflow} := Gap \cdot (PostLen - 2 \cdot HexH) \cdot (No_{post} + 1)$

$$A_{hdflow} = 12.2787\,ft^2$$

Velocity $Vel := \dfrac{W_{tot}}{A_{hdflow} \cdot \rho_{He}(T_{out}, P_{He})}$ $Vel = 259.4822\,ft\,sec^{-1}$

Heat Transfer for flow past a cylinder

$$Re_{post} := \frac{Vel \cdot Postdia}{\dfrac{\mu_{He}(T_{out})}{\rho_{He}(T_{out}, P_{He})}} \qquad Re_{post} = 8.6388 \times 10^5$$

$$Nu_{post} := .0239 \cdot Re_{post}^{\,.805} \qquad Nu_{post} = 1436.2876$$

$$h_{post} := Nu_{post} \cdot \frac{k_{He}(T_{out})}{Postdia} \qquad h_{post} = 503.9677 \frac{BTU}{hr \cdot ft^2 \cdot R}$$

Heat transfer in the inlet plenum

Plenum average diameter $Pl_{dia} := \frac{Pl_{od} + Pl_{id}}{2}$ $Pl_{dia} = 16.2106\,ft$

Plenum flow area $Pl_{area} := Pl_{dia} \cdot Pl_h$ $Pl_{area} = 26.5922\,ft^2$

$Dh_{pl} := 2 \cdot Pl_h$ $Dh_{pl} = 3.2808\,ft$

$\alpha_{pl} := \frac{Pl_h}{Pl_{od} - Pl_{id}}$ $\alpha_{pl} = 0.1225$

$Re_{pl} := \frac{4 \cdot W_{tot}}{2 \cdot \pi \cdot Pl_{dia} \cdot \mu_{He}(T_{in})}$ $Re_{pl} = 8.696 \times 10^5$

$Nu_{pl} := Nu_{slot}(Re_{pl}, Pr_{He}(T_{in}), Rel, Ret, \alpha_{pl})$ $Nu_{pl} = 1044.0404$

$h_{pl} := Nu_{pl} \cdot \frac{k_{He}(T_{in})}{Dh_{pl}}$ $h_{pl} = 53.4883 \frac{BTU}{hr \cdot ft^2 \cdot R}$

Establish the overall U for heating at the inside faces of the hexagonal portion of the core support posts. These surfaces are at station 2 and 3 in Figure 1.

$U4_{post} := \frac{1}{\frac{1}{h_{post}} + \frac{HexH}{k_{gr}}}$ $U4_{post} = 25.9347 \frac{BTU}{hr \cdot ft^2 \cdot R}$

Thickness of the two insulation layers:

$X_{cer1} := 3in$ $X_{cer2} := 3in$

The circular portion of the support posts act as fins. The UA product for circular fins is: $UA = \left(h \cdot \pi \cdot D \cdot k \cdot \frac{\pi}{4} \cdot D^2\right)^{.5}$ where:

1) h is the heat transfer coefficient
2) D is the diameter of the post and
3) k is the thermal conductivity

$$mfin := \left[\frac{h_{post} \cdot \pi Postdia}{k_{gr} \cdot \left(\frac{\pi}{4}\right) \cdot Postdia^2}\right]^{.5} \qquad mfin = 13.0428\, ft^{-1}$$

$$UA_{post} := \left[h_{post} \cdot \pi Postdia \cdot k_{gr} \cdot \left(\frac{\pi}{4}\right) \cdot Postdia^2\right]^{.5} \cdot \tanh[mfin \cdot (PostLen - 2 \cdot HexH)]$$

$$UA_{post} = 79.9146 \frac{BTU}{hr \cdot R}$$

Solve for Temperatures

There are 15 unknown temperatures in this model. At each station (1-8) in Figure 1 there are two possible temperatures Tu and Td. Tu is the temperature on the upper side of the station Td is the temperature at the lower side of the station. For stations 1-3 Tu = Td. Station 8 does not have a Td

First estimate of Temperatures Tu and Td

$Tu_1 := (T_{out})$ $Td_1 := Tu_1$ $Tu_2 := T_{out}$ $Td_2 := Tu_2$

$Tu_3 := (938 + tc) \cdot K$ $Td_3 := Tu_3$ $Tu_4 := (909 + tc) \cdot K$ $Td_4 := (907 + tc) \cdot K$

$Tu_5 := (763 + tc) \cdot K$ $Td_5 := (761 + tc) \cdot K$ $Tu_6 := (700 + tc) \cdot K$ $Td_6 := (698 + tc) \cdot K$

$Tu_7 := (547 + tc) \cdot K$ $Td_7 := (544 + tc) \cdot K$ $Tu_8 := (509 + tc) \cdot K$

Estimates of mean temperatures

$$Tbar_1 := \frac{Td_2 + Tu_3}{2} \qquad Tbar_2 := \frac{Td_3 + Tu_4}{2} \qquad Tbar_3 := \frac{Td_4 + Tu_5}{2}$$

$$Tbar_4 := \frac{Td_5 + Tu_6}{2} \qquad Tbar_5 := \frac{Td_6 + Tu_7}{2} \qquad Tbar_6 := \frac{Td_7 + Tu_8}{2}$$

Use a Solve Block to solve for the unknown temperatures

Given

Fixed Restraints

$$Tu_1 = T_{out} \qquad Td_2 = Tu_2 \qquad Td_3 = Tu_3$$

HEAT BALANCE EQUATIONS

Heat Balance on the upper hexagonal cap of the core support post

$$\begin{bmatrix} U4_{post} \cdot (A_{hex} - A_{post}) \cdot 2 \cdot (T_{out} - Td_1) \ ... & = (Td_1 - Tu_2) \cdot \dfrac{A_{post} \cdot k_{gr}}{.5 \cdot HexH} \\ + 6 \cdot 8.18 \cdot in \cdot HexH \cdot \dfrac{1}{\dfrac{1}{h_{post}} + \dfrac{4 \cdot in}{k_{gr}}} \cdot (T_{out} - Td_1) & \end{bmatrix}$$

Heat Balance on the Core Support Post

$$UA_{post} \cdot (T_{out} - Td_3) = (Td_3 - Tu_4) \cdot \frac{k_{gr} \cdot A_{hex}}{HexH}$$

Heat Balance on the lower hexagonal cap of the Post

$$(Td_3 - Tu_4)\cdot\frac{k_{gr}\cdot A_{hex}}{HexH} + \left[U4_{post}\cdot(A_{hex} - A_{post})\cdot(T_{out} - Tu_4)\right] = (Tu_4 - Td_4)\cdot\left(\frac{1}{Res_{gap}}\cdot A_{hex}\right)$$

Heat Balances for the gap at station 4 and the hexagonal support block .

$$(Tu_4 - Td_4)\cdot\left(\frac{1}{Res_{gap}}\cdot A_{hex}\right) = (Td_4 - Tu_5)\cdot\frac{A_{hex}\cdot k_{gr}}{GraH_1}$$

Heat Balances for the gap at station 5 and the hexagonal support block .

$$(Td_4 - Tu_5)\cdot\frac{A_{hex}\cdot k_{gr}}{GraH_1} = (Tu_5 - Td_5)\cdot\left(\frac{1}{Res_{gap}}\cdot A_{hex}\right)$$

Heat Balances for the gap at station 5 and the upper Macor insulator .

$$\frac{1}{Res_{gap}}\cdot A_{hex}\cdot(Tu_5 - Td_5) = (Td_5 - Tu_6)\cdot\frac{k_{mac}\cdot A_{hex}}{X_{cer1}}$$

Heat Balances for the gap at station 6 and the upper Macor insulator .

$$(Td_5 - Tu_6)\cdot\frac{k_{mac}\cdot A_{hex}}{X_{cer1}} = \frac{1}{Res_{gap}}\cdot A_{hex}\cdot(Tu_6 - Td_6)$$

Heat Balances for the gap at station 6 and the lower insulator .

$$\frac{1}{Res_{gap}}\cdot A_{hex}\cdot(Tu_6 - Td_6) = (Td_6 - Tu_7)\cdot\frac{k_{mac}\cdot A_{hex}}{X_{cer2}}$$

NGNP COMPOSITES
Calculation By: D. P. Carosella

General Atomics
Calculation Sheet
System CORE SUPPORT
Title: Establish Steady State Thermals and Input for TAC2D

Page No.: 20 of 23
Calculation No.:

Heat Balances for the gap at station 7 and the lower Macor insulator .

$$\left(Td_6 - Tu_7\right)\cdot\frac{k_{mac}\cdot A_{hex}}{X_{cer2}} = \frac{1}{Res_{gap}}\cdot A_{hex}\cdot\left(Tu_7 - Td_7\right)$$

Heat balance for the gap at station 7 and the metallic core support floor

$$\frac{1}{Res_{gap}}\cdot A_{hex}\cdot\left(Tu_7 - Td_7\right) = \left(Td_7 - Tu_8\right)\cdot\frac{k_{800H}\left(Tbar_6\right)\cdot A_{hex}}{\Delta_{ms}}$$

Heat Balance for the metallic core support floor and the helium in the lower plenum

$$\left(Td_7 - Tu_8\right)\cdot\frac{k_{800H}\left(Tbar_6\right)\cdot A_{hex}}{\Delta_{ms}} = \left(Tu_8 - T_{in}\right)\cdot h_{pl}\cdot A_{hex}$$

Overall Heat Balance

$$\begin{aligned}&\left[UA_{post}\cdot\left(T_{out} - Tu_3\right) + U4_{post}\cdot\left(A_{hex} - A_{post}\right)\cdot\left(T_{out} - Tu_4\right)\right] \ldots = \left(Tu_8 - T_{in}\right)\cdot h_{pl}\cdot A_{hex}\\ &+ \left[U4_{post}\cdot\left(A_{hex} - A_{post}\right)\cdot 2\cdot\left(T_{out} - Td_1\right) \ldots \right.\\ &\left. + 6\cdot 8.18\cdot in\cdot HexH\cdot\frac{1}{\frac{1}{h_{post}} + \frac{4\cdot in}{k_{gr}}}\cdot\left(T_{out} - Td_1\right)\right]\end{aligned}$$

IV. RESULTS

The results of this analysis are tabulated below. These results will be used to calculate the heat transfer from the outlet helium to the inlet helium.

$$\begin{pmatrix} AA \\ BB \end{pmatrix} := \text{Find}(Tu, Td)$$

$$Tu := AA \qquad Td := BB$$

$$Tu = \begin{pmatrix} 1223.16 \\ 1223.16 \\ 1218.8681 \\ 1208.4799 \\ 1126.9561 \\ 960.75 \\ 794.5439 \\ 773.5816 \end{pmatrix} K \qquad Td = \begin{pmatrix} 1223.16 \\ 1223.16 \\ 1218.8681 \\ 1207.4744 \\ 1125.9506 \\ 959.7445 \\ 793.5385 \end{pmatrix} K$$

Solution in °K

$$TCu := TC(Tu) \qquad TCd := TC(Td)$$

Solution in °C

$$TCu = \begin{pmatrix} 950 \\ 950 \\ 945.7081 \\ 935.3199 \\ 853.7961 \\ 687.59 \\ 521.3839 \\ 500.4216 \end{pmatrix} {}^\circ C \qquad TCd = \begin{pmatrix} 950 \\ 950 \\ 945.7081 \\ 934.3144 \\ 852.7906 \\ 686.5845 \\ 520.3785 \end{pmatrix} {}^\circ C$$

Estimate the component average temperature

$$Tbar_1 := \frac{Td_2 + Tu_3}{2} \qquad Tbar_2 := \frac{Td_3 + Tu_4}{2} \qquad Tbar_3 := \frac{Td_4 + Tu_5}{2}$$

$$Tbar_4 := \frac{Td_5 + Tu_6}{2} \qquad Tbar_5 := \frac{Td_6 + Tu_7}{2} \qquad Tbar_6 := \frac{Td_7 + Tu_8}{2}$$

$$TCbar := TC(Tbar)$$

$$TCbar = \begin{pmatrix} 947.8541 \\ 940.514 \\ 894.0553 \\ 770.1903 \\ 603.9842 \\ 510.4 \end{pmatrix} °C \quad \begin{array}{l} \text{Core Support Post} \\ \text{Lower Hexagonal Cap} \\ \text{Graphite Support Block} \\ \text{Upper Insulator} \\ \text{Lower Insulator} \\ \text{800H Support plate} \end{array}$$

Calculate Heat Transfered from the outlet helium to the inlet helium

Assume tha each of the core support columns transfer the same quanity of heat. This is a conservative assumption.

$$Q := No_{col} \cdot \left(Tu_8 - T_{in}\right) \cdot h_{pl} \cdot A_{hex} \qquad Q = 0.092\,MW \qquad Qpc := \frac{Q}{Q_{tot}}$$

$$Qpc = 0.0153\,\%$$

Calculate the temperature change of the helium

$$\Delta T_{He} := \frac{Q}{W_{tot} \cdot Cp_{He}} \qquad \Delta T_{He} = 0.0705\,K$$

NGNP **COMPOSITES** Calculation By: D. P. Carosella	General Atomics **Calculation Sheet** System CORE SUPPORT Title: Establish Steady State Thermals and Input for TAC2D	Page No.: 23 of 23 Calculation No.:

V. REFERENCES

1. Rohsenow & Hartnett, HANDBOOK OF HEAT TRANSFER, 1st edition 1973, Page 7-92
2. London, A.L. & Shah, R. K., Laminar Flow Forced Convection in Ducts, Academic Press, 1978
3. McDowell, J. Spotts, A Study of the Silica Refractories, page 22, 1917

APPENDIX D – Thermal Analysis Supporting the Hot Duct Design

SUMMARY The cross duct insulation system (Figure D-1) must be designed so as to prevent excessive heat transfer from the hot outlet helium (950°C) to the cold inlet helium (490°C). The maximum allowable temperature increase for the inlet helium is 1°C. A parametric study was performed to determine the required insulation thickness as a function of insulation conductivity. This study considered two cases. The first case considered a 1°C helium temperature change. The second case considered a 0.25°C helium temperature change. The results of these two cases are shown in Figures D-2 & D-3.

MODEL DESCRIPTION (Refer to Figure D-1) The overall conductance between the hot duct and the cold duct includes the heat transfer coefficients, the resistance across the carbon-carbon layers and the resistance across the insulation. In the MATHCAD model, the overall conductance is set so as to meet the cold helium temperature rise criteria. The heat transfer coefficients and resistance across the carbon-carbon layers are known values, thus, for any given insulation conductivity, the required thickness can be calculated based on the required overall conductance. In the MATHCAD model the insulation thickness was calculated as a function of the insulation conductivity. Thus, for any given insulation the required thickness can be found.

RESULTS Figures D-2 & D-3 are plots of the required thickness as a function of conductivity for two cases: 1°C temperature rise of the cold helium and 0.25°C temperature rise of the cold helium.

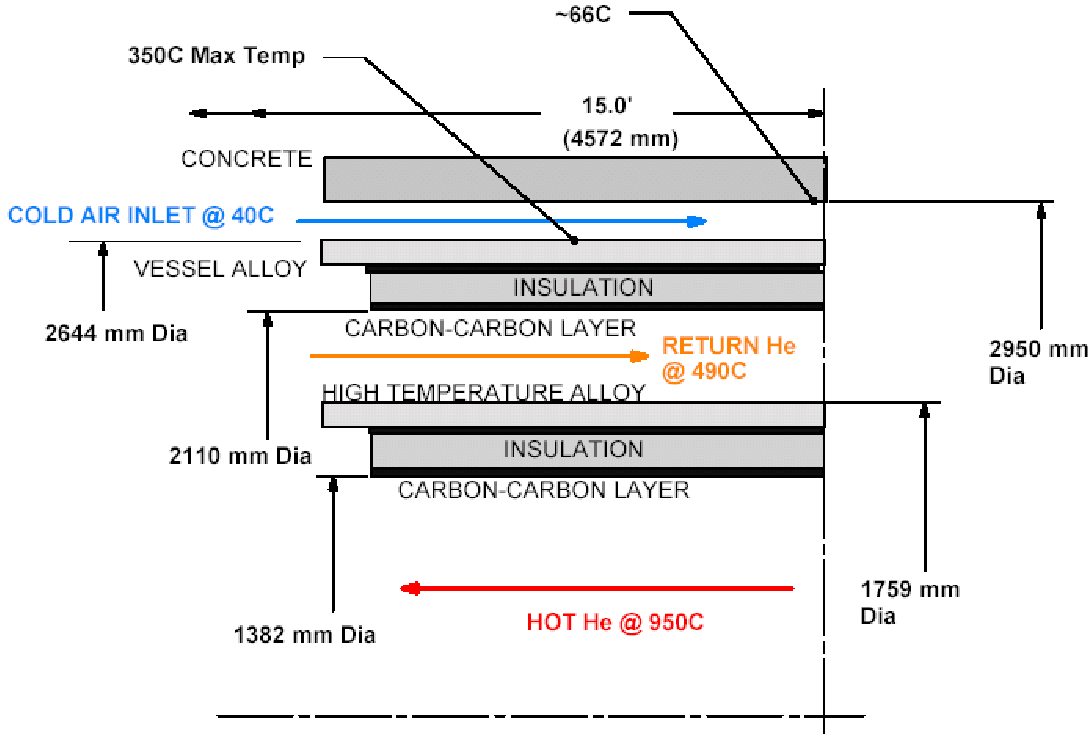

Figure D-1. Cross Duct

CASE 1

CONTROL PARAMETERS $\Delta T_{duct} = 1\,K$ $TC_c = 490\,^{\circ}C$ $TC_h = 950\,^{\circ}C$

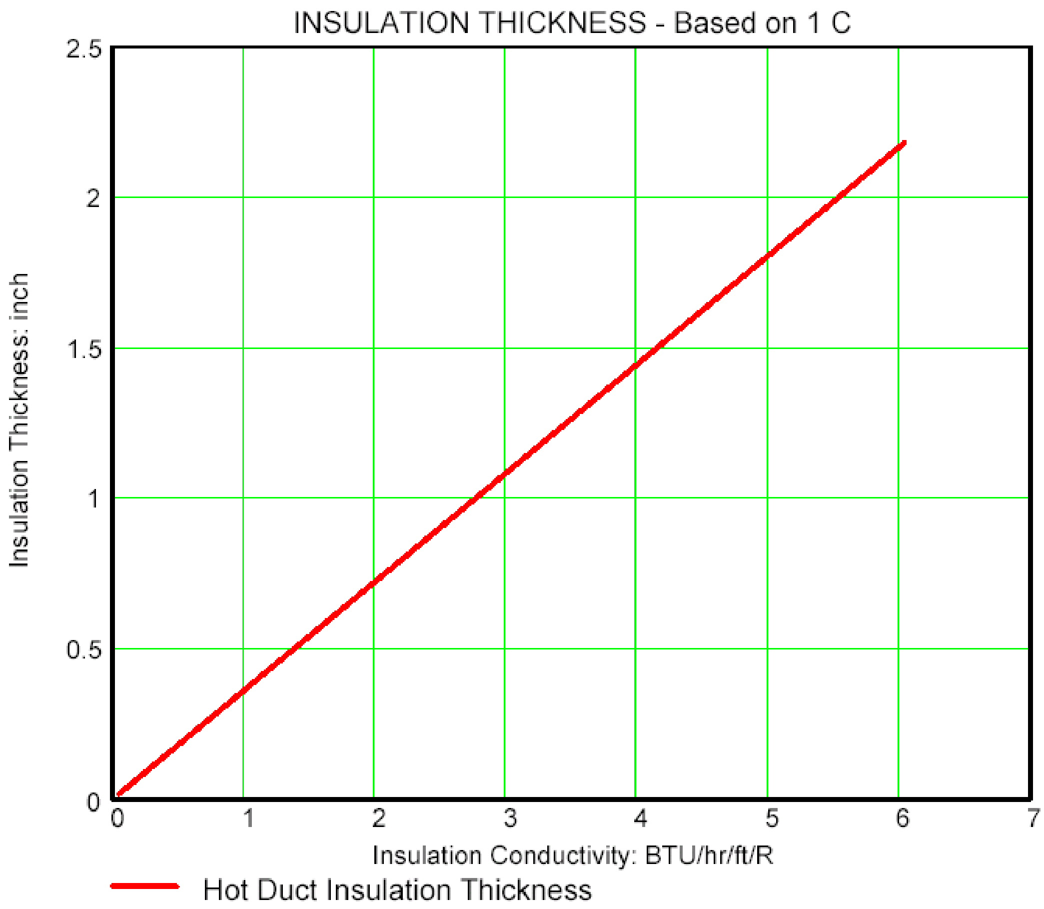

Figure D-2. $1^{o}C$ Temperature Rise

CASE 2

CONTROL PARAMETERS $\Delta T_{duct} = 0.25\,K$ $TC_c = 490\,°C$ $TC_h = 950\,°C$

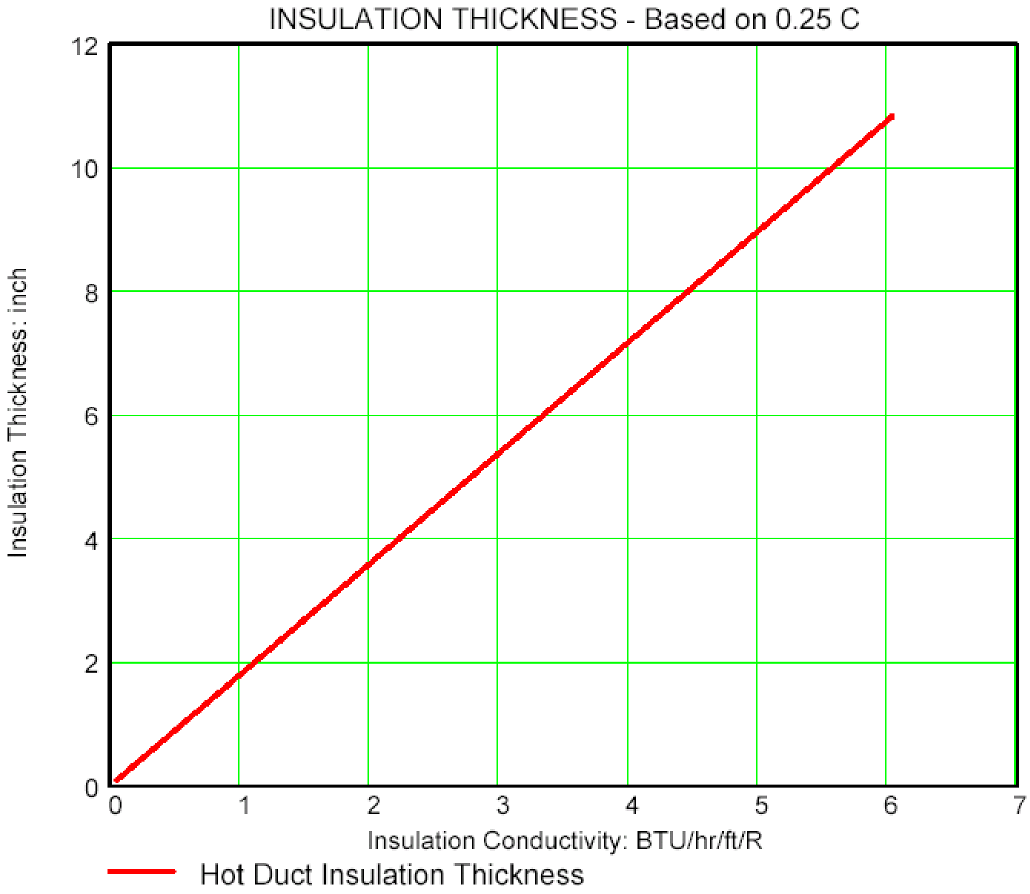

Figure D-3. 0.25^{o}C Temperature Rise

REFERENCES

1. MATHCAD 11. Technical Calculation Tool

MATHCAD MODEL

NGNP
COMPOSITES
Calculation By: D. P. Carosella
Date Saved: 9/30/2008

General Atomics
Calculation Sheet
System HOT DUCT
Title: Evaluation of Insulation Thickness Tcold = 490C Thot = 950C C-C 0.25"

Page No.: 1 of 15

Calculation No.: A30302-01

I. INTRODUCTION

The cross duct system (two concetntric ducts) transports hot helium from the reactor to the PCS and cold helium from the PCS back to the reactor. This concentric configuration results in regenerative between the hot helium and the cold helium. The criteria for allowable regenerative heating has been set at $\Delta T_{duct} := 1K$ or less. This model will be used to determine the required insulation thickness between the concentric ducts. The cross duct is shown in Figure 1. The constants, heat transfer functions and material properties are tabulated below.

Constants, Properties and Functions

$ORIGIN \equiv 1$

TC(T) converts the absolute temperature (T) to °C. TF(T) converts the absolute temperature to °F

$$TC(T) := \left(\frac{T}{K} - tc\right)\cdot °C \qquad TF(T) := \left(\frac{T}{R} - tr\right)\cdot °F$$

$kPa := Pa\cdot 1000$

$tc \equiv 273.16$

$tr \equiv 459.69$

$°C \equiv K$

$°F \equiv R$

$MPa \equiv Pa\cdot 10^{6}$

$bar \equiv .1\cdot MPa$

$CFM \equiv ft^{3}\cdot min^{-1}$

$MW := watt\cdot 10^{6}$

$kW := watt\cdot 10^{3}$

$R_{gas} := 1545\dfrac{lbf\cdot ft}{lb\cdot R}$

Properties of Helium

$Cp_{He} := 1.242\dfrac{BTU}{lb\cdot R}$

$k_{He}(T) := 1.29\cdot 10^{-3}\dfrac{BTU}{hr\cdot ft\cdot R}\cdot\left(\dfrac{T}{R}\right)^{.674}$

$\mu_{He}(T) := 6.9\cdot 10^{-4}\dfrac{lb}{ft\cdot hr}\cdot\left(\dfrac{T}{R}\right)^{.674}$

$Pr_{He}(T) := \dfrac{Cp_{He}\cdot\mu_{He}(T)}{k_{He}(T)}$

$Mol_{He} \equiv 4$

$R_{He} := \dfrac{R_{gas}}{Mol_{He}}$

$\gamma_{He} \equiv 1.667$

$\rho_{He}(T,P) := \dfrac{P}{R_{He}\cdot T}$

NGNP **COMPOSITES** Calculation By: D. P. Carosella Date Saved: 9/30/2008	General Atomics **Calculation Sheet** System HOT DUCT Title: Evaluation of Insulation Thickness Tcold = 490C Thot = 950C C-C 0.25"	Page No.: 2 of 15 Calculation No.: A30302-01

Properties of Kaowool

$$k_{ins}(T) := \left[.113 + 1.154 \cdot 10^{-4} \cdot \left(\frac{T}{R} - tr \right) \right] \cdot \frac{BTU}{hr \cdot ft \cdot R}$$

Air Properties:

Conductivity

$$K6 := 0.0146 \cdot \frac{BTU}{R \cdot ft \cdot hr} \qquad K7 := 1.695 \cdot 10^{-5} \cdot \frac{BTU}{R^2 \cdot ft \cdot hr} \qquad k_{air}(T) := K6 + K7 \cdot (T - tr \cdot R)$$

Viscosity

$$K9 := .04176 \cdot \frac{lb}{ft \cdot hr} \qquad K10 := 4.914 \cdot 10^{-05} \cdot \frac{lb}{ft \cdot hr \cdot R}$$

$$\mu_{air}(T) := K9 + K10 \cdot (T - tr \cdot R)$$

Specific Heat:

$$Cp_{air}(T) := .23578 \cdot \frac{BTU}{lb \cdot R} + \left(8.1532 \cdot 10^{-06} \cdot \frac{BTU}{lb \cdot R^2} \cdot T \right) \qquad R_{air} := \frac{1546}{29} \cdot \frac{lbf \cdot ft}{lb \cdot R}$$

$$Pr_{air}(T) := \frac{Cp_{air}(T) \cdot \mu_{air}(T)}{k_{air}(T)} \qquad \gamma_{air} := 1.38$$

$$P_{air} := 14.7 psi$$

Density $$\rho_{air}(P_{air}, T) := \frac{P_{air}}{T \cdot R_{air}}$$

$$\beta_{air}(T) := \frac{1}{T}$$

HEAT TRANSFER CORRELATION

For the turbulent region the following heat transfer correlation was based on data on page 7-92 of the Handbook of Heat Transfer, 1st Edition, 1973. For the laminar region the heat transfer correlation is based on data in Table 7.1 in Heat, Mass, and Momentum Transfer by Rohsenow and Choi, 1st edition, 1961. This correlation has a correction factor to account for the channel width to length ratio (α) The laminar flow correlation is taken from London, A.L. & Shah, R. K., Laminar flow Forced Convection in Ducts (Ref. 2). The transition zone heat transfer is a linear approximation that fits between the limits of laminar and turbulent flow. The limits set in model are laminar flow: $Rel := 2300$ and turbulent flow: $Ret := 10000$. It should be noted that the transition zone heat transfer coefficient is only an approximation. It should also be noted that in the transition zone it is possible to oscillate between turbulent and laminar heat transfer.

$$
Nu_{slot}(Re, Pr, Rel, Ret, \alpha) := \left|
\begin{array}{l}
Nu_t \leftarrow 0.0275 \cdot Re^{0.78} \cdot Pr^{0.3} \\
Nu_l \leftarrow 8.2449 - 17.005 \cdot \alpha + 25.512 \cdot \alpha^2 - 19.062 \cdot \alpha^3 + 5.8566 \cdot \alpha^4 \\
Nu1 \leftarrow 8.2449 - 17.005 \cdot \alpha + 25.512 \cdot \alpha^2 - 19.062 \cdot \alpha^3 + 5.8566 \cdot \alpha^4 \\
Nu2 \leftarrow .0275 \cdot Ret^{0.78} \cdot Pr^{0.3} \\
slope \leftarrow \dfrac{Nu2 - Nu1}{Ret - Rel} \\
B \leftarrow Nu1 - Rel \cdot slope \\
Nu_{tran} \leftarrow slope \cdot Re + B \\
Nu_t \quad \text{if} \quad Re \geq Ret \\
Nu_l \quad \text{if} \quad Re \leq Rel \\
Nu_{tran} \quad \text{otherwise}
\end{array}
\right.
$$

NOTE: The following correlations for heat transfer coefficients include approximate solutions for the transition zone between laminar and turbulent flow. In these functions Rel is the Reynolds number at the upper end of the laminar region and Ret is the Reynolds number at the start of the turbulent region.

Heat Transfer in a pipe: $Rel := 2300, \quad Ret := 10000$

$$Nu_{pipe}(Re, Pr, Rel, Ret) := \left| \begin{array}{l} Nu_t \leftarrow 0.023 \cdot Re^{0.8} \cdot Pr^{0.4} \\ Nu_l \leftarrow 4 \\ Nu1 \leftarrow 4 \\ Nu2 \leftarrow .023 \cdot Ret^{0.8} \cdot Pr^{0.4} \\ slope \leftarrow \dfrac{Nu2 - Nu1}{Ret - Rel} \\ B \leftarrow Nu1 - Rel \cdot slope \\ Nu_{tran} \leftarrow slope \cdot Re + B \\ Nu_t \quad \text{if} \quad Re \ge Ret \\ Nu_l \quad \text{if} \quad Re \le Rel \\ Nu_{tran} \quad \text{otherwise} \end{array} \right.$$

II. INPUT:

Reactor Heat Load	$Q_{tot} := 600MW$
Reactor Outlet Temperature	$T_h := (950 + tc) \cdot K$
Reactor Inlet Temperature	$T_c := (490 + tc) \cdot K$
Helium Pressure	$P_{He} := 7MPa$
Diameter of the hot duct	$Dia_{hot} := 1382mm$
Inside Diameter of the return duct	$Dia_{in} := 1759mm$
Outside Diameter of the return duct	$Dia_{out} := 2110mm$
Outside Diameter of cross duct	$Dia_{cross} := 2644mm$
Cross Duct Length	$Len_{duct} := 15ft$
Carbon-Carbon layer thickness	$\Delta_{cc} := .25in$

III. CALCULATIONS:

Calculate the flow rates:

$$W_{He} := \frac{Q_{tot}}{Cp_{He} \cdot (T_h - T_c)} \qquad W_{He} = 552.9984\,lb\,sec^{-1}$$

Calculate the heat transfer across the duct wall

$$Q_{vw} := W_{He} \cdot Cp_{He} \cdot \Delta T_{duct} \qquad Q_{vw} = 1.3043\,MW$$

$$U_{duct} = \frac{1}{\frac{1}{h_h} + \frac{2 \cdot \Delta_{cc}}{k_{cc}} + \frac{Dia_{hot}}{Dia_{in} \cdot h_c} + \frac{x_{ins}}{k_{ins}}}$$

$$k_{ins} \cdot \frac{-U_{duct} \cdot k_{cc} \cdot Dia_{in} \cdot h_c - 2 \cdot U_{duct} \cdot \Delta_{cc} \cdot h_h \cdot Dia_{in} \cdot h_c - U_{duct} \cdot Dia_{hot} \cdot h_h \cdot k_{cc} + h_h \cdot k_{cc} \cdot Dia_{in} \cdot h_c}{U_{duct} \cdot h_h \cdot k_{cc} \cdot Dia_{in} \cdot h_c}$$

$$x_{ins} = k_{ins} \cdot \frac{-U_{duct} \cdot k_{cc} \cdot Dia_{in} \cdot h_c - 2 \cdot U_{duct} \cdot \Delta_{cc} \cdot h_h \cdot Dia_{in} \cdot h_c - U_{duct} \cdot Dia_{hot} \cdot h_h \cdot k_{cc} + h_h \cdot k_{cc} \cdot Dia_{in} \cdot h_c}{U_{duct} \cdot h_h \cdot k_{cc} \cdot Dia_{in} \cdot h_c}$$

$$x_{ins} = k_{ins} \cdot \frac{\left[\begin{array}{l} \left[-\left(k_{cc} \cdot Dia_{in} \cdot h_c\right)\right] - 2 \cdot \Delta_{cc} \cdot h_h \cdot Dia_{in} \cdot h_c \;... \\ + \left[-Dia_{hot} \cdot h_h \cdot k_{cc} + \left(\frac{h_h}{U_{duct}} \cdot k_{cc} \cdot Dia_{in} \cdot h_c\right)\right] \end{array}\right]}{h_h \cdot k_{cc} \cdot Dia_{in} \cdot h_c}$$

$A_{hot} := \pi \cdot Dia_{hot} \cdot Len_{duct}$ $\quad A_{hot} = 213.6654\,ft^2$

Required overall U

$$U_{duct} := \frac{Q_{vw}}{A_{hot} \cdot (T_h - T_c)} \qquad U_{duct} = 25.1568 \frac{BTU}{hr \cdot ft^2 \cdot R}$$

Heat Transfer Coefficients

Hot Side

$$Re_{hot} := \frac{4 \cdot W_{He}}{\pi \cdot Dia_{hot} \cdot \mu_{He}(T_h)} \qquad Re_{hot} = 4.5246 \times 10^6$$

$Nu_h := Nu_{pipe}(Re_{hot}, Pr_{He}(T_h), Rel, Ret)$ $\quad Nu_h = 4122.3206$

$$h_h := \frac{Nu_h \cdot k_{He}(T_h)}{Dia_{hot}} \qquad h_h = 210.0176 \frac{BTU}{hr \cdot ft^2 \cdot R}$$

Return Duct

$$Re_{cold} := \frac{4 \cdot W_{He}}{\pi \cdot (Dia_{in} + Dia_{out}) \cdot \mu_{He}(T_c)} \qquad Re_{cold} = 2.2211 \times 10^6$$

$$Aflow_c := \frac{\pi}{4} \cdot \left(Dia_{out}^2 - Dia_{in}^2\right) \qquad Aflow_c = 11.4806\,ft^2$$

$$D_h := \frac{4Aflow_c}{\pi \cdot (Dia_{in} + Dia_{out})} \qquad D_h = 1.1516\,ft$$

$$\alpha_{duct} := \frac{(Dia_{out} - Dia_{in}) \cdot .5}{(Dia_{in} + Dia_{out}) \cdot .5 \cdot \pi} \qquad \alpha_{duct} = 0.0289$$

$$Nu_c := Nu_{slot}\left(Re_{cold}, Pr_{He}(T_c), Rel, Ret, \alpha_{duct}\right) \qquad Nu_c = 2169.5481$$

$$h_c := Nu_c \cdot \frac{k_{He}(T_c)}{D_h} \qquad h_c = 316.6674 \frac{BTU}{hr \cdot ft^2 \cdot R}$$

$$k_{cc} := 30 \frac{watt}{m \cdot K}$$

$$k_{cc} = 17.3337 \frac{BTU}{hr \cdot ft \cdot R} \qquad k_{ins} := 10 \frac{BTU}{hr \cdot ft \cdot R}$$

$$X_{ins} := k_{ins} \cdot \frac{\left[\begin{array}{l} \left[-(k_{cc} \cdot Dia_{in} \cdot h_c)\right] - 2 \cdot \Delta_{cc} \cdot h_h \cdot Dia_{in} \cdot h_c \; ... \\ + \left[-Dia_{hot} \cdot h_h \cdot k_{cc} + \left(\frac{h_h}{U_{duct}} \cdot k_{cc} \cdot Dia_{in} \cdot h_c\right)\right] \end{array}\right]}{h_h \cdot k_{cc} \cdot Dia_{in} \cdot h_c} \qquad X_{ins} = 3.6125\,in$$

$$TC_c := TC(T_c) \qquad TC_h := TC(T_h)$$

$$Line := 0$$

NGNP
COMPOSITES
Calculation By: D. P. Carosella
Date Saved: 9/30/2008

General Atomics
Calculation Sheet
System HOT DUCT
Title: Evaluation of Insulation Thickness Tcold = 490C Thot = 950C C-C 0.25"

Page No.: 9 of 15
Calculation No.: A30302-01

```
karray := | $i \leftarrow 1$
          | $k_{ins_i} \leftarrow .05 \cdot \frac{BTU}{hr \cdot ft \cdot R}$
          | $X_{ins_i} \leftarrow k_{ins_i} \cdot \frac{\left[\left[-(k_{cc} \cdot Dia_{in} \cdot h_c)\right] - 2 \cdot \Delta_{cc} \cdot h_h \cdot Dia_{in} \cdot h_c \ldots + \left[-Dia_{hot} \cdot h_h \cdot k_{cc} + \left(\frac{h_h}{U_{duct}} \cdot k_{cc} \cdot Dia_{in} \cdot h_c\right)\right]\right]}{h_h \cdot k_{cc} \cdot Dia_{in} \cdot h_c}$
          | $Resi_i \leftarrow \frac{X_{ins_i}}{k_{ins_i}} + \frac{2 \cdot \Delta_{cc}}{k_{cc}}$
          | $array_1 \leftarrow \frac{k_{ins}}{\frac{BTU}{hr \cdot ft \cdot R}}$
          | $array_2 \leftarrow \frac{X_{ins}}{in}$
          | $array_3 \leftarrow Resi \cdot \frac{BTU}{hr \cdot ft^2 \cdot R}$
          | for $i \in 2 .. 600$
          |     $k_{ins_i} \leftarrow k_{ins_{i-1}} + .01 \frac{BTU}{hr \cdot ft \cdot R}$
          |     $X_{ins_i} \leftarrow k_{ins_i} \cdot \frac{\left[\left[-(k_{cc} \cdot Dia_{in} \cdot h_c)\right] - 2 \cdot \Delta_{cc} \cdot h_h \cdot Dia_{in} \cdot h_c \ldots + \left[-Dia_{hot} \cdot h_h \cdot k_{cc} + \left(\frac{h_h}{U_{duct}} \cdot k_{cc} \cdot Dia_{in} \cdot h_c\right)\right]\right]}{h_h \cdot k_{cc} \cdot Dia_{in} \cdot h_c}$
          |     $Resi_i \leftarrow \frac{X_{ins_i}}{k_{ins_i}} + \frac{2 \cdot \Delta_{cc}}{k_{cc}}$
          |     $array_1 \leftarrow \frac{k_{ins}}{\frac{BTU}{hr \cdot ft \cdot R}}$
          |     $Dummy \leftarrow line$
          |     $Dummy \leftarrow line$
```

$$array_2 \leftarrow \frac{X_{ins}}{in}$$

$$array_3 \leftarrow Resi \cdot \frac{BTU}{hr \cdot ft^2 \cdot R}$$

array

$$k_{ins} := karray_1 \cdot \frac{BTU}{hr \cdot ft \cdot R} \qquad X_{ins} := karray_2 \cdot in \qquad Resi := karray_3 \cdot \frac{hr \cdot ft^2 \cdot R}{BTU}$$

$$Resi_1 = 0.0325 \frac{hr \cdot ft^2 \cdot R}{BTU} \qquad Resh := \frac{Dia_{hot}}{Dia_{in} \cdot h_c} + \frac{1}{h_h} \qquad Resh = 0.0072 \frac{hr \cdot ft^2 \cdot R}{BTU}$$

$$\Delta T_i := \frac{Resi_1}{Resi_1 + Resh} \cdot (T_h - T_c) \qquad \Delta T_i = 376.1879\,K \qquad \Delta T_{tot} := T_h - T_c$$

$$\Delta T_{hot} := \frac{(T_h - T_c) \cdot \frac{1}{h_h}}{Resi_1 + Resh} \qquad \Delta T_{hot} = 55.1008\,K$$

$$\Delta T_{cold} := \frac{(T_h - T_c) \cdot \frac{Dia_{hot}}{Dia_{in} \cdot h_c}}{Resi_1 + Resh} \qquad \Delta T_{cold} = 28.7113\,K$$

$$T_{surf} := \Delta T_{cold} + T_c \qquad T_{surf} = 791.8713\,K$$

$$TC_{surf} := TC(T_{surf}) \qquad TC_{surf} = 518.7113\,°C$$

CASE 1

CONTROL PARAMETERS $\Delta T_{duct} = 1\,K$ $TC_c = 490\,°C$ $TC_h = 950\,°C$

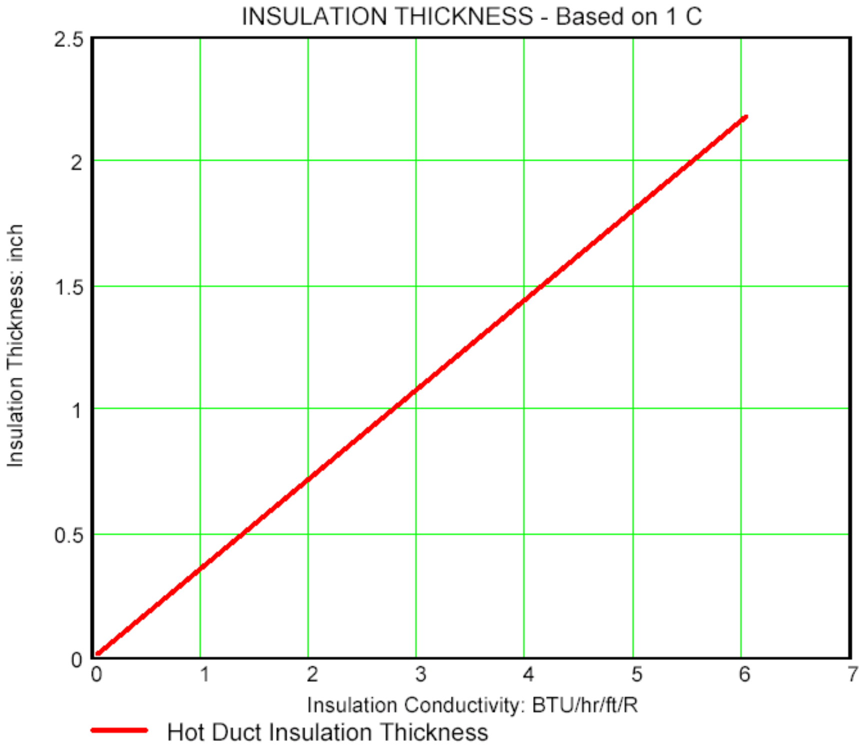

$$\Delta T_{duct} := .25K$$

$$Q_{vw} := W_{He} \cdot Cp_{He} \cdot \Delta T_{duct} \qquad Q_{vw} = 0.3261\,MW$$

$$U_{duct} := \frac{Q_{vw}}{A_{hot} \cdot (T_h - T_c)} \qquad U_{duct} = 6.2892\,\frac{BTU}{hr \cdot ft^2 \cdot R}$$

```
karray := | $i \leftarrow 1$
          | $k_{ins_i} \leftarrow .05 \cdot \frac{BTU}{hr \cdot ft \cdot R}$
          | $X_{ins_i} \leftarrow k_{ins_i} \cdot \frac{\left[\left[-\left(k_{cc} \cdot Dia_{in} \cdot h_c\right)\right] - 2 \cdot \Delta_{cc} \cdot h_h \cdot Dia_{in} \cdot h_c \ldots + \left[-Dia_{hot} \cdot h_h \cdot k_{cc} + \left(\frac{h_h}{U_{duct}} \cdot k_{cc} \cdot Dia_{in} \cdot h_c\right)\right]\right]}{h_h \cdot k_{cc} \cdot Dia_{in} \cdot h_c}$
          | $Resi_i \leftarrow \frac{X_{ins_i}}{k_{ins_i}} + \frac{2 \cdot \Delta_{cc}}{k_{cc}}$
          | $array_1 \leftarrow \frac{k_{ins}}{\frac{BTU}{hr \cdot ft \cdot R}}$
          | $array_2 \leftarrow \frac{X_{ins}}{in}$
          | $array_3 \leftarrow Resi \cdot \frac{BTU}{hr \cdot ft^2 \cdot R}$
          | for $i \in 2 .. 600$
          |     | $k_{ins_i} \leftarrow k_{ins_{i-1}} + .01 \frac{BTU}{hr \cdot ft \cdot R}$
          |     | $X_{ins_i} \leftarrow k_{ins_i} \cdot \frac{\left[\left[-\left(k_{cc} \cdot Dia_{in} \cdot h_c\right)\right] - 2 \cdot \Delta_{cc} \cdot h_h \cdot Dia_{in} \cdot h_c \ldots + \left[-Dia_{hot} \cdot h_h \cdot k_{cc} + \left(\frac{h_h}{U_{duct}} \cdot k_{cc} \cdot Dia_{in} \cdot h_c\right)\right]\right]}{h_h \cdot k_{cc} \cdot Dia_{in} \cdot h_c}$
          |     | $Resi_i \leftarrow \frac{X_{ins_i}}{k_{ins_i}} + \frac{2 \cdot \Delta_{cc}}{k_{cc}}$
          |     | $array_1 \leftarrow \frac{k_{ins}}{\frac{BTU}{hr \cdot ft \cdot R}}$
          |     | Dummy $\leftarrow$ line
          |     | Dummy $\leftarrow$ line
```

$$\text{array}_2 \leftarrow \frac{X_{ins}}{in}$$

$$\text{array}_3 \leftarrow \text{Resi}\cdot\frac{BTU}{hr\cdot ft^2\cdot R}$$

$$\text{array}$$

$$k_{ins} := \text{karray}_1\cdot\frac{BTU}{hr\cdot ft\cdot R} \qquad X_{ins} := \text{karray}_2\cdot in \qquad \text{Resi} := \text{karray}_3\cdot\frac{hr\cdot ft^2\cdot R}{BTU}$$

$$\text{Resi}_1 = 0.1518\frac{hr\cdot ft^2\cdot R}{BTU} \qquad \text{Resh} := \frac{\text{Dia}_{hot}}{\text{Dia}_{in}\cdot h_c} + \frac{1}{h_h} \qquad \text{Resh} = 0.0072\frac{hr\cdot ft^2\cdot R}{BTU}$$

$$\Delta T_i := \frac{\text{Resi}_1}{\text{Resi}_1 + \text{Resh}}\cdot\left(T_h - T_c\right) \qquad \Delta T_i = 439.047\,K \qquad \Delta T_{tot} := T_h - T_c$$

$$\Delta T_{hot} := \frac{\left(T_h - T_c\right)\cdot\frac{1}{h_h}}{\text{Resi}_1 + \text{Resh}} \qquad \Delta T_{hot} = 13.7752\,K$$

$$\Delta T_{cold} := \frac{\left(T_h - T_c\right)\cdot\frac{\text{Dia}_{hot}}{\text{Dia}_{in}\cdot h_c}}{\text{Resi}_1 + \text{Resh}} \qquad \Delta T_{cold} = 7.1778\,K$$

$$T_{surf} := \Delta T_{cold} + T_c \qquad T_{surf} = 770.3378\,K$$

$$TC_{surf} := TC\left(T_{surf}\right) \qquad TC_{surf} = 497.1778\,^\circ C$$

NGNP

COMPOSITES

Calculation By: D. P. Carosella
Date Saved: 9/30/2008

General Atomics
Calculation Sheet
System HOT DUCT
Title: Evaluation of Insulation Thickness Tcold = 490C Thot = 950C C-C 0.25"

Page No.: 15 of 15

Calculation No.: A30302-01

CASE 2

CONTROL PARAMETERS $\Delta T_{duct} = 0.25\,K \quad TC_c = 490\,°C \quad TC_h = 950\,°C$

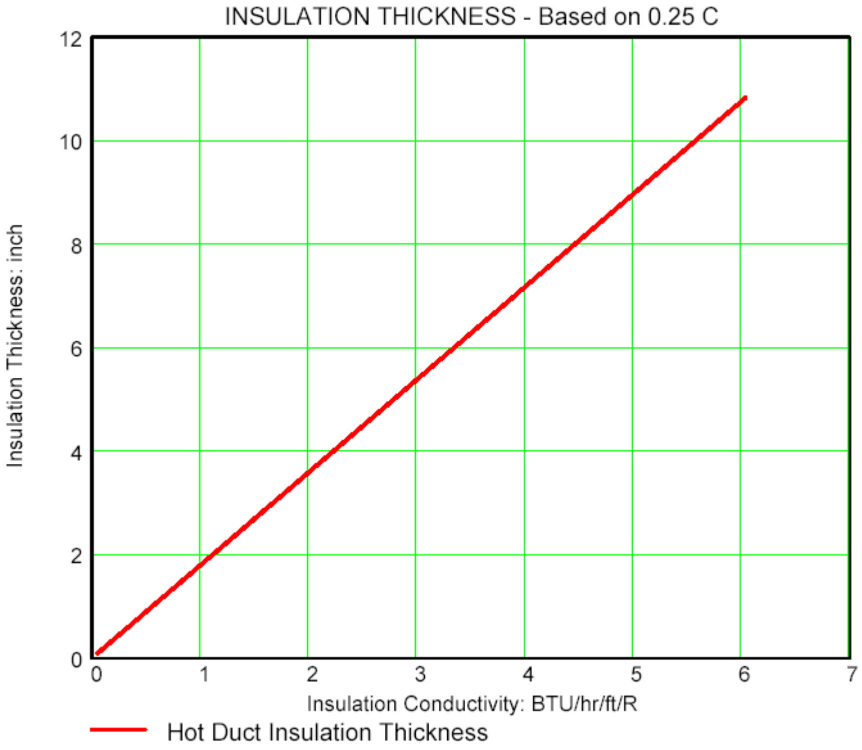

Cross Duct Vessel Cooling

SUMMARY: It is required to keep the cross-vessel temperature at or below 350°C (662°F) during steady state operation. It is also necessary to keep the concrete surrounding the cross duct at or below 66°C (150°F). These objectives can be achieved by insulating the inside of the cross vessel and by cooling the annulus between the cross vessel and the concrete with air at 40°C (104°F). Based on these criteria a study was initiated to evaluate the required insulation and airflow to achieve the desired objectives. Figure D-4 shows a set of results that met the objectives with reasonable insulation and airflow requirements. The following is a brief description of how the results in Figure D-4 were obtained.

MODEL DESCRIPTION: (See Figure D-1 above) The cross vessel radiates heat to the concrete enclosure. Thus the air in the annular space between the cross-vessel and the concrete must remove heat from both the cross-vessel and the concrete. Since the concrete has a low upper temperature limit, the temperature of the concrete becomes the controlling factor in the cooling process. The following items are included in the MATHCAD model.

1. The return helium flow in the cross duct is at 590°C (1094°F).
2. The helium is insulated from the vessel wall with two thin (6.35mm) layers of carbon-carbon and a layer of insulation. The thermal resistance of the insulation is one of the unknowns in this model.
3. The outer surface of the vessel radiates to the concrete. The emissivity of the vessel is 0.8. The emissivity of the concrete is 0.95.
4. HVAC air enters the cavity at one end and is blown to the other end. The air is at 40°C (104°F). Heat is transferred to the air from both the vessel wall and the concrete wall. The total heat transferred to the air must equal the heat conducted through the vessel wall insulation. The airflow and the air exit temperature are both unknowns in this model.
5. The thermal model includes a total of 11 unknowns and 11 simultaneous equations. By setting the vessel surface temperature, the set of equations can be solved for the following: the required airflow, the air exit temperature the insulation thermal resistance, the heat transferred and other unknown parameters.

RESULTS: It is important to note that because the average cooling air temperature cannot exceed the maximum concrete temperature limit, the range of possible results is limited.

1. Figure D-4 shows the effect of the vessel temperature on the insulation requirements.
2. Figure D-5 shows an estimate of required pumping power as function of vessel temperature. The increase of pumping power with vessel surface temperature is the result of requiring more cooling airflow as the temperature of the surface increases.

CONCLUSION:

As shown in Figure D-4, a reasonable design solution is possible using the HVAC system for cooling.

REFERENCES:

1. MATHCAD 11. Technical Calculation Tool

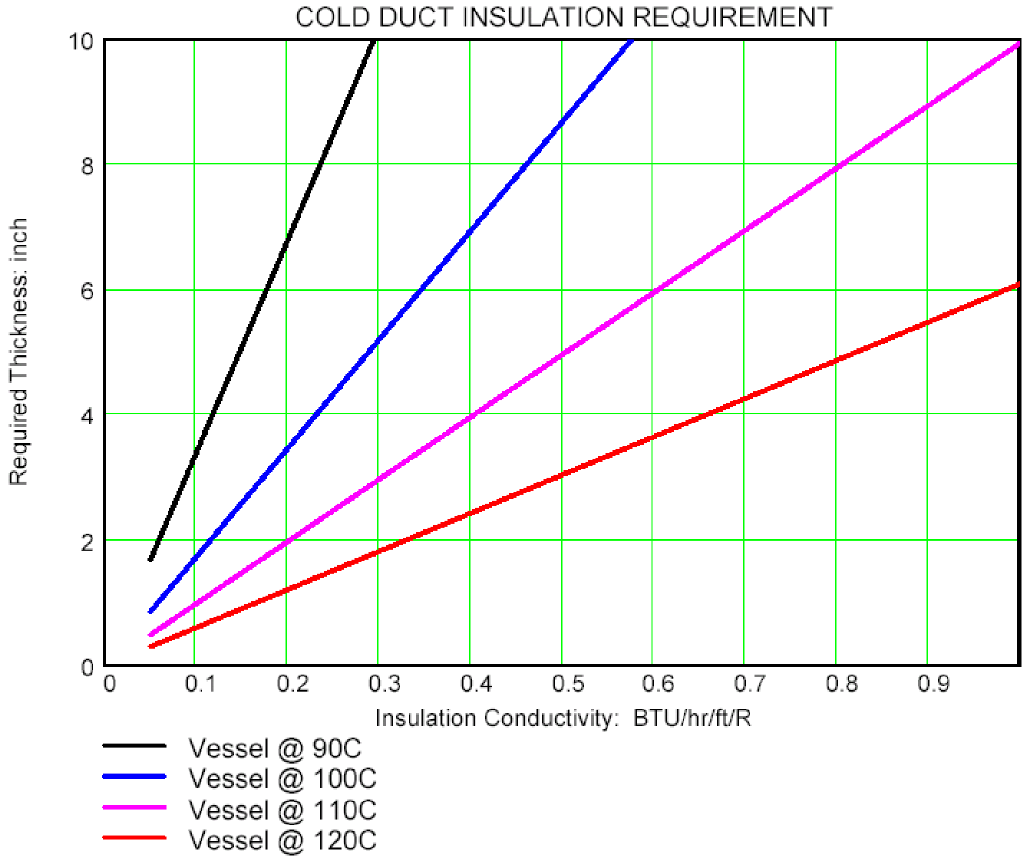

Figure D-4. Effect of vessel temperature on required insulation thickness

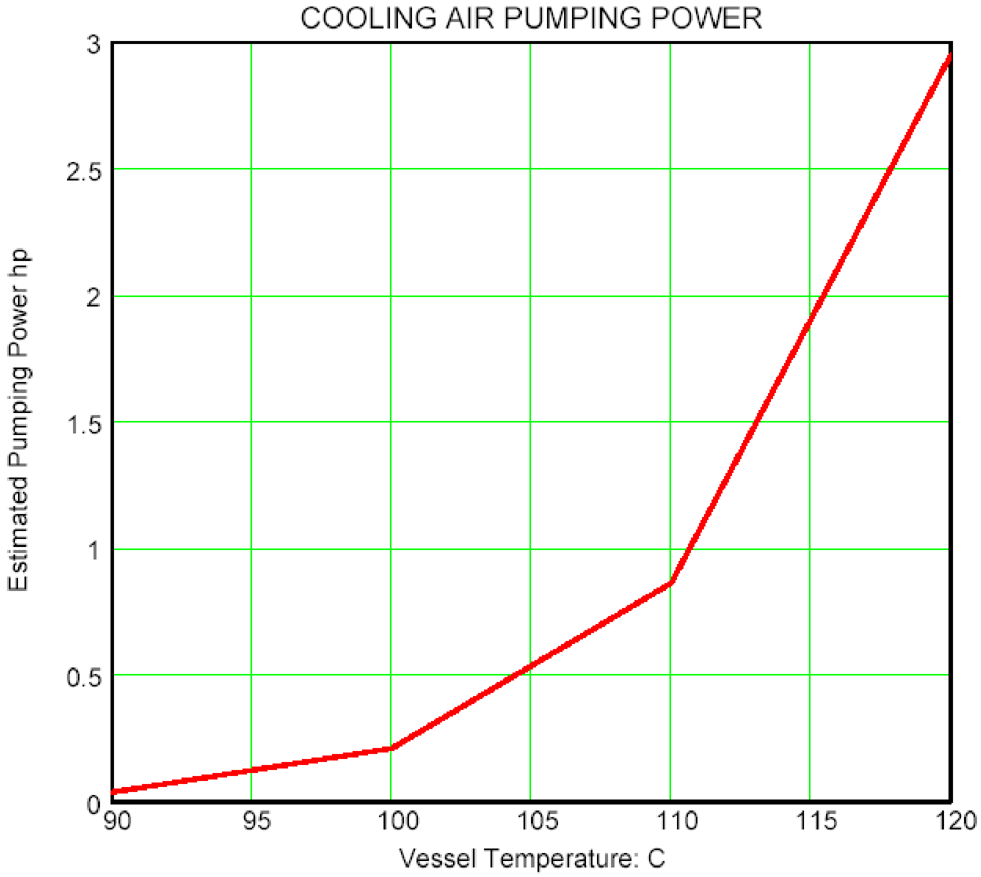

Figure D-5. Effect of vessel temperature on required air flow pumping power

MATHCAD MODEL

NGNP
COMPOSITES
Calculation By: D. P. Carosella

General Atomics
Calculation Sheet
System CROSS DUCT
Title: Insulation Requirement

Page No.: 1 of 27
Calculation No.:

I. INTRODUCTION:

This model will establish the cold duct insulation and cooling requirements to keep the concrete containment temperature at or below $T_{limit} := (66 + tc)\cdot K$. The required functions constants and properties are listed below. The configuration being considered is shown in Figure 1.

Constants, Properties and Functions

$ORIGIN \equiv 1$

TC(T) converts the absolute temperature (T) to °C. TF(T) converts the absolute temperature to °

$$TC(T) := \left(\frac{T}{K} - tc\right)\cdot °C \qquad TF(T) := \left(\frac{T}{R} - tr\right)\cdot °F$$

$kPa := Pa\cdot 1000$

$tc \equiv 273.16$

$tr \equiv 459.69$

$°C \equiv K$

$°F \equiv R$

$MPa \equiv Pa\cdot 10^{6}$

$bar \equiv .1\cdot MPa$

$CFM \equiv ft^{3}\cdot min^{-1}$

$MW := watt\cdot 10^{6}$

$kW := watt\cdot 10^{3}$

$R_{gas} := 1545\dfrac{lbf\cdot ft}{lb\cdot R}$

Properties of Helium

$Cp_{He} := 1.242\dfrac{BTU}{lb\cdot R}$

$k_{He}(T) := 1.29\cdot 10^{-3}\dfrac{BTU}{hr\cdot ft\cdot R}\cdot\left(\dfrac{T}{R}\right)^{.674}$

$\mu_{He}(T) := 6.9\cdot 10^{-4}\dfrac{lb}{ft\cdot hr}\cdot\left(\dfrac{T}{R}\right)^{.674}$

$Pr_{He}(T) := \dfrac{Cp_{He}\cdot\mu_{He}(T)}{k_{He}(T)}$

$Mol_{He} \equiv 4$

$R_{He} := \dfrac{R_{gas}}{Mol_{He}}$

$\gamma_{He} \equiv 1.667$

$\rho_{He}(T,P) := \dfrac{P}{R_{He}\cdot T}$

$\sigma_{rad} := .173\cdot 10^{-8}\cdot\dfrac{BTU}{hr\cdot ft^{2}\cdot R^{4}}$

$Z_{H2O}(\Delta P) := \dfrac{\Delta P}{g\cdot\rho_{H2O}}$

$inH2O := \dfrac{psi}{(g\cdot\rho_{H2O})}$

NGNP
COMPOSITES
Calculation By: D. P. Carosella

General Atomics
Calculation Sheet
System CROSS DUCT
Title: Insulation Requirement

Page No.: 2 of 27
Calculation No.:

Properties of Kaowool

$$k_{kw}(T) := \left[.113 + 1.154\cdot 10^{-4}\cdot\left(\frac{T}{R} - tr\right)\right]\cdot\frac{BTU}{hr\cdot ft\cdot R} \qquad \rho_{H2O} \equiv 62.4\frac{lb}{ft^3}$$

Air Properties:

Conductivity

$$K6 := 0.0146\cdot\frac{BTU}{R\cdot ft\cdot hr} \qquad K7 := 1.695\cdot 10^{-5}\cdot\frac{BTU}{R^2\cdot ft\cdot hr} \qquad k_{air}(T) := K6 + K7\cdot(T - tr\cdot R)$$

Viscosity

$$K9 := .04176\cdot\frac{lb}{ft\cdot hr} \qquad K10 := 4.914\cdot 10^{-05}\cdot\frac{lb}{ft\cdot hr\cdot R}$$

$$\mu_{air}(T) := K9 + K10\cdot(T - tr\cdot R)$$

Specific Heat:

$$Cp_{air}(T) := .23578\cdot\frac{BTU}{lb\cdot R} + \left(8.1532\cdot 10^{-06}\cdot\frac{BTU}{lb\cdot R^2}\cdot T\right) \qquad R_{air} := \frac{1546}{29}\cdot\frac{lbf\cdot ft}{lb\cdot R}$$

$$Pr_{air}(T) := \frac{Cp_{air}(T)\cdot\mu_{air}(T)}{k_{air}(T)} \qquad \gamma_{air} := 1.38$$

$$P_{air} := 14.7psi$$

Density

$$\rho_{air}(P_{air}, T) := \frac{P_{air}}{T\cdot R_{air}}$$

$$\beta_{air}(T) := \frac{1}{T}$$

HEAT TRANSFER CORRELATION

For the turbulent region the following heat transfer correlation was based on data on page 7-92 of th Heat Transfer Handbook, 1st Edition, 1973. For the laminar region the heat transfer correlation is based on data in Table 7.1 in Heat, Mass, and Momentum Transfer by Rohsenow and Choi, 1st edition, 1961. This correlation has a correction factor to account for the channel width to length ratic (α) The transition zone heat transfer is a linear approximation that fits between the limits of laminar and turbulent flow. The limits set in model are laminar flow: $Rel := 2300$ and turbulent flow: $Ret := 10000$. It should be noted that the transition zone heat transfer coefficient is only an approximation. It should also be noted that in the transition zone it is possible to oscillate between turbulent and laminar heat transfer.

$$
Nu_{slot}(Re, Pr, Rel, Ret, \alpha) := \left|
\begin{array}{l}
Nu_t \leftarrow 0.0275 \cdot Re^{0.78} \cdot Pr^{0.3} \\
Nu_l \leftarrow 8.2449 - 17.005 \cdot \alpha + 25.512 \cdot \alpha^2 - 19.062 \cdot \alpha^3 + 5.8566 \cdot \alpha^4 \\
Nu1 \leftarrow 8.2449 - 17.005 \cdot \alpha + 25.512 \cdot \alpha^2 - 19.062 \cdot \alpha^3 + 5.8566 \cdot \alpha^4 \\
Nu2 \leftarrow .0275 \cdot Ret^{0.78} \cdot Pr^{0.3} \\
slope \leftarrow \dfrac{Nu2 - Nu1}{Ret - Rel} \\
B \leftarrow Nu1 - Rel \cdot slope \\
Nu_{tran} \leftarrow slope \cdot Re + B \\
Nu_t \quad \text{if} \quad Re \geq Ret \\
Nu_l \quad \text{if} \quad Re \leq Rel \\
Nu_{tran} \quad \text{otherwise}
\end{array}
\right.
$$

NOTE: The following correlations for heat transfer coefficients include approximate solutions for the transition zone between laminar and turbulent flow. In these functions Rel is the Reynolds number at the upper end of the laminar region and Ret is the Reynolds number at the start of the turbulent region.

Heat Transfer in a pipe: $Rel := 2300,\ \ Ret := 10000$

$$Nu_{pipe}(Re, Pr, Rel, Ret) := \left| \begin{array}{l} Nu_t \leftarrow 0.023 \cdot Re^{0.8} \cdot Pr^{0.4} \\ Nu_l \leftarrow 4 \\ Nu1 \leftarrow 4 \\ Nu2 \leftarrow .023 \cdot Ret^{0.8} \cdot Pr^{0.4} \\ slope \leftarrow \dfrac{Nu2 - Nu1}{Ret - Rel} \\ B \leftarrow Nu1 - Rel \cdot slope \\ Nu_{tran} \leftarrow slope \cdot Re + B \\ Nu_t \ \text{ if } \ Re \ge Ret \\ Nu_l \ \text{ if } \ Re \le Rel \\ Nu_{tran} \ \text{ otherwise} \end{array} \right.$$

NGNP
COMPOSITES
Calculation By: D. P. Carosella

General Atomics
Calculation Sheet
System CROSS DUCT
Title: Insulation Requirement

Page No.: 5 of 27
Calculation No.:

FRICTION FACTOR CORRELATION:

The following friction factor correlation is based on the Moody Friction Factor (Reference 1) for turbulent flow. The laminar flow correlation has a correction factor to account for the channel width to length ratio (α) The laminar flow correlation is taken from London, A.L. & Shah, R. K., Laminar flow Forced Convection inDucts (Reference. 2). The transition zone is a best estimate. This zone is highly uncertain. The transition zone goes from a Reynold's number of $Rel := 2300$, to a Reynold's number of $Ret := 8000$

$$ff_{slot}(Ref, D, \varepsilon, Rel, Ret, \alpha) := \left| \begin{array}{l} ft \leftarrow \left[1 + \left(20000 \cdot \frac{\varepsilon}{D} + \frac{10^6}{Ref} \right)^{.333} \right] \cdot .0055 \\ fl \leftarrow \frac{4 \cdot \left(23.916 - 30.011 \cdot \alpha + 32.552 \cdot \alpha^2 - 12.362 \cdot \alpha^3 \right)}{Ref} \\ f1 \leftarrow \frac{4 \cdot \left(23.916 - 30.011 \cdot \alpha + 32.552 \cdot \alpha^2 - 12.362 \cdot \alpha^3 \right)}{Rel} \\ f2 \leftarrow \left[1 + \left(20000 \cdot \frac{\varepsilon}{D} + \frac{10^6}{Ret} \right)^{.333} \right] \cdot .0055 \\ slope \leftarrow \frac{f2 - f1}{Ret - Rel} \\ B \leftarrow \frac{96}{Rel} - Rel \cdot slope \\ ftran \leftarrow slope \cdot Ref + B \\ ft \ \text{ if } \ Ref \geq Ret \\ fl \ \text{ if } \ Ref \leq Rel \\ ftran \ \text{ otherwise} \end{array} \right.$$

NGNP
COMPOSITES
Calculation By: D. P. Carosella

General Atomics
Calculation Sheet
System CROSS DUCT
Title: Insulation Requirement

Page No.: 6 of 27
Calculation No.:

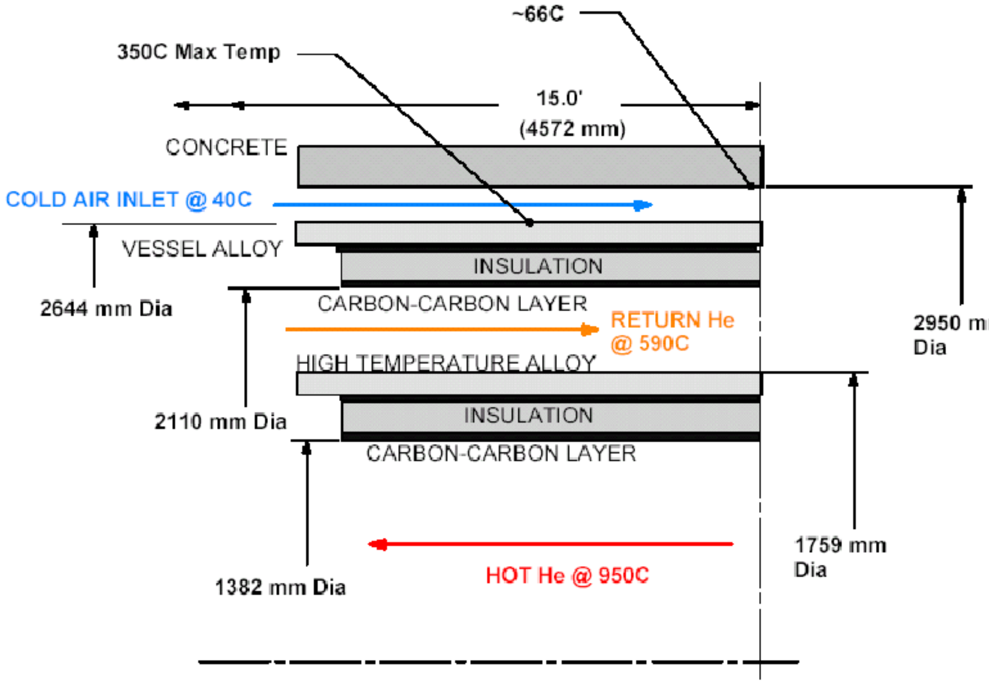

Figure 1: CROSS DUCT

II. INPUT:

Reactor Heat Load	$Q_{tot} := 600MW$
Reactor Outlet Temperature	$T_h := (950 + tc) \cdot K$
Reactor Inlet Temperature	$T_c := (590 + tc) \cdot K$
Helium Pressure	$P_{He} := 7MPa$
Cooling Helium Temperature	$T_{cool} := (40 + tc) \cdot K$
Diameter of the hot duct	$Dia_{hot} := 1382mm$
Inside Diameter of the return duct	$Dia_{in} := 1759mm$
Outside Diameter of the return duct	$Dia_{out} := 2110mm$
Outside Diameter of cross duct	$Dia_{cross} := 2644mm$
Outside Diameter of cooling channel	$Dia_{cool} := 2705mm$
Cross Duct Length	$Len_{duct} := 15ft$
Carbon-Carbon layer thickness	$\Delta_{cc} := .25in$
Carbon-Carbon conductivity	$k_{cc} := 30 \frac{watt}{m \cdot K}$
Emissivity of metallic surfaces	$\varepsilon_{met} := .8$
Emissivity of concrete	$\varepsilon_{con} := .9$

NGNP
COMPOSITES
Calculation By: D. P. Carosella

General Atomics
Calculation Sheet
System CROSS DUCT
Title: Insulation Requirement

Page No.: 8 of 27
Calculation No.:

III. CALCULATIONS:

This calculation will consist of solving a set of simulatenous equations to determine the required insulation thickness, the air flow requirements and to estimate air flow pumping requirements. This calculation will be repeated 11 times for 11 different cross vessel temperatures. The temperatures to be used are 90°C, 100°C, 110°C and 120°C.

Total helium flow

$$W_{tot} := \frac{Q_{tot}}{Cp_{He} \cdot (T_h - T_c)} \qquad W_{tot} = 706.6091\, lb\, sec^{-1}$$

Cooling Flow (estimate)

$$W_{cf} := 1 \frac{lb}{sec}$$

Coolant Heat Transfer Coefficient

$$\alpha_{cf} := \frac{(Dia_{cool} - Dia_{cross}) \cdot .5}{\pi \cdot (Dia_{cool} + Dia_{cross}) \cdot .5} \qquad \alpha_{cf} = 0.0036$$

$$A_{cf} := \frac{\pi}{4} \cdot \left(Dia_{cool}^2 - Dia_{cross}^2\right) \qquad A_{cf} = 2.7584\, ft^2$$

$$WP_{cf} := \pi \cdot (Dia_{cool} + Dia_{cross}) \qquad WP_{cf} = 55.1325\, ft$$

$$Dh_{cf} := \frac{4 \cdot A_{cf}}{WP_{cf}} \qquad Dh_{cf} = 0.2001\, ft$$

$$Re_{cf} := \frac{4 \cdot W_{cf}}{WP_{cf} \cdot \mu_{air}(T_{cool})} \qquad Re_{cf} = 5572.5728$$

$$Nu_{cf} := Nu_{slot}\left(Re_{cf}, Pr_{air}(T_{cool}), Rel, Ret, \alpha_{cf}\right) \qquad Nu_{cf} = 19.1215$$

$$h_{cf} := Nu_{cf} \cdot \frac{k_{air}(T_{cool})}{Dh_{cf}} \qquad h_{cf} = 1.5634 \frac{BTU}{hr \cdot ft^2 \cdot R}$$

NGNP
COMPOSITES
Calculation By: D. P. Carosella

General Atomics
Calculation Sheet
System CROSS DUCT
Title: Insulation Requirement

Page No.: 9 of 27
Calculation No.:

Heat Transfer in the return duct

$A_{rd} := \frac{\pi}{4} \cdot \left(Dia_{out}^2 - Dia_{in}^2\right)$ $A_{rd} = 11.4806\,ft^2$

$WP_{rd} := \pi \cdot \left(Dia_{out} + Dia_{in}\right)$ $WP_{rd} = 39.878\,ft$

$Dh_{rd} := \frac{4 \cdot A_{rd}}{WP_{rd}}$ $Dh_{rd} = 1.1516\,ft$

$Re_{rd} := \frac{4 \cdot W_{tot}}{WP_{rd} \cdot \mu_{He}\left(T_c\right)}$ $Re_{rd} = 2.612 \times 10^6$

$\alpha_{rd} := \frac{\left(Dia_{out} - Dia_{in}\right) \cdot .5}{\pi \cdot \left(Dia_{out} + Dia_{in}\right) \cdot .5}$ $\alpha_{rd} = 0.0289$

$Nu_{rd} := Nu_{slot}\left(Re_{rd}, Pr_{He}\left(T_c\right), Rel, Ret, \alpha_{rd}\right)$ $Nu_{rd} = 2462.0178$

$h_{rd} := Nu_{rd} \cdot \frac{k_{He}\left(T_c\right)}{Dh_{rd}}$ $h_{rd} = 390.4523 \frac{BTU}{hr \cdot R \cdot ft^2}$

First Estimates:

Temperature of coolant channel inside wall: $T_x := (96 + tc) \cdot K$

Coolant temperature at the exit: $Tc_{out} := (69 + tc) \cdot K$

Coolant Mean Temperature $Tc_{bar} := (57 + tc) \cdot K$

Insulation Resistance $Res_{ins} := \frac{1.5 \cdot ft^2 \cdot hr \cdot R}{BTU}$

Radiation Heat Transfer

$A_{in} := \pi \cdot Dia_{cross} \cdot Len_{duct}$ $A_{out} := \pi Dia_{cool} \cdot Len_{duct}$

$Tbar_{cd} := \frac{Dia_{cross} \cdot T_x + Dia_{cool} \cdot T_{limit}}{Dia_{cross} + Dia_{cool}}$ $Tbar_{cd} = 353.9889\,K$

Radiation Factor

$$\Im := \frac{1}{\frac{1}{\varepsilon_{met}} + \frac{A_{in}}{A_{out}} \cdot \left(\frac{1}{\varepsilon_{con}} - 1\right)} \qquad \Im = 0.736$$

Radiation Heat Transfer from the Duct to the Concrete

$$Q_{rad} := \sigma_{rad} \cdot \Im \cdot A_{in} \cdot \left(T_x^{\,4} - T_{limit}^{\,4}\right) \qquad Q_{rad} = 2.918 \times 10^{4} \frac{BTU}{hr}$$

Return Duct Overall U

$$U_{rd} := \frac{1}{\frac{1}{h_{rd}} + Res_{ins} + 2 \cdot \frac{\Delta_{cc}}{k_{cc}}} \qquad U_{rd} = 0.6645 \frac{BTU}{hr \cdot ft^2 \cdot R}$$

$$Q_{rd} := U_{rd} \cdot \pi \cdot Dia_{out} \cdot Len_{duct} \cdot \left(T_c - T_x\right) \qquad Q_{rd} = 1.9274 \times 10^{5} \frac{BTU}{hr}$$

Solve for 11 Unknowns: Case 1

Given

Heat Balances

$$Q_{rd} = U_{rd} \cdot \pi \cdot Dia_{out} \cdot Len_{duct} \cdot \left(T_c - T_x\right) \qquad 1$$

$$U_{rd} = \frac{1}{\frac{1}{h_{rd}} + Res_{ins} + 2 \cdot \frac{\Delta_{cc}}{k_{cc}}} \qquad 2$$

$$Q_{rad} = \sigma_{rad} \cdot \Im \cdot A_{in} \cdot \left(T_x^{\,4} - T_{limit}^{\,4}\right) \qquad 3$$

$$Q_{rad} = h_{cf} \cdot A_{out} \cdot \left(T_{limit} - Tc_{bar}\right) \qquad 4$$

Vessel Temperature

$$T_x = (90 + tc) \cdot K$$

$$Tbar_{cd} = \frac{Dia_{cross} \cdot T_x + Dia_{cool} \cdot T_{limit}}{Dia_{cross} + Dia_{cool}} \qquad 5$$

$$\left[Tc_{out} = Tbar_{cd} - \left(Tbar_{cd} - T_{cool}\right) \cdot e^{\frac{-\left(h_{cf} \cdot A_{out} + h_{cf} \cdot A_{in}\right)}{W_{cf} \cdot Cp_{air}\left(T_{cool}\right)}} \right] \qquad 6$$

$$W_{cf} \cdot Cp_{air}\left(T_{cool}\right) \cdot \left(Tc_{out} - T_{cool}\right) = Q_{rd} \qquad 7$$

$$Tc_{bar} = Tbar_{cd} - \frac{1}{\frac{h_{cf} \cdot A_{out} + h_{cf} \cdot A_{in}}{W_{cf} \cdot Cp_{air}\left(T_{cool}\right)}} \cdot \left(Tbar_{cd} - T_{cool}\right) \cdot \left[1 - e^{\frac{-\left(h_{cf} \cdot A_{out} + h_{cf} \cdot A_{in}\right)}{W_{cf} \cdot Cp_{air}\left(T_{cool}\right)}} \right] \qquad 8$$

$$Re_{cf} = \frac{4 \cdot W_{cf}}{WP_{cf} \cdot \mu_{air}\left(T_{cool}\right)} \qquad 9$$

$$h_{cf} = Nu_{slot}\left(Re_{cf}, Pr_{air}\left(T_{cool}\right), Rel, Ret, \alpha_{cf}\right) \cdot \frac{k_{air}\left(T_{cool}\right)}{Dh_{cf}} \qquad 10$$

$$Q_{rd} = h_{cf} \cdot A_{in} \cdot \left(T_x - Tc_{bar}\right) + Q_{rad} \qquad 11$$

$$\begin{pmatrix} AA \\ BB \\ CC \\ DD \\ EE \\ FF \\ GG \\ HH \\ II \\ JJ \\ KK \end{pmatrix} := \mathrm{Find}\left(Q_{rd}, Q_{rad}, U_{rd}, T_x, Tc_{out}, Res_{ins}, Tbar_{cd}, Tc_{bar}, W_{cf}, Re_{cf}, h_{cf}\right)$$

Results

$Q_{rd} := AA$ $Q_{rd} = 1.0349 \times 10^{5} \frac{BTU}{hr}$ $Q_{rad} := BB$ $Q_{rad} = 2.2742 \times 10^{4} \frac{BTU}{hr}$

$U_{rd} := CC$ $U_{rd} = 0.3525 \frac{BTU}{hr \cdot ft^{2} \cdot R}$ $T_x := DD$ $T_x = 363.16\,K$

$Tc_{out} := EE$ $Tc_{out} = 340.9597\,K$ $Res1_{ins} := FF$ $Res1_{ins} = 2.832\,hr \cdot ft^{2} \cdot \frac{R}{BTU}$

$Tbar_{cd} := GG$ $Tbar_{cd} = 351.0232\,K$

$TCx_1 := TC(T_x)$ $TCx_1 = 90\,°C$ $W_{cf} := II$ $W_{cf} = 2.3899\,lb\,sec^{-1}$

$Tc_{bar} := HH$ $Tc_{bar} = 330.0433\,K$ $TC_{surf_2} := TC(T_{limit})$ $TC_{surf_2} = 66\,°C$

$TCc_{bar} := TC(Tc_{bar})$ $TCc_{bar} = 56.8833\,°C$

$TCc_{out} := TC(Tc_{out})$ $TCc_{out} = 67.7997\,°C$ $Re_{cf} := JJ$ $h_{cf} := KK$

$TCcool_2 := TC(T_{cool})$ $TCcool_2 = 40\,°C$ $Re_{cf} = 1.3318 \times 10^{4}$

$kins_1 := .05 \frac{BTU}{hr \cdot ft \cdot R}$ $h_{cf} = 3.3138 \frac{BTU}{hr \cdot ft^{2} \cdot R}$

$i := 2 .. 100$

$kins_i := kins_{i-1} + .05 \frac{BTU}{hr \cdot ft \cdot R}$

Calculate the Insulation Thickness Knowing the Required Resistance and Conductivity

$i := 1 .. 100$

$X1_{ins_i} := k_{ins_i} \cdot Res1_{ins}$

Calculate the pressure drop

Flow Area $A_{cf} = 2.7584\,ft^2$ $WP_{cf} = 55.1325\,ft$

$Dh_{cf} = 0.2001\,ft$ $Len_{duct} = 15\,ft$ $Tc_{bar} = 330.0433\,K$

$\rho_{air}(P_{air}, Tc_{bar}) = 0.0668\,lb\,ft^{-3}$

$ff_{slot}(Ref, D, \varepsilon, Rel, Ret, \alpha)$ $\varepsilon_{st} := .00015ft$ $\varepsilon con := .001ft$

Average Surface Roughness $\varepsilon_{bar} := \dfrac{Dia_{cross} \cdot \varepsilon_{st} + Dia_{cool} \cdot \varepsilon con}{Dia_{cross} + Dia_{cool}}$ $\varepsilon_{bar} = 5.7985 \times 10^{-4}\,ft$

$mf := ff_{slot}(Re_{cf}, Dh_{cf}, \varepsilon_{bar}, Rel, Ret, \alpha_{cf})$ $mf = 0.0335$ Friction factor

$$\Delta P_f := \frac{mf \cdot \dfrac{Len_{duct}}{Dh_{cf}} \cdot \left(\dfrac{W_{cf}}{A_{cf}}\right)^2}{2 \cdot \rho_{air}(P_{air}, Tc_{bar})} \qquad \Delta P_f = 0.003\,psi$$

$Z_{H2O}(\Delta P_f) = 0.0844\,in$ Inches of H_2O

$\Delta_{kw_1} := Res1_{ins} \cdot k_{kw}(T_x)$ $\Delta_{kw_1} = 4.601\,in$

Pumping Power

$Anu := \dfrac{Dh_{cf}}{2}$

$$PP_1 := \frac{\Delta P_f \cdot W_{cf}}{\rho_{air}(P_{air}, T_{cool}) \cdot .7} \qquad PP_1 = 0.0387\,hp$$

$Anu = 30.5\,mm$

This calculation is repeated for 3 more vessel temperatures

Appendix E – PSR Seal Leakage Analysis

SUMMARY: A series of flow analyses were performed to establish the flow leakage characteristics of the Permanent Side Reflector (PSR) inlet flow channel seal rings (Figure 1) that are used to prevent leakage from the inlet flow channels to the reactor coolant flow. This analysis has shown that the leakage flow rate is highly dependent on the gap size of both the horizontal gaps between the PSR graphite blocks and the radial gap between the seal ring and the PSR blocks. Typical results can be seen in Figures 2 & 3. From these figures it is clear that the gap size of the radial and horizontal gaps and the number of horizontal gaps are the controlling factors in defining the leakage rate. For example, reducing the nominal horizontal gap size from 0.01” to 0.005” for an 8 gap configuration with a 0.008” radial gap reduces the leakage flow rate from about 2% to about 0.5%.

MODEL DESCRIPTION and CALCULATION METHOD (Refer to Figure 1) The helium pressure in the reactor can be summarized as follows. The inlet pressure at the bottom of the inlet tubes is about 1025 psi. The pressure at the core inlet is about 1023 psi. The pressure at the core outlet is about 1011 psi. Based on these values the mean pressure differential between the inlet channels and the core flow is about 7 psid. This pressure differential drives leakage flow from the inlet channel to the core flow system. As defined in the attached MATHCAD file (Appendix A) the flow path includes inlet and outlet losses, 90^o bends and friction. Since the flow can be in the laminar Reynolds number range the friction factor can be highly sensitive to flow rate. Thus the calculation required several iterations to establish confirmed results. The flow values shown in the MATHCAD file are converged flow rates. The basic calculation method consists of the following steps.

1. Establish the geometric parameters for a specific case. These include the gap sizes and the flow lengths.
2. Estimate the flow rate for the case and use the flow rate and geometry to calculate the friction factors.
3. Set the flow dependent pressure drop equation to the given pressure drop (7psid).
4. Solve for the flow rate.
5. Repeat as necessary until the flow rates converge.

RESULTS The results of this analysis are shown in Figures 2 & 3. These results indicate that in order to minimize flow leakage from the inlet channels to the main flow path it is necessary to control the gap sizes and number. These results were based on the assumption of 8 horizontal gaps and 8 seal rings per flow column. Using longer PSR blocks thus reducing the number of horizontal gaps and seal rings will reduce the leakage rates.

The solution method (MATHCAD solve block as shown on pages 13 & 14 of the MATHCAD file) is repeated for each radial gap size, ring height and inlet temperature until all of the flow rates are established. This data is then plotted as shown in Figures 2 & 3.

REFERENCES
MATHCAD 11. Technical Calculation Tool

Figure 1

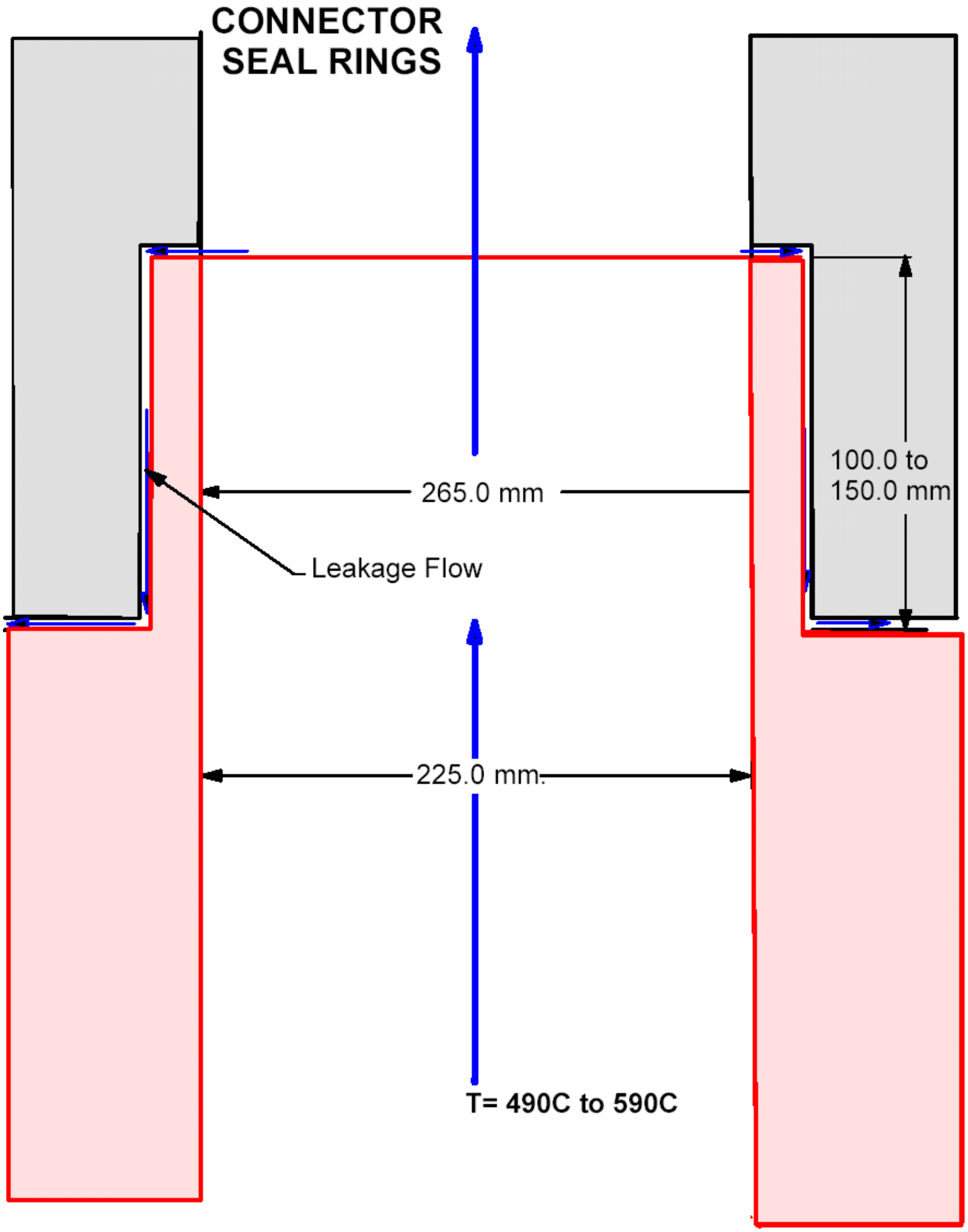
CONNECTOR
SEAL RINGS
265.0 mm
100.0 to
150.0 mm
Leakage Flow
225.0 mm
T= 490C to 590C

Figure 2: Seal Ring Leakage Flow - 0.005” Horizontal Gap

CRITICAL PARAMETERS

Block Gap	$gap_{bl} = 0.005\,in$
Number of Horizontal Gaps	$No_{sr} = 8$
Coolant Hole Diameter	$Dia_{in} = 8.86\,in$

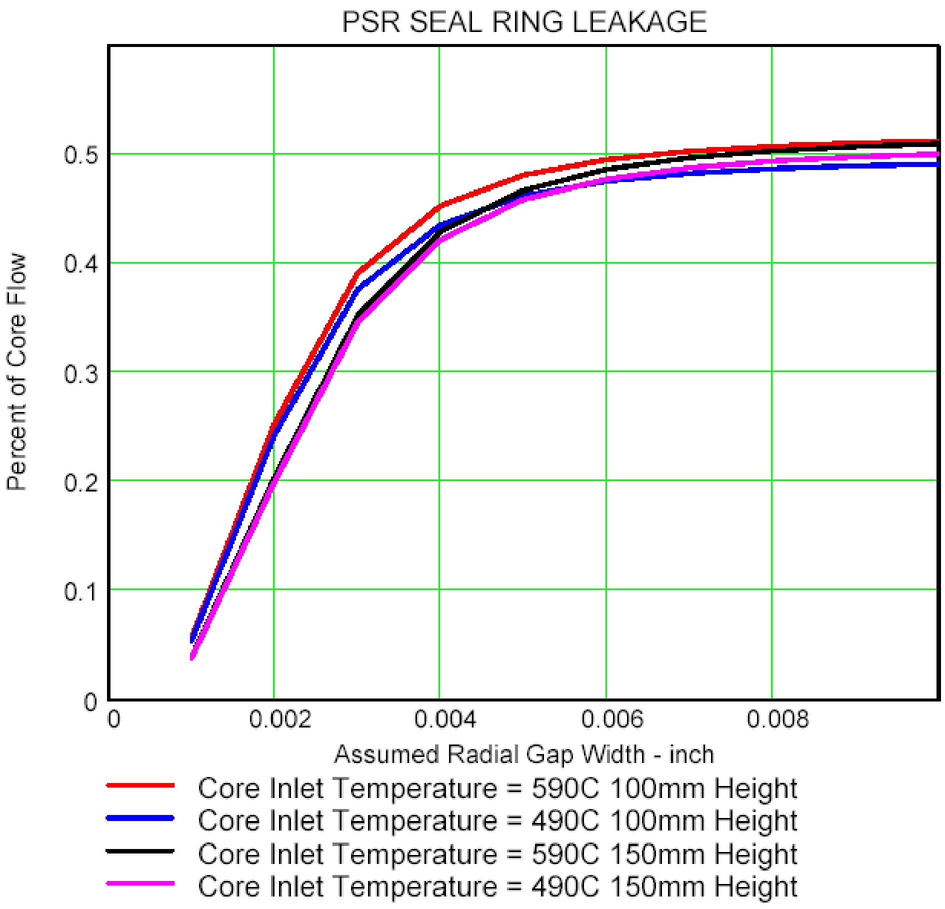

Figure 3: Seal Ring Leakage Flow - 0.01" Horizontal Gap

CRITICAL PARAMETERS

Block Gap	$gap_{bl} = 0.01\,in$
Number of Horizontal Gaps	$No_{sr} = 8$
Coolant Hole Diameter	$Dia_{in} = 8.86\,in$

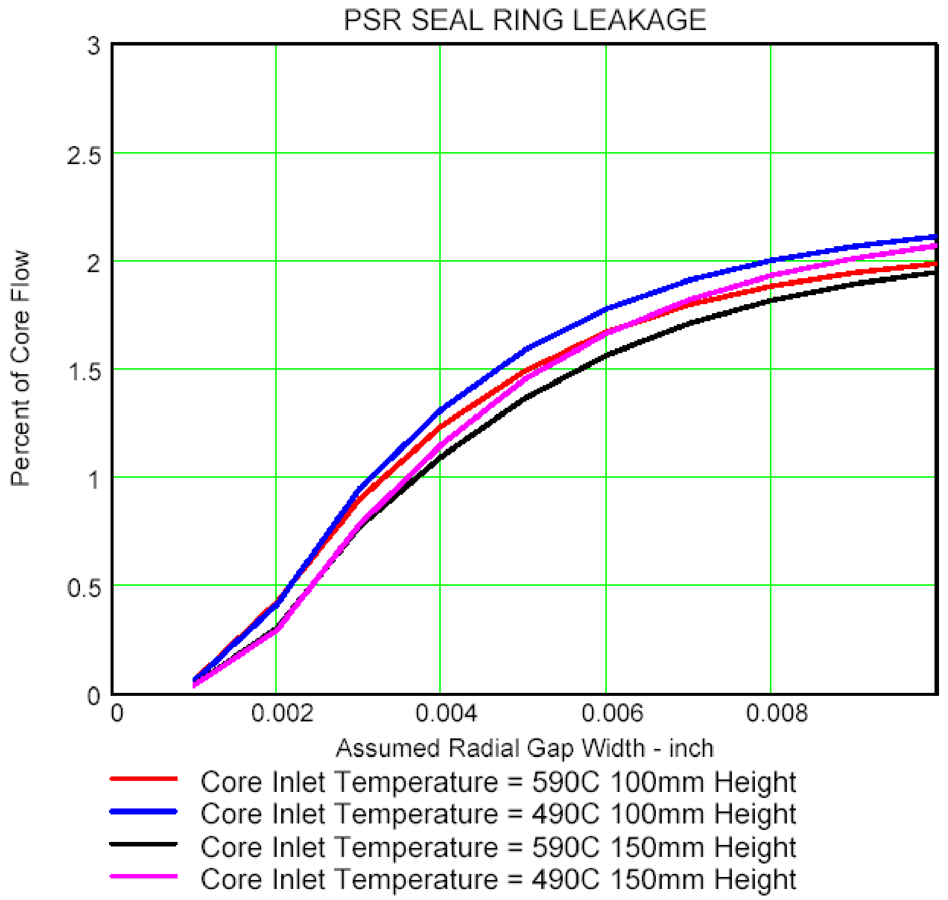

MATHCAD MODEL

NGNP **COMPOSITES** Calculation By: D. P. Carosella	General Atomics **Calculation Sheet** System PSR Seal Rings Title: Leakage Determination 0.01" Horizontal Gap	Page No.: 1 of 43 Calculation No.:

I. INTRODUCTION:

This model will be used to investigate the magnitude of helium leakage around the PSR seal rings. These rings (Figure 1) are installed in the Helium inlet lines at the interface between the blocks that make up the PSR. These rings reduce the leakage, but they can not totally eliminated the leakage. The following constants, properties and functions will be used in this model.

Constants, Properties and Functions

$\mathrm{ORIGIN} \equiv 1$

TC(T) converts the absolute temperature (T) to °C. TF(T) converts the absolute temperature to °F

$$TC(T) := \left(\frac{T}{K} - tc\right)\cdot {}^{\circ}C \qquad TF(T) := \left(\frac{T}{R} - tr\right)\cdot {}^{\circ}F$$

$kPa := Pa \cdot 1000$ $tc \equiv 273.16$ $tr \equiv 459.69$

${}^{\circ}C \equiv K$ ${}^{\circ}F \equiv R$

$MPa \equiv Pa \cdot 10^{6}$ $bar \equiv .1 \cdot MPa$ $CFM \equiv ft^{3} \cdot min^{-1}$

$MW := watt \cdot 10^{6}$ $kW := watt \cdot 10^{3}$ $R_{gas} := 1545 \frac{lbf \cdot ft}{lb \cdot R}$

Properties of Helium

$$Cp_{He} := 1.242 \frac{BTU}{lb \cdot R} \qquad k_{He}(T) := 1.29 \cdot 10^{-3} \frac{BTU}{hr \cdot ft \cdot R} \cdot \left(\frac{T}{R}\right)^{.674}$$

$$\mu_{He}(T) := 6.9 \cdot 10^{-4} \frac{lb}{ft \cdot hr} \cdot \left(\frac{T}{R}\right)^{.674} \qquad Pr_{He}(T) := \frac{Cp_{He} \cdot \mu_{He}(T)}{k_{He}(T)} \qquad Mol_{He} \equiv 4$$

$$R_{He} := \frac{R_{gas}}{Mol_{He}} \qquad \gamma_{He} \equiv 1.667 \qquad \rho_{He}(T, P) := \frac{P}{R_{He} \cdot T}$$

NGNP
COMPOSITES
Calculation By: D. P. Carosella

General Atomics
Calculation Sheet
System PSR Seal Rings
Title: Leakage Determination 0.01" Horizontal Gap

Page No.: 2 of 43
Calculation No.:

FRICTION FACTOR CORRELATION:

The following friction factor correlation is based on the Moody Friction Factor (Reference 1) for turbulent flow. The laminar flow correlation has a correction factor to account for the channel width to length ratio (α) The laminar flow correlation is taken from London, A.L. & Shah, R. K., Laminar flow Forced Convection inDucts (Reference. 2). The transition zone is a best estimate. This zone is highly uncertain. The transition zone goes from a Reynold's number of $Rel := 2300$, to a Reynold's number of $Ret := 8000$

$$ff_{slot}(Ref, D, \varepsilon, Rel, Ret, \alpha) := \left| \begin{array}{l} ft \leftarrow \left[1 + \left(20000 \cdot \frac{\varepsilon}{D} + \frac{10^6}{Ref}\right)^{.333}\right] \cdot .0055 \\ fl \leftarrow \frac{4 \cdot \left(23.916 - 30.011 \cdot \alpha + 32.552 \cdot \alpha^2 - 12.362 \cdot \alpha^3\right)}{Ref} \\ f1 \leftarrow \frac{4 \cdot \left(23.916 - 30.011 \cdot \alpha + 32.552 \cdot \alpha^2 - 12.362 \cdot \alpha^3\right)}{Rel} \\ f2 \leftarrow \left[1 + \left(20000 \cdot \frac{\varepsilon}{D} + \frac{10^6}{Ret}\right)^{.333}\right] \cdot .0055 \\ slope \leftarrow \frac{f2 - f1}{Ret - Rel} \\ B \leftarrow \frac{4 \cdot \left(23.916 - 30.011 \cdot \alpha + 32.552 \cdot \alpha^2 - 12.362 \cdot \alpha^3\right)}{Rel} - Rel \cdot slope \\ ftran \leftarrow slope \cdot Ref + B \\ ft \quad \text{if} \quad Ref \ge Ret \\ fl \quad \text{if} \quad Ref \le Rel \\ ftran \quad \text{otherwise} \end{array} \right.$$

II. ASSUMPTIONS

The following assumptions were used in this analysis (refer to Figure 1).

1. The seal dowel is concentric to the coolant hole in the permanent side reflector (PSR).
2. The leakage flow path is as shown in figure 1. The reactor inlet coolant flows upward in the inlet holes. There are 60 such holes. These holes are 225 mm in diameter.
3. At the top of the seal, helium flows radially outward to the gap between the seal and the PSR.
4. This flow proceeds downward to the gap between reflector blocks.
5. The flow proceeds radially inward until it reaches a vertical gap which contains reactor coolant flow.
6. The leakagae flow mixes with the reactor coolant.
7. The following factors control the leakage flow.
    a) The size of the radial gap.
    b) The size of the horizontal gap.
    c) The flow area between the dowel and the coolant sink. This area was estimated considering the following parameters: the height of the gap, the radial location of the dowel and the radial location of the reactor coolant. The number of horizontal gaps. Two gap heights were considered in this evaluation.
    d) The pressure differential between the inlet helium and the helium in the coolant flow path. At the top of the reactor this difference is zero. At the bottom of the reactor this difference is the full reactor pressure drop. For this study the average value was used.
    e) Loss coefficients due to turns, inlets and exits. The turning losses were based on the best avilable data for bends. the inlet loss was taken as 0.5 velocity heads. The outlet loss was taken as 1 velocity head
    f) Friction factors for flow in a gap.
    g) The length of the flow path. Note: two cases will be considered. One for the flow length being 100mm and the second for the length being 150mm as illustrated in Figure 1.
    h) This analysis will consider inlet flow at both 490°C and 590°C.

NGNP **COMPOSITES** Calculation By: D. P. Carosella	General Atomics **Calculation Sheet** System PSR Seal Rings Title: Leakage Determination 0.01" Horizontal Gap	Page No.: 4 of 43 Calculation No.:

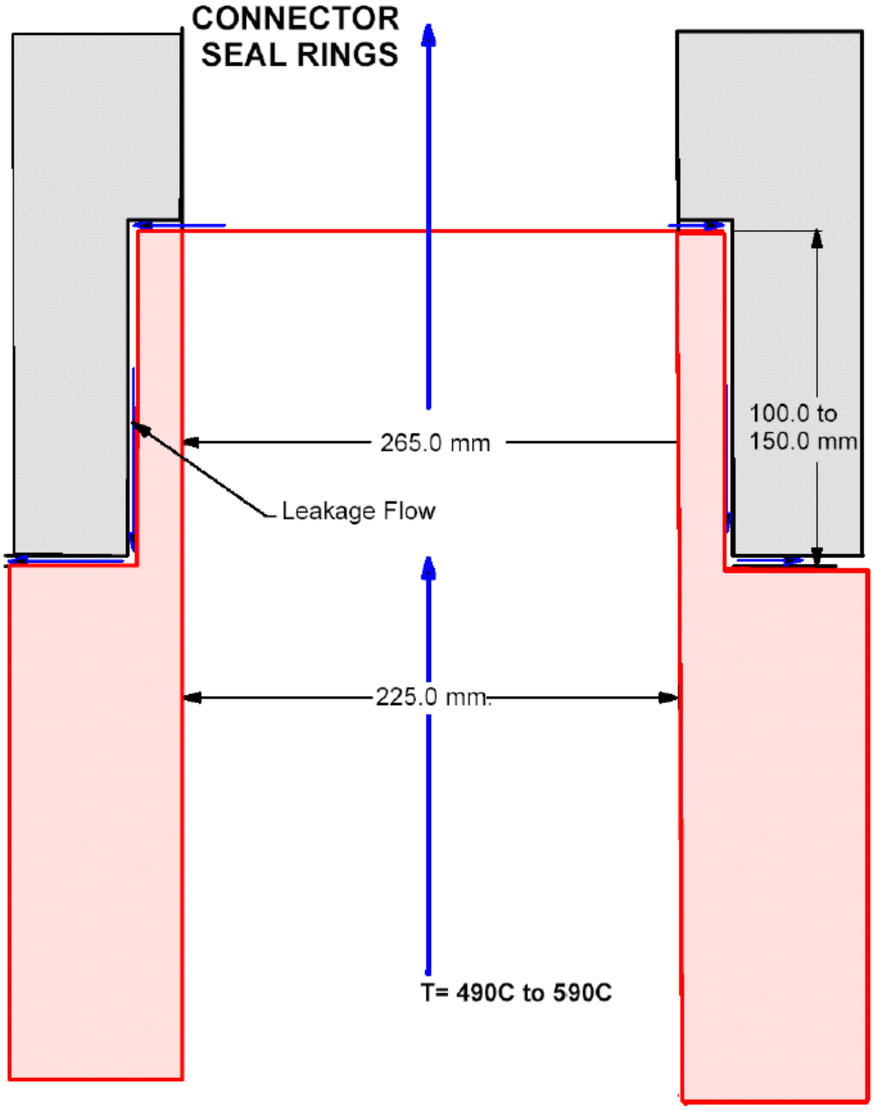

Figure 1: PSR Seal Ring Configuration & Leakage Flow Paths

SEAL RING 100mm.mcd 9/30/2008 9:51 AM

NGNP
COMPOSITES
Calculation By: D. P. Carosella

General Atomics
Calculation Sheet
System PSR Seal Rings
Title: Leakage Determination 0.01" Horizontal Gap

Page No.: 5 of 43
Calculation No.:

III. INPUT:

Number of seal rings per channel	$No_{sr} := 8$
Number of channels	$No_{ch} := 60$
Seal ring dimensions	
OD	$Dia_{out} := 265mm$
ID	$Dia_{in} := 225mm$
Height	$H_{sr} := 100mm$
Centerline radius	$R_{cl} := 3300mm$
Effective radius of replaceable reflector	$R_{ac} := 3016mm$
Estimate corner radius	$r_c := .0005in$
Gap width	Variable
Max helium temp	$THe_{max} := (590 + tc) \cdot K$
Minimum helium temp	$THe_{min} := (490 + tc) \cdot K$
Core Outlet Temp	$THe_{out} := (950 + tc) \cdot K$
Core Heat Duty	$Q_{core} := 600MW$
Pressure @ the inlet	$P_{in} := 1025psi$
Pressure @ the top	$P_{top} := 1023psi$
Pressure @ the outlet	$P_{out} := 1011psi$
Roughness	$\varepsilon_f := 8 \cdot 10^{-6} \cdot ft$

NGNP
COMPOSITES
Calculation By: D. P. Carosella

General Atomics
Calculation Sheet
System PSR Seal Rings
Title: Leakage Determination 0.01" Horizontal Gap

Page No.: 6 of 43
Calculation No.:

IV. CALCULATIONS:

Referring to Figure 1 the flow paths around a single seal ring consists of a radial flow outward, a 90° bend, a downward flow in a gap, another 90° bend and a horizontal flow outward to the core region. Since the actual gap size is unknown, this study will investigate gap size ranging from 0.001" to .01". Calculate flow rates for this range of gaps

$$gap_1 := .001in$$

$$i := 2 .. 10$$

$$gap_i := gap_{i-1} + .001in$$

$$i := 1 .. 10$$

$$Dh_i := 2 \cdot gap_i \qquad gap_{bl} := .010in$$

$Dh =$

	1
1	0.002
2	0.004
3	0.006
4	0.008
5	0.01
6	0.012
7	0.014
8	0.016
9	0.018
10	0.02

in

Calculation of flow areas based on 60 coolant channels

Area around the seal ring $Asr_i := \pi \cdot Dia_{out} \cdot gap_i \cdot No_{sr} \cdot No_{ch}$

Area between the blocks: $Abl_i := \pi \cdot (R_{cl} \cdot 2 + R_{ac} \cdot 2) \cdot .5 \cdot gap_{bl} \cdot No_{sr}$

$$Dh_{bl} := 2 \cdot gap_{bl}$$

$Asr =$

	1
1	0.1093
2	0.2185
3	0.3278
4	0.437
5	0.5463
6	0.6555
7	0.7648
8	0.874
9	0.9833
10	1.0925

ft^2

$Abl =$

	1
1	0.434
2	0.434
3	0.434
4	0.434
5	0.434
6	0.434
7	0.434
8	0.434
9	0.434
10	0.434

ft^2

Pressure differential

At the bottom $\Delta P_b := P_{in} - P_{out}$ $\Delta P_b = 14\,psi$

At the top $\Delta P_t := 0psi$

$$\Delta P_{bar} := \frac{\Delta P_b + \Delta P_t}{2} \qquad \Delta P_{bar} = 7\,psi$$

Core Flow Rate

$$W_{tot_1} := \frac{Q_{core}}{Cp_{He}\cdot\left(THe_{out} - THe_{max}\right)} \qquad W_{tot_1} = 706.6091\,lb\,sec^{-1}$$

$$W_{tot_2} := \frac{Q_{core}}{Cp_{He}\cdot\left(THe_{out} - THe_{min}\right)} \qquad W_{tot_2} = 552.9984\,lb\,sec^{-1}$$

Density of helium at inlet

$$\rho_{in_1} := \rho_{He}\left(THe_{max}, P_{in}\right) \qquad \rho_{in_1} = 0.246\,lb\,ft^{-3}$$

$$\rho_{in_2} := \rho_{He}\left(THe_{min}, P_{in}\right) \qquad \rho_{in_2} = 0.2782\,lb\,ft^{-3}$$

The pressure loss in this system consists of the following:
1. Entrance effect
2. 90° bend
3. Exit
4. Friction

Since friction is flow rate dependent, it is necessary to iterate on the flow rate.
For a first estimate assume that the leakage flow is 1% of the total flow

After the first iteration the calculated flows for all cases is input into this table as a next guess at flow rates.

$$\begin{pmatrix} Wfind1 \\ Wfind2 \end{pmatrix} :=$$

Wfind1	Wfind2	Wfind3	Wfind4			
0.442962	0.334191	0.298176	0.225611			
2.954884	2.250145	2.120418	1.611617			
6.345017	5.22841	5.447803	4.24015			
8.755703	7.266211	7.752971	6.369199			
10.52804	8.772795	9.634699	8.030461			
11.80759	9.831087	11.05496	9.206341			
12.69712	10.56628	12.09671	10.0679			
13.31086	11.07362	12.84301	10.68502			
13.73844	11.42729	13.37582	11.1258			

$$W_{find1} := Wfind1 \cdot \frac{lb}{sec} \qquad W_{find2} := Wfind2 \cdot \frac{lb}{sec}$$

Calculate the Reynolds numbers

$$wp_{sr} := 2 \cdot \pi \cdot Dia_{out} \cdot No_{ch} \qquad wp_{bl} := 2 \cdot \pi \cdot \left(R_{cl} + R_{ac}\right) \cdot No_{sr}$$

$$wp_{sr} = 327.7646\,ft \qquad wp_{bl} = 1041.5905\,ft$$

$$Re_{sr1_i} := \frac{4 \cdot W_{find1_i}}{wp_{sr} \cdot \mu_{He}\left(THe_{max}\right)} \qquad Re_{bl1_i} := \frac{4 \cdot W_{find1_i} \cdot 2}{wp_{bl} \cdot \mu_{He}\left(THe_{max}\right)}$$

$Re_{sr1} =$

	1
1	199.2225
2	1328.9622
3	2853.678
4	3937.8866
5	4734.9946
6	5310.4758
7	5710.5418
8	5986.5718
9	6178.8784
10	6315.2736

$Re_{bl1} =$

	1
1	125.3815
2	836.3877
3	1795.9737
4	2478.3247
5	2979.9879
6	3342.1693
7	3593.9525
8	3767.673
9	3888.7019
10	3974.5429

$$Re_{sr2_i} := \frac{4 \cdot W_{find2_i}}{wp_{sr} \cdot \mu_{He}\left(THe_{min}\right)}$$

$$Re_{bl2_i} := \frac{4 \cdot W_{find2_i} \cdot 2}{wp_{bl} \cdot \mu_{He}\left(THe_{min}\right)}$$

$Re_{sr2} =$

	1
1	163.309
2	1099.5762
3	2554.9621
4	3550.772
5	4286.9931
6	4804.1473
7	5163.4154
8	5411.337
9	5584.1642
10	5706.8361

$Re_{bl2} =$

	1
1	102.7792
2	692.0227
3	1607.9756
4	2234.6926
5	2698.0364
6	3023.5094
7	3249.6162
8	3405.6467
9	3514.4162
10	3591.6202

$$\alpha_{sr} := \frac{gap}{\pi \cdot Dia_{out}}$$

$$\alpha_{bl} := \frac{gap_{bl}}{\pi \cdot \left(R_{cl} + R_{ac}\right)}$$

$$mf1_{sr_i} := ff_{slot}\left(Re_{sr1_i}, Dh_i, \varepsilon_f, Rel, Ret, \alpha_{sr_i}\right)$$

$$mf1_{bl_i} := ff_{slot}\left(Re_{bl1_i}, Dh_{bl}, \varepsilon_f, Rel, Ret, \alpha_{bl}\right)$$

$$mf2_{sr_i} := ff_{slot}\left(Re_{sr2_i}, Dh_i, \varepsilon_f, Rel, Ret, \alpha_{sr_i}\right)$$

$$mf2_{bl_i} := ff_{slot}\left(Re_{bl2_i}, Dh_{bl}, \varepsilon_f, Rel, Ret, \alpha_{bl}\right)$$

$mf1_{sr} =$

	1
1	0.4802
2	0.072
3	0.0422
4	0.0425
5	0.0422
6	0.0416
7	0.041
8	0.0405
9	0.04
10	0.0395

$mf1_{bl} =$

	1
1	0.763
2	0.1144
3	0.0533
4	0.0415
5	0.0412
6	0.0411
7	0.0409
8	0.0408
9	0.0408
10	0.0407

$mf2_{sr} =$

	1
1	0.5858
2	0.087
3	0.0418
4	0.0423
5	0.0421
6	0.0416
7	0.0411
8	0.0406
9	0.0402
10	0.0399

$mf2_{bl} =$

	1
1	0.9308
2	0.1382
3	0.0595
4	0.0428
5	0.0414
6	0.0412
7	0.0411
8	0.041
9	0.041
10	0.0409

Calculate the velocities in each region

$$Vel1_{sr_i} := \frac{W_{find1_i}}{A_{sr_i} \cdot \rho in_1} \qquad Vel1_{bl_i} := \frac{W_{find1_i} \cdot 2}{A_{bl_i} \cdot \rho in_1}$$

$$Vel2_{sr_i} := \frac{W_{find2_i}}{A_{sr_i} \cdot \rho in_2} \qquad Vel2_{bl_i} := \frac{W_{find2_i} \cdot 2}{A_{bl_i} \cdot \rho in_2}$$

$Vel1_{sr} =$ $ft\,sec^{-1}$

	1
1	16.4843
2	54.9814
3	78.7076
4	81.4585
5	78.3578
6	73.2344
7	67.5013
8	61.9186
9	56.8068
10	52.2547

$Vel1_{bl} =$ $ft\,sec^{-1}$

	1
1	8.2996
2	55.3644
3	118.8839
4	164.0519
5	197.2593
6	221.2338
7	237.9005
8	249.3999
9	257.4113
10	263.0935

NGNP
COMPOSITES
Calculation By: D. P. Carosella

General Atomics
Calculation Sheet
System PSR Seal Rings
Title: Leakage Determination 0.01" Horizontal Gap

Page No.: 11 of 43
Calculation No.:

$Vel2_{sr} =$

	1
1	10.9957
2	37.0177
3	57.3427
4	59.7692
5	57.7295
6	53.9113
7	49.6654
8	45.5438
9	41.7763
10	38.4247

$\mathrm{ft\,sec^{-1}}$

$Vel2_{bl} =$

	1
1	5.5362
2	37.2756
3	86.6132
4	120.3712
5	145.3291
6	162.8606
7	175.0398
8	183.4443
9	189.3032
10	193.4617

$\mathrm{ft\,sec^{-1}}$

90° Bend

$$Georatio_i := \frac{gap_i}{\pi \cdot Dia_{out}}$$

$$K_{90} := 1.24 \cdot 1.5$$

$Georatio =$

	1
1	$3.051 \cdot 10^{-5}$
2	$6.1019 \cdot 10^{-5}$
3	$9.1529 \cdot 10^{-5}$
4	$1.2204 \cdot 10^{-4}$
5	$1.5255 \cdot 10^{-4}$
6	$1.8306 \cdot 10^{-4}$
7	$2.1357 \cdot 10^{-4}$
8	$2.4408 \cdot 10^{-4}$
9	$2.7459 \cdot 10^{-4}$
10	$3.051 \cdot 10^{-4}$

NGNP
COMPOSITES
Calculation By: D. P. Carosella

General Atomics
Calculation Sheet
System PSR Seal Rings
Title: Leakage Determination 0.01" Horizontal Gap

Page No.: 12 of 43

Calculation No.:

$K_{90} = 1.86$

$K_{in} := .5$

$K_{out} := 1$

Pressure Drop Calculation

$$\Delta P1_i := \frac{\left[\left(mf1_{sr_i}\cdot\frac{H_{sr}}{Dh_i}\right) + K_{in} + K_{90}\cdot 2.5\right]\cdot\left(\frac{Wfind1_i}{A_{sr_i}}\right)^2 \; \ldots \\ + \left[\frac{\left(R_{cl} - R_{ac} - .5\cdot Dia_{out}\right)}{Dh_{bl}}\cdot mf1_{bl_i} + K_{out}\right]\cdot\left(\frac{Wfind1_i}{A_{bl_i}}\right)^2}{2\cdot\rho_{in_1}}$$

$\Delta P1 =$

	1
1	6.9592
2	6.8119
3	6.9786
4	6.9789
5	6.9788
6	6.9785
7	6.9782
8	6.9779
9	6.9777
10	6.9775

psi

Solve for flow $\Delta P_{bar} = 7\,psi$

Given

$$\Delta P_{bar} = \frac{\left[\left(mf1_{sr_1}\cdot\frac{H_{sr}}{Dh_1}\right)+K_{in}+K_{90}\cdot 2.5\right]\cdot\left(\frac{W_{find1_1}}{A_{sr_1}}\right)^2 \dots + \left[\frac{(R_{cl}-R_{ac}-.5\cdot Dia_{out})}{Dh_{bl}}\cdot mf1_{bl_1}+K_{out}\right]\cdot\left(\frac{W_{find1_1}}{A_{bl_1}}\right)^2}{2\cdot\rho_{in_1}}$$

$AA := Find\left(W_{find1_1}\right)$ $AA = 0.4443\,lb\,sec^{-1}$ $W_{find1_1} := AA$

Given

$$\Delta P_{bar} = \frac{\left[\left(mf1_{sr_2}\cdot\frac{H_{sr}}{Dh_2}\right)+K_{in}+K_{90}\cdot 2.5\right]\cdot\left(\frac{W_{find1_2}}{A_{sr_2}}\right)^2 \dots + \left[\frac{(R_{cl}-R_{ac}-.5\cdot Dia_{out})}{Dh_{bl}}\cdot mf1_{bl_2}+K_{out}\right]\cdot\left(\frac{W_{find1_2}}{A_{bl_2}}\right)^2}{2\cdot\rho_{in_1}}$$

$K_{in} = 0.5$

$K_{out} = 1$

$K_{90} = 1.86$

$AA := Find\left(W_{find1_2}\right)$ $AA = 2.9954\,lb\,sec^{-1}$ $W_{find1_2} := AA$

Given

$$\Delta P_{bar} = \frac{\left[\left(mf1_{sr_3}\cdot\frac{H_{sr}}{Dh_3}\right) + K_{in} + K_{90}\cdot 2.5\right]\cdot\left(\frac{W_{find1_3}}{A_{sr_3}}\right)^2 \ldots + \left[\frac{\left(R_{cl} - R_{ac} - .5\cdot Dia_{out}\right)}{Dh_{bl}}\cdot mf1_{bl_3} + K_{out}\right]\cdot\left(\frac{W_{find1_3}}{A_{bl_3}}\right)^2}{2\cdot\rho_{in_1}}$$

$AA := Find\left(W_{find1_3}\right)$ $AA = 6.3547\,lb\,sec^{-1}$ $W_{find1_3} := AA$

Given

$$\Delta P_{bar} = \frac{\left[\left(mf1_{sr_4}\cdot\frac{H_{sr}}{Dh_4}\right) + K_{in} + K_{90}\cdot 2.5\right]\cdot\left(\frac{W_{find1_4}}{A_{sr_4}}\right)^2 \ldots + \left[\frac{\left(R_{cl} - R_{ac} - .5\cdot Dia_{out}\right)}{Dh_{bl}}\cdot mf1_{bl_4} + K_{out}\right]\cdot\left(\frac{W_{find1_4}}{A_{bl_4}}\right)^2}{2\cdot\rho_{in_1}}$$

$AA := Find\left(W_{find1_4}\right)$ $AA = 8.7689\,lb\,sec^{-1}$ $W_{find1_4} := AA$

APPENDIX F – General Material Aspects

The purpose of this appendix is to explain the anisotropic nature of ceramic composites for those who do not already understand this aspect of composite materials.

Anisotropy

It should be noted that the properties of nearly all the materials considered in this report are anisotropic. In particular, fiber-reinforced composites exhibit extreme anisotropy of all properties, given that fiber properties dominate in the fiber direction and matrix properties dominate normal to the fibers. This problem is alleviated slightly by the weaving of fabrics, but matrix properties still dominate normal to the weave plane and in interlaminar shear.

Less obviously, many monolithic ceramics exhibit great anisotropy of properties because their complex bonding often causes their crystal structures to have low symmetry. Also, even in high symmetry structures such as graphite or boron nitride, the bonding orientation within the material can lead to high anisotropy of properties – in graphite, for example, conductivity is two orders of magnitude higher parallel to the graphene sheets than perpendicular to them. This problem is less apparent with polycrystalline bulk ceramics.

Radiation Damage

In monolithic ceramics, it is routinely found that atomic displacements affect thermo physical properties long before they affect mechanical properties, and it is also found that these types of damage are readily annealed out of the material. Indeed, within specific temperature ranges and at low fluence several materials reach equilibrium between damage and annealing (ref. 11).

Experience of the irradiation damage of materials, especially by neutron irradiation, is dominated by graphite. The irradiation experience base of graphite is dominated by Magnox and AGR applications in the United Kingdom, but with substantial extension of the data from high-temperature reactor testing.

The graphite experience base is complemented by a substantial body of theoretical study and experimental investigation, which supports understanding of the roles that the micro structural effects of neutron irradiation play in the overall mechanical changes.

The other CMC and monolithic materials here may be more or less susceptible to irradiation damage. However, the great majority of the components under consideration for use of CMCs or other ceramics are well outside the reactor core, so that they will only be exposed to neutron fluence that are orders of magnitude below those that can be tolerated by graphite. Hence, it is considered that irradiation degradation is unlikely to be a priority issue, except in materials where there is concern about identified processes specific to the material (such as the reaction of neutrons with boron).

This report contains appraisals of candidate materials based on their unirradiated properties. Subsequent work would be required to confirm that the expected radiation doses would not invalidate the conclusions presented here.

Operating Environment

Ceramics and composites are affected by a variety of design considerations which require study. In particular, two classes of issues should be studied further:

Thermal effects: ceramics and composites are often subject to thermal shock limits, but are also susceptible to thermal and thermo mechanical fatigue. Therefore, for lifing of a ceramic or composite component it is not sufficient to calculate temperature transients and ensure these remain within the thermal shock limit of the proposed material; the rate of cycling between transients must also be considered, and an evaluation made as to whether this cycling and the thermal stresses induced in a structure pose a risk of thermal fatigue. Also, system thermal analysis should evaluate the effect of localized hot-spots on components, transient or permanent, as the effect of thermal gradients in 3 dimensions can be considerable in ceramics and composites.

Corrosion effects: while ceramics are generally exceptionally resistant to all forms of corrosion save occasional attack by strong acids and alkalis, the compositional transients in the primary circuit must be understood in order to accurately predict the performance of candidate materials, especially in conjunction with the reactor temperature cycle. For example, a rapid heating cycle after refueling while a significant transient O_2 or H_2O partial pressure remains in the primary circuit would be likely to damage SiC or Si_3N_4 materials. Furthermore, it is known that there will be a certain level of particulate content in the primary coolant. The composition of this particulate matter should be defined.

APPENDIX G - Material Suppliers

This supplier review section was put together through review of manufacturer's websites and manufacturer supplied literature and experience Rolls-Royce has had through interaction with these companies.

Snecma Propulsion Solide (SPS)

SNECMA Propulsion Solide (SPS) are part of the Safran Group of companies that includes SNECMA and Turbomeca. SPS are based in Bordeaux, France. The expertise of SPS is in the production of carbon and silicon carbide matrices using the CVI process. SPS have a large market for their C/C composites in brake disc applications and for exhaust components in space vehicle applications where they manufacture components of up to approximately 2 m diameter by 2 m axial length. SPS may be capable of manufacturing larger components than this, up to 3m diameter, in C/C. SPS also offer a number of other composite materials. Their C/SiC material (A262) has been used in the outer flaps of the SNECMA M88-2 for past 10 years and the A500 (C/SiC) and A410 (SiC/SiC) grades have been rig tested for the divergent seals of a US fighter aircraft (F100) in the exhaust system. SPS have a history of continuous materials development as demonstrated by the property improvements achieved on moving from the A262 grade to the current A410/A415 grades. Currently, their most advanced materials are the A500 and the A410/A415 in the C/SiC and SiC/SiC systems, respectively. Both of these systems have a self healing matrix, which relies on the formation of a glassy phase to heal cracks that form in the matrix. Recently, SPS have introduced a lower cost CMC that utilizes polymer impregnation and pyrolysis (PIP) for the hardening route and the CVI process for the subsequent infiltration and formation of the matrix. Materials manufactured by SPS can have 2D or 3D fiber architecture. SPS also have a good grounding in CMC component design, manufacture and lifing due to the use of their materials in aerospace and aero-engine applications.

Goodrich

Goodrich Corporation is a global supplier of systems, products and services to the aerospace, defense and homeland security markets. The headquarters of Goodrich are in Charlotte, North Carolina. Goodrich employs more than 24,000 people worldwide in over 90 facilities across 16 countries.

Goodrich have a High Temperature Composites team (HTC) located in Santa Fe Springs, California that forms part of the Goodrich Aircraft Wheels & Brakes division. Goodrich have a history of providing steel and carbon brakes to aircraft manufacturers worldwide and it is through building on a core competency developed in the manufacture of carbon/carbon aircraft brakes that Goodrich has transitioned in to the manufacture of ceramic matrix composites

(CMC). A CMC produced by Goodrich is currently used in afterburner flaps and seals of the F-18 E/F and the Company is looking to expand the application of their MI-SiC/SiC composites to the hot section of gas turbine engines.

General Electric

General Electric offers a number of ceramic composite materials for turbine parts, aerospace structures and rocket propulsion applications through GE Aviation. The GE Global Research organization also has a section that is working on these materials. GE offer SiC/SiC and C/SiC material systems that are produced by either the melt infiltration or CVI processes.

General Electric has a history of obtaining technology through acquisition and in the recent past has obtained the ceramics technology of Honeywell.

Hyper-Therm HTC

The headquarters of Hyper-Therm HTC are located in Huntington Beach, CA. Hyper-Therm HTC's intellectual property portfolio includes patents on ceramic matrix composites (CMCs), functionally engineered fiber coatings for CMCs, nano-engineered materials, and the manufacture of actively cooled CMC components. Hyper-Therm HTC is a world-recognized producer of high-performance ceramic composite materials, engineered coatings and thermal-structural components using patented chemical vapor infiltration (CVI) and chemical vapor deposition (CVD) process technology. Since 1992, Hyper-Therm HTC has been active in the research and development of advanced materials primarily serving the military aerospace and energy generation markets, and building on their history of innovation are well positioned to serve these markets in the future. For more information please visit: http://www.htcomposites.com

Starfire – Pre-ceramic polymers

The headquarters of Starfire are in Malta, NY. Starfire offer a range of polymer precursor materials for the manufacture of ceramics, CMC's and coatings that can be used in a range of industrial and aerospace applications. These precursors offer new material options that combine the flexible processing and design advantages of plastics with the added benefits and durability of ceramics. The products offered by Starfire are matrix polymers, CVD/CVI precursors, ceramic forming molding compounds and fiber interface coatings.

The family of matrix polymers offered by Starfire® Systems can be used to form highly pure nano-structured silicon carbide (SiC) ceramics. The polymers available offer ease of processing, produce stoichiometric SiC, have a high ceramic yield, provide good thermal stability and high hardness.

Starfire also offer a polymer precursor for the formation of a ceramic matrix via the CVI process which provides improved efficiency over the conventional CVI process.

The family of low-cost fiber interface coatings offered by Starfire is compatible with a wide range of fibers used in carbon and silicon carbide composites and provides the required interfacial properties to produce composite behavior.

The family of Ceramic Forming Molding compounds derived from the Starfire proprietary polymers offer a cost-effective way of producing high quality near-net shape Silicon Carbide (SiC) components at low firing temperatures. These molding compounds yield high-strength ceramics that are resistant to corrosion and wear, even at high temperatures.

MT Aerospace

MT Aerospace is based in Augsburg, Germany. The company was previously known as MAN Technology. Since 2005 MT Aerospace has become part of OHB-Technology AG. MT Aerospace is a leading player in the European Aerospace sector supplying components for the launcher and orbiter systems of the Ariane 4 and 5 space programs. This technology is now being utilized in the aviation and industrial sectors. MT Aerospace offers a C/SiC and a SiC/SiC system for aerospace applications. These are used for multiple re-use on re-entry vehicles, but although temperatures up to 1800°C (3270ºF) may be experienced on re-entry this is in a non-oxidizing environment for short durations. MT Aerospace uses a forced gas CVI process to produce the C/SiC and SiC/SiC materials that they produce. The materials produced by MT Aerospace use a 2D fiber architecture. MT Aerospace has expertise in the manufacture, design and lifing of CMC structures and has manufactured some large 3D structures for re-entry vehicles from the 2D lay-ups that they produce. The main unknowns of the materials produced by MT aerospace regards there use in a long term structural application as currently the materials have only been used in short term, high temperature applications in an inert environment. http://www.mt-aerospace.de/frameset_de.html

Horizon Composites

Horizon Composites are based at the AMRC in Sheffield, UK whilst maintaining a small development facility in Cumbria, UK. Horizon is a small company, run by an individual who has considerable experience working with ceramic materials. Their past experience covers work with oxide/oxide, C/SiC and SiC/SiC composite systems. The facility in Cumbria is small, but has the basic equipment required for the development of ceramic/CMC technology. Horizon have established links with the AMRC and CAMTEC in Sheffield which gives the company access to advanced processing equipment and university based facilities. Horizon possesses novel ideas on material systems and manufacturing processes for CMCs that are worthy of consideration, and currently are considered capable of manufacturing prototype components.

Morgan Technical Ceramics

Morgan Technical Ceramics is a Global Business Unit of the Morgan Crucible Company and manufactures products from a comprehensive range of advanced ceramics, glass, precious metals, piezoelectric and dielectric materials. MTC offer a range of materials and products that are used in markets that include the aerospace, automotive, power generation and transmission, and thermal processing industries.

MTC was formed in 2003 when two former businesses units of The Morgan Crucible Company plc, Morgan Advanced Ceramics and Morgan Electro Ceramics, were combined. Since this time MTC has continued to grow through a number of strategic company acquisitions and consolidations. The resources and expertise of the constituent companies in the group enable MTC to offer a broad product range and technical capability. Morgan Technical Ceramics has manufacturing plants located throughout Europe, North America, South America, Australasia and Asia, each fully supported by a comprehensive customer service and technical support network. The company has the structure and the capability to work with global businesses at international and national level.

Kyocera

The headquarters of Kyocera are located in Kyoto, Japan. Kyocera was established in 1959 as a small suburban workshop by 28 colleagues. Their first product was a U-shaped ceramic insulator for use within early television picture tubes. Today Kyocera is a highly diversified global enterprise that offers a range of materials and products to a diversified range of businesses and industries. Of interest to this program are the fine ceramic materials and components that Kyocera produce. These are based on alumina, zirconia, silicon carbide and silicon nitride ceramics.

Saint-Gobain

Saint-Gobain Ceramics is a worldwide manufacturer and expert of specialty refractory products for the ceramics, metallurgy, chemical, petrochemical, power generation, waste processing and glass making industries. Saint Gobain has expertise in the design, engineering and manufacture of refractory systems for high temperature applications in these industries.

Saint-Gobain Ceramics has more than 70 years experience in providing refractories to industry and the company has been formed through the full integration of several leading worldwide refractory producers. These include: SEPR (1929); Savoie Refractaires (1985); Corhart (1987); Hamilton porcelain (1989); Norton Company (1990); Carborundum (1996); Cesiwid (1997); AnnaWerk (1999) and Toshiba Monofrax (2003).

Saint-Gobain Ceramics operates 22 sites dedicated to the manufacture of specialty refractory products around the world and benefits from two state-of-the-art primary Research & Development facilities located in France and in the USA.

The major product categories offered by Saint-Gobain include:

- **Advanced SiC products:** Recrystallized Silicon Carbide, Silicon infiltrated reaction bonded SiC, Advanced Silicon Nitride bonded SiC, pressureless sintered SiC.
- **Bonded refractories:** Silicon Nitride and Sialon bonded materials, Silicate bonded SiC, as well as Mullite, High Alumina, Alumina-Chrome, Chromium oxide, Tin oxide, Zirconia, Zirconium silicate, Cordierite and Spinel materials;
- **Pre-Formed Castable blocks** based on low and Ultra-low cement castables;
- **Resin bonded Alumina-Carbon bricks ;**
- **High purity Insulating Fire Bricks ;**
- **Fused cast refractories :** AZS, High Alumina, High Zirconia and Magnesia-Chrome;
- **Monolithics:** Regular and low cement castables, Dry Vibratable Cements, Blast furnace tap hole mixes, Gunning, Ramming and Trovelling mixes.

Surface Transforms

Surface Transforms are based in Cheshire, UK. The business was started in 1992 when technology was acquired from ICI. The company is now quoted on the AIM stock market. Surface Transforms produce their C/SiC material for friction applications (brakes, clutches). This is a low cost manufacturing route with material cost estimated to be at least an order of magnitude lower than other such composites. This C/SiC composite is produced by depositing carbon in the carbon fiber preform via the CVI process followed by melt infiltration with molten silicon, which reacts with the carbon to form the SiC matrix. Both unreacted C and Si are also present in the matrix.

This material is likely to be seriously degraded by thermal exposure in air at temperatures above 600°C (1100ºF) owing to the presence of carbon in the fibers and matrix; however in an inert environment the material may offer higher temperature capabilities.

DLR

DLR comprises a number of research institutes based throughout Germany. These institutes specialize in materials, structures and design, and propulsion technology. The Institute of materials has developed a filament winding process to produce an oxide/oxide composite known as Whippox. This technology is reported to have been licensed to a German company, which currently uses the facilities at DLR to fulfill commercial orders.

Corning

Corning Incorporated is a world leader in specialty glass and ceramics. They have more than 150 years of materials science and process engineering knowledge to draw on to create and make keystone components that enable high-technology systems for consumer electronics, mobile emissions control, telecommunications and life sciences. A key to Corning's success has been its sustained commitment to developing and supplying premier glass and glass-ceramics for many different applications on a global basis. Corning is a world leader in delivering advanced optical solutions for a broad array of commercial and industrial markets. They have an unparalleled understanding of fundamental glass science and deliver more than 150 material formulations; including glass, glass ceramics and fluoride crystals to a range of industries.

Composites Optics Inc (COI Ceramics Inc.)

Composite Optics, Inc. began operation in 1999 and is a division of ATK Space Systems, a division of ATK, Alliant Techsystems, Inc. COIC have a history in the manufacture of oxide/oxide composites using Nextel™ oxide fibres from 3M in their San Diego facility and are a supplier of ceramic fibre reinforcement from the Salt Lake City facility. A composite combustion liner produced in the oxide/oxide CMC has been run in a SOLAR industrial gas turbine programme that was set up to demonstrate CMC technology in collaboration with Siemens.

Teledyne Rockwell

The Teledyne Scientific Company was established in 1962 as a corporate R&D laboratory serving the business units of Rockwell International. The main facility in Thousand Oaks opened in 1964 on a 77 acre campus. Major operations at this facility include electronics, information sciences, materials, and optics research and product development. Initially, Teledyne Scientific focused solely on R&D for the U.S. Government and the Rockwell International Corporation, but latterly have transitioned to a for-profit enterprise by expanding the customer base, and offering cutting-edge R&D services, products and licensing deals to address the needs of external customers.

Research and development in the Materials Technology Division ranges from the frontiers of basic materials science to novel device technologies. Through decades of aerospace research Teledyne Scientific offer a world-class capability in ultra-high performance ceramic composite design, modeling, and fabrication. Within the Materials Technology Division the Composite Materials Department offers a capability in developing novel composite structures based on integrally formed 3-D textile fiber preforms. These composites are designed for aerospace applications that demand optimum thermal and mechanical performance. Key applications include actively cooled rocket nozzles, space vehicle thermal protection, polymeric composites for aircraft, microelectronic packaging, hot structures for hypersonic vehicles, and efficient turbine engine combustor components.

APPENDIX H – Rolls Royce Ceramics Technology Program Elements

The introduction of ceramic or ceramic composites for components operating in civil nuclear power generating applications will require a significant level of effort that should not be underestimated and a highly disciplined approach to achieve a successful outcome. Some of the issues that will need to be addressed in a ceramic or CMC development program are given below together with an indication of the perceived man power effort and time for technology development. These resource requirements are rough estimates based on the introduction of materials in aerospace applications and do no take in to account any special considerations or costs associated with neutron irradiation. These estimates are not intended to be authoritative, nor are they intended to be used for budgetary purposes.

- A detailed review to establish the knowledge base that exists globally for the application of ceramics and ceramic composites in nuclear and high temperature extreme environments. (Stage 1 – one man year over one year).
- Detailed component design requirements (operating environment, stresses, and temperatures). (Stage 1 - Supplied by General Atomics)
- A detailed preliminary evaluation with the supply network to establish manufacturing options and capabilities for candidate materials in the proposed applications. (Stage 1 – half a man over one year plus travel budget).
- Detailed risk reviews at a component, sub-assembly and system level. (Stage 1 – equivalent of 1/10 man year in one year)
- Assembly of a consortium that includes the raw material supplier through to the end user, which involves the participation of specialists from the materials design, lifing and manufacturing community. (Stage 1 - equivalent of 1/10 man year in one year)
- Development of enabling technologies such as design, lifing, stressing, joining, protective coatings and manufacturing to enable the successful implementation and operation of ceramics and ceramic composites in the proposed applications. (Stage 2 – a two or three man year effort per year per technology for 5 years – 60 to 90 man years effort over 5 years total)
- Material property testing to establish the behavior of proposed materials in a high temperature nuclear environment. This should also form part of the material selection exercise. (Stage 1 – estimate of $4M per material and 3 years testing).
- Understanding the degradative effect of long term thermal and nuclear exposure on the microstructure, phase stability and properties of a material. (Included in above)
- Understanding the effect of corrosive and oxidative species in the environment on the long term degradation of a material. (Included in above)

- Development of detailed property databases to support the design, stressing and lifing of a component. (stage 2 - $6M to $10M per material over a five year timeframe)
- Design for manufacture. This is especially important for a composite where the fiber architecture determines the properties of a component.
- Adoption of a process that takes a structured approach to the introduction of new materials and technologies.
- Production of required documentation and specifications. (stage 2 & 3 – probably a 3 man-year effort for material specifications).
- Development of a mature supply chain, especially for ceramic matrix composites.
- Early identification of a methodology that can be used to fully validate the materials in the proposed applications. (stage 3 – validation test – allow several million dollars)

Appendix I – KAERI Report NHDD-RD-08-005, Rev. 1

KAERI

Nuclear Hydrogen Project

Calculation Note

Document No: NHDD-RD-CA-08-005, Rev. 01

Title : A Thermal-fluid analysis for the selection of operating conditions of reactor internals

Prepared by :	Min-Hwan Kim	Date : Sep. 10. 2008
Reviewed by :	Jisu Jun	Date : Sep. 11. 2008
Approved by :	Won Jae Lee	Date : Sep. 12, 2008

SUMMARY

This report addresses the results of thermal-fluid analysis that will be used in defining the material requirements of the candidate reactor internal components. This work has been performed as a part of NGNP Phase B Conceptual Design Study, WBS HTS.000.S15-Composites R&D Technical Issues Study. The selected NGNP reactor design has a block type core with reactor power of 600MWt. The reactor pressure vessel (RPV) material is SA508/533 and it is cooled by a vessel cooling system in which slipstream of the reactor coolant flows through the bottom plenum, helium side of the shutdown cooling system, the gap between the RPV and the core barrel to the upper plenum. In order to obtain reasonable estimate of temperatures for candidate composite components, the reactor pressure vessel is modeled in detail using the GAMMA+ code. The GAMMA+ code solves the transient multi-dimensional fluid-dynamics and heat conduction equations as well as radiation heat transfer. The calculation was performed for both normal operating conditions and the LPCC/HPCC accident conditions at the initial core inlet/outlet temperatures of 490/950°C and 590/950°C. The maximum temperatures of candidate components were obtained and provided for defining the material requirements.

Record of Revisions

No.	Date	Description	Prepared by
00	Aug. 14, 2008	Initial Issue	Min-Hwan Kim
01	Sep. 11, 2008	Add the Results for T_{in} = 590^{o}C	Jisu Jun

NHDD-RD-CA-08-005, Rev.01

A Thermal-fluid Analysis for the Selection of Operating Conditions of Reactor Internals

September 10, 2008

Revision 01

WBS HTH.000.S15. Composites R&D Technical Issues Study
NGNP Phase B Conceptual Design Studies

Korea Atomic Energy Research Institute

TABLE OF CONTENTS

LIST OF FIGURES

LIST OF TABLES

1. INTRODUCTION

Material selection for reactor internals is one of important issues in the NGNP design with an increase of the core outlet temperature for the multi-purpose heat applications. Reactor internals such as control rod structural elements may undergo high temperature and stress conditions during a normal operation and accidents, at which the structural integrity could not be assured. Thus, the use of composite material which sustains its material integrity at high temperature is not avoidable in the NGNP reactor internals design.

The purpose of this study is to perform thermo-fluid analyses by the GAMMA+ code to calculate operating conditions for various reactor internals that are candidates for composite or ceramic construction. The analyses are performed for a normal operating condition, and the HPCC and LPCC accidents. The results of the GAMMA+ analysis will be used for defining the material requirements for the reactor internal components.

2. Identification of Components

The reactor vessel design selected for the present analysis is a cooled-vessel design and its geometric configuration is mostly the same as used in the previous KAERI analysis [Kim, 2008] during NGNP Phase-A PCD studies. The only difference is the upper plenum design where the upper plenum shroud exists based on the GA's design.

Reactor internal components of concern should be identified before the detail thermo-fluid analyses. Based on the results of pre-conceptual design studies, the following internal components are derived as candidates for the use of composite material as follows. The location of each component is indicated in Figure 2.1.

- Side reflector seals
- Control rod structural elements
- Control rod guide tubes
- Upper plenum shroud insulation canisters
- Upper core restraint blocks
- Lower metallic core support insulation blocks
- Hot duct insulation canisters
- Bottom Plenum/SCS insulation tubes

2.1 Side reflector seals

As shown in Figure 2.2, side reflector seals are formed in a shape of an annular ring and installed in each riser holes and at each vertical interface between the permanent side reflector blocks to minimize leakage flow associated with the change of the core inlet flow path through the riser holes in the SA508/533 vessel design.

2.2 Control rod structural elements

Each complete control rod assembly consists of a series of 18 interconnected annular cylinders that provide mechanical flexibility. For the reference GT-MHR control rod elements, the control rod channels allows bypass flow, approximately 3% of core coolant flows, into them to maintain adequate cooling for the alloy 800H canister. [GA, 1990] However, the NGNP control rod elements do not require the cooling flow because the composite material can sustain much higher temperature than alloy 800H. Detail of the control rod structural elements is shown in Figure 2.3.

2.3 Control rod guide tubes

The control rod guide tubes, as shown in Figure 2.4, extend from the control rod drive assembly housing down to the top of the core, which form an integral part of the control rod drive assembly, and provide a guided passage for the control rods between the drive assembly housing and the entrance to the control rod hole in the upper core restraint blocks at the top of the core.

2.4 Upper plenum shroud insulation canisters

These are cover sheets used to cover both sides of the enclosed layers of the thermal insulation in the reactor upper plenum area of the reactor vessel. The upper plenum shroud protects the reactor vessel wall from high temperature not only during normal operation but also during a postulated conduction cool-down accident when the upper plenum helium temperature becomes very high. Figure 2.5 shows the upper plenum shroud.

2.5 Upper core restraint blocks

A single core restraint block of which the height is a half of the core block element is located at the top of each column of hexagonal core blocks, and also above each column of the permanent reflector elements, as shown in Figure 2.6. These blocks have the same cross section as the column of blocks upon which they are installed. The blocks are interlocked each other to provide stability during refueling and to maintain relatively uniform and small gaps between columns during operation.

2.6 Lower metallic core support insulation blocks

Two layers of insulation blocks, as shown in Figure 2.7, are installed directly on the top of the metallic core support floor near the bottom of the reactor vessel. Each of these blocks are intended to support one entire column of core elements, the associated top and bottom core reflector elements, the core support pedestal, and one layer of either graphite or composite blocks. The blocks are sized to the same hexagonal cross section as the standard graphite block but have a length of 450mm.

2.7 Hot duct insulation canisters

Figure 2.8 shows hot duct insulation canisters, a type of cover sheets which are formed as short cylinders and wrap the thermal insulation to protect the duct from creep damage.

2.8 Bottom plenum and SCS insulation cover sheets

SCS insulation tubes and cover sheets shown in Figure 2.9 are a part of reactor vessel lower plenum insulation assembly that is installed below the metallic core support floor, which protects the lower section of the reactor vessel and provides a pathway for a reactor vessel cooling system that utilizes the shutdown cooling system as a source of cooled helium. The insulation material also extend upward slightly around shutdown cooling system heat exchanger to prevent imposition of an unacceptable heat load into that system.

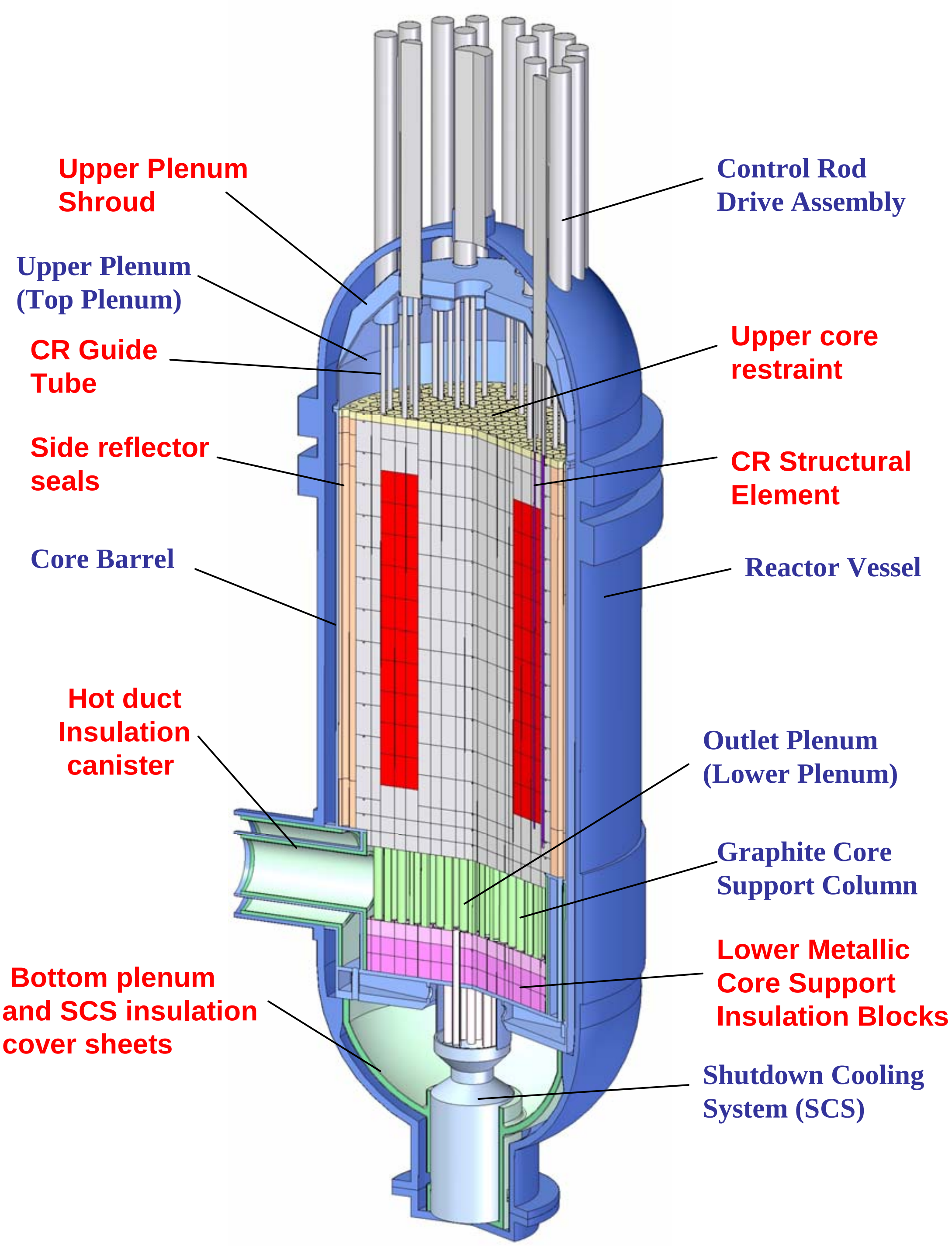

Figure 2.1 Reactor internal components for composite materials

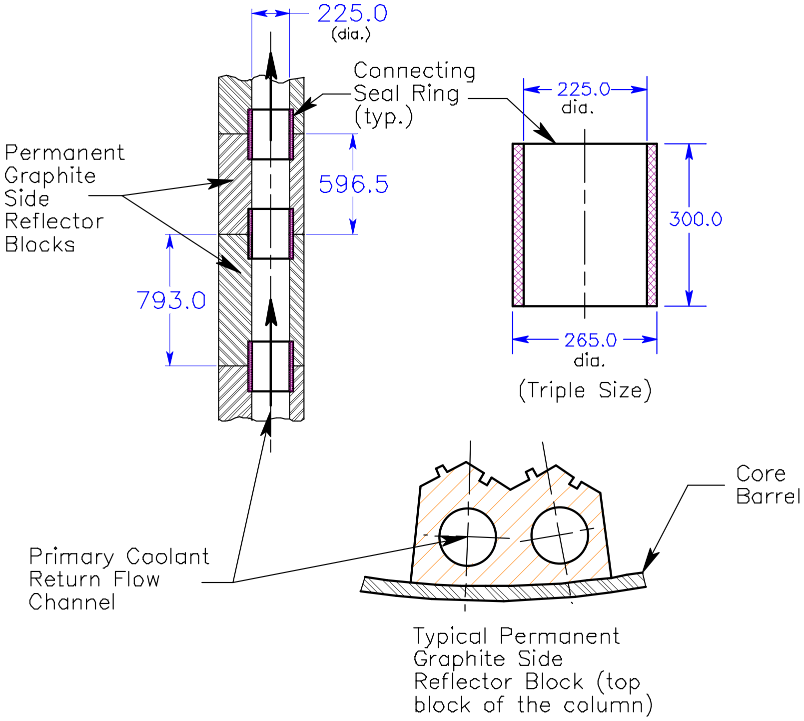

Figure 2.2 Side reflector seals in the permanent side reflector

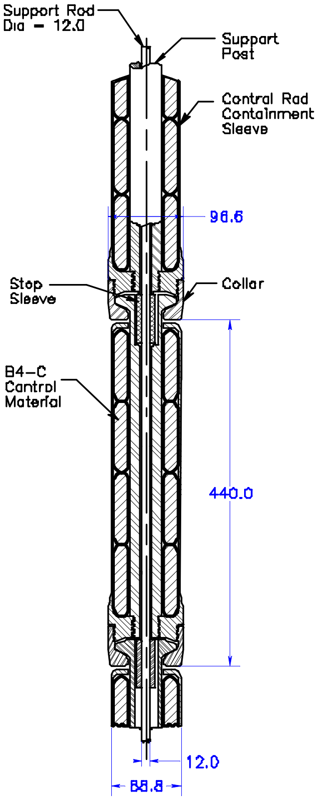

Figure 2.3 Control rod structural elements

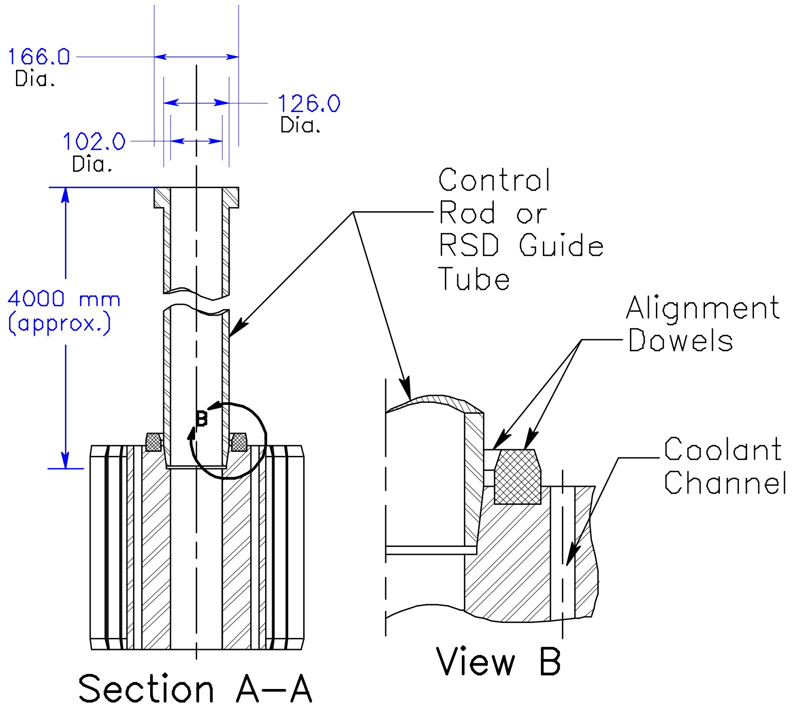

Figure 2.4 Control rod guides tubes

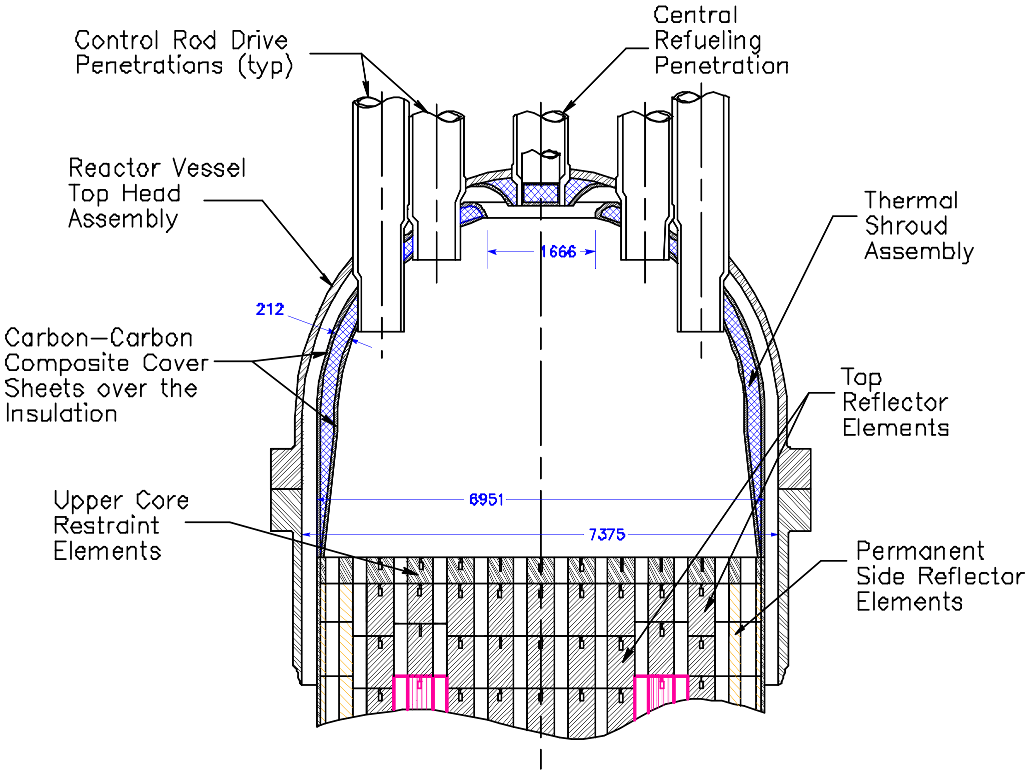

Figure 2.5 Upper plenum shroud insulation canisters

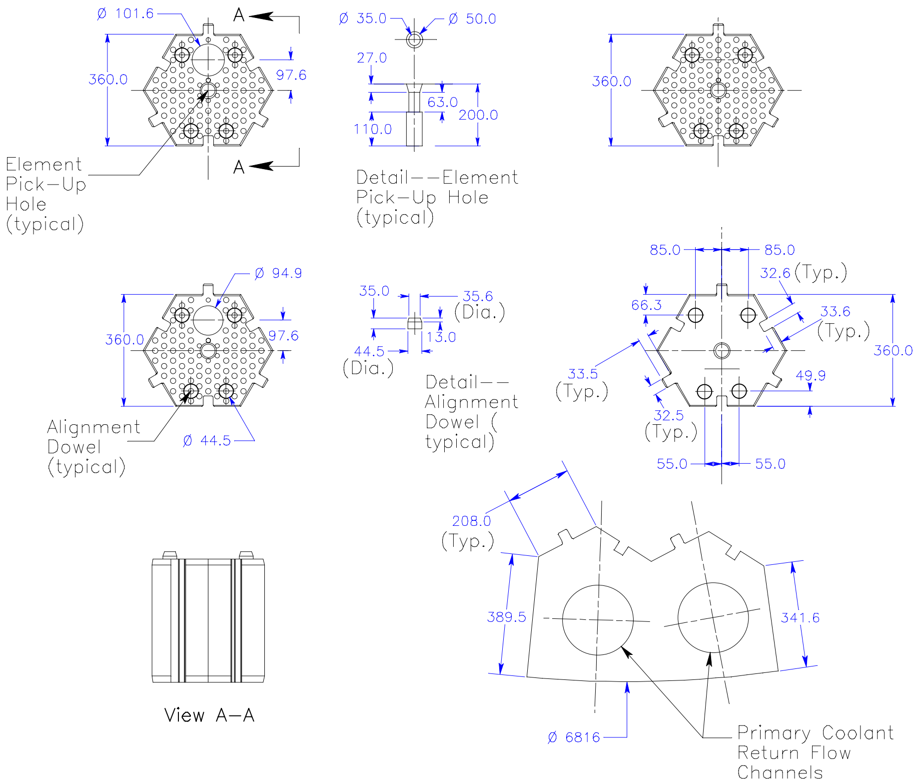

Figure 2.6 Upper core restraint blocks

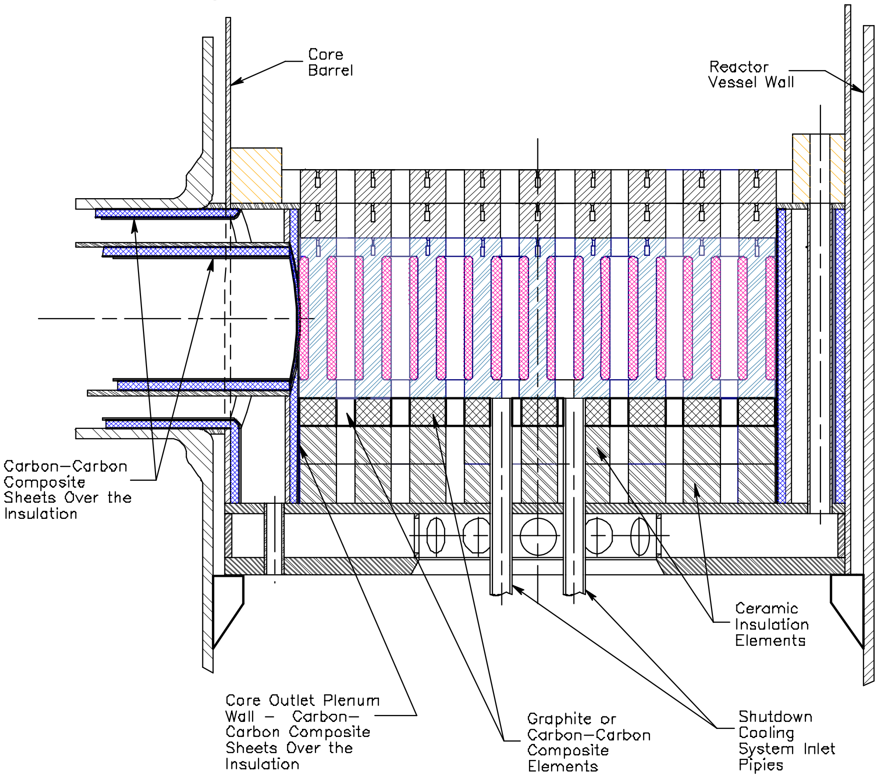

Figure 2.7 Metallic core support insulation blocks

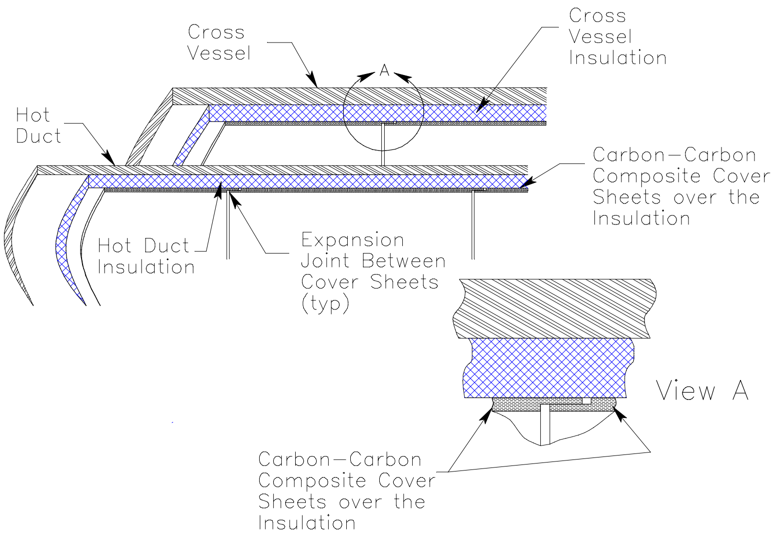

Figure 2.8 Hot duct insulation canisters

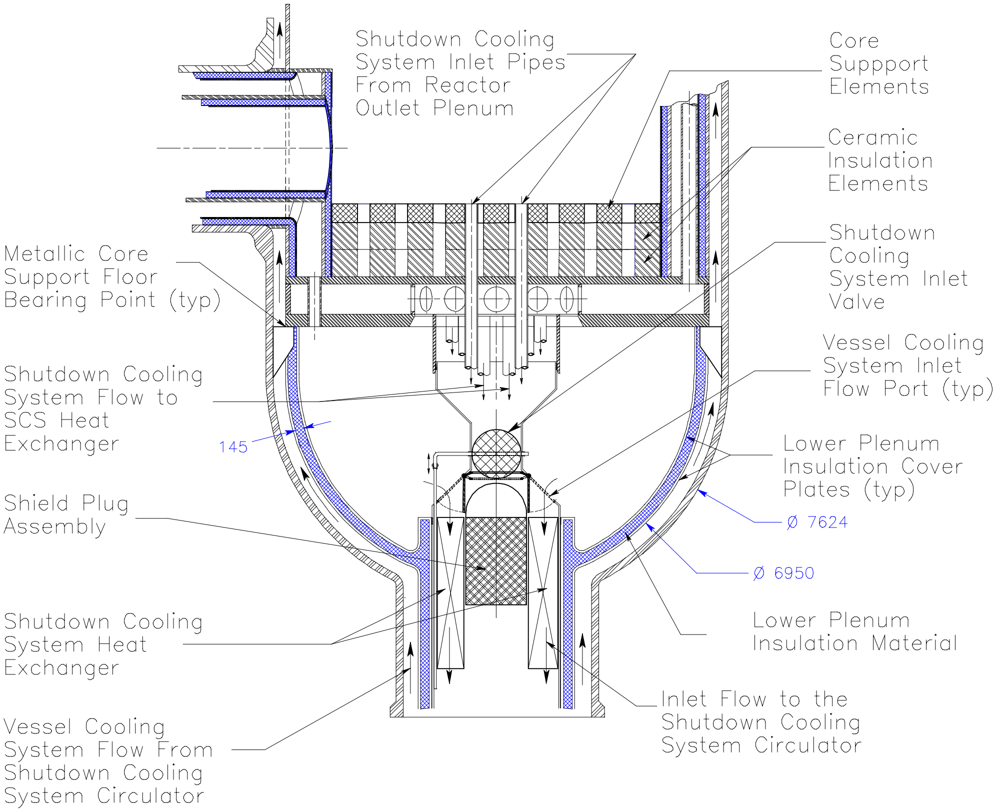

Figure 2.9 Bottom plenum and SCS insulation cover sheets

3. THERMAL-FLUID ANALYSIS USING GAMMA+ CODE

3.1 Description of thermal-fluid analysis model

The GAMMA code [Lim, 2006] was developed for the analysis of VHTR thermo-fluid transients including air ingress phenomena. The code capability was extended and the GAMMA+ code was developed to have enhanced capability for the following models; fluid transport and material properties, multi-dimensional heat conduction, multi-dimensional fluid flow, chemical reactions, multi-component molecular diffusion, fluid heat transfer and pressure drop, heat generation and dissipation, and radiation heat transfer.

The input used for the NGNP cooled-vessel study [Kim, 2008] is selected as a reference for the present analysis. Detailed modeling of the reactor internals are incorporated in the GAMMA+ model to obtain reasonable estimates of the temperatures distribution in the inlet plenum, the upper plenum, the lower plenum, the vessel cooling flow path.

Figure 3.1 shows the GAMMA+ model for the whole system. The model of fluid parts is composed of the reactor coolant system (RCS), the air-cooled reactor cavity cooling system (RCCS), the vessel cooling system (VCS) and the water-cooled shutdown cooling system (SCS). The flow from the cold inlet duct is supplied to the inlet plenum and sent down to the bottom plenum. Most of the flow is sent to the riser holes in the permanent side reflectors through the flow paths provided in the metallic core support. In the bottom plenum, part of the flow is bypassed to the shutdown cooling system through which the temperature of helium coolant decrease and then sent to the annular space between the reactor vessel and the core barrel to maintain the reactor vessel temperature below the normal operational limit of SA508/533 steel. After that, the vessel cooling flow is combined with the main flow at the upper plenum.

Solid regions for the reactor internals composites are two-dimensionally modeled. Inner and outer control rods are modeled as 3x36 meshes for the region of a series of 18 interconnected annular cylinders, and as 3x13 meshes for the upper structure. Guide tubes for the inner control rods, the outer control rods, and the reserve shutdown control (RSC) material are modeled as 3x10 meshes, respectively. The other regions for the reactor internals of interest are also modeled as two-dimensional meshes as shown in Table 3.1. Total mesh number for the solid regions is 1216.

The fluid regions are modeled by the combination of two- and one-dimensional flow networks with 505 meshes. The thermal radiation heat transfers are considered in the top plenum, the bottom plenum, the annulus between the core barrel and the RPV, the reactor cavity containing the RCCS panels, and the annulus between the downcomer wall and the reactor cavity wall.

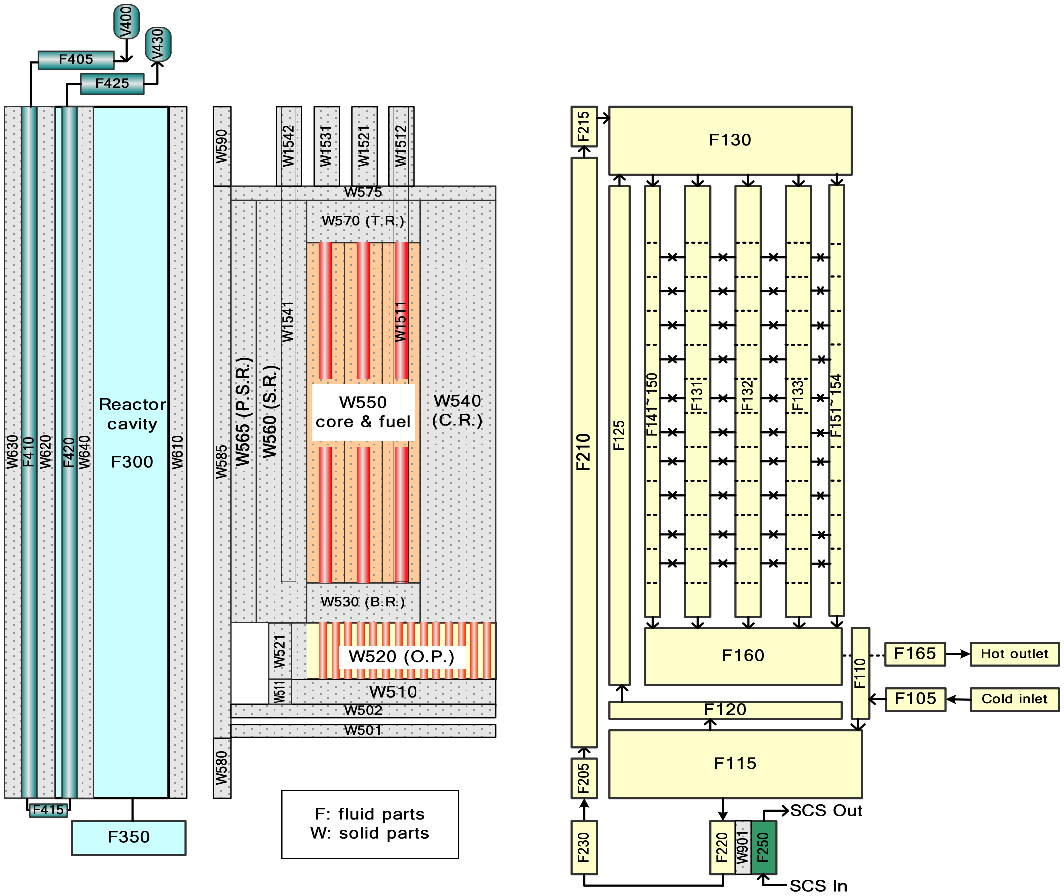

Figure 3.1 Analysis model of the GAMMA+ code for the cooled-vessel concept

Figure 3.2 shows a flow network model of the GAMMA+ code for the inlet riser, core coolant channels, FA gap bypasses, and RSC/CR channels. The active core flow is modeled as three flow channels with 15 axial nodes including 10 nodes for fuel blocks, 1 for upper restraint block, 2 for top reflector blocks, and 2 for bottom reflector blocks. The other bypass flow from the top plenum and the outlet plenum is modeled as 10 flow channels which consist of 5 channels for gap flow between inner reflector blocks, 3 channels for the gap flow between FA blocks, and 2 channels for gap flow between outer reflector blocks. These gap flow channels are interconnected each other and also interconnected to the FA coolant flow channels and RSC/CR flow channels through cross-flow junctions. The gap sizes considered in the present analysis are 2 mm for the horizontal gaps and 1.5 mm for the vertical gaps between the fuel blocks, respectively.

Table 3.1 Description of GAMMA+ model Components and their meshes

Component	Description	Meshes
F105	Inlet cold pipe	5
F110	Inlet plenum	3
F115	Lower plenum	2
F120	Metal support zone	1
F125	Inlet riser holes	18
F130	Upper plenum	3
F131~133	Core coolant channels	15 (all)
F141~150	IR, FA, SR, PSR bypass channels	15 (all)
F151~154	CR, RSC bypass channels	15 (all)
F160	Outlet plenum	1
F165	Outlet hot pipe	7
F205,F210,F215	CB/RPV annulus (VCS flow path)	1,3x21,1
F220	SCS HX - He side	20
F230	VCS inlet riser	4
F250	SCS HX - water side	20
F300	Reactor cavity (RCCS)	3x23
F350	Reactor cavity (remain)	1
F405	RCCS inlet header	1
F410	RCCS downcomer	14
F415	RCCS lower plenum	1
F420	RCCS tube riser	14
F425	RCCS outlet header	1
W501,502	Lower metal support plate	5x1,10x1
W510	Bottom support	9x2
W511	Bottom support insulation cover	3x2
W520	Outlet plenum	9x3
W521	Outlet plenum insulation cover	3x2
W530	Bottom reflector	3x2
W540	Central reflector	5x14
W550	Fuel & core reflector	3x10
W560	Side reflector	2x14
W565	Permanent side reflector	3x14
W570	Top reflector	3x2
W575	Top support shroud	11x1
W580	Lower plenum cover	4x2
W585	Core barrel	3x19
W590	Upper shroud	4x3
W610	Reactor pressure vessel	5x23
W620	RCCS downcomer wall	3x23
W630	Reactor cavity wall	4x23
W640	RCCS panel	2x23x4
W1511,1541	Inner and outer CRs	3x49
W1512,1542	CR guide tubes	3x10
W1521,1531	RSC guide tubes	3x10

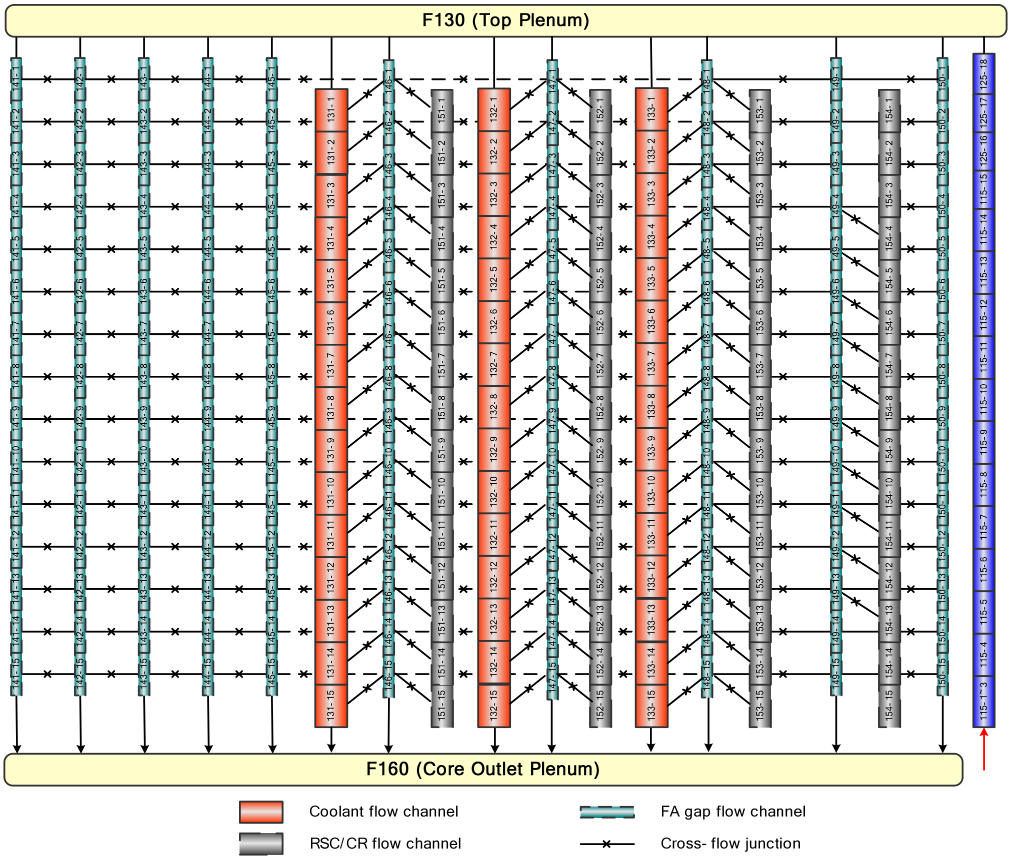

Figure 3.2 Flow network model of the GAMMA+ code for the inlet riser, core coolant, FA gap bypasses, and RSC/CR channels

In the present analysis, the riser holes in the permanent side reflector are connected directly to the upper plenum to which the core coolant channels are connected. This configuration is expected to result in much higher temperature in the upper plenum during accidents than the previous NGNP cooled-vessel study [Kim, 2008] and is selected to be conservative in determination of the temperature requirement of composite material components.

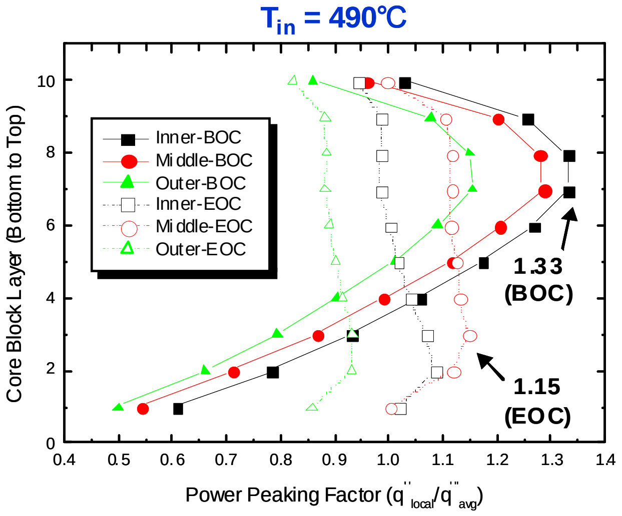

Figure 3.3 Core power distributions from the GAMMA+/VSOP linkage calculation

The core power distribution is obtained from the GAMMA+/VSOP linkage calculation. Figure 3.3 shows the power distributions for the helium inlet temperature of 490°C. The beginning-of-cycle (BOC) power peaking factor for T_{in}=490 °C is higher than that for T_{in}=590 °C condition [Kim, 2008] and, thus, is conservatively applied for all the calculations.

The air-cooled RCCS is considered in the analysis, the model of which is one-dimension and refers the GT-MHR design with assumption of the inlet pressure and temperature of 1 bar and 43°C, respectively. The heat loss from the outside of the reactor concrete wall to an environment is modeled using a constant heat transfer coefficient of 5 W/m^2-K and an emissivity of 0.6 at an air temperature of 30°C.

Reference coordinates in the radial and axial directions for the main components are shown in Figure 3.4. A variety of materials can be used for the candidate components according to the purpose and the operating conditions. In the present analysis, however, just carbon composite is assumed as the material for all the components considered.

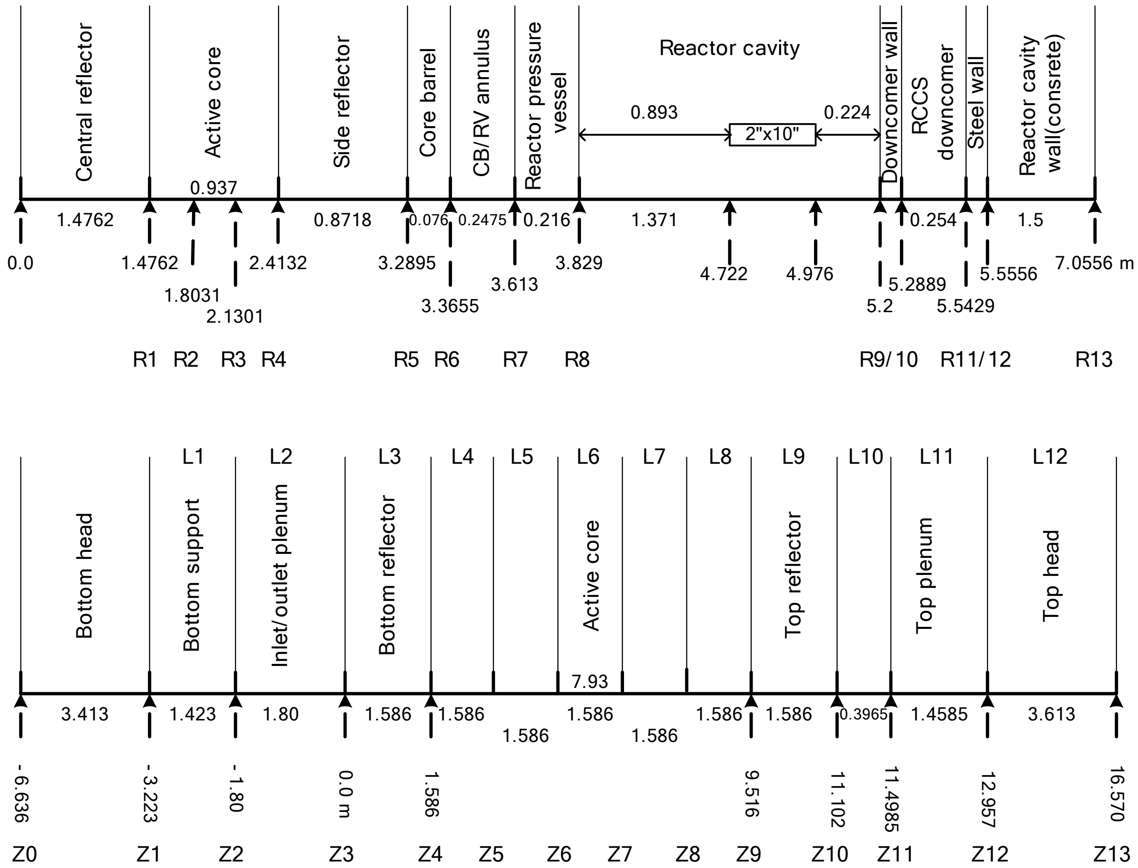

Figure 3.4 Radial and axial coordinates used in the GAMMA+ analysis

3.2 Steady-state analysis

Steady state analysis is performed using the GAMMA+ model described in the section 3.1. The operating conditions and the calculated maximum temperatures of main components at steady state are shown in Table 3.2 and 3.3, respectively. The VCS helium flow rate, which is bypassed from the bottom plenum to the upper plenum, is calculated as 4.143 kg/s and 5.325 kg/s for two core inlet temperature conditions with the fixed flow rate of 12.0 kg/s at the SCS water side. The temperature of the VCS flow after going through the SCS heat exchanger is 260^{o}C and 268^{o}C, respectively. The predicted maximum RPV temperature is 333^{o}C for T_{in}=490 ^{o}C condition and 390 ^{o}C for T_{in}=590 ^{o}C. Heat loss to the RCCS for T_{in} =490 ^{o}C during steady state is computed to be 1.6MWt which is lower than that of the cooled-vessel analysis, 1.76MWt [Kim, 2008]. This is because the RPV temperature of the present analysis is relatively low. Maximum fuel temperature of 1110^{o}C for T_{in}=590^{o}C less than that of 1133^{o}C for T_{in}=590^{o}C condition, which is caused by the higher RCS helium flow rate for T_{in}=590^{o}C. Among the reflectors, the highest temperature occurs in the bottom reflector.

Table 3.2 Operating conditions at steady state

Parameters	For T_{in}=490 ^oC	For T_{in}=590 ^oC
Power, MWt	600 (BOC)	600 (BOC)
RCS helium P, MPa	7.0	7.0
RCS helium T_{in}/T_{out}, ^oC	490/950	590/950
RCS helium flow rate, kg/s	248.5	315.15
SCS water Pin, MPa	5.0	5.0
SCS water T_{in}/T_{out}, ^oC	64/158	66/230
SCS water flow rate, kg/s	12.0	12.0
SCS helium T_{in}/T_{out}, ^oC	474/260	568/268
VCS helium flow rate, kg/s	4.143	5.325
Heat loss to RCCS, MWt	1.6	2.0
RCCS air T_{in}/T_{ex} , ^oC	43/171	43/197
RCCS air flow rate, kg/s	12.28	12.84

Table 3.3 Maximum Temperature of main components at steady state

Components	For T_{in}=490 ^oC Max. Temperature ,^oC	For T_{in}=590 ^oC Max. Temperature ,^oC
Fuel Compact	1133	1110
Fuel Block	1081	1057
Bottom Reflector	1018	1004
Central Reflector	900	897
Side Reflector	762	788
Top Reflector	553	637
RPV	333	390
Core Barrel	481	578

Table 3.4 shows steady state temperatures at the side reflector seals. Modeling all seal rings in the permanent reflector requires a lot of computer resource. Therefore, the permanent side reflector is just divided into three regions in the radial direction, and the middle one corresponding to both the seal rings and the riser holes is modeled as a porous region. The highest temperature of the seal rings occurs at the bottom side of the permanent reflector.

Table 3.5 shows steady state temperatures at the control rod structural elements in the inner ring. In the 18 interconnected annular cylinders, each cylinder is modeled as 2 cells in the axial direction in which one has a length corresponding to the B4C control material region and the other to the region composing the articulate parts. The mesh size for the control rod assembly is 3x36. It is assumed that the control rod is fully inserted both normal operation and accidents to estimate the peak temperature conservatively. The results show that the maximum temperature occurs at the bottom region of the core.

Table 3.4 Steady state temperatures at the side reflector seals

For T_{in}=490 °C T (°C)	For T_{in}=590 °C T (°C)	Axial Location Z (m)
483.908	582.317	10.71
484.049	582.455	9.913
484.274	582.599	9.120
484.499	582.735	8.327
484.699	582.867	7.534
484.920	583.040	6.741
485.021	583.210	5.947
485.096	583.283	5.155
485.192	583.323	4.361
485.311	583.373	3.568
485.477	583.446	2.776
485.715	583.595	1.982
485.610	583.652	1.190
486.794	584.799	0.3965

The guide tubes for both the control rod and the reserve shutdown control material are modeled as 3x10 meshes. The results for the inner control rod and the outer reserve shutdown control guide tubes are shown in Table 3.6. The guide tubes are located in upper plenum zone, and so the height of the inner guide tube is greater than that of the outer guide tube. It is assumed that the CR guide tubes are filled with the CR drive structures, but the RSC holes are empty. Thus, it is modeled that the flow area of the inside CR guide tube is less than that of RSC guide tube although the diameter of the CR guide tube (0.1016 m) is greater than that of the RSC hole (0.09525 m). All the temperature during the steady state is lower than the core inlet temperature. Bottom regions mating with the upper core restraint blocks reveal higher temperature than others.

The upper plenum shroud is modeled as an annular cylinder which has an equivalent heat transfer area to the shroud. The temperatures at steady state are given in Table 3.7. The temperature of the inside canister is higher than the outside one, and the maximum occurs near the riser outlet.

The results for the upper core restrain blocks are shown in Table 3.8. Total 13 solid sells are used in the radial direction, which are 5 meshes in the central replaceable reflector column, 3 meshes in the fuel assembly column, 2 meshes in the replaceable side reflector, and 3 meshes in the permanent side reflector. The maximum temperatures of 486°C and 584°C occur at the riser location in the permanent side reflector column for both the inlet temperature conditions.

Metallic core support insulation blocks are modeled as 9 solid cells in the radial direction among which 5 cells corresponds to the SCS inlet pipe region and is treated as a porous region. The results are shown in Table 3.9. Maximum temperature occurs at the center. Temperature distribution at cover sheets wrapping the outlet plenum and the insulation blocks is also estimated and shown in Table 3.9. The locations of the hottest temperatures of 857 °C and 877 °C are in the part contacting with the outlet plenum for both inlet temperature conditions.

Both hot and cold ducts are modeled as annular cylinders, the mesh sizes of which are 5x7 and 5x5 respectively. Table 3.10 shows the temperature at each cell. The temperature of the hot duct insulation canisters is close to the core outlet temperature while that of the cold side is nearly same as the reactor inlet temperature.

The results for the bottom plenum shroud of which the structure is the same as the upper plenum shroud are shown in Table 3.11. The temperature of the cover sheet at hot side is close to the reactor inlet temperature because the inlet coolant is supplied into this bottom plenum. The cold side temperature of the cover sheet is much lower than the hot side due to a coolant temperature drop through the shutdown cooling system.

Table 3.5 Steady state temperatures at the CR structural elements

T (^oC) for T_{in}=490 ^oC			T (^oC) for T_{in}=590 ^oC			Z (m)
513.531	513.831	514.065	605.772	606.010	606.195	9.491
514.204	514.206	514.207	606.294	606.295	606.296	9.266
514.229	514.223	514.213	606.312	606.307	606.300	9.046
514.468	514.397	514.325	606.492	606.436	606.379	8.826
549.699	550.578	552.435	634.550	635.256	636.723	8.606
553.475	553.483	553.489	637.454	637.460	637.464	8.386
553.522	553.515	553.504	637.488	637.483	637.475	8.166
553.807	553.724	553.639	637.703	637.637	637.569	7.946
595.434	596.470	598.640	670.856	671.688	673.412	7.726
599.907	599.906	599.905	674.304	674.303	674.302	7.506
604.955	603.769	601.331	678.184	677.243	675.305	7.286
650.869	650.961	651.054	714.658	714.731	714.805	7.066
651.185	651.193	651.204	714.896	714.902	714.910	6.846
651.243	651.232	651.224	714.939	714.930	714.924	6.626
656.641	655.370	652.758	719.121	718.105	716.010	6.406
705.790	705.888	705.988	758.415	758.494	758.573	6.186
706.129	706.137	706.149	758.673	758.679	758.688	5.966
706.188	706.178	706.170	758.715	758.707	758.701	5.746
711.398	710.178	707.659	762.706	761.740	759.740	5.526
758.681	758.776	758.871	800.141	800.216	800.292	5.306
759.036	759.036	759.037	800.406	800.406	800.406	5.086
759.379	759.289	759.196	800.661	800.590	800.517	4.866
804.541	805.663	807.993	836.409	837.304	839.168	4.646
809.446	809.447	809.448	840.169	840.170	840.170	4.426
814.032	812.986	810.812	843.596	842.782	841.087	4.206
854.800	854.881	854.964	875.291	875.354	875.418	3.986
855.098	855.105	855.116	875.508	875.513	875.521	3.766
855.146	855.139	855.134	875.541	875.536	875.532	3.546
858.669	857.879	856.232	878.148	877.538	876.264	3.326
889.636	889.698	889.761	902.022	902.069	902.118	3.106
889.892	889.899	889.909	902.206	902.210	902.217	2.886
889.921	889.920	889.920	902.225	902.224	902.224	2.666
890.472	890.359	890.123	902.577	902.501	902.342	2.446
894.986	894.995	895.004	905.595	905.601	905.607	2.226
895.124	895.127	895.132	905.688	905.690	905.693	2.006
895.162	895.162	895.162	905.712	905.713	905.713	1.786
0.01238	0.03308	0.04290	0.01238	0.03308	0.04290	R (m)

Table 3.6 Steady state temperatures at the CR and RSC guide tubes

Temperature (^{o}C) for T$_{in}$=490 ^{o}C			Z (m)
Inner-CR (CR hole dia.=0.1016, Tube Thickness=0.012)			
330.581	330.581	330.581	16.01
330.598	330.597	330.597	15.53
330.766	330.764	330.763	15.06
334.159	334.160	334.161	14.58
334.371	334.371	334.371	14.11
334.604	334.602	334.600	13.64
337.966	337.913	337.853	13.16
481.518	481.567	481.623	12.69
485.226	485.228	485.230	12.21
485.499	485.499	485.500	11.74
0.05280	0.05680	0.06080	R (m)
Outer-RSC (CR hole dia.=0.09525, Tube Thickness=0.012)			
330.581	330.581	330.581	14.45
330.598	330.597	330.597	14.14
330.766	330.764	330.763	13.83
334.159	334.160	334.161	13.52
334.371	334.371	334.371	13.21
334.604	334.602	334.600	12.89
337.966	337.913	337.853	12.58
481.518	481.567	481.623	12.27
485.226	485.228	485.230	11.96
485.499	485.499	485.500	11.65
0.04963	0.05362	0.05762	R (m)

Temperature (^{o}C) for T$_{in}$=590 ^{o}C			Z (m)
Inner-CR (CR hole dia.=0.1016, Tube Thickness=0.012)			
364.989	364.989	364.989	16.01
365.014	365.014	365.014	15.53
365.234	365.233	365.231	15.06
369.724	369.725	369.727	14.58
369.986	369.986	369.986	14.11
370.311	370.309	370.306	13.64
374.956	374.880	374.794	13.16
578.017	578.087	578.164	12.69
583.281	583.284	583.287	12.21
583.673	583.673	583.673	11.74
0.05280	0.05680	0.06080	R (m)
Outer-RSC (CR hole dia.=0.09525, Tube Thickness=0.012)			
364.988	364.988	364.988	14.45
365.012	365.012	365.012	14.14
365.251	365.251	365.249	13.83
369.704	369.705	369.707	13.52
369.974	369.974	369.974	13.21
370.269	370.268	370.266	12.89
375.382	375.333	375.255	12.58
577.518	577.562	577.633	12.27
583.322	583.323	583.325	11.96
583.684	583.684	583.685	11.65
0.04963	0.05362	0.05762	R (m)

Table 3.7 Steady state temperatures at the upper plenum shroud

Temperature (°C) for T_{in}=490 °C (C-C thickness=0.0125, Kaowool thickness=0.06)				Z (m)
C-C(hot)	K-Wool	B4C-Graphite	C-C(cold)	
341.672	334.050	326.540	326.534	15.42
374.042	343.989	314.380	314.077	13.78
458.255	386.914	316.685	316.061	12.23
3.16	3.196	3.290	3.359	R (m)

Temperature (°C) for T_{in}=590 °C (C-C thickness=0.0125, Kaowool thickness=0.06)				Z (m)
C-C(hot)	K-Wool	B4C-Graphite	C-C(cold)	
382.789	370.525	358.437	358.389	15.42
432.644	388.656	345.305	344.840	13.78
540.703	444.046	348.829	347.859	12.23
3.16	3.196	3.290	3.359	R (m)

Table 3.8 Steady state temperatures at the upper core restraint blocks

	Temperature (°C) for T_{in}=490 °C					Z (m)
Center Reflector Column	456.755	456.876	456.904	456.917	456.930	11.50
	484.724	485.088	485.174	485.214	485.253	11.30
	0.1476	0.4429	0.7381	1.033	1.329	R (m)
Fuel Block Column	460.096	460.132	460.187			11.50
	485.504	485.519	485.520			11.30
	1.640	1.967	2.272			R (m)
Side Reflector Column	461.435	460.797				11.50
	485.326	483.183				11.30
	2.571	2.868				R (m)
Permanent Side Reflector Column	461.349	466.271	440.558			11.50
	484.565	485.589	417.391			11.30
	3.011	3.148	3.285			R (m)

	Temperature (°C) for T_{in}=590 °C					Z (m)
Center Reflector Column	538.020	538.183	538.219	538.236	538.252	11.50
	582.625	583.129	583.242	583.293	583.342	11.30
	0.1476	0.4429	0.7381	1.033	1.329	R (m)
Fuel Block Column	542.877	543.000	543.148			11.50
	583.682	583.703	583.704			11.30
	1.640	1.967	2.272			R (m)
Side Reflector Column	543.901	542.994				11.50
	583.431	580.289				11.30
	2.571	2.868				R (m)
Permanent Side Reflector Column	543.894	555.416	518.211			11.50
	582.611	583.981	498.376			11.30
	3.011	3.148	3.285			R (m)

Table 3.9 Steady state temperatures at the metallic core support insulation blocks

Temperature (^{o}C) for T_{in}=490 ^{o}C					Z (m)
SCS inlet pipe zone of core bottom support ceramic insulation blocks					
837.407	837.193	836.617	835.267	832.166	-2.006
631.118	630.881	630.264	628.900	625.993	-2.417
0.1476	0.4429	0.7381	1.033	1.329	R (m)
Core zone of core bottom support ceramic insulation blocks					
824.970	806.972	762.884	654.944		-2.006
619.956	607.764	585.177	549.361		-2.417
1.640	1.967	2.272	2.571		R (m)
Outlet Plenum Cover Sheets (C-C thickness=0.005, Kaowool thickness=0.005)					
C-C(hot)	K-Wool	C-Steel(cold)			
676.270	584.212	493.660			-0.300
857.224	676.510	499.001			-0.900
686.298	589.308	493.911			-1.50
596.740	546.951	497.955			-2.006
529.061	510.629	492.476			-2.417
2.732	2.737	2.742			R (m)

Temperature (^{o}C) for T_{in}=590 ^{o}C					Z (m)
SCS inlet pipe zone of core bottom support ceramic insulation blocks					
860.461	860.298	859.857	858.822	856.422	-2.006
696.912	696.742	696.297	695.310	693.192	-2.417
0.1476	0.4429	0.7381	1.033	1.329	R (m)
Core zone of core bottom support ceramic insulation blocks					
850.764	836.334	800.538	712.606		-2.006
688.733	679.189	661.204	632.536		-2.417
1.640	1.967	2.272	2.571		R (m)
Outlet Plenum Cover Sheets (C-C thickness=0.005, Kaowool thickness=0.005)					
C-C(hot)	K-Wool	C-Steel(cold)			
726.863	659.051	592.448			-0.300
874.099	733.894	596.321			-0.900
732.469	661.894	592.579			-1.50
664.871	629.717	595.180			-2.006
616.212	603.695	591.390			-2.417
2.732	2.737	2.742			R (m)

Table 3.10 Steady state temperatures at the hot duct

Temperature (^{o}C) for T_{in}=490 ^{o}C					Pipe Length, L (m)
Hot Duct (C-C thickness=0.0125, Kaowool thickness=0.06)					
C-C	K-Wool	800H	800H	800H	
948.414	712.124	494.814	493.020	491.334	2.255 (Outlet Plenum wall)
948.413	712.118	494.802	493.010	491.328	1.974 (Outlet Plenum wall)
948.439	712.089	494.723	492.926	491.235	1.711 (Core Barrel)
948.466	712.094	494.708	492.910	491.216	1.479 (RPV)
948.290	712.059	494.802	493.010	491.327	1.143 (Reactor Cavity)
948.288	712.061	494.808	493.015	491.329	0.6855 (Reactor Cavity)
948.286	712.059	494.807	493.014	491.328	0.2285 (Reactor Cavity)
0.6837	0.7200	0.7750	0.8250	0.8750	Pipe Radius, R (m)
Cold Duct (C-C thickness=0.0125, Kaowool thickness=0.06)					
C-C	K-Wool	SA508	SA508	SA508	
489.581	378.583	273.196	272.925	272.778	1.711 (Core Barrel)
489.582	377.246	270.574	270.262	270.037	1.479 (RPV)
489.540	374.172	264.586	264.172	263.752	1.143 (Reactor Cavity)
489.529	370.918	258.248	257.821	257.383	0.6855 (Reactor Cavity)
489.522	368.869	254.252	253.801	253.321	0.2285 (Reactor Cavity)
1.149	1.186	1.240	1.291	1.341	Pipe Radius, R (m)

Temperature (^{o}C) for T_{in}=590 ^{o}C					Pipe Length, L (m)
Hot Duct (C-C thickness=0.0125, Kaowool thickness=0.06)					
C-C	K-Wool	800H	800H	800H	
948.735	764.011	594.074	592.435	590.894	2.255 (Outlet Plenum wall)
948.734	764.018	594.088	592.446	590.901	1.974 (Outlet Plenum wall)
948.754	764.075	594.182	592.547	591.013	1.711 (Core Barrel)
948.774	764.091	594.193	592.553	591.009	1.479 (RPV)
948.645	764.065	594.261	592.625	591.087	1.143 (Reactor Cavity)
948.644	764.067	594.266	592.629	591.089	0.6855 (Reactor Cavity)
948.642	764.066	594.266	592.628	591.089	0.2285 (Reactor Cavity)
0.6837	0.7200	0.7750	0.8250	0.8750	Pipe Radius, R (m)
Cold Duct (C-C thickness=0.0125, Kaowool thickness=0.06)					
C-C	K-Wool	SA508	SA508	SA508	
589.311	414.185	247.841	247.185	246.555	1.711 (Core Barrel)
589.320	414.188	247.841	247.185	246.554	1.479 (RPV)
589.270	414.164	247.839	247.184	246.553	1.143 (Reactor Cavity)
589.270	414.163	247.838	247.183	246.552	0.6855 (Reactor Cavity)
589.270	414.163	247.838	247.182	246.552	0.2285 (Reactor Cavity)
1.149	1.186	1.240	1.291	1.341	Pipe Radius, R (m)

Table 3.11 Steady state temperatures at the Bottom plenum/SCS insulation cover

Temperature (^{o}C) for T_{in}=490 ^{o}C (C-C thickness=0.0125, Kaowool thickness=0.06)				Z (m)
C-C(hot)	K-Wool	B4C-Graphite	C-C(cold)	
483.372	366.771	252.273	251.609	-4.076
483.173	367.917	254.741	254.089	-5.783
3.227	3.263	3.323	3.359	R (m)

Temperature (^{o}C) for T_{in}=590 ^{o}C (C-C thickness=0.0125, Kaowool thickness=0.06)				Z (m)
C-C(hot)	K-Wool	B4C-Graphite	C-C(cold)	
580.140	421.463	265.621	264.588	-4.076
579.922	423.317	269.513	268.499	-5.783
3.227	3.263	3.323	3.359	R (m)

3.3 Transient Analysis

The transient analyses are performed for the High Pressure Conduction Cooldown (HPCC) and the Lower Pressure Conduction Cooldown (LPCC) accidents. Figure 3.5 shows the transient conditions of the helium flow rate and outlet pressure of the RCS, and the water flow rate of SCS for both the HPCC and LPCC accidents. It is assumed that the flow rate in the RCS is decreased to zero in 10 seconds after the initiation of both the HPCC and LPCC accidents. The reactor trip signal occurs by low RCS flow of 90% normal flow for the HPCC event and occurs by low system pressure of 6.24MPa for the LPCC, respectively. For both events, the decay heat loading and SCS flow isolation start with one second delay time after the trip signal. After then, the SCS flow is decreased to zero in 5 seconds. The RCS pressure is set as a boundary condition, the value of which is 6.98MPa for the HPCC and 0.1MPa for the LPCC.

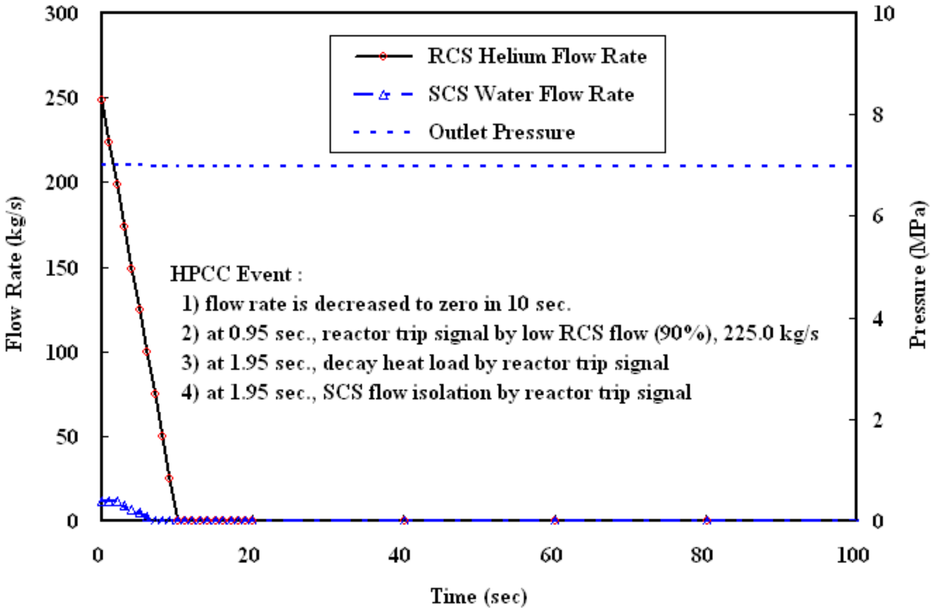

(a) HPCC for T_{in}=490 ^{o}C

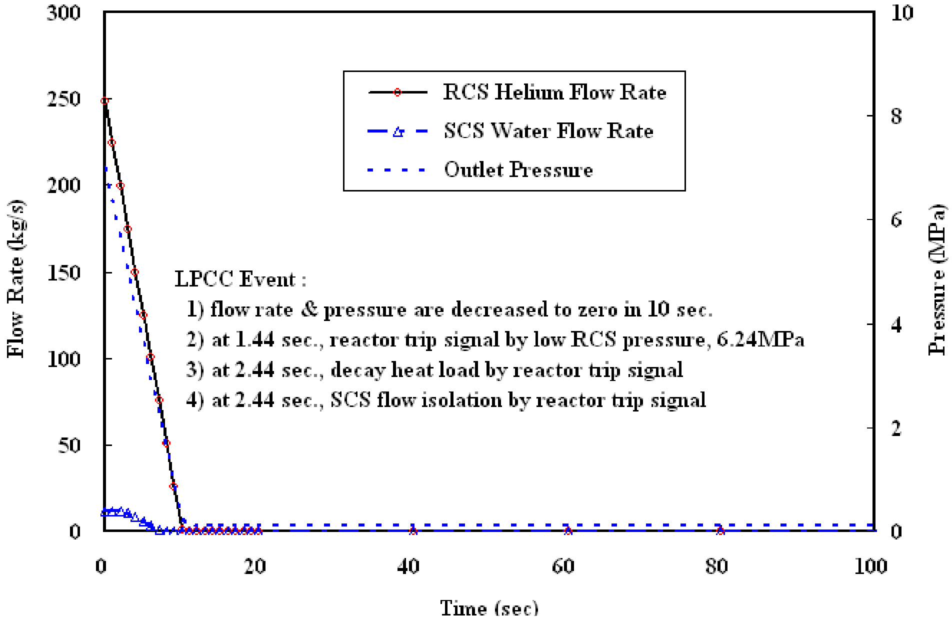

(b) LPCC for T_{in}=490 ^{o}C

Figure 3.5 Transient conditions for the HPCC and LPCC accidents

Maximum temperatures of main components during the HPCC and LPCC accidents for both inlet temperature conditions are summarized in Table 3.12. The maximum fuel temperatures for the HPCC and the LPCC are 1243^{o}C and 1487^{o}C for T_{in}=490^{o}C, and 1280^{o}C and 1511^{o}C for T_{in}=590^{o}C condition, respectively. This shows that the higher inlet temperature condition during the accident results in the higher peak temperatures. It is noted that the temperature of the top reflector for the HPCC is higher than that of the LPCC due to a natural convective flow during the HPCC accidents.

Table 3.12 Maximum temperature of main components during the HPCC and LPCC accidents

Components	T_{max} (^oC) for LPCC		T_{max} (^oC) for HPCC	
	T_{in}=490 ^oC	T_{in}=590 ^oC	T_{in}=490 ^oC	T_{in}=590 ^oC
Fuel Compact	1487	1511	1243	1280
Fuel Block	1487	1511	1243	1279
Bottom Reflector	1018	1004	1019	1005
Inner Reflector	1473	1497	1232	1267
Side Reflector	1153	1174	951	980
Top Reflector	964	990	1195	1225
RPV	540	553	456	468
Core Barrel	693	706	597	608

The temperature transients of the side reflector seals are shown in Figure 3.6. The seals at the top core region are exposed to higher temperature than the others during the HPCC, whereas those of the middle core region are in the higher temperatures during the LPCC. The LPCC accident results in the peak temperature of the seals of 729 ^oC at 87.81 hr for T_{in}=490^oC and 743 ^oC at 81.42 hr for T_{in}=590^oC, respectively.

Figure 3.7 shows the temperature transient of the control rod structural elements. Only the results for the inner control rod are presented, which is a higher temperature region. The peak temperature of the control rod canister for the LPCC is 1474^oC at around 2/3 height of the core, the thirteenth canister from the bottom. Whereas, the peak temperature of 1236 ^oC for the HPCC occurs at the top core due to the natural convection. The difference of the peak temperature between two accidents is nearly the same as that of the fuel temperature. Increase of peak temperature is 26 ^oC for LPCC and 37 ^oC for HPCC, respectively, by increasing the core inlet temperature from 490 ^oC to 590 ^oC. Occurrence of peak temperature for T_{in}=590 ^oC is faster than that of T_{in}=490 ^oC condition.

Figure 3.8 shows the results for the control rod guides tubes. The peak temperature is much higher in the HPCC than in the LPCC due to the natural circulation formed during the HPCC which results in a direct movement of high temperature coolant in the core to the upper plenum. The peak temperature of the guide tubes is as high as 974^oC at 75.14hr for T_{in}=490^oC and 989 ^oC at 63.22 hr for T_{in}=590 ^oC during the HPCC condition. The RSC guide tubes undergo nearly the same peak temperature as that for the control rod guide tubes.

Upper plenum shroud insulation canisters are also exposed to the peak temperatures of 914^oC for T_{in}=490^oC and 926 ^oC for T_{in}=590^oC during the HPCC as shown in Figure 3.9. This is because the hot coolant coming from the core directly impinges onto the canisters during the HPCC. The temperature difference between hot and cold side canisters is as much as 500^oC in its maximum. Increase of peak temperature is 27 ^oC for LPCC and 12 ^oC for HPCC, respectively, by increasing the core inlet temperature from 490 ^oC to 590 ^oC.

The temperature transient of core upper restrain blocks during the HPCC and LPCC accidents is shown in Figure 3.10. Various transient temperature changes are observed in the upper core restraint blocks according to their radial positions. Relatively low temperature is observed in the PSR column compared to the steady state results. The peak temperature of 1075^{o}C for 490^{o}C inlet temperature condition is observed in the HPCC accident and its location corresponds to the inner ring of the core.

Temperature transient of core bottom ceramic insulation blocks is shown in Figure 3.11. The peak temperatures continue to decrease after the initiation of accidents. Temperature transient of hot duct canisters is shown in Figure 3.12. The LPCC results show that the temperature decreases below the steady state and approaches as low as 300^{o}C. In the HPCC accidents, the temperatures continue to decrease after 5^{o}C increase in a few seconds but maintains above 500^{o}C due to the heat supplied by the natural circulating flow in the core.

The results for the bottom plenum/SCS insulation cover sheets are shown in Figure 3.13. Both the results of the HPCC and LPCC decrease at the beginning of the accidents. The HPCC case reveals a relatively steep decrease of the temperature.

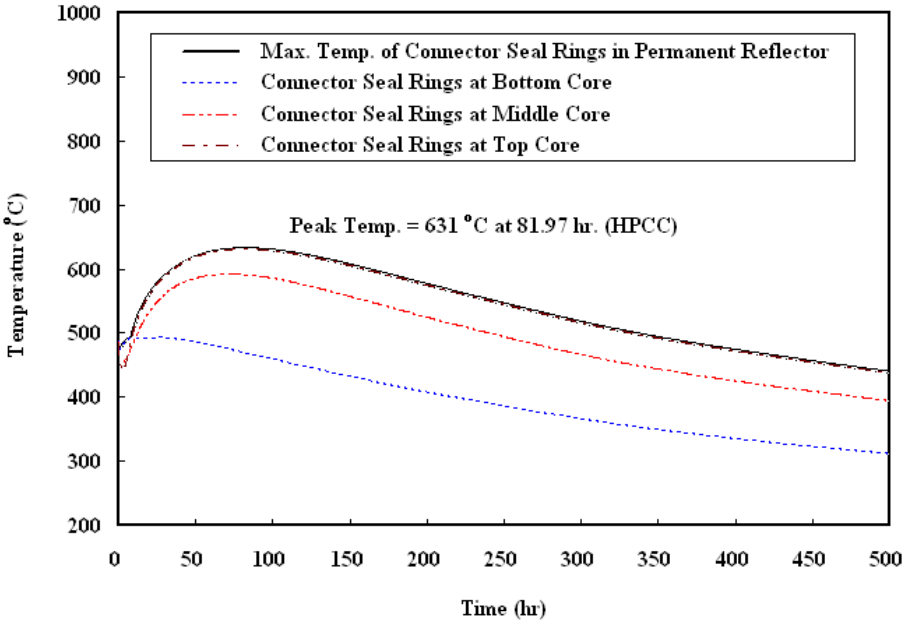

(a) HPCC for T_{in}=490 °C

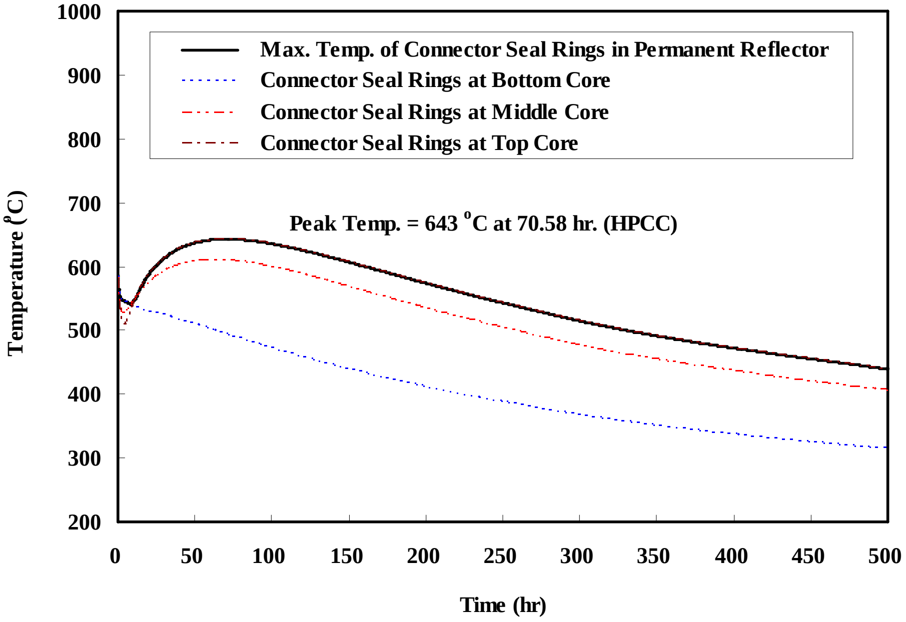

(b) HPCC for T_{in}=590 °C

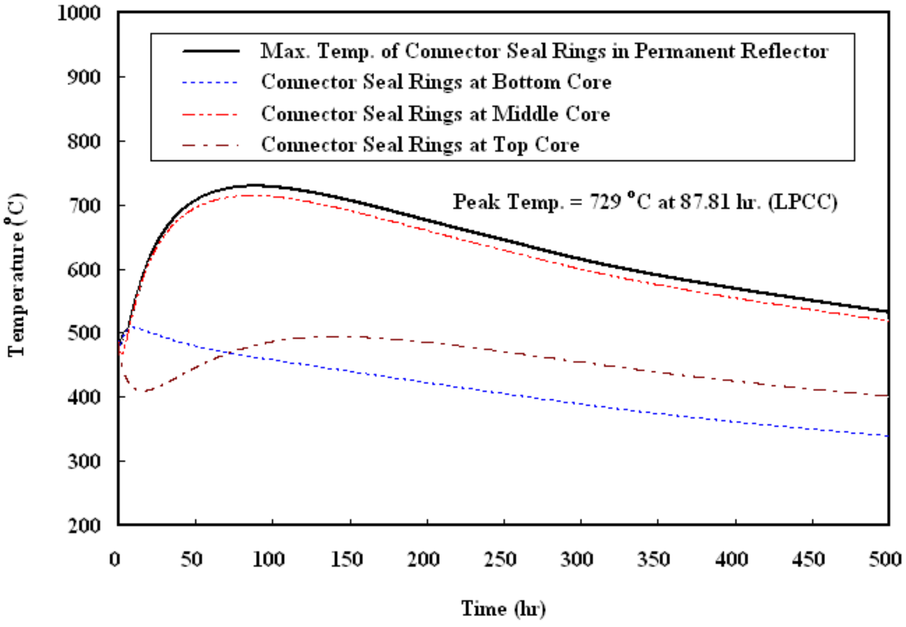

(c) LPCC for T_{in}=490 °C

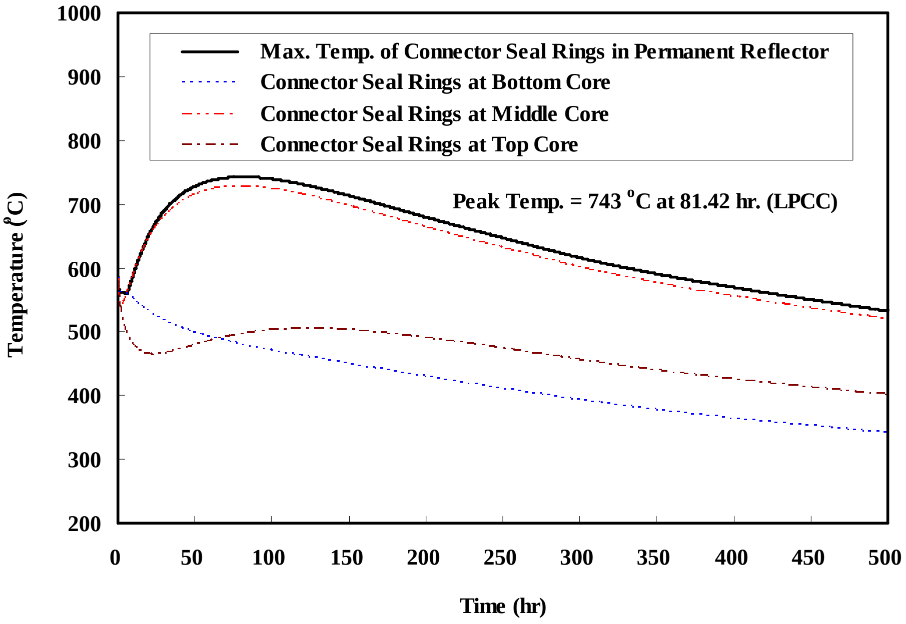

(d) LPCC for T_{in}=590 °C

Figure 3.6 Temperature transients at the side reflector seals

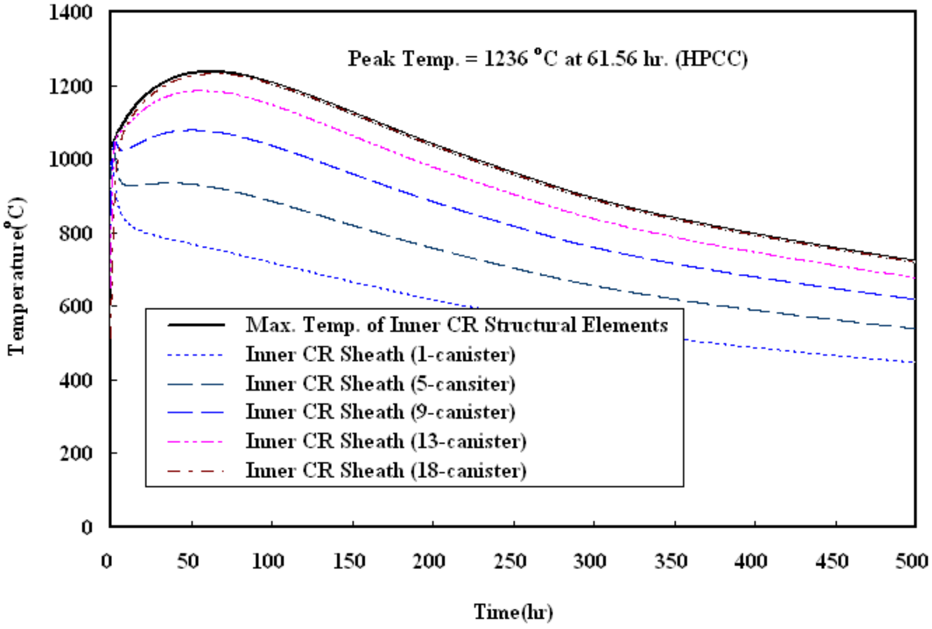

(a) HPCC for T_{in}=490 ^{o}C

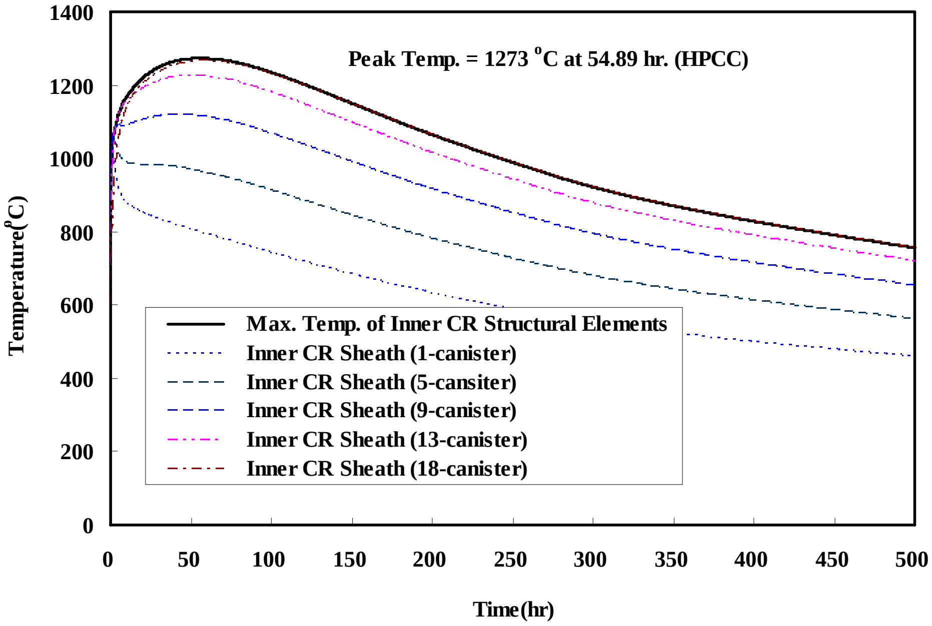

(b) HPCC for T_{in}=590 ^{o}C

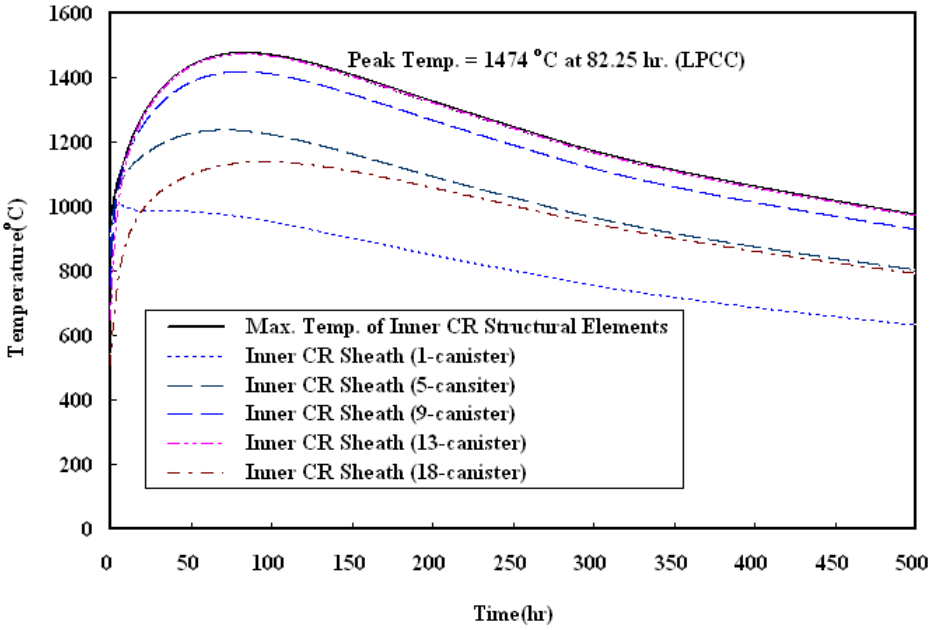

(c) LPCC for T_{in}=490 °C

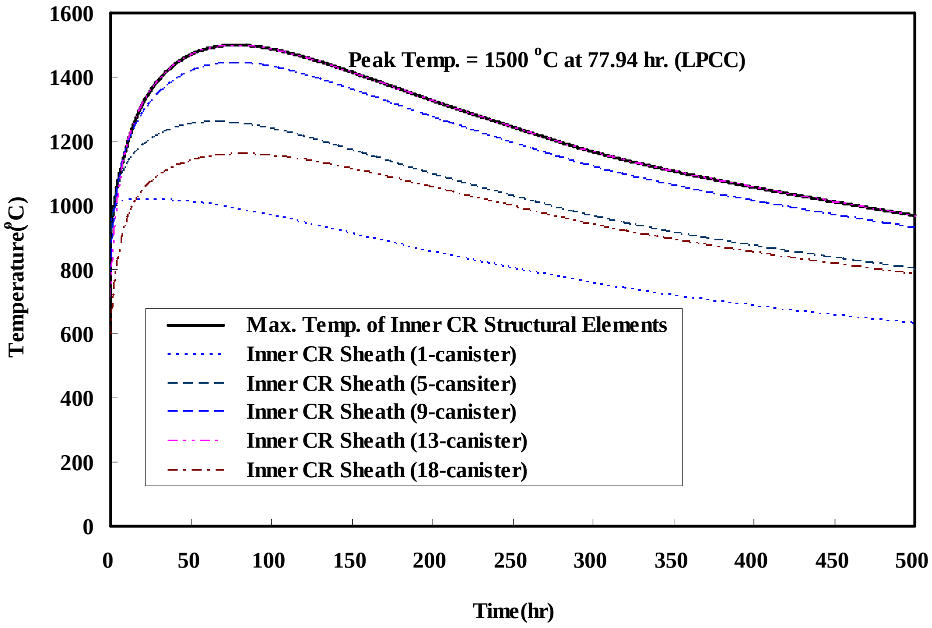

(d) LPCC for T_{in}=590 °C

Figure 3.7 Temperature transients at the inner CR structural elements

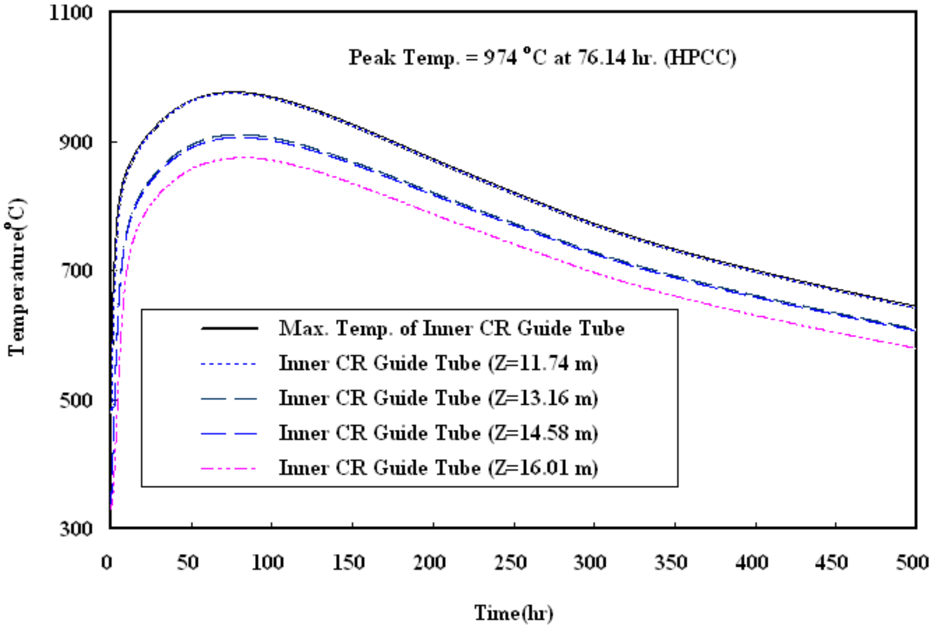

(a) HPCC for T_{in}=490 °C

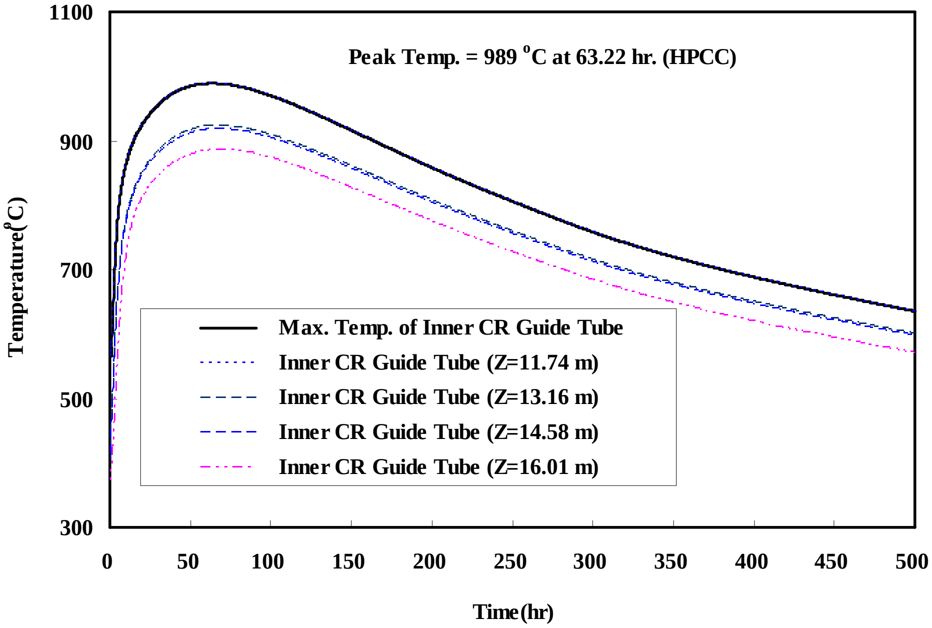

(b) HPCC for T_{in}=590 °C

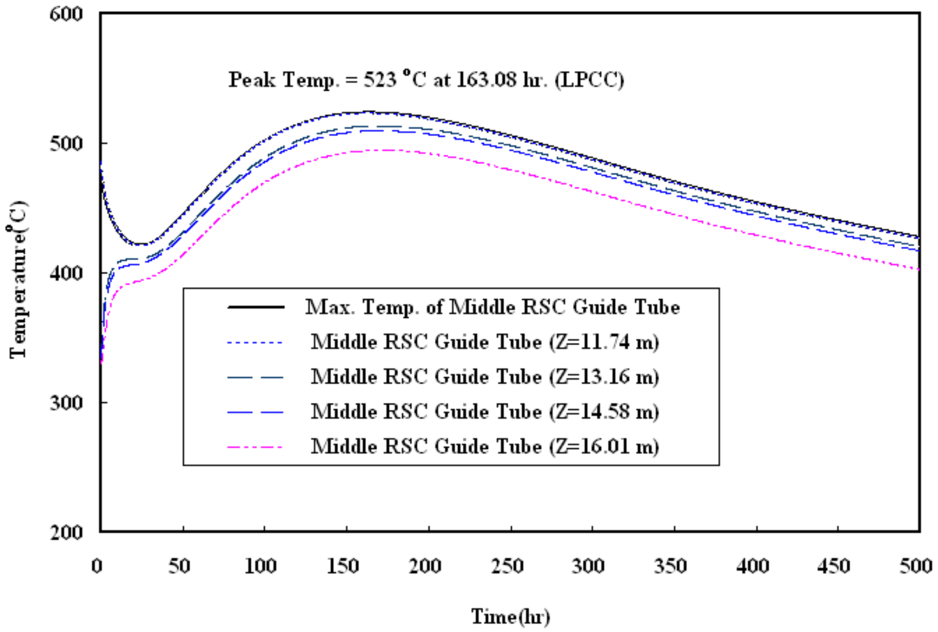

(c) LPCC for T_{in}=490 °C

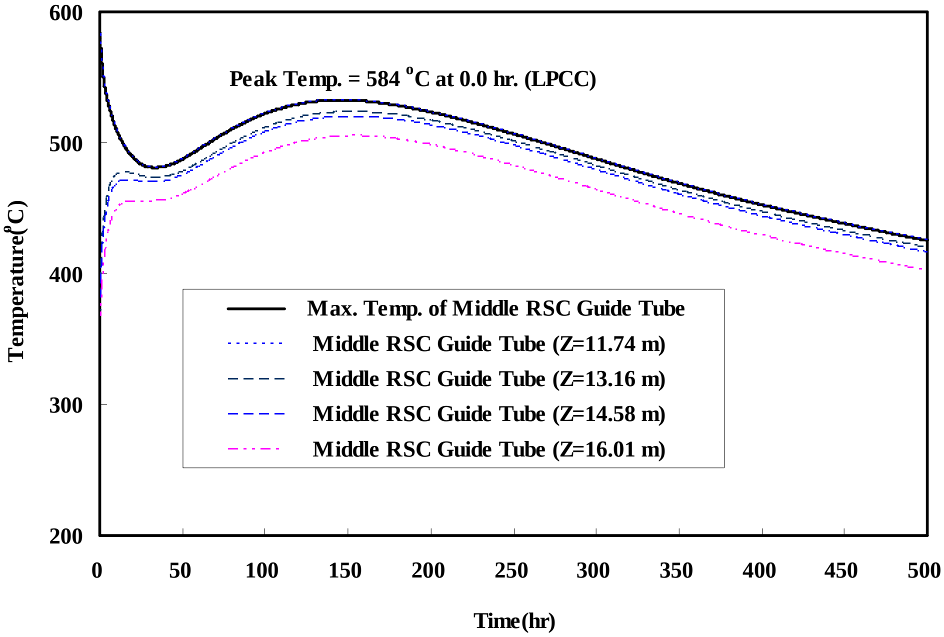

(d) LPCC for T_{in}=590 °C

Figure 3.8 Temperature transients at the CR/RSC guide tubes

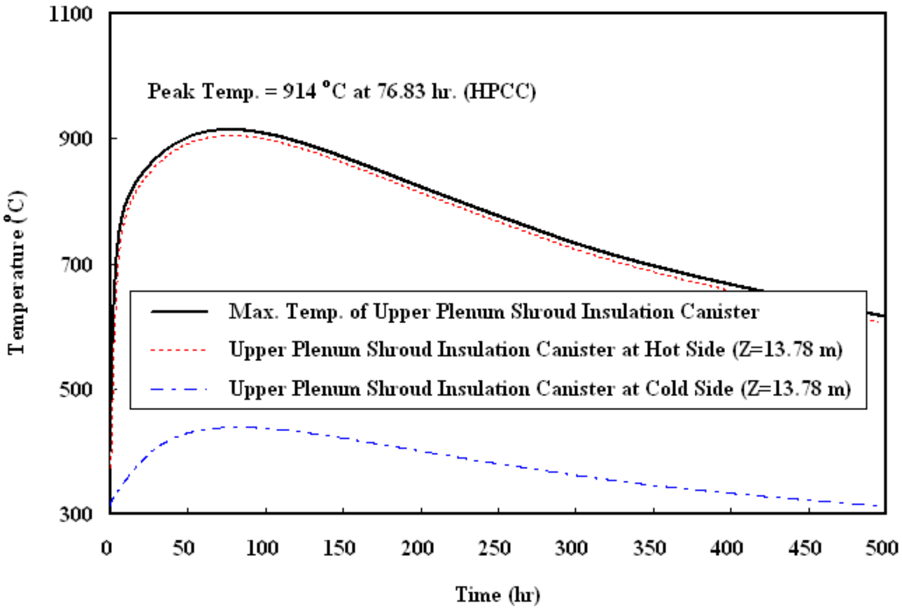

(a) HPCC for T_{in}=490 °C

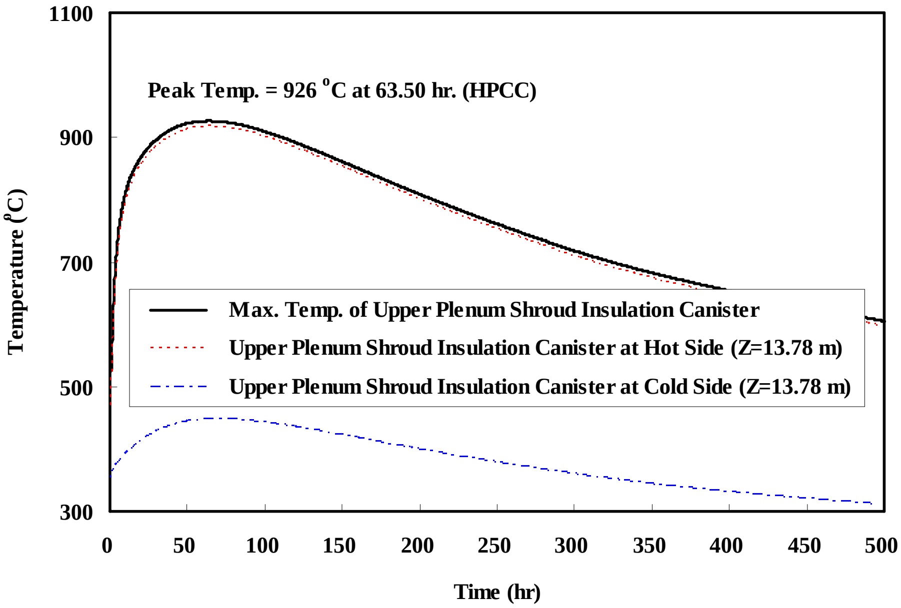

(b) HPCC for T_{in}=590 °C

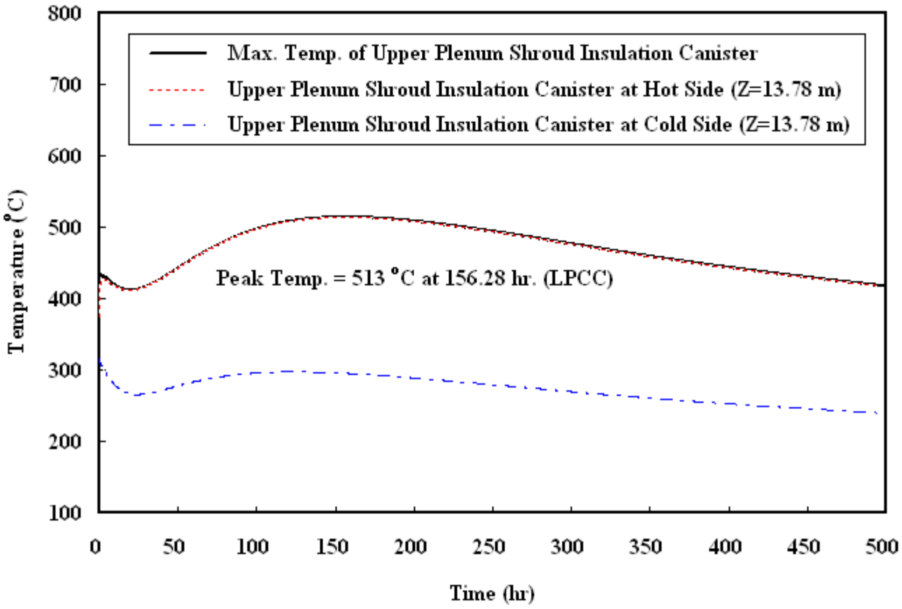

(c) LPCC for T_{in}=490 °C

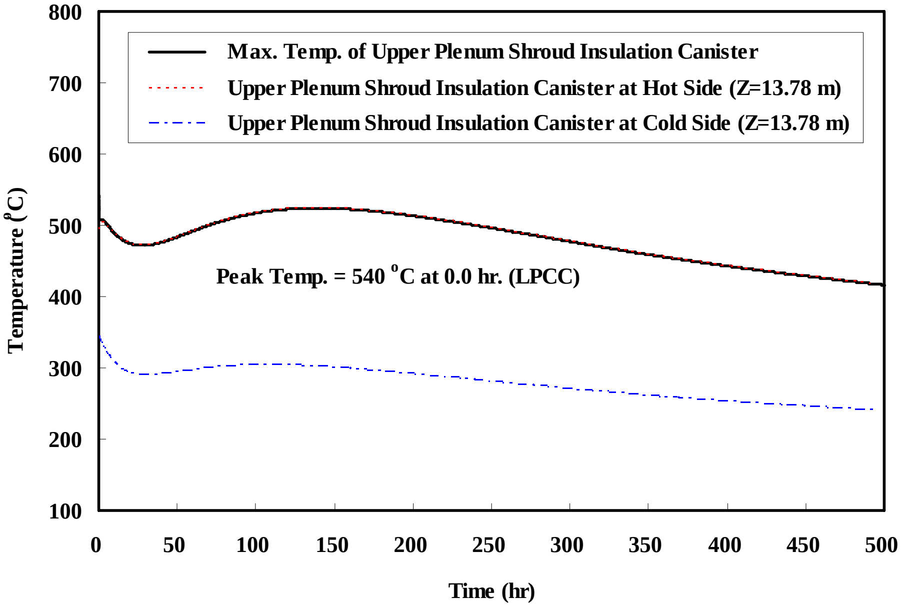

(d) LPCC for T_{in}=590 °C

Figure 3.9 Temperature transients at the upper plenum shroud insulation canisters

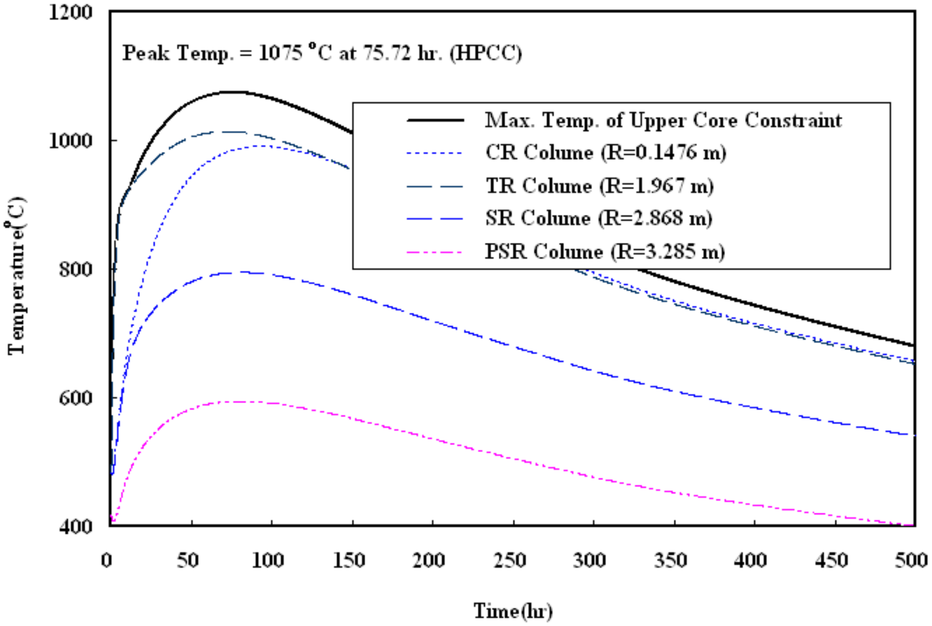

(a) HPCC for T_{in}=490 °C

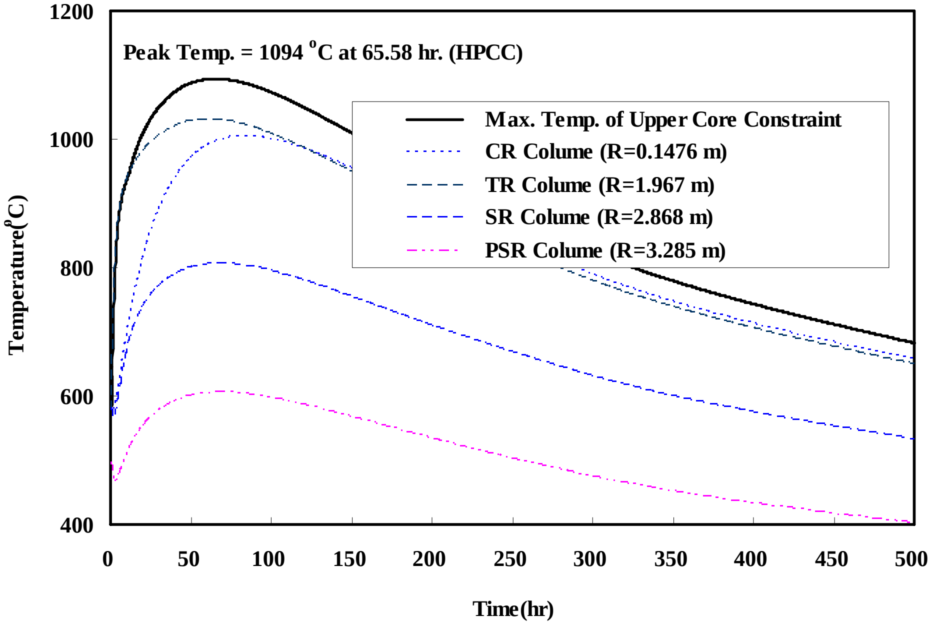

(b) HPCC for T_{in}=590 °C

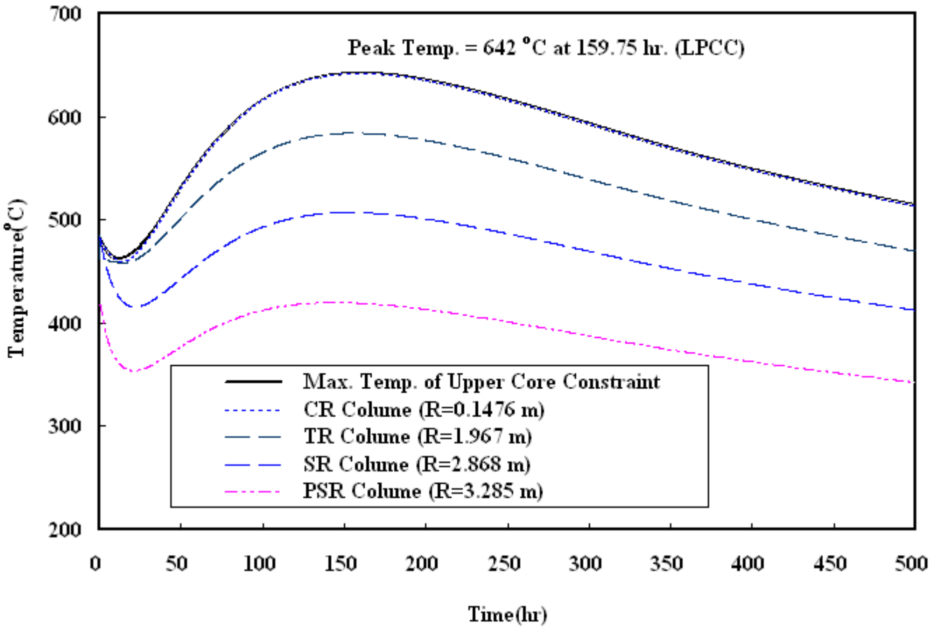

(c) LPCC for T_{in}=490 °C

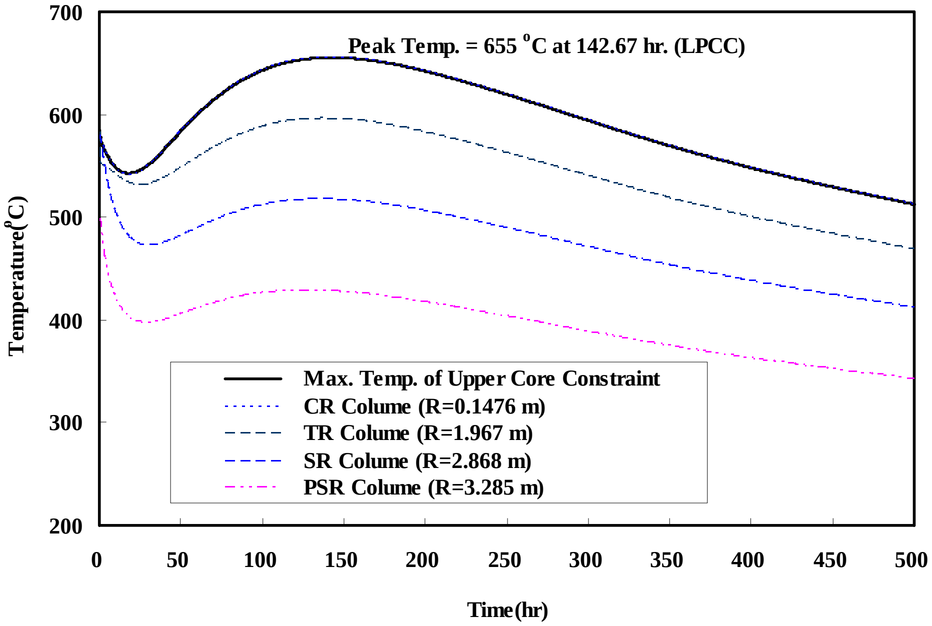

(d) LPCC for T_{in}=590 °C

Figure 3.10 Temperature transients at the upper core restraint blocks

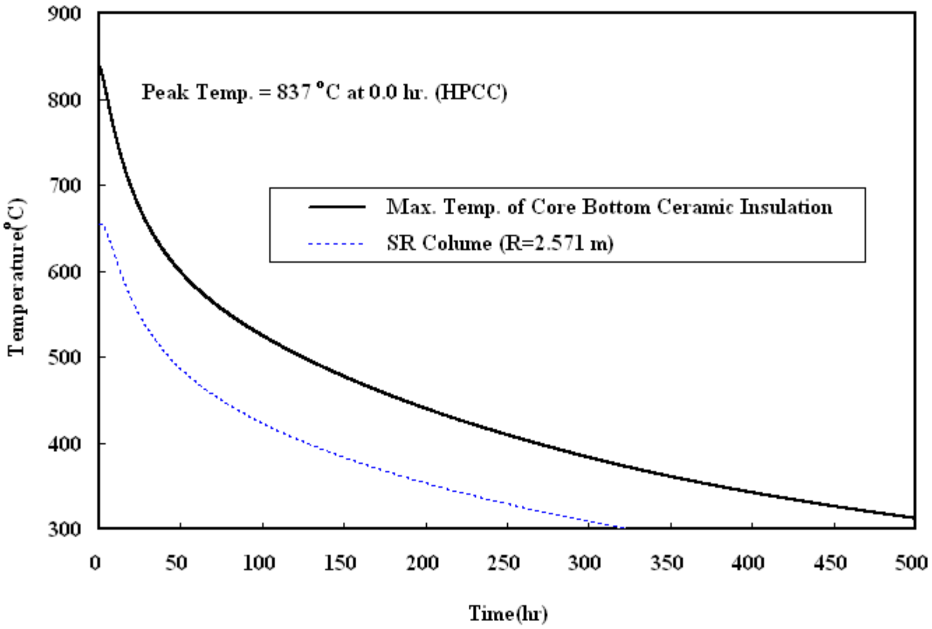

(a) HPCC for T_{in}=490 °C

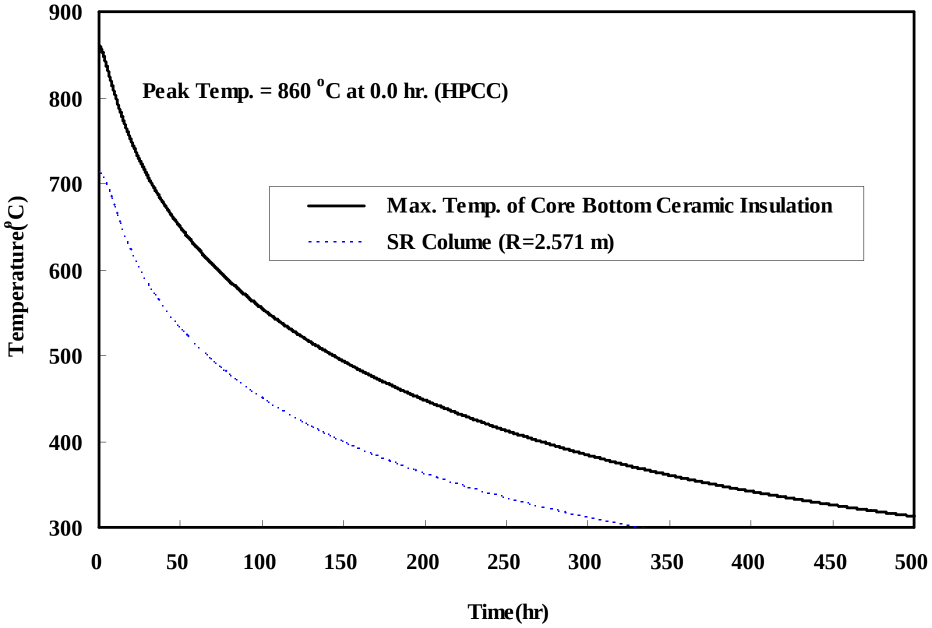

(b) HPCC for T_{in}=590 °C

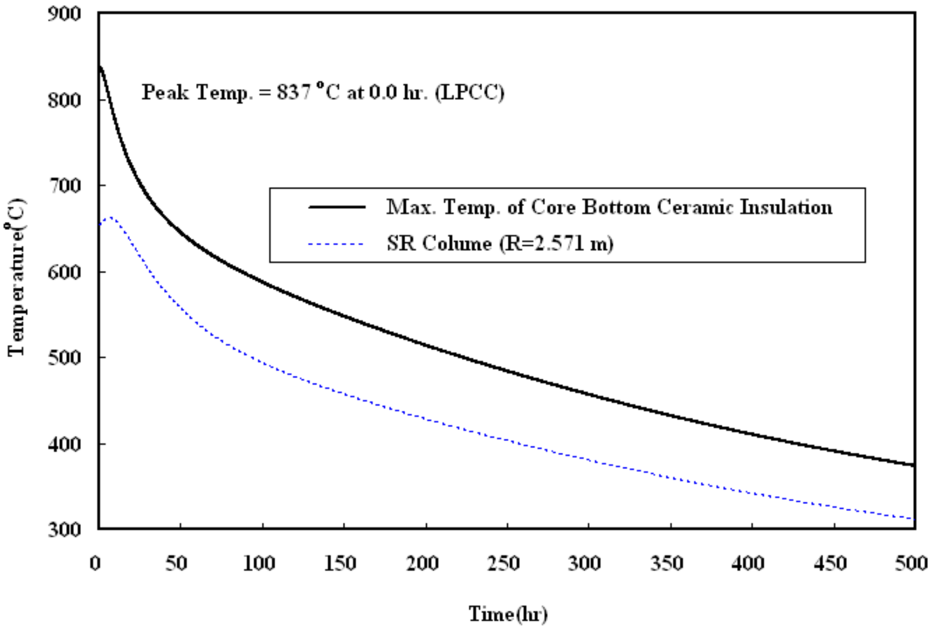

(c) LPCC for T_{in}=490 °C

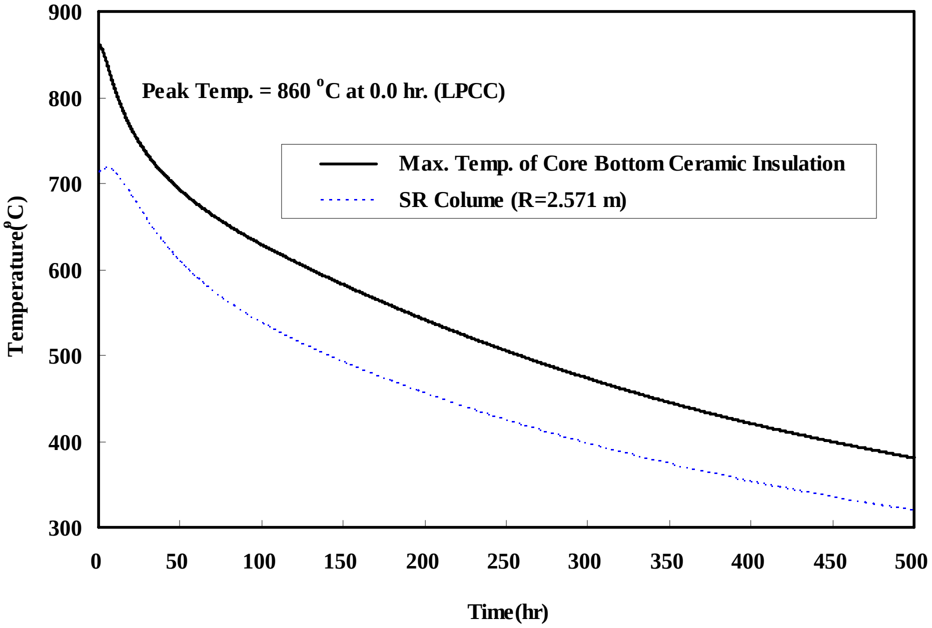

(d) LPCC for T_{in}=590 °C

Figure 3.11 Temperature transients at the metallic core support insulation blocks

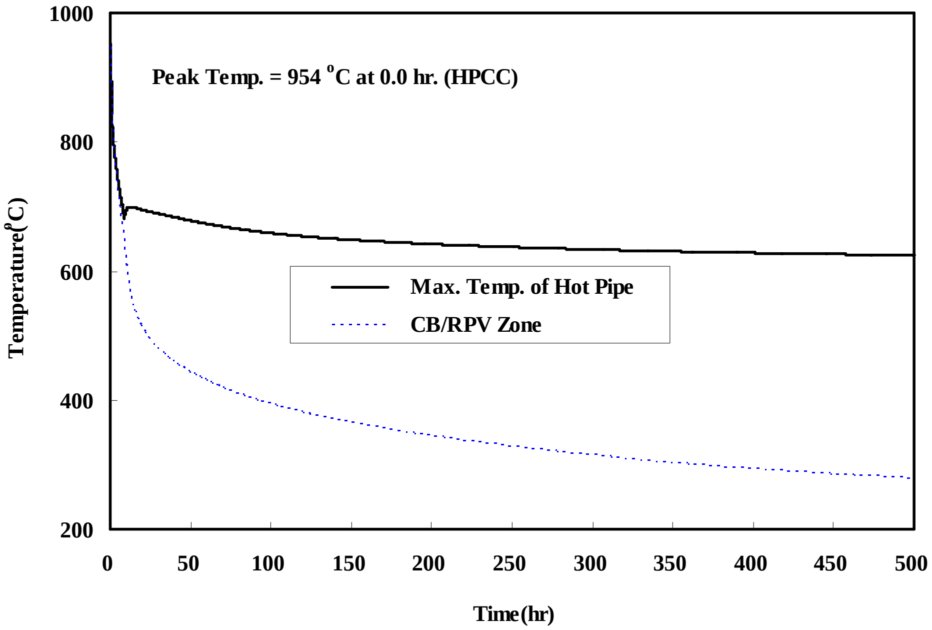

(a) HPCC for T_{in}=490 °C

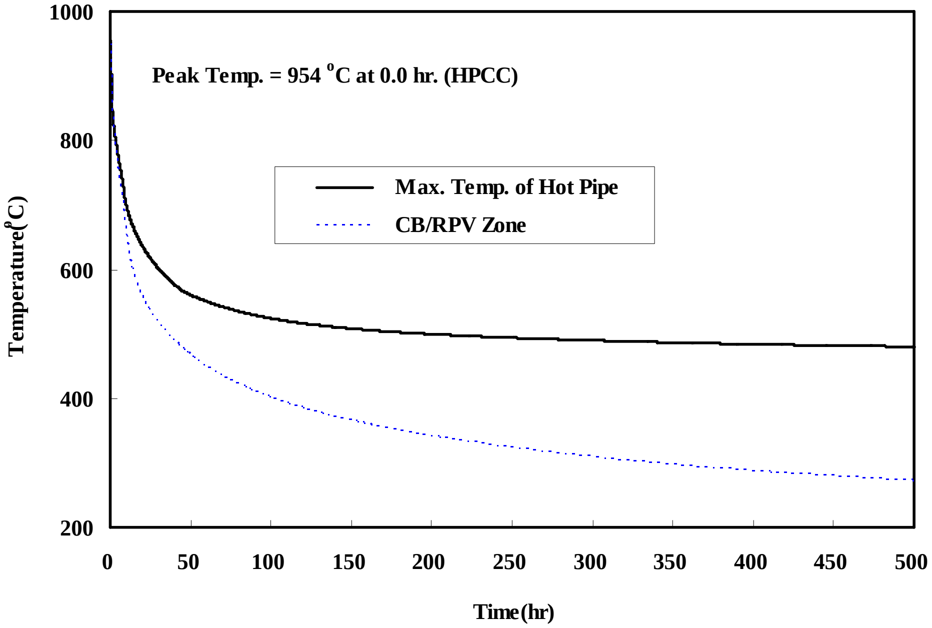

(b) HPCC for T_{in}=590 °C

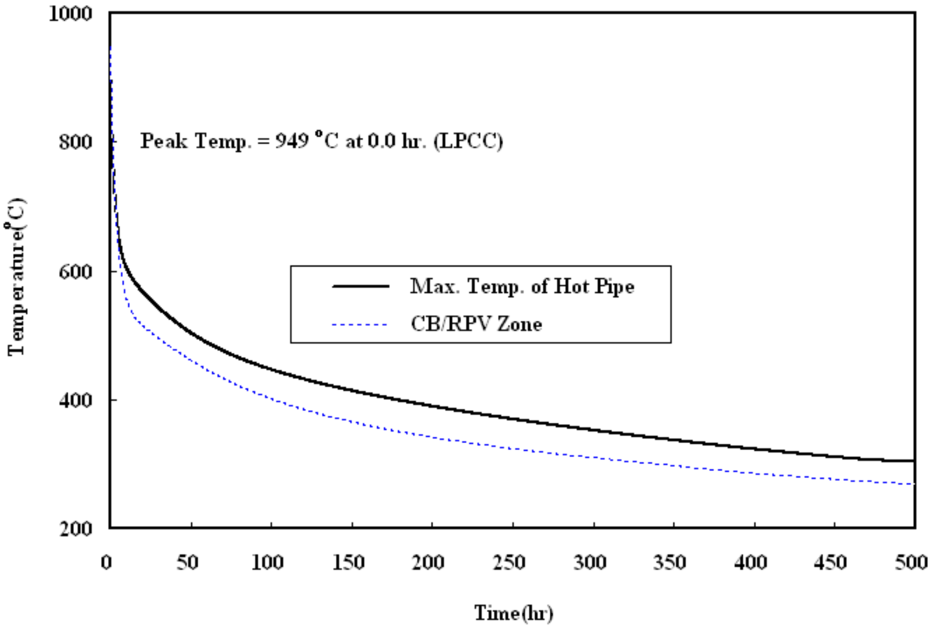

(c) LPCC for T_{in}=490 °C

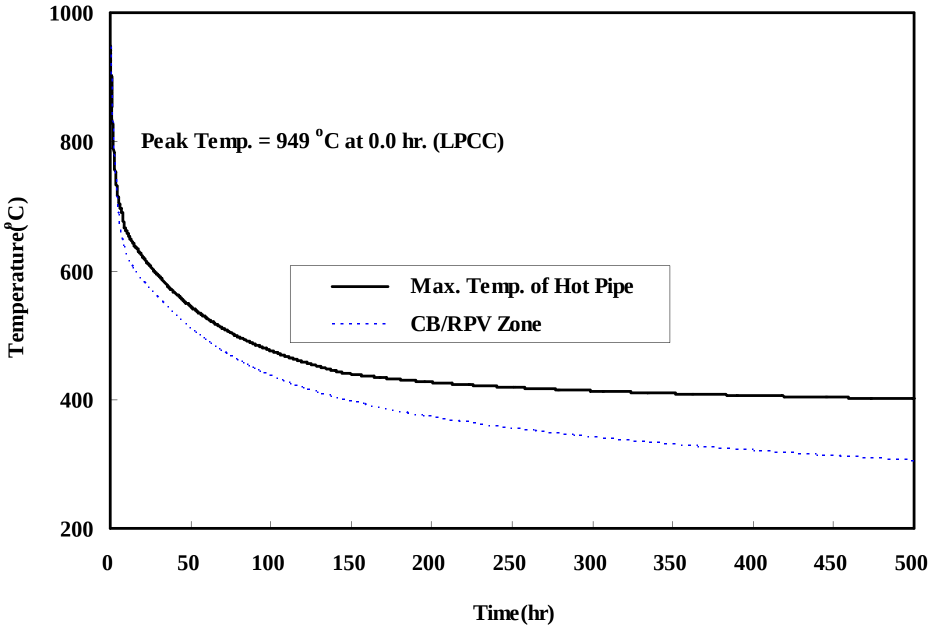

(d) LPCC for T_{in}=590 °C

Figure 3.12 Temperature transient at the hot duct insulation canisters

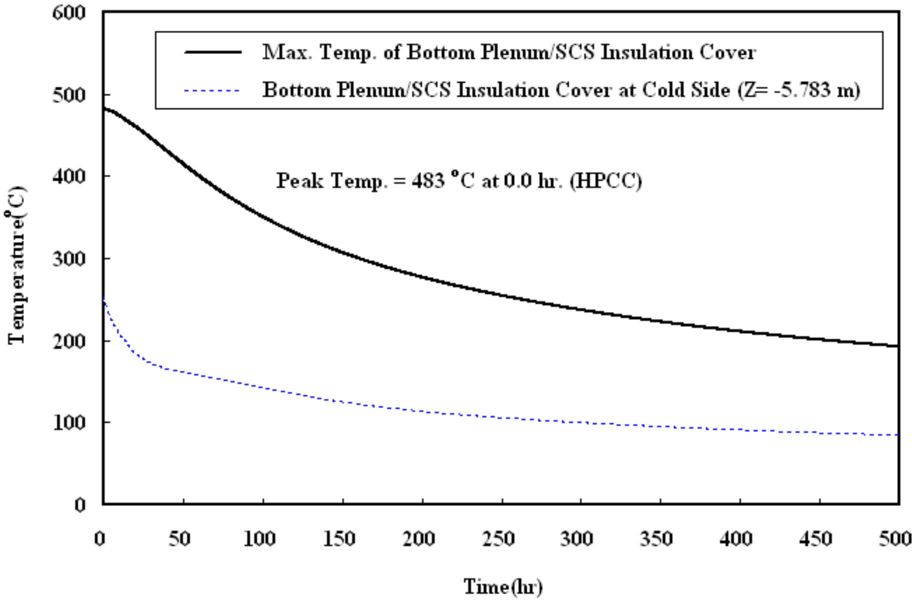

(a) HPCC for T_{in}=490 °C

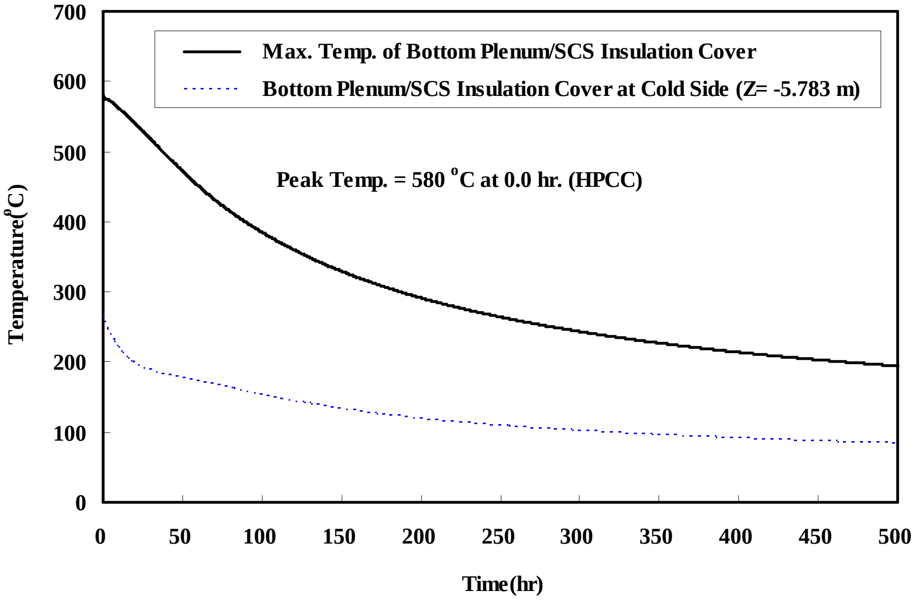

(b) HPCC for T_{in}=590 °C

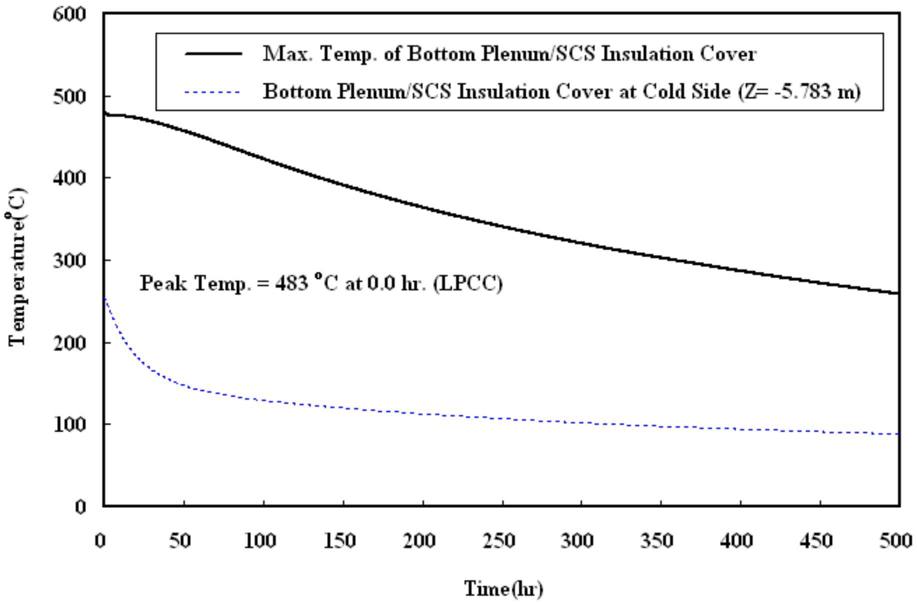

(c) LPCC for T_{in}=490 °C

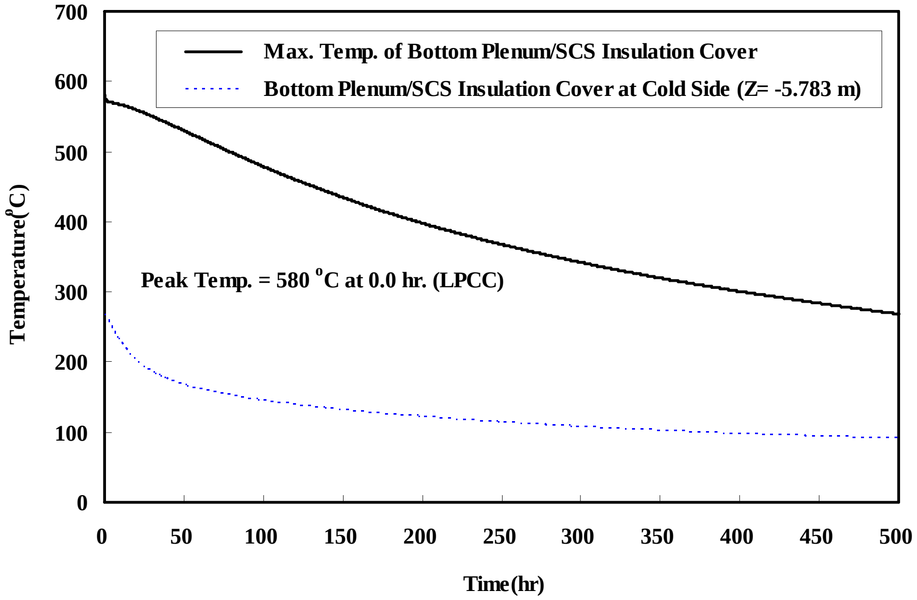

(d) LPCC for T_{in}=590 °C

Figure 3.13 Temperature transients at the bottom plenum and SCS insulation cover sheets

4. SUMMARY

Thermal-fluid analyses to calculate operating conditions for various reactor internals, which are candidates for the use of composite materials, have been performed as a part of NGNP Phase B Conceptual Design Study, WBS HTS.000.S15-Composites R&D Technical Issues Study. Cooled vessel configuration, which use SA-508/533 steel as a material for the reactor vessel, is selected for the analysis except for the upper plenum configuration. It is assumed that the upper plenum is directly connected to the coolant flow channel and it results in higher temperature in the upper plenum during accidents.

The peak temperature of each composite component is derived from the GAMMA+ code analysis results and summarized in Table 4.1. It is seen that some components are exposed to lower temperatures during the accidents than those during the steady state. They are the low metallic core support insulation blocks, the outlet plenum cover sheets, the hot duct insulation canisters, and the bottom plenum/SCS insulation cover sheets. The control rod structural elements undergo the highest temperature during the LPCC accident. The HPCC accident has large influence on the peak temperature of composites around the upper plenum such as the CR/RSC guide tubes, the upper plenum shroud insulation canisters and the upper core restraint blocks.

These peak temperatures will be used as a reference to determine the requirement of materials for the reactor internal components.

Table 4.1 Peak temperatures of the composite components in the postulated conditions.

	Steady		LPCC		HPCC	
Reactor Internal Components	T_{in}=490 °C	T_{in}=590 °C	T_{in}=490 °C	T_{in}=590 °C	T_{in}=490 °C	T_{in}=590 °C
Side reflector seals	487	602	729	743	631	643
Control rod structural elements Inner CR : Outer CR :	 895 535	 905 621	 1474 1029	 1500 1050	 1236 969	 1273 983
Guide tubes of control rod Inner CR : Outer CR :	 485 485	 583 583	 533 526	 584 583	 974 969	 989 984
Guide tubes of RSC Middle RSC : Outer RSC :	 485 485	 583 583	 523 522	 584 584	 971 971	 985 985
Upper plenum shroud insulation	458	541	513	540	914	926
Upper core restraint blocks	485	584	642	655	1075	1094
Lower metallic support insulation Ceramic Blocks : Core Outlet Plenum Wall :	 837 857	 860 877	 837 857	 860 874	 837 857	 860 874
Hot/Cold duct insulation of CV Hot Pipe : Cold Pipe :	 948 489	 949 589	 949 493	 949 589	 954 492	 954 590
Bottom plenum/SCS insulation	483	580	483	580	483	580

REFERENCES

[Kim, 2008]	Kim, M. H., “A preliminary analysis for a cooled SA-508/533 NGNP Reactor Pressure Vessel,” NHDD-KA-07-RD-CA-022, Rev. 01, March 2008.
[GA, 1996]	General Atomics, “Gas Turbine-Modular Helium Reactor (GT-MHR) Conceptual Design Description Report,” Jul. 1996.
[Lim, 2006]	Lim, H.S. and No, H.C. "GAMMA Multi-dimensional Multi-component Mixture Analysis to Predict Air Ingress Phenomena in an HTGR," Nuclear Science and Engineering, Vol. 152, pp. 87-97, Jan. 2006.

GENERAL ATOMICS
P.O. BOX 85608 SAN DIEGO, CA 92186-5608 (858) 455-3000